NASA/TM—2002-211914

Fractional-Order Viscoelasticity (FOV): Constitutive Development Using the Fractional Calculus: First Annual Report

Alan Freed
Glenn Research Center, Cleveland, Ohio

Kai Diethelm
Technische Universität Braunschweig, Braunschweig, Germany

Yury Luchko
Europe University Viadrina, Frankfurt, Germany

December 2002

The NASA STI Program Office . . . in Profile

Since its founding, NASA has been dedicated to the advancement of aeronautics and space science. The NASA Scientific and Technical Information (STI) Program Office plays a key part in helping NASA maintain this important role.

The NASA STI Program Office is operated by Langley Research Center, the Lead Center for NASA's scientific and technical information. The NASA STI Program Office provides access to the NASA STI Database, the largest collection of aeronautical and space science STI in the world. The Program Office is also NASA's institutional mechanism for disseminating the results of its research and development activities. These results are published by NASA in the NASA STI Report Series, which includes the following report types:

- TECHNICAL PUBLICATION. Reports of completed research or a major significant phase of research that present the results of NASA programs and include extensive data or theoretical analysis. Includes compilations of significant scientific and technical data and information deemed to be of continuing reference value. NASA's counterpart of peer-reviewed formal professional papers but has less stringent limitations on manuscript length and extent of graphic presentations.

- TECHNICAL MEMORANDUM. Scientific and technical findings that are preliminary or of specialized interest, e.g., quick release reports, working papers, and bibliographies that contain minimal annotation. Does not contain extensive analysis.

- CONTRACTOR REPORT. Scientific and technical findings by NASA-sponsored contractors and grantees.

- CONFERENCE PUBLICATION. Collected papers from scientific and technical conferences, symposia, seminars, or other meetings sponsored or cosponsored by NASA.

- SPECIAL PUBLICATION. Scientific, technical, or historical information from NASA programs, projects, and missions, often concerned with subjects having substantial public interest.

- TECHNICAL TRANSLATION. English-language translations of foreign scientific and technical material pertinent to NASA's mission.

Specialized services that complement the STI Program Office's diverse offerings include creating custom thesauri, building customized databases, organizing and publishing research results . . . even providing videos.

For more information about the NASA STI Program Office, see the following:

- Access the NASA STI Program Home Page at ***http://www.sti.nasa.gov***

- E-mail your question via the Internet to help@sti.nasa.gov

- Fax your question to the NASA Access Help Desk at 301–621–0134

- Telephone the NASA Access Help Desk at 301–621–0390

- Write to:
  NASA Access Help Desk
  NASA Center for AeroSpace Information
  7121 Standard Drive
  Hanover, MD 21076

NASA/TM—2002-211914

Fractional-Order Viscoelasticity (FOV): Constitutive Development Using the Fractional Calculus: First Annual Report

Alan Freed
Glenn Research Center, Cleveland, Ohio

Kai Diethelm
Technische Universität Braunschweig, Braunschweig, Germany

Yury Luchko
Europe University Viadrina, Frankfurt, Germany

National Aeronautics and
Space Administration

Glenn Research Center

December 2002

Acknowledgments

Alan Freed would like to thank Prof. Ronald Bagley, University of Texas-San Antonio (then Col. Bagley, USAF), for encouraging him to study the fractional calculus and to use FOV in his research on polymers and soft tissues. This work was supported in part by the U.S. Army Medical Research and Material Command to the Cleveland Clinic Foundation with NASA Glenn Research Center being a subcontractor through Space Act Agreement SAA 3–445. Numerous discussions with the PI, Dr. Ivan Vesley, and two of his research associates, Dr. Evelyn Carew and Dr. Todd Doehring, are gratefully acknowledged. Additional support was supplied by the UltraSafe Project at the NASA Glenn Research Center. Alan Freed also gratefully acknowledges the encouragement and support of project manager, Mr. Dale Hopkins, and supervisor, Dr. Michael Meador, at the NASA Glenn Research Center.

This report contains preliminary findings, subject to revision as analysis proceeds.

The Aerospace Propulsion and Power Program at NASA Glenn Research Center sponsored this work.

Available from

NASA Center for Aerospace Information
7121 Standard Drive
Hanover, MD 21076

National Technical Information Service
5285 Port Royal Road
Springfield, VA 22100

Available electronically at http://gltrs.grc.nasa.gov

Contents

Nomenclature

Numbers

$\mathbb{N}$	natural numbers, $\mathbb{N} := \{1, 2, 3, \ldots\}$
$\mathbb{N}_0$	counting numbers, $\mathbb{N}_0 := \{0, 1, 2, \ldots\}$
$\mathbb{R}$	real numbers
$\mathbb{R}_+$	positive real numbers, $\mathbb{R}_+ := \{a \in \mathbb{R} \ : \ a > 0\}$
$\mathbb{C}$	complex numbers, $\mathbb{C} := \left\{x + i\,y : x, y \in \mathbb{R}; i := \sqrt{-1}\right\}$

Functions

C^n	set of all continuous n-differentiable functions
$E_\alpha(x)$	Mittag-Leffler function in one parameter, α
$E_{\alpha,\beta}(x)$	Mittag-Leffler function in two parameters, α & β
${}_1F_1(a; b; x)$	Kummer confluent hypergeometric function
${}_2F_1(a, b; c; x)$	Gauss hypergeometric function
$U(x - x_0)$	unit step function
$\delta(x)$	Dirac delta distribution (the generalized function usually characterized by the property that $\int_{-\infty}^{\infty} \delta(x)\, f(x)\, dx := \delta[f] := f(0)$ whenever f is continuous at 0)
$\Gamma(x)$	Euler's continuous gamma function
$\psi(x)$	digamma function

Differential and Integral Operators

D^n	differential operator, $n \in \mathbb{N}$
D^α	Riemann-Liouville fractional differential operator, $\alpha \in \mathbb{R}_+$
$D_\star^\alpha$	Caputo fractional differential operator, $\alpha \in \mathbb{R}_+$
J^n	Cauchy n-fold integral operator, $n \in \mathbb{N}$
J^α	Riemann-Liouville fractional integral operator, $\alpha \in \mathbb{R}_+$

Scalar Fields

A_i	surface area whose normal points in the i^{th} coordinate direction
dA	differential element for area-of-surface
dC	reference distance separating neighboring planes
dH	differential element for height-of-separation between planes
dS	differential element for distance-of-separation between points

dV	differential element for volume-of-mass
e	dilatation
f	force in 1D
f_i	force in the i^{th} coordinate direction
f_{ij}	force in the i^{th} coordinate direction acting on a surface whose unit normal is in the j^{th} coordinate direction
G	viscoelastic (or relaxation) modulus
G' & G''	viscoelastic storage and loss (dynamic) moduli
$\mathfrak{G}_i$	i^{th} relaxation function
I_n	n^{th} invariant of an integrity basis
J	viscoelastic compliance
ℓ	current length of gauge section
ℓ_0	gauge length
$\mathfrak{M}_i$	i^{th} memory function
p	hydrostatic pressure
$\wp$	Lagrange multiplier forcing an isotropic constraint
s	Laplace transform variable
s	magnitude of shear
t	time
T	absolute temperature
v_s	speed of sound
W	work
$\mathfrak{W}$	potential function representing work
α, α_i	fractal order of evolution
$\bar{\alpha}$	fractal order of evolution in bulk response
β_i	viscoelastic material constant
γ	engineering shear strain
δ	dilatation, classic definition
Δ	dilatation, Hencky's definition
ε	strain in 1-D
η	viscosity
κ	bulk modulus
λ	principal stretch ratio
λ	stretch along fiber direction
λ_i	i^{th} principal stretch ratio
μ	elastic shear modulus
ρ, ρ_i	characteristic retardation time
$\bar{\rho}$	characteristic bulk retardation time
ϱ	mass density
σ	stress in 1-D
σ_i	i^{th} principal stress
ς	reaction stress

τ	shear stress
τ, τ_i	characteristic relaxation time
$\bar{\tau}$	characteristic bulk relaxation time
Ψ_1	first normal-stress difference
Ψ_2	second normal-stress difference
ω	angular frequency (rad/sec)

Outer Products

$\underline{a} \otimes \underline{b}$	vector outer product with components $\mathrm{a}_i \mathrm{b}_j$ where $i, j = 1, 2, 3$
$\underline{\underline{A}} \otimes \underline{\underline{B}}$	tensor outer product with components $\mathrm{A}_{ij}\mathrm{B}_{k\ell}$ where $i, j, k, \ell = 1, 2, 3$
$\underline{\underline{A}} \boxtimes \underline{\underline{b}}$	symmetric tensor outer product with components $\frac{1}{2}\left(\mathrm{A}_{ik}\mathrm{B}_{j\ell} + \mathrm{A}_{i\ell}\mathrm{B}_{jk}\right)$ where $i, j, k, \ell = 1, 2, 3$

Body

$\mathbb{B}$	manifold, $\mathbb{B} \in \mathbb{R}^3$
$\mathcal{B}$	coordinate system
$\mathfrak{P}$	particle (a material point)
ξ	coordinates, $\xi = (\xi^1, \xi^2, \xi^3)$

Body Vector and Tensor Fields

$\underline{\underline{\underline{\underline{\mathfrak{C}}}}}$	fourth-order, contravariant, tangent operator
$d\underline{\xi}$ & $\widehat{d\underline{\xi}}$	coordinate differences between neighboring particles
$d\underline{\phi}$	contact force acting on differential area
$\underline{\alpha}_0$	contravariant unit vector in preferred material direction
$\underline{\underline{\beta}}$	contravariant areal strain tensor
$\underline{\underline{\delta}}$	mixed idem tensor
$\underline{\underline{\gamma}}$	covariant metric tensor
$\underline{\underline{\gamma}}^{-1}$	contravariant metric tensor
$\underline{\underline{\epsilon}}$	covariant strain tensor (strain between material points)
$\underline{\underline{\zeta}}$	contravariant strain tensor (strain between material planes)
$\underline{\underline{\eta}}$	arbitrary contravariant tensor
$\underline{\underline{\theta}}$	tensor of arbitrary weight, kind and rank
$\underline{\underline{\Lambda}}$	mixed stretch tensor
$\underline{\underline{\mu}}$	arbitrary covariant tensor
$\underline{\nu}$	covariant unit normal vector
$\underline{\underline{\pi}}$	contravariant stress tensor
$\underline{\underline{\widetilde{\pi}}}$	contravariant deviatoric stress tensor
$\underline{\underline{\Pi}}$	contravariant extra-stress tensor

Body Tensor Rates

D	partial derivative
$D^{\alpha}_{\star}$	Caputo fractional derivative
J^{α}	Riemann-Liouville fractional integral

Field Transfer

$\overset{t}{\longmapsto}$	Eulerian transfer of field: body into Cartesian space
$\overset{t_0}{\longmapsto}$	Lagrangian transfer of field: body into Cartesian space

Cartesian Space

$\mathbb{S}$	manifold, $\mathbb{S} \in \mathbb{R}^3$
$\mathcal{C}$	(rectangular) Cartesian coordinate system
$\mathfrak{X}_0$	place containing particle $\mathfrak{P}$ in initial state t_0
$\underline{X}$	reference (Lagrangian) position vector to $\mathfrak{X}_0$ with coordinates $\mathbb{X} = (\mathrm{X}_1, \mathrm{X}_2, \mathrm{X}_3)$ in $\mathcal{C}$
$\mathfrak{X}$	place containing particle $\mathfrak{P}$ in current state t
$\underline{x}$	current (Eulerian) position vector to $\mathfrak{X}$ with coordinates $x = (\mathrm{x}_1, \mathrm{x}_2, \mathrm{x}_3)$ in $\mathcal{C}$
$\underline{\underline{I}}$	unit tensor

Kinematic Fields

$\underline{a}$	acceleration vector
$\underline{v}$	velocity vector
$\underline{\underline{F}}$	deformation gradient tensor
$\underline{\underline{L}}$	velocity gradient tensor
$\underline{\underline{R}}$	orthogonal rotation tensor

Eulerian Vector and Tensor Fields

$\underline{a}$	unit vector in preferred material direction
$d\underline{x}$ & $\widehat{d\underline{x}}$	coordinate differences between neighboring places
$\underline{f}$	body-force vector
$\underline{n}$	unit-normal vector
$\underline{\underline{A}}$	Almansi strain tensor (strain between material points)
$\underline{\underline{A}}^{(n)}$	generalized anisotropic strain tensor of order n
$\underline{\underline{B}}$	Finger deformation tensor
$\underline{\underline{\underline{\underline{\mathcal{C}}}}}$	fourth-order tangent operator
$\underline{\underline{\underline{\underline{\mathcal{C}}}}}^{a}$	anisotropic part of elastic tangent operator
$\underline{\underline{\underline{\underline{\mathcal{C}}}}}^{e}$	isotropic elastic part of viscoelastic tangent operator
$\underline{\underline{\underline{\underline{\mathcal{C}}}}}^{ea}$	anisotropic elastic part of viscoelastic tangent operator
$\underline{\underline{\underline{\underline{\mathcal{C}}}}}^{v}$	isotropic viscous part of viscoelastic tangent operator

$\underline{\underline{\underline{\underline{\mathcal{C}}}}}^{va}$	anisotropic viscous part of viscoelastic tangent operator
$\underline{\underline{E}}^{(n)}$	generalized strain tensor of order n
$\underline{\underline{G}}$	arbitrary contravariant-like tensor
$\underline{\underline{\underline{\underline{G}}}}$	fourth-order relaxation modulus
$\underline{J}$	arbitrary tensor
$\underline{\underline{M}}$	arbitrary covariant-like tensor
$\underline{\underline{\underline{\underline{M}}}}$	fourth-order memory function
$\underline{\underline{T}}$	Cauchy stress tensor
$\underline{\underline{\widetilde{T}}}$	deviatoric Cauchy stress tensor
$\underline{\underline{V}}$	left stretch tensor
$\underline{\underline{Z}}$	Signorini strain tensor (strain between material planes)
$\underline{\nabla}$	spatial-gradient operator, $\partial/\partial\underline{x}$

Eulerian Tensor Rates

$\underline{a}_0$	unit vector in preferred material direction
D, $\partial/\partial t$	partial derivative
$\dot{\ }$	material derivative
$\underline{\underline{D}}$	rate-of-deformation tensor
$\overset{\alpha\uparrow}{\underline{\underline{D}}}$	upper-fractal rate-of-deformation tensor of order α
$\overset{\alpha\downarrow}{\underline{\underline{D}}}$	lower-fractal rate-of-deformation tensor of order α
$\overset{\vartriangle}{\underline{\underline{G}}}$	upper-convected (Oldroyd) derivative of a contravariant-like tensor $\underline{\underline{G}}$
$\mathfrak{D}_\star^{\alpha\uparrow}\underline{\underline{G}}$	upper-fractal derivative of order α of a contravariant-like tensor $\underline{\underline{G}}$
$\mathfrak{J}^{\alpha\uparrow}\underline{\underline{G}}$	upper-fractal integral of order α of a contravariant-like tensor $\underline{\underline{G}}$
$\overset{\circ}{\underline{J}}$	corotational (Zaremba-Jaumann) derivative of an arbitrary tensor $\underline{J}$
$\overset{\triangledown}{\underline{\underline{M}}}$	lower-convected (Oldroyd) derivative of a covariant-like tensor $\underline{\underline{M}}$
$\mathfrak{D}_\star^{\alpha\downarrow}\underline{\underline{M}}$	lower-fractal derivative of order α of a covariant-like tensor $\underline{\underline{M}}$
$\mathfrak{J}^{\alpha\downarrow}\underline{\underline{M}}$	lower-fractal integral of order α of a covariant-like tensor $\underline{\underline{M}}$
$\underline{\underline{W}}$	vorticity tensor

Lagrangian Vector and Tensor Fields

$d\underline{X}$ & $\widehat{d\underline{X}}$	coordinate differences between neighboring places
$\underline{N}$	unit-normal vector
$\underline{\underline{C}}$	Green deformation tensor
$\underline{\underline{\underline{\underline{C}}}}$	fourth-order tangent operator
$\underline{\underline{E}}$	Green strain tensor (strain between material points)
$\underline{\underline{H}}$	arbitrary contravariant-like tensor
$\underline{\underline{N}}$	arbitrary covariant-like tensor

$\underline{\underline{P}}$	second Piola-Kirchhoff stress tensor
$\underline{\underline{\tilde{P}}}$	deviatoric part of second Piola-Kirchhoff stress tensor
$\underline{\underline{P}}^{\star}$	Lagrangian stress tensor
$\underline{\underline{U}}$	right stretch tensor
$\underline{\underline{Y}}$	Lagrangian strain tensor (strain between material planes)
Div	spatial-gradient operator, $\partial/\partial\underline{X}$

Lagrangian Tensor Rates

D	partial derivative
$D^{\alpha}_{\star}$	Caputo fractional derivative
J^{α}	Riemann-Liouville fractional integral

Preface

This is the first annual report to the U.S. Army Medical Research and Material Command for the three year project "Advanced Soft Tissue Modeling for Telemedicine and Surgical Simulation" supported by grant No. DAMD17-01-1-0673 to The Cleveland Clinic Foundation, to which the NASA Glenn Research Center is a subcontractor through Space Act Agreement SAA 3-445.

The objective of this report is to extend popular one-dimensional (1D) fractional-order viscoelastic (FOV) material models into their three-dimensional (3D) equivalents for finitely deforming continua, and to provide numerical algorithms for their solution. The present report is organized into seven chapters and three appendices.

The first chapter serves as an introduction to the fractional calculus. Algorithms for computing fractional derivatives, fractional integrals, fractional-order differential equations (FDE's), and the Mittag-Leffler function (which apprears in analytic solutions of FDE's) are provided.

One of the oldest applications of the fractional calculus is viscoelasticity. Chapter two presents an overview of 1D FOV. Definitions for the standard FOV fluid and the standard FOV solid are put forth along with formulæ that are useful in their characterization, assuming infinitesimal strains and rotations.

The third chapter provides an overview of continuum mechanics using body (i.e., convected) tensor fields. Three strain fields are introduced that are measures of strain based on changes in: length of line, separation of non-intersecting surfaces, and volume of mass. Introduced here for the first time are fractal rates of arbitrary tensor fields. Body fields are useful when deriving contitutive equations.

In the fourth chapter, the body fields defined in the previous chapter are mapped into objective, Cartesian, space fields. A useful by-product of field transfer is that those spatial fields created by field transfer are frame invariant. Spatial fields are useful when solving boundary-value problems.

The fifth chapter derives isotropic and transverse-isotropic theories for elastic and viscoelastic materials by applying a work potential to an integrity basis. Both compressible and incompressible materials are considered. These theories are derived in the body and then transferred into Cartesian space in both the Eulerian and Lagrangian frames. The tangent modulus is derived for the general theoretical structures of elastic and viscoelastic solids.

A suite of homogeneous experiments used to characterize material models is presented in the sixth chapter. The suite includes the homogeneous deformations of: shear-free extension (e.g., uniaxial elongation, biaxial extension, pure shear, and dilational compression) and simple shear. The deformation, stress and strain fields

defined in the prior chapter, along with their various rates, are all quantified for this suite of experiments.

Chapters seven through nine provide elastic and viscoelastic constitutive models appropriate for 3D analysis. Chapter seven provides material models for bulk response. Chapter eight will introduce material models for isotropic elastomers, while chapter nine will introduce material models for soft biological tissues, which are generally transverse isotropic; they will be completed for the second annual report. Both classical and fractional-order viscoelastic models are presented. Included are solutions for the characterization experiments of chapter six.

There are three appendices. The first appendix tabulates Caputo fractional derivatives for a few of the more common mathematical functions. The second appendix outlines an automatic procedure for numerical integration that is required by the algorithm which computes the Mittag-Leffler function. And the third appendix provides an efficient scheme for approximating a specific form of the Mittag-Leffler function that arises in FOV.

Chapter 1

Fractional Calculus: numerical methods

1.1 Riemann-Liouville Fractional Integral

In the classical calculus of Newton and Leibniz, Cauchy reduced the calculation of an n-fold integration of the function $\mathbf{y}(x)$ into a single convolution integral possessing an Abel (power law) kernel,

$$\begin{aligned} J^n\mathbf{y}(x) &:= \int_0^x \int_0^{x_{n-1}} \cdots \int_0^{x_1} \mathbf{y}(x_0)\, dx_0 \ldots dx_{n-2}\, dx_{n-1} \\ &= \frac{1}{(n-1)!} \int_0^x \frac{1}{(x-x')^{1-n}}\, \mathbf{y}(x')\, dx', \quad n \in \mathbb{N}, \quad x \in \mathbb{R}_+, \end{aligned} \tag{1.1}$$

where J^n is the n-fold integral operator with $J^0\mathbf{y}(x) = \mathbf{y}(x)$, $\mathbb{N}$ is the set of positive integers, and $\mathbb{R}_+$ is the set of positive reals. Liouville and Riemann* analytically continued Cauchy's result by replacing the discrete factorial $(n-1)!$ with Euler's continuous gamma function $\Gamma(n)$, noting that $(n-1)! = \Gamma(n)$, thereby producing [67, ¶5, Eqn. A]

$$J^\alpha\mathbf{y}(x) := \frac{1}{\Gamma(\alpha)} \int_0^x \frac{1}{(x-x')^{1-\alpha}}\, \mathbf{y}(x')\, dx', \quad \alpha, x \in \mathbb{R}_+, \tag{1.2}$$

where J^α is the Riemann-Liouville integral operator of order α, which commutes (i.e., $J^\alpha J^\beta \mathbf{y}(x) = J^\beta J^\alpha \mathbf{y}(x) = J^{\alpha+\beta}\mathbf{y}(x)\ \forall\ \alpha, \beta \in \mathbb{R}_+$). Equation (1.2) is the cornerstone of the fractional calculus, although it may vary in its assignment of limits of integration. In this report we take the lower limit to be zero and the upper limit to be some positive finite real. Actually, α can be complex [102], but for our purposes we only need it to be real.

A brief history of the development of fractional calculus can be found in Ross [100] and Miller and Ross [78, Chp. 1]. A survey of many emerging applications of the fractional calculus in areas of science and engineering can be found in the recent text by Podlubny [86, Chp. 10].

*Riemann's pioneering work in the field of fractional calculus was done during his student years, but published posthumous—forty-four years after Liouville first published in the field [100].

1.2 Caputo-Type Fractional Derivative

From this single definition for fractional integration one can construct several definitions for fractional differentiation (cf. e.g., [86, 102]). The special operator $D_\star^\alpha$ that we choose to use, which requires the dependent variable $\mathbf{y}$ to be continuous and $\lceil\alpha\rceil$-times differentiable in the independent variable x, is defined by

$$D_\star^\alpha \mathbf{y}(x) \coloneqq J^{\lceil\alpha\rceil-\alpha} D^{\lceil\alpha\rceil}\mathbf{y}(x), \tag{1.3}$$

such that

$$\lim_{\alpha\to n_-} D_\star^\alpha \mathbf{y}(x) = D^n\mathbf{y}(x) \quad \text{for} \quad n\in\mathbb{N}, \tag{1.4}$$

with $D_\star^0\mathbf{y}(x) = \mathbf{y}(x)$, where $\lceil\alpha\rceil$ is the ceiling function giving the smallest integer greater than (or equal to) α, and where $\alpha\to n_-$ means α goes to n from below. The operator D^n, $n\in\mathbb{N}$, is the classical differential operator. It is accepted practice to call $D_\star^\alpha$ the Caputo differential operator of order α, after Caputo [12] who was the amoung the first to use this operator in applications and to study some of its properties.[†] Appendix A presents a table of Caputo derivatives for some of the more common mathematical functions.

The Caputo differential operator is a linear operator

$$D_\star^\alpha\big(\mathbf{y}+\mathbf{z}\big)(x) = D_\star^\alpha\mathbf{y}(x) + D_\star^\alpha\mathbf{z}(x) \tag{1.5a}$$

that commutes

$$D_\star^\alpha D_\star^\beta\mathbf{y}(x) = D_\star^\beta D_\star^\alpha\mathbf{y}(x) = D_\star^{\alpha+\beta}\mathbf{y}(x) \quad \forall\ \alpha,\beta\in\mathbb{R}_+ \tag{1.5b}$$

if $\mathbf{y}(x)$ is sufficiently smooth, and it possesses the desirable property that

$$D_\star^\alpha c = 0 \quad \text{for any constant } c. \tag{1.5c}$$

The more common Riemann-Liouville fractional derivative D^α, although linear, need not commute [86, pg. 74]; furthermore, $D^\alpha c = D^{\lceil\alpha\rceil}J^{\lceil\alpha\rceil-\alpha}c = cx^{-\alpha}/\Gamma(1-\alpha)$, which is a function of x! Ross [100] attributes this startling fact as the main reason why the fractional calculus has historically had a difficult time being embraced by the mathematics and physics communities.

[†]Actually, Liouville introduced the operator in his historic first paper on the topic [67, ¶6, Eqn. B]. Still, nothing in Liouville's works suggests that he ever saw any difference between $D_\star^\alpha = J^{\lceil\alpha\rceil-\alpha}D^{\lceil\alpha\rceil}$ and $D^\alpha = D^{\lceil\alpha\rceil}J^{\lceil\alpha\rceil-\alpha}$, D^α being his accepted definition [67, first formula on pg. 10]—the Riemann-Liouville differential operator of order α. Liouville freely interchanged the order of integration and differentiation, because the class of problems that he was interested in happened to be a class where such an interchange is legal, and he made only a few terse remarks about the general requirements on the class of functions for which his fractional calculus works [74]. The accepted naming of the operator $D_\star^\alpha$ after Caputo therefore seems warrented.

Rabotnov [90, pg. 129] introduced this same differential operator into the Russian viscoelastic literature a year before Caputo's paper was published. Regardless of this fact, operator $D_\star^\alpha$ is commonly named after Caputo in the current liturature.

The Riemann-Liouville integral operator J^α and the Caputo differential operator $D^\alpha_\star$ are inverse operators in the sense that

$$D^\alpha_\star J^\alpha \mathbf{y}(x) = \mathbf{y}(x) \quad \text{and} \quad J^\alpha D^\alpha_\star \mathbf{y}(x) = \mathbf{y}(x) - \sum_{k=0}^{\lfloor\alpha\rfloor} \frac{x^k}{k!}\, \mathbf{y}^{(k)}_{0^+}, \quad \alpha \in \mathbb{R}_+, \tag{1.6}$$

with $\mathbf{y}^{(k)}_{0^+} := D^k \mathbf{y}(0^+)$, where $\lfloor\alpha\rfloor$ is the floor function giving the largest integer less than α. The classic n-fold integral and differential operators of integer order satisfy like formulæ, viz.: $D^n J^n \mathbf{y}(x) = \mathbf{y}(x)$ and $J^n D^n \mathbf{y}(x) = \mathbf{y}(x) - \sum_{k=0}^{n-1} \frac{x^k}{k!}\, \mathbf{y}^{(k)}_{0^+}$, $n \in \mathbb{N}$.

A word of caution. Fractional derivatives do not satisfy the Leibniz product rule of classical calculus. For example, whenever the Caputo derivative is restricted so that $0 < \alpha < 1$, the Leibniz product rule is given by

$$\begin{aligned} D^\alpha_\star\big(\mathbf{y} \times \mathbf{z}\big)(x) = \frac{\mathbf{y}(0^+)}{\Gamma(1-\alpha)} \times \frac{\mathbf{z}(x) - \mathbf{z}(0^+)}{x^\alpha} + \big(D^\alpha_\star \mathbf{y}\big)(x) \times \mathbf{z}(x) \\ + \sum_{k=1}^{\infty} \binom{\alpha}{k} \big(J^{k-\alpha}\mathbf{y}\big)(x) \times \big(D^k \mathbf{z}\big)(x), \end{aligned} \tag{1.7}$$

where, unlike the Leibniz product rule for integer-order derivatives, the binomial coefficients $\binom{\alpha}{k} = \frac{\alpha(\alpha-1)(\alpha-2)\cdots(\alpha-k+1)}{k!}$ (with $\binom{\alpha}{0} = 1$, $\alpha \in \mathbb{R}_+$ and $k \in \mathbb{N}$) do not become zero whenever $k > \alpha$ because $\alpha \notin \mathbb{N}$ (i.e., the binomial sum is now of infinite extent). A similar infinite sum exists for the Leibniz product rule of the Riemann-Liouville fractional derivative (cf. Podlubny [86, pp. 91–97]).

1.2.1 Integral Expressions

The Caputo derivative (1.3) can be expressed in more explicit notation as the integral

$$D^\alpha_\star \mathbf{y}(x) = \frac{1}{\Gamma(\lceil\alpha\rceil - \alpha)} \int_0^x \frac{1}{(x-x')^{\alpha-\lfloor\alpha\rfloor}} \big(D^{\lceil\alpha\rceil}\mathbf{y}\big)(x')\, dx', \quad \alpha, x \in \mathbb{R}_+, \tag{1.8a}$$

where the weak singularity caused by the Abel kernel of the integral operator is readily observed. This singularity can be removed through an integration by parts

$$D^\alpha_\star \mathbf{y}(x) = \frac{1}{\Gamma(1 + \lceil\alpha\rceil - \alpha)} \left(x^{\lceil\alpha\rceil-\alpha}\, \mathbf{y}^{(\lceil\alpha\rceil)}_{0^+} + \int_0^x \big(x-x'\big)^{\lceil\alpha\rceil-\alpha} \big(D^{1+\lceil\alpha\rceil}\mathbf{y}\big)(x')\, dx' \right), \tag{1.8b}$$

provided that the dependent variable $\mathbf{y}$ is continuous and $(1+\lceil\alpha\rceil)$-times differentiable in the independent variable x over the interval of differentiation (integration) $[0, x]$. In (1.8b) the power-law kernel is bounded over the entire interval of integration; whereas, in (1.8a) the kernel is singular at the upper limit of integration.

The two representations of (1.8a) and (1.8b) are quite useful for pen-and-paper calculations, but in order to obtain a numerical scheme for the approximation of such fractional derivatives, we found it even more helpful to look at yet another

representation that seems to have been introduced into this context by Elliott [30]; namely,

$$D_\star^\alpha \mathbf{y}(x) = \frac{1}{\Gamma(-\alpha)} \int_0^x \frac{1}{(x-x')^{\alpha+1}} \mathbf{y}(x')\, dx', \quad \alpha, x \in \mathbb{R}_+. \tag{1.8c}$$

This representation can also be obtained from (1.8a) using the method of integration by parts, but with the roles of the two factors interchanged. The advantage here is that the function $\mathbf{y}$ itself appears in the integrand instead of its derivative. The disadvantage is that the singularity of the kernel is now strong rather than weak, and thus we have to interpret this integral as a Hadamard-type finite-part integral. This is cumbersome in pen-and-paper calculations but, as we shall see below, it is not a problem to devise an algorithm that makes the computer do this job. We provide a brief description of such an algorithm in the following pages. For more details, the interested reader is referred to [20, 30] and the references cited therein.

1.3 Caputo-Type FDE's

Fractional material models, the subject of this report, are systems of fractional-order differential equations (FDE's) that need to be solved in accordance with appropriate initial and boundary conditions. A FDE of the Caputo type has the form

$$D_\star^\alpha \mathbf{y}(x) = \mathbf{f}\big(x, \mathbf{y}(x)\big), \quad \alpha, x \in \mathbb{R}_+, \tag{1.9a}$$

satisfying the (possibly inhomogeneous) initial conditions

$$\mathbf{y}_{0^+}^{(k)} = D^k \mathbf{y}(0^+), \quad k = 0, 1, \ldots, \lfloor \alpha \rfloor, \tag{1.9b}$$

and whose solution is sought over an interval $[0, X]$, say, where $X \in \mathbb{R}_+$. It turns out that under some very weak conditions placed on the function $\mathbf{f}$ of the right-hand side, a unique solution to (1.9) does exist [21].

A typical feature of differential equations (both classical and fractional) is the need to specify additional conditions in order to produce a unique solution. For the case of Caputo FDE's, these additional conditions are just the static initial conditions listed in (1.9b), which are akin to those of classical ODE's, and are therefore familiar to us. In contrast, for Riemann-Liouville FDE's, these additional conditions constitute certain fractional derivatives (and/or integrals) of the unknown solution at the initial point $x = 0$ [57], which are functions of x! These initial conditions are not physical; furthermore, it is not clear how such quantities are to be measured from experiment, say, so that they can be appropriately assigned in an analysis.[‡] If for no

[‡]We explicitly note, however, the very recent paper of Podlubny [87] who attempts to give highly interesting geometrical and physical interpretations for fractional derivatives of both the Riemann-Liouville and Caputo types. These interpretations are deeply related to the questions: What precisely is time? Is it absolute or not? And can it be measured correctly and accurately, and if so, how? Thus, we are still a long way from a full understanding of the geometric and physical nature of a fractional derivative, let alone from an idea of how we can measure it in an experiment, but our mental picture of what fractional derivatives and integrals 'look like' continues to improve.

other reason, the need to solve FDE's is justification enough for choosing Caputo's definition (i.e., $D_*^\alpha = J^{\lceil\alpha\rceil-\alpha} D^{\lceil\alpha\rceil}$) for fractional differentiation over the more commonly used (at least in mathematical analysis) definition of Liouville and Riemann (viz., $D^\alpha = D^{\lceil\alpha\rceil} J^{\lceil\alpha\rceil-\alpha}$).

1.4 Numerical Approximations

1.4.1 Caputo-type Fractional Derivatives

Unlike ordinary derivatives, which are point functionals, fractional derivatives are hereditary functionals possessing a total memory of past states. A numerical algorithm for computing Caputo derivatives has been derived by Diethelm [20][§] and is listed in Alg. 1.1. Validity of its Richardson extrapolation scheme for $1 < \alpha < 2$, or one similar to it, has to date not been proven, or disproven. Here $\mathbf{y}_n$ denotes $\mathbf{y}(x_n)$, while $\mathbf{y}_N$ represents $\mathbf{y}(X)$ where $[0, X]$ is the interval of integration (fractional differentiation) with $0 \le x_n \le X$. This algorithm was arrived at by approximating the integral (1.8c) with a trapezoidal product method, thereby restricting $0 < \alpha < 2$. Similar algorithms applicable to larger ranges of α can be constructed by using the general procedure derived in Ref. [20], if they become needed.

The Grünwald-Letnikov algorithm is often used to numerically approximate the Riemann-Liouville fractional derivative (cf., e.g., with Oldham and Spanier [82, §8.2] and Podlubny [86, Chp. 7]) and it was the first algorithm to appear for approximating fractional derivatives (and integrals).

The extent of rememberance of past states exhibited by the hereditary nature of a fractional derivative is manifest, for example, in its weights of quadrature, as illustrated in Fig. 1.1. This operator exhibits a fading memory: $0.001 < |a_{8,8}| < 0.01$ for the six cases plotted in this figure. If $D\mathbf{y}(X)$ were to be approximated by a backward difference with $h = X/8$, then the effective weights of quadrature would be $a_{0,8} = 1$ and $a_{1,8} = -1$ with all remaining weights being zero, as represented by the line segments in this figure. Similarly, if $D^2\mathbf{y}(X)$ were to be approximated by a like backward-difference scheme, then $a_{0,8} = 1$, $a_{1,8} = -2$ and $a_{2,8} = 1$ with all remaining weights being zero. It is evident from the data presented in Fig. 1.1 that the weights of quadrature $a_{n,8}$ for approximating $D_*^\alpha \mathbf{y}(X)$ are compatible with those for the first- and second-order backward differences, and that fractional quadratures have additional contributions that monotonically diminish with increasing nodal number from node $n = 2$ fading all the way back to the origin at node $n = N$. This suggests that a truncation scheme may be able to be used to enhance algorithmic efficiency for some classes of functions, but not all.

[§]Apparently this algorithm first appeared in the PhD thesis of Chern [15], unbeknownst to us (KD) at the time of writing Ref. [20]. Chern used this algorithm to differentiate a Kelvin-Voigt, fractional-order, viscoelastic, material model in a finite element code. He did not address stability or uniqueness of solution issues; he did not compute error estimates; and he did not utilize an extrapolation scheme to enhance solution accuracy.

Algorithm 1.1 Computation of a Caputo fractional derivative ($0 < \alpha < 2, \alpha \neq 1$).

For interval $[0, X]$ with grid $\{x_n = nh\colon n = 0, 1, 2, \ldots, N\}$ where $h = X/N$, compute

$$D_\star^\alpha \mathbf{y}_N(h) = \frac{1}{h^\alpha \Gamma(2-\alpha)} \sum_{n=0}^{N} a_{n,N} \left(\mathbf{y}_{N-n} - \sum_{k=0}^{\lfloor \alpha \rfloor} \frac{(N-n)^k h^k}{k!} \mathbf{y}_{0+}^{(k)} \right),$$

$$D_\star^\alpha \mathbf{y}(X) = D_\star^\alpha \mathbf{y}_N(h) + O(h^{2-\alpha}),$$

using the quadrature weights (derived from a trapezoidal product rule)

$$a_{n,N} = \begin{cases} 1, & \text{if } n = 0, \\ 2^{1-\alpha} - 2, & \text{if } n = 1, \\ (n+1)^{1-\alpha} - 2n^{1-\alpha} + (n-1)^{1-\alpha}, & \text{if } 2 \leq n \leq N-1, \\ (1-\alpha)N^{-\alpha} - N^{1-\alpha} + (N-1)^{1-\alpha}, & \text{if } n = N. \end{cases}$$

Refine, if desired, using Richardson extrapolation

$$D_\star^\alpha \mathbf{y}_v^u = \left(D_\star^\alpha \mathbf{y}_{v-1}^{u-1} - 2^{r_{u-1}} D_\star^\alpha \mathbf{y}_v^{u-1} \right) / \left(1 - 2^{r_{u-1}} \right),$$

$$D_\star^\alpha \mathbf{y}(X) = D_\star^\alpha \mathbf{y}_u^u + O(h^{r_u}),$$

such that if $0 < \alpha < 1$ then r_{u-1} is assigned as

$$r_0 = 2 - \alpha,$$

$$r_1 = 2, \quad r_2 = 3 - \alpha, \quad r_3 = 4 - \alpha,$$

$$r_4 = 4, \quad r_5 = 5 - \alpha, \quad r_6 = 6 - \alpha,$$

$$r_7 = 6, \quad \cdots.$$

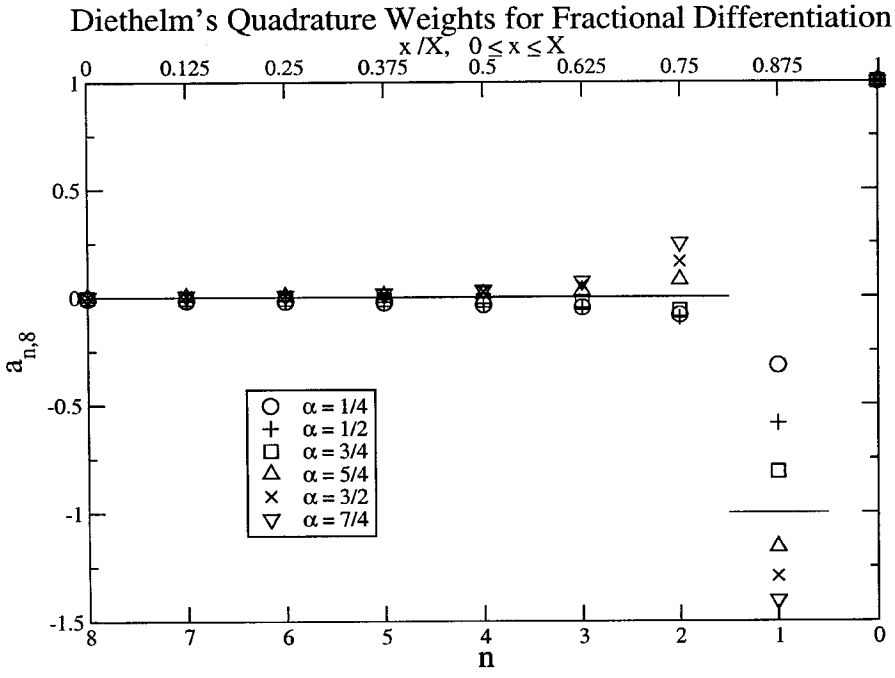

Figure 1.1: Weights of quadrature $a_{n,N}$ for approximating Caputo's fractional derivative (1.8) over interval $[0, X]$ using Diethelm's [20] Alg. 1.1, plotted here for various values of α with $N = 8$.

Richardson extrapolation

Richardson extrapolation is a technique that can often be used to increase the accuracy of results [24]. As we utilize it, this technique follows a triangular scheme—a Romberg tableau—that has the form

$$\begin{array}{cccccc} D_\star^\alpha \mathbf{y}_0^0 & & & & & \\ D_\star^\alpha \mathbf{y}_1^0 & D_\star^\alpha \mathbf{y}_1^1 & & & & \\ D_\star^\alpha \mathbf{y}_2^0 & D_\star^\alpha \mathbf{y}_2^1 & D_\star^\alpha \mathbf{y}_2^2 & & & \\ D_\star^\alpha \mathbf{y}_3^0 & D_\star^\alpha \mathbf{y}_3^1 & D_\star^\alpha \mathbf{y}_3^2 & D_\star^\alpha \mathbf{y}_3^3 & & \\ \vdots & \vdots & \vdots & \vdots & \ddots & \end{array} \tag{1.10}$$

Constructing the first column of the tableau constitutes the bulk of the computational effort. Here $D_\star^\alpha \mathbf{y}_0^0 := D_\star^\alpha \mathbf{y}_N(h)$ denotes the value of $D_\star^\alpha \mathbf{y}$ evaluated numerically at X over $[0, X]$ using an initial stepsize of h $(= X/N)$, $D_\star^\alpha \mathbf{y}_1^0 := D_\star^\alpha \mathbf{y}_N(h/2)$ is computed using the refined stepsize of $\frac{1}{2}h$ $(= X/2N)$, $D_\star^\alpha \mathbf{y}_2^0 := D_\star^\alpha \mathbf{y}_N(h/4)$ is computed using the more refined stepsize of $\frac{1}{4}h$ $(= X/4N)$, while $D_\star^\alpha \mathbf{y}_3^0 := D_\star^\alpha \mathbf{y}_N(h/8)$ is computed using the further refined stepsize of $\frac{1}{8}h$ $(= X/8N)$, etc. The remaining columns are quickly evaluated using the recursive formula listed in Alg. 1.1. The advantage of constructing this tableau is that the elements $D_\star^\alpha \mathbf{y}_v^u(X)$ in the u^{th} column converge for fixed u and increasing v towards the true value of the Caputo derivative as $O(h^{r_u})$. Hence, the further one moves to the right in the tableau the faster the column converges, and this level of convergence requires less computational effort to achieve than a direct computation of $D_\star^\alpha \mathbf{y}_N(X; \bar{h})$ when computed to a similar accuracy of $O(\bar{h}^{r_0}) \sim O(h^{r_u})$.

Step-size choice

The error analysis mentioned above is only a truncation error analysis. It assumes that the calculations are done in exact arithmetic, and it does not take into account effects like roundoff. When one needs to look at these effects too, it is possible to ask for a step size $h = X/N$ whose combined effect arising from both error sources is minimized. As we have seen above, it is likely that the truncation error decreases with the step size h, whereas roundoff tends to have the opposite behavior, so we should be looking for a sort of compromise. The considerations in this context are very similar to those for integer-order derivatives [89, §5.7]. Roughly speaking, it turns out that the roundoff error behaves as $h^{-\alpha}\epsilon_y f(\eta)$, where ϵ_y is the relative accuracy with which one can compute y, and where η designates some number within the interval $[0, X]$. Moreover, the truncation error is close to $c_\alpha h^{2-\alpha} f''(\xi)$, where c_α is some constant independent of f, and ξ is some other number also contained in the interval $[0, X]$. Consequently, an optimum step size would be of order $h \sim (\epsilon_y f(\eta)/f''(\xi))^{1/2}$ when minimizing with respect to both trucation and roundoff errors.

Unless specific information indicating the contrary is available, one may assume that f and f'' are not too irregularly behaved. Under these conditions $f(\eta) \approx f(X)$ and $f''(\eta) \approx f''(X)$, and one can then follow the suggestion of Press et al. [89, p. 187] by setting $f(X)/f''(X) \approx X$ (except near $X = 0$ where some other estimate for this

quantity should be used). This scheme provides some advice on the choice of step size if roundoff effects are considered problematic in some specific application at hand.

1.4.2 Riemann-Liouville Fractional Integrals

In the course of our work we shall not only have to approximate fractional derivatives, but also fractional integrals. As indicated above, the natural concept for the fractional integral to be used in connection with Caputo derivatives is the Riemann-Liouville integral described in (1.2). We therefore present a numerical scheme for the solution of this problem, too. The underlying idea of the algorithm, stated in a formal way in Alg. 1.2 below, is completely identical to the idea presented above for the Caputo derivative; that is, we use a product integration technique based on the trapezoidal quadrature rule. Said differently, we replace the given function $\mathbf{f}$ on the right-hand side of (1.2) by a piecewise linear interpolant, and then we calculate the resulting integral exactly. As a matter of fact, this algorithm will also be part of the scheme introduced in Alg. 1.3 in the pages that follow for the numerical solution of certain Caputo-type differential equations.

It is easily seen that the error of this algorithm is of the order $O(h^2)$ where, as above, h denotes the step size. Once again, we can improve the accuracy by adding a Richardson extrapolation procedure to the plain algorithm. The required exponents are known (cf. [52, §4]) and the resulting scheme is detailed in Alg. 1.2. Both the fundamental algorithm itself, and the Richardson extrapolation procedure, may be used for any positive value of α; there is no need to impose an upper bound on the legal range for α. This is due to the fact that the Abel (power law) kernel in the definition (1.2) of the Riemann-Liouville integral is regular, or at worst, weakly singular, and hence, integrable (at least in the improper sense) for any $\alpha > 0$. In contrast, the corresponding kernel in the definition (1.8c) of the Caputo derivative is not integrable. This kernel requires special regularization methods that are compatible with our approximation method, and as such, our scheme for approximating Caputo derivatives is only valid for $0 < \alpha < 2$, whereas, our corresponding scheme for approximating Riemann-Liouville integrals is valid for all $\alpha > 0$.

Notice the formal correspondence between Alg. 1.2 (for fractional *integration* of order α) and Alg. 1.1 (for fractional *differentiation* of order α). Except for the initial conditions that have to be taken into account additionally, the latter is simply obtained from the former by replacing the parameter α by $-\alpha$.[¶] This relates to the intuitive (but not mathematically strictly correct) interpretation of fractional differentiation and integration being inverse operations. Also notice that the index ordering is inverted between these two algorithms, which is in keeping with accepted indexing conventions. Algorithm 1.1 indexes from $x_0 = X$ to $x_N = 0$, while Alg. 1.2 indexes from $x_0 = 0$ to $x_N = X$.

A visualization of quadrature weight versus nodal index for several values of α pertaining to Alg. 1.2 is presented in Fig. 1.2. What is striking about this figure is the

[¶]Similarly, the Grünwald-Letnikov algorithm for approximating Riemann-Liouville fractional derivatives of order α also applies for approximating Riemann-Liouville fractional integrals by replacing their algorithmic parameter α with $-\alpha$ [82, §8.2].

Algorithm 1.2 Computation of a Riemann-Liouville fractional integral ($\alpha > 0$).

For interval $[0, X]$ with grid $\{x_n = nh\colon n = 0, 1, 2, \ldots, N\}$ where $h = X/N$, compute

$$J^\alpha \mathbf{y}_N(h) = \frac{h^\alpha}{\Gamma(2+\alpha)} \sum_{n=0}^{N} c_{n,N}\, \mathbf{y}_n,$$

$$J^\alpha \mathbf{y}(X) = J^\alpha \mathbf{y}_N(h) + O(h^2),$$

using the quadrature weights (derived from a trapezoidal product rule)

$$c_{n,N} = \begin{cases} (1+\alpha)N^\alpha - N^{1+\alpha} + (N-1)^{1+\alpha}, & \text{if } n = 0, \\ (N-n+1)^{1+\alpha} - 2(N-n)^{1+\alpha} + (N-n-1)^{1+\alpha}, & \text{if } 0 < n < N, \\ 1, & \text{if } n = N. \end{cases}$$

Refine, if desired, using Richardson extrapolation

$$J^\alpha \mathbf{y}_v^u = \left(J^\alpha \mathbf{y}_{v-1}^{u-1} - 2^{r_{u-1}}\, J^\alpha \mathbf{y}_v^{u-1} \right) / \left(1 - 2^{r_{u-1}} \right),$$

$$J^\alpha \mathbf{y}(X) = J^\alpha \mathbf{y}_u^u + O(h^{r_u}),$$

such that if $0 < \alpha < 1$ then r_{u-1} is assigned as

$$r_0 = 2, \quad r_1 = 2 + \alpha,$$
$$r_2 = 3, \quad r_3 = 3 + \alpha,$$
$$r_4 = 4, \quad r_5 = 4 + \alpha,$$
$$r_6 = 5, \quad \cdots.$$

Note: Whenever $\alpha > 1$, the same values appear in the sequence $r_0, r_1, r_2, \ldots$, but they now have to be ordered in a different way to keep the sequence monotonic. (For example, if $1 < \alpha < 2$ then we have $r_0 = 2, r_1 = 3, r_2 = 2 + \alpha, r_3 = 4, r_4 = 3 + \alpha, \ldots$).

obvious difference between domains $0 < \alpha < 1$ and $1 < \alpha < 2$. Whenever $\alpha = 1$, the algorithm reduces to classic trapezoidal integration. Whenever $0 < \alpha < 1$, the earlier states will contribute less to the overall solution than will the more recent states, but they do not entirely fade out. Fractional integration exhibits long-term memory loss when $0 < \alpha < 1$ but, unlike fractional differentiation, fractional integration does not experience a total loss (or fading away) of past memories. Also, the smaller the value of α (i.e., the closer it is to zero) the greater the degree of long-term memory loss will be. In contrast, whenever $1 < \alpha < 2$, the earlier states will contribute more to the overall solution than will the more recent states. Fractional integration therefore exhibits short-term memory loss when $1 < \alpha < 2$. This is like an elderly person who remembers in vivid detail what happened years ago, but who cannot recall what took place yesterday. Furthermore, the greater the value of α (i.e., the closer it is to two) the more pronounced the short-term memory loss will be.

The line segments displayed in Fig. 1.2 represent averaged and normalized weights of quadrature over each subinterval. The actual nodal weights, $c_{n,N}$, are often observed to be non-monotonic at either of the two nodal endpoints. In this integration scheme there are $N + 1$ nodal weights that apply to N subintervals, but there should be exactly one weight per subinterval. So how the algorithm works (internally, and roughly speaking) is to average these weights in a trapezoidal fashion, as outlined in Table 1.1. In other words, the inner weights are divided into two equal halves with each half going to one of the two adjoining subintervals. In addition to averaging, the displayed line segments have been normalized to the interval $[0, 1]$. Normalizing allows

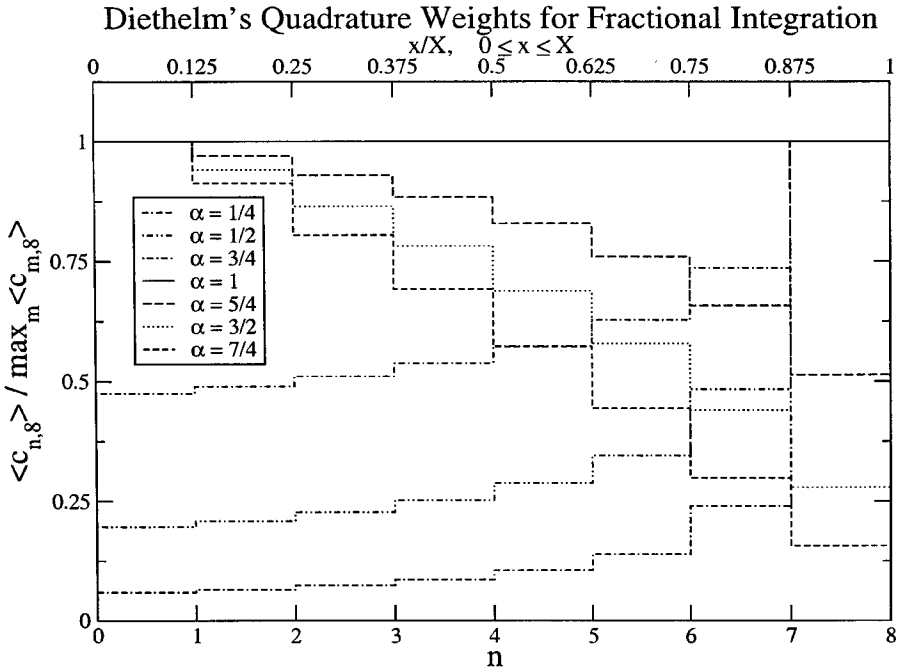

Figure 1.2: Effective weights of quadrature $\langle c_{n,N} \rangle$ for approximating the Riemann-Liouville fractional integral (1.2) over interval $[0, X]$ using Alg. 1.2, plotted here for various values of α with $N = 8$.

Subinterval	Averaged Quadrature Weight $\langle c_{n,N} \rangle$
$[0, X/N]$	$\langle c_{0,N} \rangle = c_{0,N} + \frac{1}{2}\, c_{1,N}$
$[nX/N, (n+1)X/N]$	$\langle c_{n,N} \rangle = \frac{1}{2}\big(c_{n,N} + c_{n+1,N}\big), \qquad (n = 1, 2, \ldots, N-2)$
$[(N-1)X/N, X]$	$\langle c_{N-1,N} \rangle = \frac{1}{2}\, c_{N-1,N} + c_{N,N}$

Table 1.1: Averaging procedure used to compute effective weights of quadrature for approximating Riemann-Liouville integration as they relate to Alg. 1.2.

one to discern the influence of α on quadrature in a meaningful way. The outcome is an averaged and normalized quadrature weighting that is monotonic in the nodal index number, as demonstrated by the line segments in Fig. 1.2, where there is a monotonic increase (decrease) in the effective weight of quadrature, $\langle c_{n,N} \rangle \,/\, \max_m \langle c_{m,N} \rangle$, with increasing nodal index number for $0 < \alpha < 1$ ($1 < \alpha < 2$).

1.4.3 Caputo-Type FDE's

A numerical algorithm that solves Caputo-type FDE's has been derived by Diethelm et al. [23] and is listed in Alg. 1.3. A thorough analysis of its algorithmic error is given in [22]. This algorithm is of the PECE (Predict-Evaluate-Correct-Evaluate) type. Other numerical algorithms exist that solve FDE's (e.g., Gorenflo [44] and Podlubny

Algorithm 1.3 Computation of a Caputo FDE ($0 < \alpha < 2$, $\alpha \neq 1$).

For interval $[0, X]$ with grid $\{x_n = nh\colon n = 0, 1, 2, \ldots, N\colon h = X/N\}$, *predict* with

$$\mathbf{y}_N^P(h) = \sum_{k=0}^{\lfloor \alpha \rfloor} \frac{X^k}{k!}\, \mathbf{y}_{0+}^{(k)} + \frac{h^\alpha}{\Gamma(1+\alpha)} \sum_{n=0}^{N-1} b_{n,N}\, \mathbf{f}(x_n, \mathbf{y}_n),$$

using the quadrature weights (derived from a rectangular product rule)

$$b_{n,N} = (N-n)^\alpha - (N-n-1)^\alpha,$$

and *evaluate* $\mathbf{f}(X, \mathbf{y}_N^P)$, then *correct* with

$$\mathbf{y}_N(h) = \sum_{k=0}^{\lfloor \alpha \rfloor} \frac{X^k}{k!}\, \mathbf{y}_{0+}^{(k)} + \frac{h^\alpha}{\Gamma(2+\alpha)} \left(\sum_{n=0}^{N-1} c_{n,N}\, \mathbf{f}(x_n, \mathbf{y}_n) + c_{N,N}\, \mathbf{f}(X, \mathbf{y}_N^P) \right),$$

$$\mathbf{y}(X) = \mathbf{y}_N(h) + O\big(h^{\min(1+\alpha, 2)}\big),$$

using the quadrature weights (derived from a trapezoidal product rule)

$$c_{n,N} = \begin{cases} (1+\alpha)N^\alpha - N^{1+\alpha} + (N-1)^{1+\alpha}, & \text{if } n = 0, \\ (N-n+1)^{1+\alpha} - 2(N-n)^{1+\alpha} + (N-n-1)^{1+\alpha}, & \text{if } 0 < n < N, \\ 1, & \text{if } n = N, \end{cases}$$

and finally re-*evaluate* $\mathbf{f}(X, \mathbf{y}_N)$ saving it as $\mathbf{f}(x_N, \mathbf{y}_N)$.

Refine, if desired, using Richardson extrapolation

$$\mathbf{y}_v^u = \left(\mathbf{y}_{v-1}^{u-1} - 2^{r_{u-1}}\, \mathbf{y}_v^{u-1} \right) / \left(1 - 2^{r_{u-1}} \right),$$

$$\mathbf{y}(X) = \mathbf{y}_u^u + O(h^{r_u}),$$

such that whenever $0 < \alpha < 1$ the exponent r_{u-1} is assigned as

$$r_0 = 1+\alpha,$$
$$r_1 = 2, \quad r_2 = 2+\alpha, \quad r_3 = 3+\alpha,$$
$$r_4 = 4, \quad r_5 = 4+\alpha, \quad r_6 = 5+\alpha,$$
$$r_7 = 6, \quad \cdots,$$

or whenever $1 < \alpha < 2$ it is assigned as

$$r_0 = 2, \quad r_1 = 1+\alpha, \quad r_2 = 2+\alpha,$$
$$r_3 = 4, \quad r_4 = 3+\alpha, \quad r_5 = 4+\alpha,$$
$$r_6 = 6, \quad \cdots.$$

[86, Chp. 8]), but they focus on solving Riemann-Liouville FDE's and usually restrict the class of FDE's to be linear with homogeneous initial conditions. Algorithm 1.3 solves non-linear Caputo FDE's with inhomogeneous initial conditions, if required.

The restriction that $\alpha \neq 1$ in this algorithm is purely for formal reasons. If $\alpha = 1$, then we can still implement the algorithm exactly in the indicated way. It must be noted, however, that it then is the limit case of an algorithm for *fractional* differential equations, and these equations involve *non-local* differential operators. Thus, the resulting scheme is non-local, too. In contrast, a method constructed for a first-order equation will, in practice, always make explicit use of the *local* structure of such an equation to save memory and computing time. Therefore, the case $\alpha = 1$ of our algorithm will never be a competitive alternative to the usual methods for first-order equations. In particular, our algorithm is distinct from the algorithm known as the second-order Adams-Bashforth-Moulton technique for first-order problems when $\alpha = 1$.

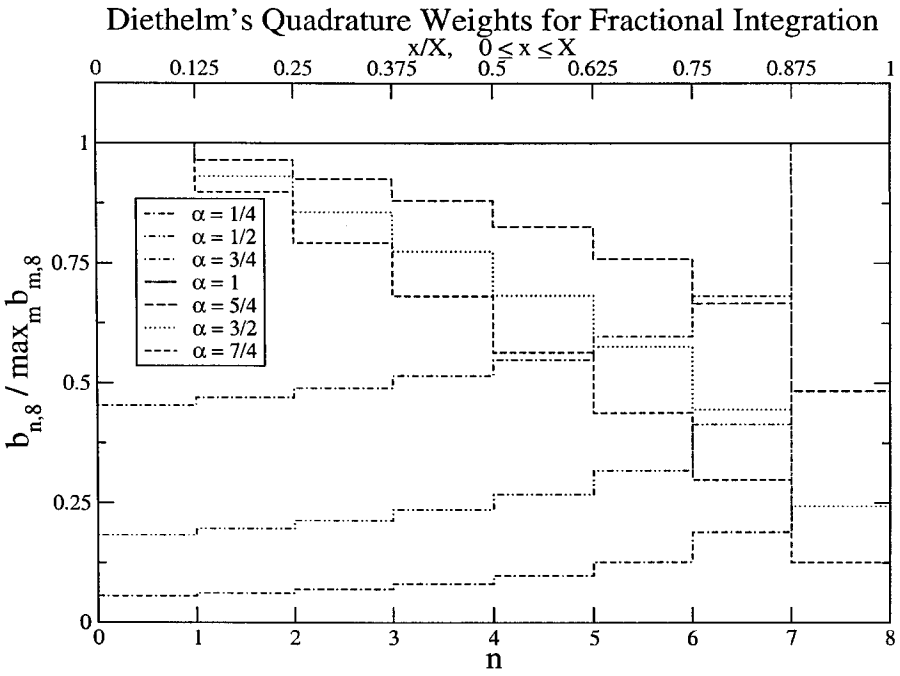

Figure 1.3: Normalized weights of quadrature $b_{n,N}$ for the predictor that approximates Caputo FDE's (1.9) over interval $[0, X]$ when using Diethelm et al.'s [23] Alg. 1.3, plotted here for various values of α with $N = 8$.

Illustrations of quadrature weight versus nodal index for several values of α, as they pertain to the PECE method of Alg. 1.3, are presented in Figs. 1.2 & 1.3 with the former figure pertaining to the corrector and the latter pertaining to the predictor. FDE's, like fractional integrals, exhibit long-term memory loss when $0 < \alpha < 1$, no memory loss when $\alpha = 1$, and short-term memory loss when $1 < \alpha < 2$.

Unlike the $\langle c_{n,N} \rangle$ in Fig. 1.2, where the $N + 1$ quadrature weights are averaged at the beginning and end of each subinterval in order to get N effective weights for N subintervals, the $b_{n,N}$ in Fig. 1.3 are fixed to the beginning of each of the N subintervals, and as such, do not require any 'effective averaging' to take place. This is a consequence of the $b_{n,N}$ quadrature weights belonging to an explicit integrator, while the $c_{n,N}$ weights belong to an implicit integrator. Contrasting Figs. 1.2 & 1.3, there is little difference between the $b_{n,N}$ and $\langle c_{n,N} \rangle$ curves, indicating that there is a much stronger influence of α on the weights of quadrature than there is on the order of accuracy (e.g., $O(h^{\min(2,1+\alpha)})$) that a particular integration scheme provides.

Differential equations of fractional order have found recent applications in a variety of fields in science and engineering (e.g., see references in [57, 86]): chemical kinetics theory, electromagnetic theory, transport (diffusion) theory, fractal theory, control theory, electronic circuit theory, porous media, etc. One of the first applications of the fractional calculus was viscoelasticity, which is the primary focus of this work.

Efficient approximations

Ford and Simpson [35] have extended Alg. 1.3, which possesses $O(n)$ operation counts at each stage and $O(n^2)$ overall, to a more efficient scheme with $O(n \log n)$ counts overall, while retaining the accuracy of the method.

1.5 Mittag-Leffler Function

The (generalized) Mittag-Leffler function $E_{\alpha,\beta}(z)$ is an entire function (in $z \in \mathbb{C}$) of order $1/\alpha$ that is defined by the power series [31, §18.1]

$$E_{\alpha,\beta}(z) = \sum_{k=0}^{\infty} \frac{z^k}{\Gamma(\beta + \alpha k)}, \quad \alpha \in \mathbb{R}^+, \ \beta \in \mathbb{R}, \ z \in \mathbb{C}, \tag{1.11}$$

with $E_\alpha(x) = E_{\alpha,1}(x)$ being the original function studied by Mittag-Leffler [79]. This function plays the same role in differential equations of fractional order as the exponential function e^z plays in ordinary differential equations; in fact, $E_{1,1}(z) = e^z$.

A special form of the Mittag-Leffler function,

$$G(t-t') := E_{\alpha,1}\Big(-\big((t-t')/\tau\big)^\alpha\Big), \quad 0 < \alpha < 1, \quad 0 < \tau, \quad 0 \le t' \le t,$$

and its derivative,

$$M(t-t') := \frac{\partial G(t-t')}{\partial t'} = \frac{-1}{t-t'} E_{\alpha,0}\Big(-\big((t-t')/\tau\big)^\alpha\Big),$$

appear in FOV, which is the subject of much of this report.

We now present some important properties of the Mittag-Leffler function, and a numerical algorithm for its rigorous solution, both of which are useful when considering differential equations of fractional order.

1.5.1 Analytical Properties

In spite of the fact that in applications to differential equations of fractional order where the Mittag-Leffler function is typically restricted to the real line, we still need to give some of its properties in the complex plane. The main reason for this is that the numerical algorithm we present in the next sub-section consists of two parts: the first part gives a numerical value for the Mittag-Leffler function with $\alpha \le 1$, while the second one uses, for $\alpha > 1$, some special formulæ that reduce this case to the previous one. These special formulæ are defined over the complex plane and are given by

$$E_{\alpha,\beta}(z) = \frac{1}{2m+1} \sum_{h=-m}^{m} E_{\alpha/(2m+1),\beta}\big(z^{1/(2m+1)} e^{2i\pi h/(2m+1)}\big), \ m = 0, 1, 2, \ldots, \tag{1.12a}$$

and

$$E_{\alpha,\beta}(z) = \frac{1}{m} \sum_{h=0}^{m-1} E_{\alpha/m,\beta}\big(z^{1/m} e^{2i\pi h/m}\big), \ m = 1, 2, \ldots, \tag{1.12b}$$

where i $(:= \sqrt{-1})$ is the imaginary unit number. Obviously, if $\alpha > 1$, and even if z is a real number, we still need to evaluate the numerical values of the Mittag-Leffler function with, in general, a complex argument (and $\alpha \leq 1$).

First, we present some important integral representations of the Mittag-Leffler function. Let us denote by $\gamma(\epsilon;\varphi)$ $(\epsilon > 0,\ 0 < \varphi \leq \pi)$ a contour in the complex λ-plane with non-decreasing $\arg\lambda$ consisting of the following parts:

1) the ray $\arg\lambda = -\varphi,\ |\lambda| \geq \epsilon$;

2) the arc $-\varphi \leq \arg\lambda \leq \varphi$ from the circumference $|\lambda| = \epsilon$;

3) the ray $\arg\lambda = \varphi,\ |\lambda| \geq \epsilon$.

In the case where $0 < \varphi < \pi$, the complex λ-plane is divided into two unbounded parts by the contour $\gamma(\epsilon;\varphi)$: domain $G^{(-)}(\epsilon;\varphi)$ is to the left of the contour, while domain $G^{(+)}(\epsilon;\varphi)$ is to its right. If $\varphi = \pi$, the contour $\gamma(\epsilon;\varphi)$ consists of the circumference $|\lambda| = \epsilon$ and the cut $-\infty < \lambda \leq -\epsilon$. In this case, domain $G^{(-)}(\epsilon;\varphi)$ becomes the circle $|\lambda| < \epsilon$, while domain $G^{(+)}(\epsilon;\varphi)$ becomes the region $\{\lambda : |\arg\lambda| < \pi,\ |\lambda| > \epsilon\}$.

Let $0 < \alpha < 2$, let β be an arbitrary (real or complex) number, and let a non-negative number φ be chosen such that

$$\frac{\alpha\pi}{2} < \varphi \leq \min\{\pi, \alpha\pi\}. \tag{1.13}$$

Then we have the following integral representations for the Mittag-Leffler function:

$$E_{\alpha,\beta}(z) = \frac{1}{2\pi i\alpha}\int_{\gamma(\epsilon;\varphi)} \frac{e^{\lambda^{1/\alpha}}\lambda^{(1-\beta)/\alpha}}{\lambda - z}\,d\lambda,\ z \in G^{(-)}(\epsilon;\varphi), \tag{1.14a}$$

and

$$E_{\alpha,\beta}(z) = \frac{z^{(1-\beta)/\alpha}e^{z^{1/\alpha}}}{\alpha} + \frac{1}{2\pi i\alpha}\int_{\gamma(\epsilon;\varphi)} \frac{e^{\lambda^{1/\alpha}}\lambda^{(1-\beta)/\alpha}}{\lambda - z}\,d\lambda,\ z \in G^{(+)}(\epsilon;\varphi). \tag{1.14b}$$

If β is a real number, as assigned in (1.11), then the formulæ of (1.14) can be rewritten in forms that are more suitable for numerical evaluation (see Gorenflo et al. [45]). In particular, if $0 < \alpha \leq 1,\ \beta \in \mathbb{R},\ |\arg z| > \alpha\pi, z \neq 0$, then

$$E_{\alpha,\beta}(z) = \int_{\epsilon}^{\infty} K(\alpha,\beta,\chi,z)\,d\chi + \int_{-\alpha\pi}^{\alpha\pi} P(\alpha,\beta,\epsilon,\varphi,z)\,d\varphi,\ \epsilon > 0,\ \beta \in \mathbb{R}, \tag{1.15a}$$

$$E_{\alpha,\beta}(z) = \int_{0}^{\infty} K(\alpha,\beta,\chi,z)\,d\chi,\ \text{if } \beta < 1 + \alpha, \tag{1.15b}$$

$$E_{\alpha,\beta}(z) = -\frac{\sin(\alpha\pi)}{\alpha\pi}\int_{0}^{\infty} \frac{e^{-\chi^{1/\alpha}}}{\chi^2 - 2\chi z\cos(\alpha\pi) + z^2}\,d\chi - \frac{1}{z},\ \text{if } \beta = 1 + \alpha, \tag{1.15c}$$

where

$$K(\alpha,\beta,\chi,z) = \frac{\chi^{(1-\beta)/\alpha}e^{-\chi^{1/\alpha}}}{\alpha\pi}\,\frac{\chi\sin\big(\pi(1-\beta)\big) - z\sin\big(\pi(1-\beta+\alpha)\big)}{\chi^2 - 2\chi z\cos(\alpha\pi) + z^2},$$

$$P(\alpha,\beta,\epsilon,\varphi,z) = \frac{\epsilon^{1+(1-\beta)/\alpha}}{2\alpha\pi}\,\frac{e^{\epsilon^{1/\alpha}\cos(\varphi/\alpha)}\big(\cos(\omega) + i\sin(\omega)\big)}{\epsilon e^{i\varphi} - z},$$

$$\omega = \epsilon^{1/\alpha} \sin(\varphi/\alpha) + \varphi(1 + (1-\beta)/\alpha).$$

The representations in (1.15), and similar formulæ for the cases $|\arg z| = \alpha\pi$ and $|\arg z| < \alpha\pi$ presented in Gorenflo et al. [45], are an essential part of the numerical algorithm listed in the next sub-section.

Using the integral representations in (1.14), it is not too difficult to get asymptotic expansions for the Mittag-Leffler function in the complex plane. Let $\alpha < 2$, β be an arbitrary number, and φ be choosen to satisfy the condition (1.13). Then we have, for any $p \in \mathbb{N}$ and $|z| \to \infty$:

1) Whenever $|\arg z| \leq \varphi$,

$$E_{\alpha,\beta}(z) = \frac{z^{(1-\beta)/\alpha} e^{z^{1/\alpha}}}{\alpha} - \sum_{k=1}^{p} \frac{z^{-k}}{\Gamma(\beta - \alpha k)} + O\big(|z|^{-1-p}\big). \tag{1.16a}$$

2) Whenever $\varphi \leq |\arg z| \leq \pi$,

$$E_{\alpha,\beta}(z) = -\sum_{k=1}^{p} \frac{z^{-k}}{\Gamma(\beta - \alpha k)} + O\big(|z|^{-1-p}\big). \tag{1.16b}$$

These formulæ are also used in our numerical algorithm.

Thorough discussions of properties of the Mittag-Leffler function can be found, for example, in Refs. [31, 76, 86].

1.5.2 Numerical Algorithms

Robust

The numerical scheme listed in Alg. 1.4 for computing the general Mittag-Leffler function $E_{\alpha,\beta}(z)$ is taken from an obscure paper written by Gorenflo et al. [45]. Their algorithm uses the defining series (Eqn. 1.11) for arguments of small magnitude, its asymptotic representation (Eqn. 1.16) for arguments of large magnitude, and special integral representations (the formulæ in (1.15) for the case where $|\arg z| > \alpha\pi$, and similar representations for the cases $|\arg z| = \alpha\pi$ and $|\arg z| < \alpha\pi$) for intermediate values of the argument that include a monotonic part $\int K(\alpha, \beta, \chi, z)\, d\chi$ and an oscillatory part $\int P(\alpha, \beta, \epsilon, \phi, z)\, d\phi$, which can themselves be evaluated using standard techniques (cf. App. B).

Efficient

Algorithm 1.4 can produce a numerical result to any desired level of accuracy, but these computations are expensive and therefore their use in a finite element setting, for example, is prohibative. To meet this need, we have constructed a table of Padé approximates for $E_\alpha(-x^\alpha)$ in App. C for $x \geq 0$ and $\alpha \in \{0.01, 0.02, 0.03, \ldots, 0.98, 0.99\}$. As we shall see in the next chapter, this form of the Mittag-Leffler function arises in many fractional-order, viscoelastic, material models, including those of interest to us.

Another algorithm for solving the Mittag-Leffler function $E_\alpha(x)$ ($0.02 < \alpha < 0.98$ with a reported relative error that is less than 1.6×10^{-5}) has been published by Welch et al. [109].

Algorithm 1.4 Computation of the Mittag-Leffler function.

GIVEN $\alpha > 0$, $\beta \in \mathbb{R}$, $z \in \mathbb{C}$ THEN
IF $z = 0$ THEN
$E_{\alpha,\beta}(z) = \frac{1}{\Gamma(\beta)}$
ELSIF $|z| < 1$ THEN
$k_0 = \max\{\lceil {}^{(1-\beta)}/_{\alpha} \rceil, \lceil \ln[\varepsilon_m(1-|z|)] / \ln(|z|) \rceil\}$
$E_{\alpha,\beta}(z) = \sum_{k=0}^{k_0} \frac{z^k}{\Gamma(\beta+\alpha k)} + O(\varepsilon_m)$
ELSIF $|z| > \lfloor 10 + 5\alpha \rfloor$ THEN
$k_0 = \lfloor -\ln(\varepsilon_m) / \ln(|z|) \rfloor$
IF $|\arg z| < {}^{\alpha\pi}/_4 + {}^1/_2 \min\{\pi, \alpha\pi\}$ THEN
$E_{\alpha,\beta}(z) = \frac{1}{\alpha} z^{(1-\beta)/\alpha} e^{z^{1/\alpha}} - \sum_{k=1}^{k_0} \frac{z^{-k}}{\Gamma(\beta-\alpha k)} + O(\varepsilon_m)$
ELSE
$E_{\alpha,\beta}(z) = -\sum_{k=1}^{k_0} \frac{z^{-k}}{\Gamma(\beta-\alpha k)} + O(\varepsilon_m)$
ELSIF $\alpha \leq 1$ THEN
$\chi_0 = \begin{cases} \max\{1, 2|z|, (-\ln({}^{\pi\varepsilon_m}/_6))^{\alpha}\}, & \beta \geq 0 \\ \max\{(|\beta|+1)^{\alpha}, 2|z|, (-2\ln({}^{\pi\varepsilon_m}/_{[6(|\beta|+2)(2|\beta|)^{|\beta|}]}))^{\alpha}\}, & \beta < 0 \end{cases}$
$K(\alpha,\beta,\chi,z) = \frac{1}{\alpha\pi} \chi^{(1-\beta)/\alpha} \exp(-\chi^{1/\alpha}) \frac{\chi \sin[\pi(1-\beta)] - z\sin[\pi(1-\beta+\alpha)]}{\chi^2 - 2\chi z \cos(\alpha\pi) + z^2}$
$P(\alpha,\beta,\epsilon,\phi,z) = \frac{1}{2\alpha\pi} \epsilon^{1+(1-\beta)/\alpha} \exp(\epsilon^{1/\alpha}\cos({}^{\phi}/_{\alpha})) \frac{\cos(\omega) + i\sin(\omega)}{\epsilon\exp(i\phi) - z}$
$\omega = \phi(1 + {}^{(1-\beta)}/_{\alpha}) + \epsilon^{1/\alpha}\sin({}^{\phi}/_{\alpha})$
IF $|\arg z| > \alpha\pi$ THEN
IF $\beta \leq 1$ THEN
$E_{\alpha,\beta}(z) = \int_0^{\chi_0} K(\alpha,\beta,\chi,z)\, d\chi + O(\varepsilon_m)$
ELSE
$E_{\alpha,\beta}(z) = \int_1^{\chi_0} K(\alpha,\beta,\chi,z)\, d\chi + \int_{-\alpha\pi}^{\alpha\pi} P(\alpha,\beta,1,\phi,z)\, d\phi + O(\varepsilon_m)$
ELSIF $|\arg z| < \alpha\pi$ THEN
IF $\beta \leq 1$ THEN
$E_{\alpha,\beta}(z) = \int_0^{\chi_0} K(\alpha,\beta,\chi,z)\, d\chi + \frac{1}{\alpha} z^{(1-\beta)/\alpha} e^{z^{1/\alpha}} + O(\varepsilon_m)$
ELSE
$E_{\alpha,\beta}(z) = \int_{|z|/2}^{\chi_0} K(\alpha,\beta,\chi,z)\, d\chi + \int_{-\alpha\pi}^{\alpha\pi} P(\alpha,\beta,{}^{|z|}/_2,\phi,z)\, d\phi + \frac{1}{\alpha} z^{(1-\beta)/\alpha} e^{z^{1/\alpha}} + O(\varepsilon_m)$
ELSE
$E_{\alpha,\beta}(z) = \int_{(|z|+1)/2}^{\chi_0} K(\alpha,\beta,\chi,z)\, d\chi + \int_{-\alpha\pi}^{\alpha\pi} P(\alpha,\beta,{}^{(|z|+1)}/_2,\phi,z)\, d\phi + O(\varepsilon_m)$
ELSIF $1 < \alpha < 2$ THEN
$E_{\alpha,\beta}(z) = E_{\alpha/2,\beta}(z^{1/2}) + E_{\alpha/2,\beta}(-z^{1/2})$
ELSE
$k_0 = \lfloor {}^{\alpha}/_2 \rfloor + 1$
$E_{\alpha,\beta}(z) = \frac{1}{k_0} \sum_{k=0}^{k_0-1} E_{\alpha/k_0,\beta}(z^{1/k_0} \exp({}^{2\pi i k}/_{k_0}))$
END
Parameter ε_m denotes machine epsilon (precision).

Chapter 2

1D FOV

In the 1940's, Scott Blair [8] and Gerasimov [42] independently proposed a material model bounded between a Hookean solid ($\alpha = 0$) and a Newtonian fluid ($\alpha = 1$). Their relationship—a fractional Newton model—can be written as $\sigma(t) = \mu\tau^{\alpha} D_{\star}^{\alpha}\varepsilon(t)$, where σ and ε denote stress and strain, respectively, which are considered here to be causal functions of time t. The coefficient $\mu\tau$ (> 0) represents a single material constant (a generalized viscosity: μ has units of stress, while τ has units of time), and exponent α ($0 < \alpha \leq 1$) can be considered as a second material constant. Experimental results motivated Scott Blair's model development. Mathematics, on the other hand, motivated Gerasimov who was the first to consider an Abel kernel for the relaxation modulus in Boltzmann's general theory of viscoelasticity.

Bagley and Torvik [4] demonstrated that the molecular theory of Rouse (for dilute solutions of *non-crosslinked* polymer molecules residing in Newtonian solvents) has a polymer contribution to stress that corresponds to a fractional Newton element whose order of evolution is a half (i.e., $\alpha = 1/2$). They also state (without proof) that the molecular theory of Zimm (for dilute solutions of *crosslinked* polymer molecules residing in Newtonian solvents) has a polymer contribution to stress that corresponds to a fractional Newton element whose order of evolution is two thirds (i.e., $\alpha = 2/3$).

Gemant [38] was the first to propose a fractional viscoelastic model. He extended the notion of a Maxwell fluid by replacing its first-order derivative on stress with the semi-derivative, and in doing so, he proposed that $\left[1 + \sqrt{\eta/\mu} D_{\star}^{1/2}\right]\sigma(t) = \eta D\varepsilon(t)$, where μ (> 0) and η (> 0) are material constants. The fractional Maxwell fluid, which is a spring in series with a fractional Newton element, actually has the form

$$\left[1 + \tau^{\alpha} D_{\star}^{\alpha}\right]\sigma(t) = \eta\tau^{\alpha-1} D_{\star}^{\alpha}\varepsilon(t), \quad \sigma_{0+} = \frac{\eta}{\tau}\varepsilon_{0+}, \tag{2.1}$$

where η (> 0) is the viscosity, τ (> 0) is the characteristic relaxation time, and exponent α ($0 < \alpha \leq 1$) is the fractal order of evolution, which is taken to be the same for both stress and strain, while σ_{0+} and ε_{0+} are the initial states of stress and strain at time $t = 0^{+}$, thereby allowing for an inhomogeneous initial state of finite stress—a characteristic that Gemant's model does not possess. The fractional Maxwell fluid was first discussed in the manuscript of Caputo and Mainardi [13] as a special case to their material model (Eqn. 2.2 below). We refer to (2.1) as the *standard FOV fluid* in 1D.

Caputo [12] introduced a fractional Voigt solid $\sigma(t) = \mu[1 + \rho^\alpha D^\alpha_\star]\varepsilon(t)$ to model the nearly rate-insensitive dynamic response of Earth's crust over large ranges in frequency when excited by earthquakes. Here μ (> 0), ρ (> 0) and α $(0 < \alpha \leq 1)$ are the material constants. As a mechanical model, this is a spring in parallel with a fractional Newton element. A more appropriate representation of solid behavior is the fractional Kelvin model, which is a spring in parallel with a fractional Maxwell element. This material model was introduced by Caputo and Mainardi [13] and has the form

$$\left[1 + \tau^\alpha D^\alpha_\star\right]\sigma(t) = \mu\left[1 + \rho^\alpha D^\alpha_\star\right]\varepsilon(t), \quad \sigma_{0+} = \mu\left(\frac{\rho}{\tau}\right)^\alpha \varepsilon_{0+}, \tag{2.2}$$

where μ (> 0) is the rubbery modulus, $\mu(\rho/\tau)^\alpha$ $(> \mu)$ is the glassy modulus, τ (> 0) is the characteristic relaxation time, ρ $(> \tau)$ is the characteristic retardation time, and exponent α $(0 < \alpha \leq 1)$ is the fractal order of evolution. This model, unlike Caputo's original model, allows for an inhomogeneous initial state of finite stress. Bagley and Torvik [5] have shown that the fractal orders of evolution in stress and strain must be the same, as written in (2.2), and as originally proposed by Caputo and Mainardi, in order for this constitutive realationship to be compatible with the second law of thermodynamics; specifically, in order to guarantee a non-negative dissipation whenever a cyclic loading history is imposed on the material. We refer to (2.2) as the *standard FOV solid* in 1D, in the spirit of Zener [111, pg. 43] referring to Kelvin's model $[1 + \tau D]\sigma(t) = \mu[1 + \rho D]\varepsilon(t)$ as the "standard linear solid".

The initial conditions present in (2.1 & 2.2) come about by taking the Laplace transform* of these constitutive formulæ. What one learns from these transformations is that if the material model is to be physically admissible, in the sense that it propagates a wave front at finite speed, then that part of the transformation which pertains to the initial state must be independent of the Laplace transform variable s in the frequency domain, or it must have like dependencies on both sides of the equation

---

*The Laplace transform $\tilde{f}(s)$ of function $f(t)$ is given by the mapping procedure $f(t) \div \tilde{f}(s) = \int_0^\infty \exp(-s\tau)\, f(\tau)\, d\tau$, where $\div$ denotes the juxtaposition of function $f(t)$ with its Laplace transform $\tilde{f}(s)$. In fractional-order viscoelasticity, the Laplace transform pairs

$$D^\alpha_\star f(t) \div s^\alpha \tilde{f}(s) - \sum_{k=0}^{\lfloor\alpha\rfloor} s^{\alpha-k-1} f^{(k)}_{0+}, \quad \frac{t^{n-1}}{\Gamma(n)} \div \frac{1}{s^n} \quad \text{and} \quad t^{\beta-1} E_{\alpha,\beta}(\pm a t^\alpha) \div \frac{s^{\alpha-\beta}}{s^\alpha \mp a}$$

have particular significance, where $\alpha, a, n, t \in \mathbb{R}_+$, $\beta \in \mathbb{R}$ and $E_{\alpha,\beta}(t) = \sum_{k=0}^\infty t^k/\Gamma(\beta + \alpha k)$ is the general Mittag-Leffler function, which plays a role in FDE's like that which the exponential function plays in ODE's; in fact, $E_{1,1}(t) = e^t$.

The above formulæ are analytic continuations of the well known Laplace transform pairs

$$D^m f(t) \div s^m \tilde{f}(s) - \sum_{k=0}^{m-1} s^{m-k-1} f^{(k)}_{0+}, \quad \frac{t^{m-1}}{(m-1)!} \div \frac{1}{s^m} \quad \text{and} \quad e^{\pm at} \div \frac{1}{s \mp a},$$

where $m \in \mathbb{N}$ and $a, t \in \mathbb{R}_+$. In contrast to the Laplace transform of Caputo's deriviative, which contains a sum of *integer-order* derivatives of the initial state, the Laplace transform of the Riemann-Liouville derivative contains a sum of *fractional-order* derivatives of the initial state, making the initialization of Riemann-Liouville based differential equations a difficult task, but not an impossible one [73].

that then cancel out in the initial state. Having derivatives of equal order on both sides of the equation, as in the standard FOV fluid and solid material models, is one way to ensure that this physical constraint is adhered to. In the aerodynamics literature, this process of addressing the initial state for consistency of initial condition in the frequency domain is known as the method of shocks, which was introduced into the FOV literature by Bagley and Calico [3]. Another very important reason to restrict the class of admissible material models to only include those that propagate waves at finite speeds has to do with stability. Material models that predict infinite wave speeds will become mathematically unstable at some critical finite velocity [65].

One objective of this paper is to derive 3D versions of the standard, FOV, fluid and solid, material models without imposing any constraints as to the magnitude of deformation. To the best of our knowledge, Drozdov [27] is the only person to have extended linear, fractional-order, viscoelastic formulations into 3D formulæ applicable to non-linear mechanics where finite strains are present. Specifically, he extended the following 1D models: $\left[1 + (\eta/\mu)^{\alpha} D_{\star}^{\alpha}\right]\sigma(t) = \eta D\varepsilon(t)$, which is a generalization of Gemant's [38] fractional Maxwell model, and $\sigma(t) = \mu[1 + \rho^{\alpha} D_{\star}^{\alpha}]\varepsilon(t)$, which is Caputo's [12] fractional Voigt model. In Chps. 7–??, we introduce 3D versions for the standard FOV fluid and the standard FOV solid, which are presented here in 1D in Eqns. (2.1 & 2.2).

2.1 Material Functions

The parameterization procedures that follow assume infinitesimal strains in homogeneous 1D deformations.

Boltzmann's [9] linear theory of viscoelasticity, which includes the standard FOV models of (2.1 & 2.2), can be expressed as an integral equation with a hereditary kernel that convolves with a change in the independent state variable according to the convolution rules of either Stieltjes or Riemann. Whenever stress responds to strain, this theory can be expressed in terms of a (relaxation) modulus $G(t)$ where [16, pp. 3–9]

$$\sigma(t) = \int_0^t G(t-t')\, d\varepsilon(t') = \varepsilon_{0+} G(t) + \int_{0+}^t G(t-t')\, D\varepsilon(t')\, dt', \tag{2.3a}$$

or conversely, whenever strain responds to stress, Boltzmann's theory can be re-expressed in terms of a (creep) compliance $J(t)$ where

$$\varepsilon(t) = \int_0^t J(t-t')\, d\sigma(t') = \sigma_{0+} J(t) + \int_{0+}^t J(t-t')\, D\sigma(t')\, dt'. \tag{2.3b}$$

These two convolution integrals can be solved analytically using Laplace transform techniques, provided that the loading histories are simple enough.

The standard FOV fluid (2.1) has a modulus $G(t)$ and a compliance $J(t)$ of [13]

$$\left.\begin{aligned} G(t) &= \frac{\eta}{\tau} E_{\alpha}\left(-(t/\tau)^{\alpha}\right) \\ J(t) &= \frac{\tau}{\eta}\left(1 + \frac{(t/\tau)^{\alpha}}{\Gamma(1+\alpha)}\right) \end{aligned}\right\}, \tag{2.4}$$

whereas, the standard FOV solid (2.2) has the material functions [13]

$$\left.\begin{aligned} G(t) &= \mu\left(\frac{\rho}{\tau}\right)^{\alpha}\left(\left(\frac{\tau}{\rho}\right)^{\alpha} + \frac{\rho^{\alpha}-\tau^{\alpha}}{\rho^{\alpha}}E_{\alpha}\left(-(t/\tau)^{\alpha}\right)\right) \\ J(t) &= \frac{1}{\mu}\left(\frac{\tau}{\rho}\right)^{\alpha}\left(1+\frac{\rho^{\alpha}-\tau^{\alpha}}{\tau^{\alpha}}\left(1-E_{\alpha}\left(-(t/\rho)^{\alpha}\right)\right)\right) \end{aligned}\right\}, \tag{2.5}$$

where $E_{\alpha}(x) = E_{\alpha,1}(x)$ is the Mittag-Leffler function (see §1.5).

2.1.1 Static Experiments

Stress relaxation experiments are often executed for the purpose of materials characterization, where

$$\frac{\sigma(t)}{\sigma_{0+}} = \begin{cases} E_{\alpha}\left(-(t/\tau)^{\alpha}\right) & \text{for standard FOV fluids,} \\ \frac{\tau^{\alpha}}{\rho^{\alpha}} + \frac{\rho^{\alpha}-\tau^{\alpha}}{\rho^{\alpha}}E_{\alpha}\left(-(t/\tau)^{\alpha}\right) & \text{for standard FOV solids.} \end{cases} \tag{2.6}$$

Figure 2.1 presents a normalized plot of stress relaxation curves for the standard FOV fluid, with $\alpha = 1$ designating the response of a classic Maxwell fluid. The stress relaxes to zero monotonically in a FOV fluid for all $\alpha \in (0, 1]$. Figure 2.2 presents a normalized plot of stress relaxation curves for the standard FOV solid, with $\alpha = 1$ designating the response of a classic Kelvin solid. For all $\alpha \in (0, 1]$, the stress monotonically relaxes to a unique non-zero value in a FOV solid as $t \to \infty$, which distinguishes solid behavior from fluid behavior. Here, and in the following figures of this chapter, the relaxation τ and retardation ρ times are assumed to scale as $(\rho/\tau)^{\alpha} = 5$ for purposes of illustration. These figures show that the fractal order of evolution controls the shape of the relaxation curve.

Relaxation, as described above, exhibits an exponential decay as $t \to \infty$ whenever $\alpha = 1$, and an algebraic decay to infinity whenever $0 < \alpha < 1$. This corresponds to a regular rate process leading to strong mixing (exponential decay) versus an intermittent rate process causing weak mixing (algebraic decay), as quantified by a probabilistic fluctuation of recurrent events (molecular collisions) governing the velocity relaxation process in polymer chain physics. Douglas [25] has shown, through probabilistic reasoning using Feller's renewal theory, that the autocorrelation function describing relaxation phenomena is governed by a fractional-order differential equation whose solution is given in terms of the Mittag-Leffler function, and whose order of evolution correlates with the degree of intermittency in the relaxation process.

Douglas [25] also states that the stretched exponential, e.g., $\exp\left(-(t/\tau)^{\alpha}\right)$, often used to empirically fit relaxation data in the literature, does not arise from probabilistic considerations in polymer chain physics. Popularity of the stretched exponential over the Mittag-Leffler function has two likely sources: many researchers are not familiar with, or have even heard of, the Mittag-Leffler function, and if they are familiar with it, they do not likely know how to compute its value. With respect to the latter, see Alg. 1.4 and App. C.

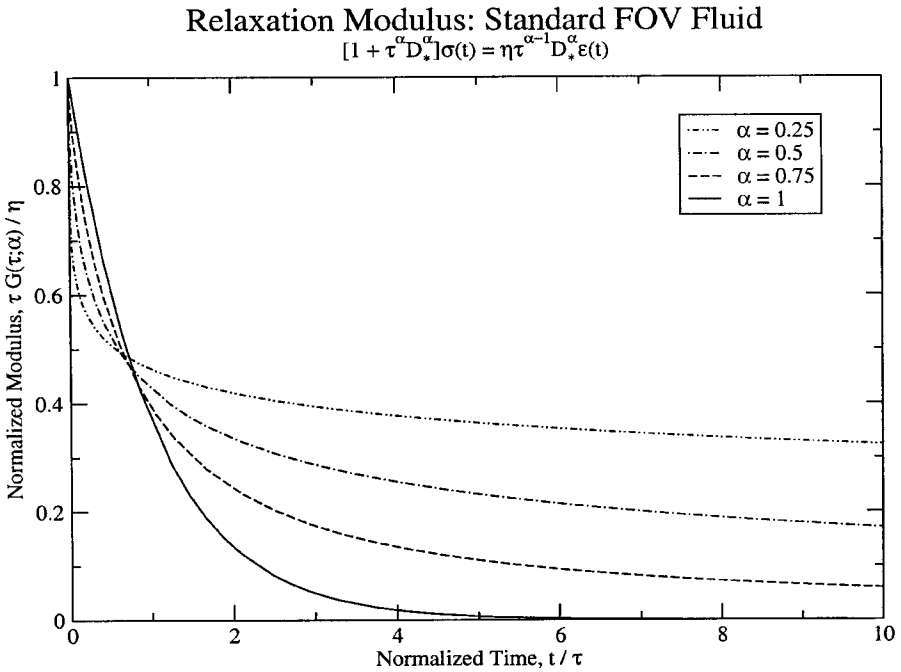

Figure 2.1: Normalized diagram for stress relaxation of a fractional Maxwell fluid.

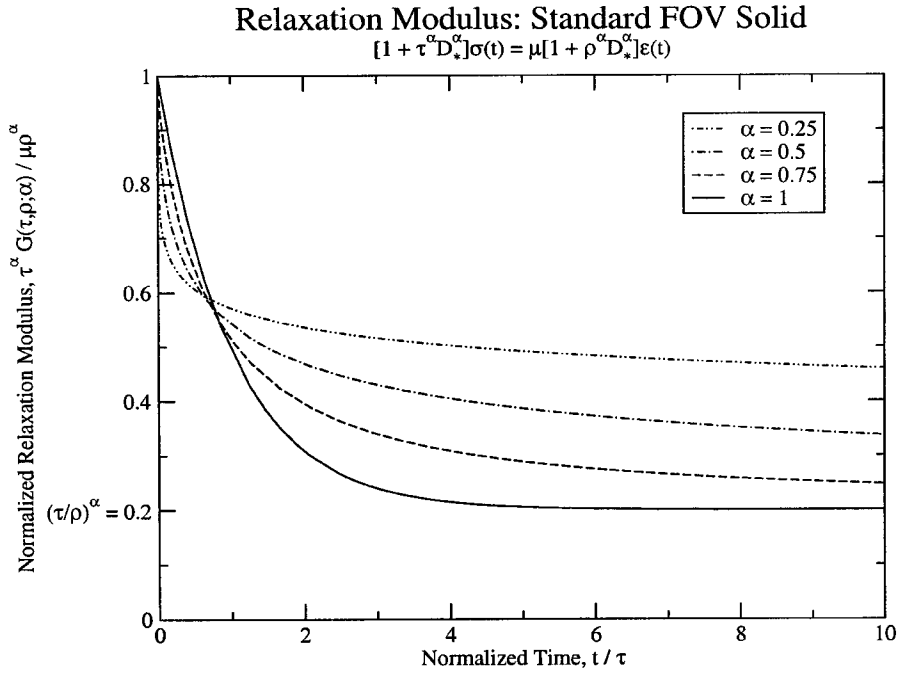

Figure 2.2: Normalized diagram for stress relaxation of a fractional Kelvin solid.

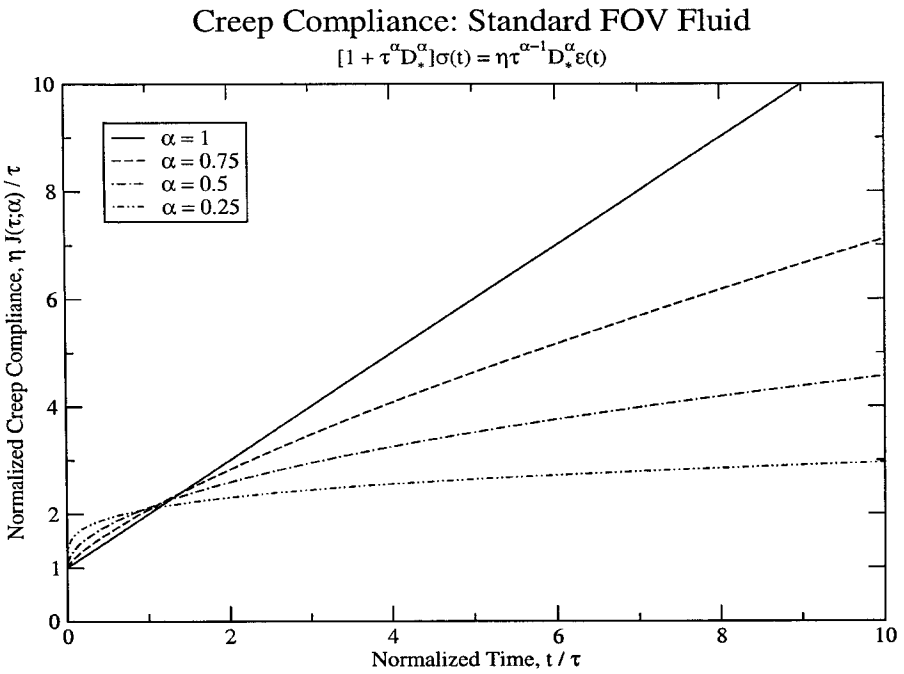

Figure 2.3: Normalized diagram for creep of a fractional Maxwell fluid.

Creep experiments are also performed for purposes of materials characterization, where

$$\frac{\varepsilon(t)}{\varepsilon_{0+}} = \begin{cases} 1 + \frac{1}{\Gamma(1+\alpha)} \left(t/\tau\right)^{\alpha} & \text{for standard FOV fluids,} \\ 1 + \frac{\rho^{\alpha} - \tau^{\alpha}}{\tau^{\alpha}} \Big(1 - E_{\alpha}\big(-(t/\rho)^{\alpha}\big) \Big) & \text{for standard FOV solids.} \end{cases} \tag{2.7}$$

Figure 2.3 shows a normalized plot of creep curves for the standard FOV fluid. A specimen will creep without bound in a FOV fluid for all $\alpha \in (0, 1]$. However, only in the case of a Maxwell fluid where $\alpha = 1$ is the 'effective' viscosity (i.e., the slope) a constant. Conversely, FOV fluids will eventually (at infinite time) stop creeping altogether (see Eqn. 2.9). Figure 2.4 shows a normalized plot of creep curves for the standard FOV solid. Here creep stops at a unique threshold level in strain for all $\alpha \in (0, 1]$. Steady-state creep behavior cannot be predicted by this class of material models. The fractal orders of evolution influence the shape of these curves, too, and in the case of a solid, they also influence the time required to attain saturation.

It is difficult to parameterize an FOV solid with only relaxation data, or with only creep data. This is because it is difficult to acquire sufficient sensitivity in the data to the parameter ρ in the case of relaxation, or to the paramter τ in the case of creep. But whenever relaxation and creep data are used together during estimation, ample sensitivty will exist for all material constants and good data fits can be expected.

Although Figs. 2.1–2.4 are informative, they are not as practical as one would like in the sense that one cannot directly extract the order of evolution, α, from them via some graphical technique. However, if one were to measure stress rates in a relaxation experiment, or strain rates in a creep experiment, then the order of evolution could,

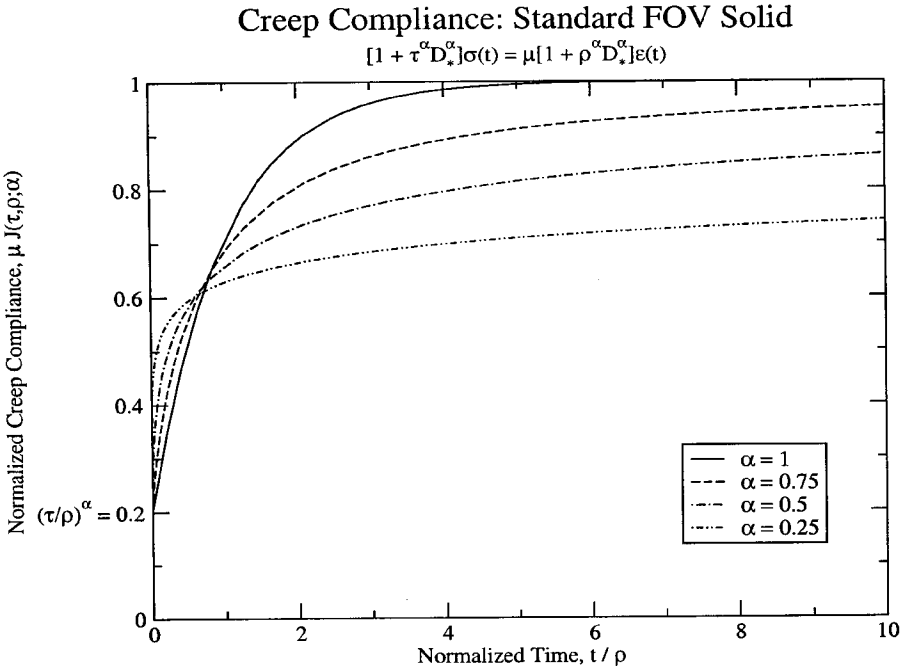

Figure 2.4: Normalized diagram for creep of a fractional Kelvin solid.

in theory, be extracted as a slope in an appropriate log-log plot of the data. In a stress relaxation experiment

$$\frac{D\sigma(t)}{\sigma_{0+}} = \begin{cases} DE_\alpha\left(-(t/\tau)^\alpha\right) & \text{for standard FOV fluids,} \\ \frac{\rho^\alpha - \tau^\alpha}{\rho^\alpha} DE_\alpha\left(-(t/\tau)^\alpha\right) & \text{for standard FOV solids,} \end{cases} \tag{2.8}$$

whereas, in a creep experiment

$$\frac{D\varepsilon(t)}{\varepsilon_{0+}} = \begin{cases} \frac{\alpha}{\tau\,\Gamma(1+\alpha)} (\tau/t)^{1-\alpha} & \text{for standard FOV fluids,} \\ \frac{\tau^\alpha - \rho^\alpha}{\tau^\alpha} DE_\alpha\left(-(t/\rho)^\alpha\right) & \text{for standard FOV solids.} \end{cases} \tag{2.9}$$

Figure 2.5 presents a graphical representation of $\partial E_\alpha(-x^\alpha)/\partial x$,[†] which appears in three of the four descriptions above, with the exception being creep rate in a standard FOV fluid, which has a power-law response. Cureously, what is observed in Fig. 2.5 is that $\partial E_\alpha(-x^\alpha)/\partial x$ approximates power-law behavior whenever $x < 0.1$. The scheme depicted in this figure for extracting α is accurate (to two significant figures) over the range of $1 \leq \alpha \leq 1/2$, but it looses accuracy as α approaches zero; for example, this graphical scheme yielded a value for α of 0.27 when it was actually $1/4$. Even so,

[†]From Podlubny [86, pp. 21–22], one finds that

$$\frac{\partial E_{\alpha,1}\left(-(x/y)^\alpha\right)}{\partial x} = \frac{E_{\alpha,0}\left(-(x/y)^\alpha\right)}{x},$$

for $0 < \alpha \leq 1$, $x \geq 0$ and $y > 0$.

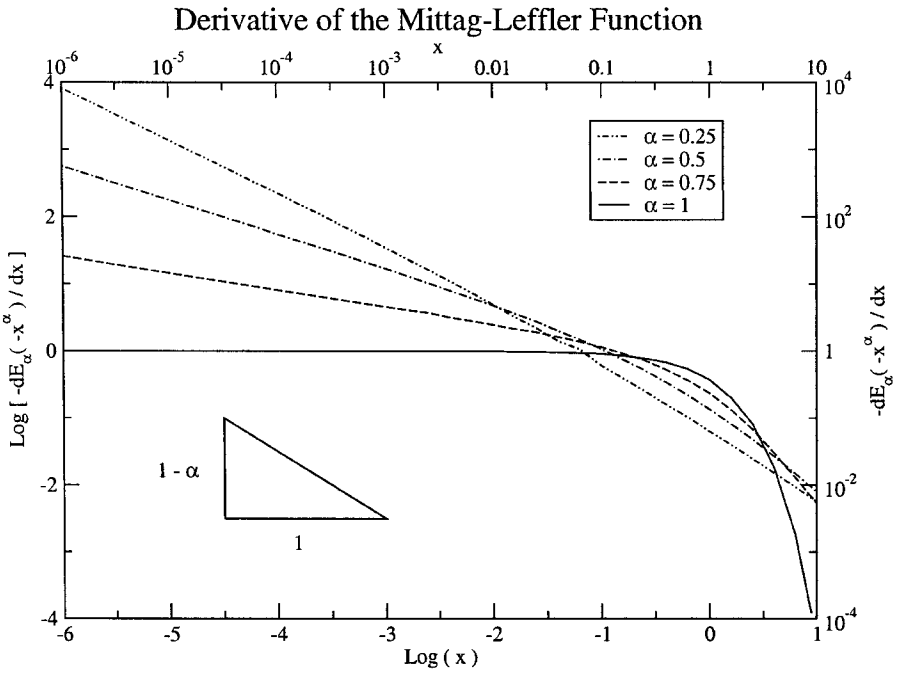

Figure 2.5: Diagram of the derivative of the Mittag-Leffler function, $\partial E_{\alpha,1}(-x^\alpha)/\partial x = E_{\alpha,0}(-x^\alpha)/x$.

this is likely to be accurate enough for material characterization purposes given the uncertainty of experiemental error. Because the time constant for creep is typically many orders of magnitude greater than the time constant for stress relaxation, it will be easier to satisfy a boundary of $x < 0.1$ in a creep experiment than it would be to satisfy it in a relaxation experiment; nevertheless, the experimental challenge remains great.

2.1.2 Dynamic Experiments

Also useful for the purpose of materials characterization are dynamic experiments where strain is controlled at a constant amplitude ε_0 and angular frequency ω according to $\varepsilon(t) = \varepsilon_0 \exp(i\omega t)$, to which stress responds with a dynamic modulus of $G^\star(\omega) = G'(\omega) + iG''(\omega)$ such that $\sigma(t) = \varepsilon_0 G^\star(\omega) \exp(i\omega t)$. The real $G'(\omega)$ and imaginary $G''(\omega)$ parts of the dynamic modulus are called the storage and loss moduli, respectively, whose ratio, $\tan\delta(\omega) = {}^{G''(\omega)}/_{G'(\omega)}$, is often reported in the literature. Figure 2.6 illustrates how these properties are extracted from experimental data obtained under steady, oscillatory, loading conditions, where the stress-strain curve is an ellipse with control $\varepsilon(t) = \varepsilon_0 \sin\omega t$ and response $\sigma(t) = \sigma_0 \sin(\omega t + \delta)$. A material is non-linear if the hysteresis is something other than an ellipse under sinusoidal loading conditions. A thorough discussion of dynamic experiments, as they relate to linear viscoelastic materials characterization, can be found in the recent text by Lakes [62, Chp. 3].

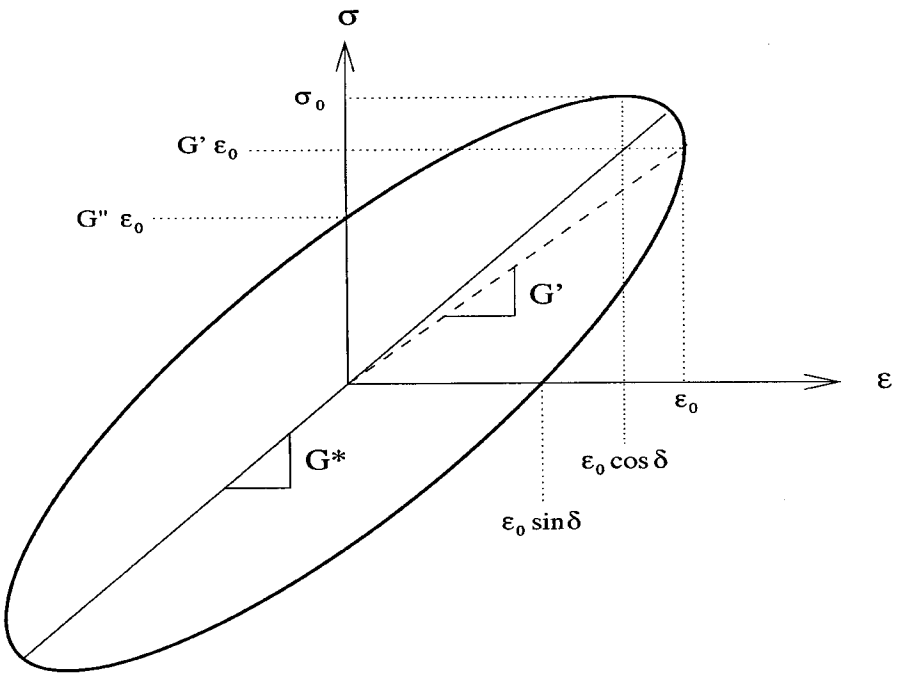

Figure 2.6: Extracting dynamic properties from linear viscoelastic materials.

For the standard FOV fluid (2.1), the dynamic modulus is given by

$$G^*(\omega) = \frac{\eta}{\tau}\,\frac{(i\,\omega\tau)^\alpha}{1+(i\,\omega\tau)^\alpha}, \tag{2.10a}$$

whose real and imaginary parts are

$$\left.\begin{aligned} G'(\omega) &= \frac{\eta}{\tau}\,\frac{(\omega\tau)^\alpha + \cos(\alpha\pi/2)}{(\omega\tau)^\alpha + (\omega\tau)^{-\alpha} + 2\cos(\alpha\pi/2)} \\ G''(\omega) &= \frac{\eta}{\tau}\,\frac{\sin(\alpha\pi/2)}{(\omega\tau)^\alpha + (\omega\tau)^{-\alpha} + 2\cos(\alpha\pi/2)} \end{aligned}\right\}, \tag{2.10b}$$

and that ratio as

$$\tan\delta(\omega) = \frac{\sin(\alpha\pi/2)}{(\omega\tau)^\alpha + \cos(\alpha\pi/2)}. \tag{2.10c}$$

For the standard FOV solid (2.2), the dynamic modulus is given by

$$G^*(\omega) = \mu\left(\frac{\rho}{\tau}\right)^\alpha \frac{(\tau/\rho)^\alpha + (i\,\omega\tau)^\alpha}{1+(i\,\omega\tau)^\alpha}, \tag{2.11a}$$

whose real and imaginary parts are

$$\left.\begin{aligned} G'(\omega) &= \mu\left(\frac{\rho}{\tau}\right)^\alpha \frac{(\omega\tau)^\alpha + (\omega\rho)^{-\alpha} + \left(1+(\tau/\rho)^\alpha\right)\cos(\alpha\pi/2)}{(\omega\tau)^\alpha + (\omega\tau)^{-\alpha} + 2\cos(\alpha\pi/2)} \\ G''(\omega) &= \mu\left(\frac{\rho}{\tau}\right)^\alpha \frac{\left(1-(\tau/\rho)^\alpha\right)\sin(\alpha\pi/2)}{(\omega\tau)^\alpha + (\omega\tau)^{-\alpha} + 2\cos(\alpha\pi/2)} \end{aligned}\right\}, \tag{2.11b}$$

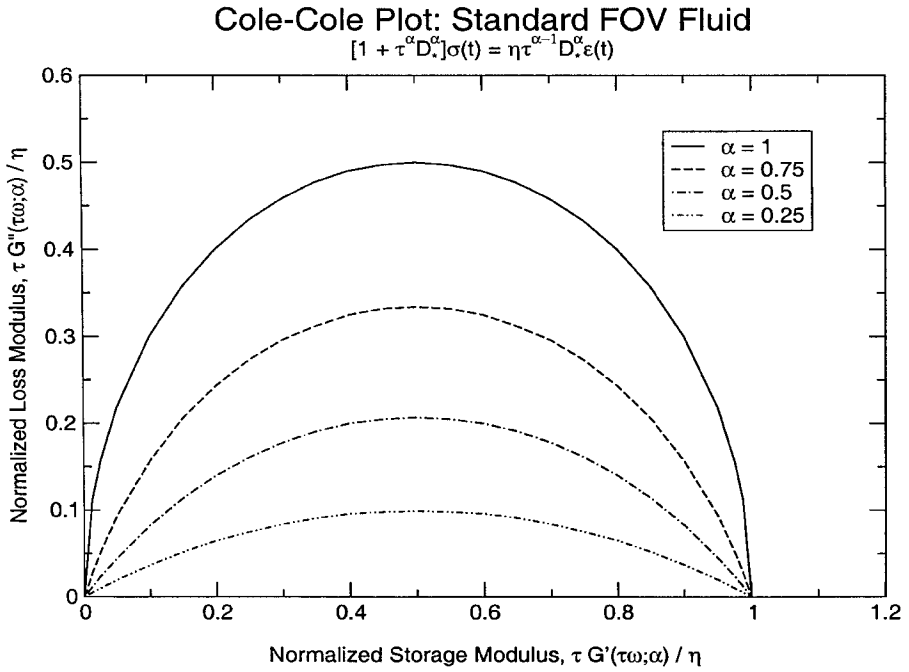

Figure 2.7: Normalized Cole-Cole diagram for a fractional Maxwell fluid.

and that ratio as

$$\tan\delta(\omega) = \frac{\left(1 - (\tau/\rho)^{\alpha}\right)\sin(\alpha\pi/2)}{(\omega\tau)^{\alpha} + (\omega\rho)^{-\alpha} + \left(1 + (\tau/\rho)^{\alpha}\right)\cos(\alpha\pi/2)}, \tag{2.11c}$$

thereby requiring $\tau < \rho$ if $G'' \geq 0$—a well-known requirement of thermodynamics—given that $\mu > 0$, $\tau > 0$, and $0 < \alpha \leq 1$.

A Cole-Cole [17] diagram—a plot of $G'(\omega)$ versus $G''(\omega)$—is a very sensitive way to view anomalous relaxation phenomena. Figure 2.7 presents the normalized Cole-Cole diagram for the standard FOV fluid, with the $\alpha = 1$ curve designating the response of a Maxwell fluid. Figure 2.8 presents a normalized Cole-Cole diagram for the standard FOV solid, which in this case translates the storage modulus of the FOV fluid by an amount $(\tau/\rho)^{\alpha} = 0.2$, with the $\alpha = 1$ curve designating the response of a Kelvin solid. The influence that the fractal order of evolution has on material response is readily apparent in a Cole-Cole diagram. Fractal order affects the extent of dissipation.

Cole-Cole–type relaxations are naturally produced by random-walk models done on fractal lattices brought about by studying the motion of a particle in restricted geometries [37]. They also result from random-walk models done in fractal time on regular lattices, where the probability distribution is now a decaying power-law in time instead of the more common decaying exponential [43]. Random walks are used to establish the mean-square end-to-end distance of polymer chains in the various statistical theories of polymer physics, both for fluids and solids (e.g., cf. Douglas [25]).

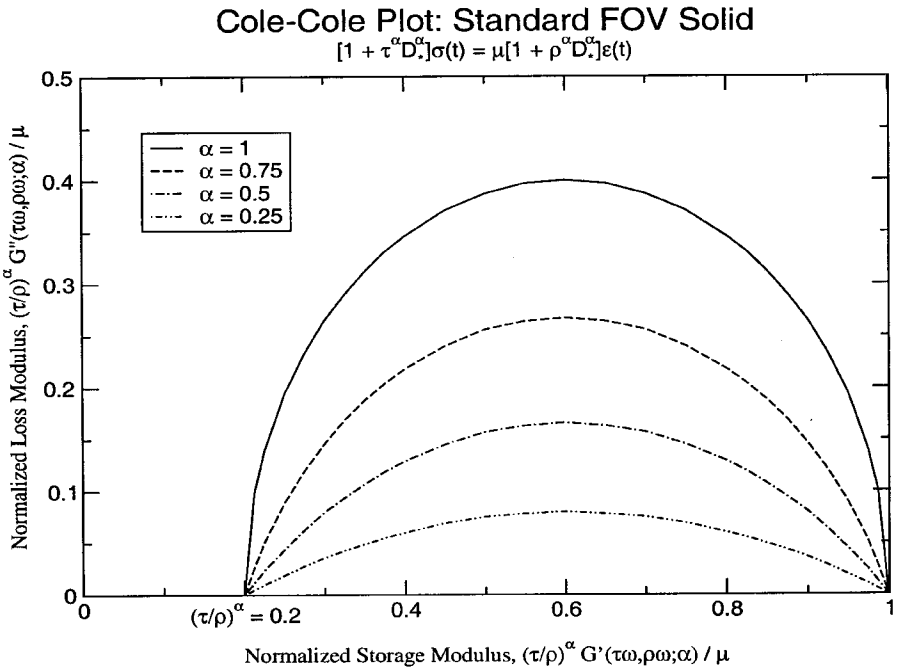

Figure 2.8: Normalized Cole-Cole diagram for a fractional Kelvin solid.

Chapter 3

Continuum Mechanics: body-tensor fields

In this report we use body-tensor fields (as defined by Lodge [68, 69, 70]) for deriving constitutive formulæ, and we use Cartesian space-tensor fields (as commonly used throughout the literature) to solve boundary-value problems. In this regard we are free to select the tensor analysis scheme best suited for a particular task at hand, since one can readily map body-tensor fields into space-tensor fields, and vice versa. In this chapter we present the basic fields used in body-tensor analysis. In the next chapter we map these fields into Cartesian space, thereby producing tensor fields that are likely to be more familiar to the reader.

Consider a continuum consisting of an infinite set of point particles, $\{\mathfrak{P}\}$, also referred to as mass elements, that fills a domain, $\mathbb{B}$, in 3-space ($\mathbb{B} \subset \mathbb{R}^3$). We call this set the body $\mathbb{B}$. In any admissible body-coordinate system, $\mathcal{B}$, defined over $\mathbb{B}$, each particle $\mathfrak{P}$ in $\mathbb{B}$ is assigned a unique set of body coordinates, $\mathfrak{\xi} = (\xi^1, \xi^2, \xi^3)$, $\xi^i \in \mathbb{R}$, that are independent of time (i.e., $\mathcal{B}$: $\mathfrak{P} \to \mathfrak{\xi}$, cf. Lodge [69]). In this sense, body-coordinate systems have been construed as being convected coordinate systems.

3.1 Metric Fields

The distance dS separating any two neighboring particles—say, $\mathfrak{P}$ and $\mathfrak{P}'$—in $\mathbb{B}$ can be quantified by using the covariant body-metric tensor, $\underline{\underline{\gamma}}$, of Lodge [68, 70] that he assigned to a Riemannian manifold with geometric measurement

$$(dS_0)^2 = d\underline{\xi} \cdot \underline{\underline{\gamma}}_0 \cdot d\underline{\xi} \quad \text{and} \quad (dS)^2 = d\underline{\xi} \cdot \underline{\underline{\gamma}} \cdot d\underline{\xi}, \tag{3.1}$$

where $\underline{\underline{\gamma}}(\mathfrak{P}; t)$ is symmetric positive-definite and, most notibly, a function of time t with $\underline{\underline{\gamma}}_0 := \underline{\underline{\gamma}}(\mathfrak{P}; t_0)$, wherein t_0 is usually taken to be zero (0). This tensor field has a matrix representation of $\mathfrak{G}$ ($= [\![\gamma_{rc}]\!]$; $r, c = 1, 2, 3$) in the coordinate system $\mathcal{B}$ with components $\gamma_{ij} = \gamma_{ji} = \gamma_{ij}(\mathfrak{\xi}; t)$. Scalar $dS(\mathfrak{P}; t)$ is the infinitesimal length-of-line of the contravariant vector $d\underline{\xi}(\mathfrak{P}) := \overrightarrow{\mathfrak{P}\mathfrak{P}'}$, with $dS_0 := dS(\mathfrak{P}; t_0)$ designating its gauge length.

A single dot placed between two tensor fields represents a contraction over one array index. Likewise, a double dot (colon) will represent a contraction over two array indices.

3.1.1 Dual

Because the metric tensor $\underline{\underline{\gamma}}$ is symmetric postitive-definite, it has a dual—the contravariant (inverse) body-metric tensor, $\underline{\underline{\gamma}}^{-1}(\mathfrak{P};t)$—whose matrix representation $\mathfrak{g}^{-1}$ $(= [\![\gamma^{rc}]\!])$ has components $\gamma^{ij} = \gamma^{ji} = \underline{\underline{\gamma}}^{ij}(\xi;t)$ in $\mathcal{B}$ such that $\underline{\underline{\gamma}}^{-1}\cdot\underline{\underline{\gamma}} = \underline{\underline{\delta}}$, where $\underline{\underline{\delta}}(\mathfrak{P})$ is the mixed idem tensor with a matrix representation of $\mathfrak{S}$ $(= [\![\delta^r_c]\!])$ possessing components δ^i_j that equal 1 whenever $i = j$, or that equal 0 whenever $i \neq j$, in every body-coordinate system.

This dual body-metric tensor, $\underline{\underline{\gamma}}^{-1}$, has two possible geometric interpretations. In the first interpretation, provided by Lodge [68, pg. 318], the distance $dH(\mathfrak{P};t)$ measuring the height-of-separation between any two, neighboring, material surfaces—say, $\sigma(\underline{\xi}) = C$ and $\sigma(\underline{\xi} + d\underline{\xi}) = C + dC$, where C and dC are constants—belonging to the same one-parameter family of non-intersecting surfaces, σ, in $\mathbb{B}$ is quantified via the contravariant body-metric tensor, $\underline{\underline{\gamma}}^{-1}$, according to

$$\left(\frac{dC}{dH_0}\right)^2 = \frac{\partial\sigma}{\partial\underline{\xi}}\cdot\underline{\underline{\gamma}}_0^{-1}\cdot\frac{\partial\sigma}{\partial\underline{\xi}} \quad \text{and} \quad \left(\frac{dC}{dH}\right)^2 = \frac{\partial\sigma}{\partial\underline{\xi}}\cdot\underline{\underline{\gamma}}^{-1}\cdot\frac{\partial\sigma}{\partial\underline{\xi}}, \quad dC = \frac{\partial\sigma}{\partial\underline{\xi}}\cdot d\underline{\xi}, \tag{3.2}$$

where $(\partial\sigma/\partial\underline{\xi})(\mathfrak{P})$ is a covariant vector, independent of time t, that is normal to this material suraface, with contravariant vector $d\underline{\xi}$ originating on one surface and terminating on the other. Scalar $dH_0 := dH(\mathfrak{P};t_0)$ is the gauge length for this height-of-separation, while $\underline{\underline{\gamma}}_0^{-1} := \underline{\underline{\gamma}}^{-1}(\mathfrak{P};t_0)$.

A second geometric interpretation for the dual metric, provided by Truesdell [108] in an analysis done using general space-tensor fields, has a description of

$$(dA_0)^2 = \left(d\underline{\xi}\times\widehat{d\underline{\xi}}\right)\cdot\frac{\underline{\underline{\gamma}}_0^{-1}}{\det\underline{\underline{\gamma}}_0^{-1}}\cdot\left(d\underline{\xi}\times\widehat{d\underline{\xi}}\right) \quad \text{and} \quad (dA)^2 = \left(d\underline{\xi}\times\widehat{d\underline{\xi}}\right)\cdot\frac{\underline{\underline{\gamma}}^{-1}}{\det\underline{\underline{\gamma}}^{-1}}\cdot\left(d\underline{\xi}\times\widehat{d\underline{\xi}}\right), \tag{3.3}$$

where $\det\underline{\underline{\gamma}}$ denotes the determinant of $\underline{\underline{\gamma}}$, which is a scalar field with a tensorial weight of two (2), and therefore the areal metric tensor, $(\det\underline{\underline{\gamma}})\,\underline{\underline{\gamma}}^{-1}$, is a relative field of like weight. Scalar $dA(\mathfrak{P};t)$ is an infinitesimal area-of-surface, with $dA_0 := dA(\mathfrak{P};t_0)$ designating its gauge area. This material surface contains neighboring particles $\mathfrak{P}$, $\mathfrak{P}'$ and $\mathfrak{P}''$. The normal to this surface lies in the direction of a covariant vector field given by the cross product $d\underline{\xi}\times\widehat{d\underline{\xi}}$, which has a tensorial weight of minus one (-1), wherein $d\underline{\xi}(\mathfrak{P}) := \overrightarrow{\mathfrak{P}\mathfrak{P}'}$ and $\widehat{d\underline{\xi}}(\mathfrak{P}) := \overrightarrow{\mathfrak{P}\mathfrak{P}''}$.

The unit normal $\underline{\nu}(\mathfrak{P};t)$ to element dA is given by $\underline{\nu}\,dA := \sqrt{\det\underline{\underline{\gamma}}}\;d\underline{\xi}\times\widehat{d\underline{\xi}}$. This is an 'absolute' (without tensorial weight) covariant vector that, in body tensor analysis, is a function of time t through the presence of $\underline{\underline{\gamma}}(\mathfrak{P};t)$, because $\|\underline{\nu}\|^2 := \underline{\nu}\cdot\underline{\underline{\gamma}}^{-1}\cdot\underline{\nu} = 1$.

3.1.2 Rates

The various descriptions for strain rate that are found in the literature can all be expressed in terms of derivatives of the metric tensor, $\underline{\underline{\gamma}}$, its inverse, $\underline{\underline{\gamma}}^{-1}$, and its determinant, $\det \underline{\underline{\gamma}}$. The time rate-of-change of the body-metric tensor, $D\underline{\underline{\gamma}}$, is defined classically through the limiting process

$$D\underline{\underline{\gamma}}(\mathfrak{P};t) = \lim_{t' \to t} \frac{\underline{\underline{\gamma}}(\mathfrak{P};t) - \underline{\underline{\gamma}}(\mathfrak{P};t')}{t - t'}, \tag{3.4}$$

while the time rate-of-change of the determinant of the body metric, $D(\det \underline{\underline{\gamma}})(\mathfrak{P};t)$, is given by

$$D\big(\det \underline{\underline{\gamma}}\big) = \big(\det \underline{\underline{\gamma}}\big)\big(\operatorname{tr} D\underline{\underline{\gamma}}\big), \tag{3.5}$$

wherein the trace, $\operatorname{tr} D\underline{\underline{\gamma}}$, is computed as $\underline{\underline{\gamma}}^{-1} : D\underline{\underline{\gamma}}$, consistent with the precepts of general tensor analysis.

The first-order body-metric rates $D\underline{\underline{\gamma}}(\mathfrak{P};t)$ and $D\underline{\underline{\gamma}}^{-1}(\mathfrak{P};t)$ are not independent. Instead, they are related through the expression

$$D\underline{\underline{\gamma}}^{-1} = -\underline{\underline{\gamma}}^{-1} \cdot \big(D\underline{\underline{\gamma}}\big) \cdot \underline{\underline{\gamma}}^{-1}. \tag{3.6a}$$

Likewise, the second-order rates $D^2\underline{\underline{\gamma}}(\mathfrak{P};t)$ and $D^2\underline{\underline{\gamma}}^{-1}(\mathfrak{P};t)$ are related through

$$D^2\underline{\underline{\gamma}}^{-1} = \underline{\underline{\gamma}}^{-1} \cdot \Big(2\,\big(D\underline{\underline{\gamma}}\big) \cdot \underline{\underline{\gamma}}^{-1} \cdot \big(D\underline{\underline{\gamma}}\big) - \big(D^2\underline{\underline{\gamma}}\big)\Big) \cdot \underline{\underline{\gamma}}^{-1}. \tag{3.6b}$$

These identities are easily derived by applying the Leibniz product rule for differentiation to the expression $\underline{\underline{\gamma}}^{-1} \cdot \underline{\underline{\gamma}} = \underline{\underline{\delta}}$, noting that $D\underline{\underline{\delta}} = \underline{\underline{0}}$. Higher-order relationships can be acquired in like manner, but they are not needed in this work.

Fractional order

From the definition of Caputo differentiation (1.8a), one can compute fractal rates for metric evolution via the formulæ*

$$\left.\begin{aligned} D^\alpha_\star \underline{\underline{\gamma}}(\mathfrak{P};t_0,t) &= \frac{1}{\Gamma(1-\alpha)} \int_{t_0}^{t} \frac{1}{(t-t')^\alpha} \big(D\underline{\underline{\gamma}}\big)(\mathfrak{P};t')\,dt' \\ D^\alpha_\star \underline{\underline{\gamma}}^{-1}(\mathfrak{P};t_0,t) &= \frac{1}{\Gamma(1-\alpha)} \int_{t_0}^{t} \frac{1}{(t-t')^\alpha} \big(D\underline{\underline{\gamma}}^{-1}\big)(\mathfrak{P};t')\,dt' \end{aligned}\right\}, \tag{3.7}$$

*Because $\binom{\alpha}{k} \neq 0$ whenever $k > \alpha$ given that $k \in \mathbb{N}$ and $\alpha \in \mathbb{R}_+$ with $\alpha \notin \mathbb{N}$, the Leibniz product rule (1.7) applicible to the Caputo derivative (1.3) leads to a more complex identity for $D^\alpha_\star \underline{\underline{\gamma}}^{-1}$ than otherwise exists in the integer case (3.6a); specifically, for $0 < \alpha < 1$,

$$D^\alpha_\star \underline{\underline{\gamma}}^{-1} = \frac{(t_0 - t)^{-\alpha}}{\Gamma(1-\alpha)} \big(\underline{\underline{\gamma}}^{-1}_{0^+} - \underline{\underline{\gamma}}^{-1}\big) - \sum_{k=1}^{\infty} \binom{\alpha}{k} \big(J^{k-\alpha}\underline{\underline{\gamma}}^{-1}\big) \cdot \big(D^k \underline{\underline{\gamma}}\big) \cdot \underline{\underline{\gamma}}^{-1},$$

where $\underline{\underline{\gamma}}^{-1}_{0^+} := \underline{\underline{\gamma}}^{-1}(\mathfrak{P};t_{0^+})$. Consequently, there is no direct relationship between $D^\alpha_\star \underline{\underline{\gamma}}$ and $D^\alpha_\star \underline{\underline{\gamma}}^{-1}$. These rate fields are independent of one another. This result follows from $D^\alpha_\star\big(\underline{\underline{\gamma}}^{-1} \cdot \underline{\underline{\gamma}}\big) = D^\alpha_\star \underline{\underline{\delta}} = \underline{\underline{0}}$.

where the fractal order of differentiation is restricted to the range $0 < \alpha < 1$. Unlike integer-order derivatives of the body metric (i.e., $D\underline{\underline{\gamma}}(\mathfrak{P};t)$ and $D\underline{\underline{\gamma}}^{-1}(\mathfrak{P};t)$), which are one-state fields in time t, fractal-order derivatives of the body metrics (viz., $D^{\alpha}_{\star}\underline{\underline{\gamma}}(\mathfrak{P};t_0,t)$ and $D^{\alpha}_{\star}\underline{\underline{\gamma}}^{-1}(\mathfrak{P};t_0,t)$) depend on all states traversed along the time interval $[t_0,t]$, where we shall typically take t_0 to be zero in this work.

3.2 Strain Fields

Strain tensors are the preferred measures for describing deformations in solids, because solids have a quantifyible reference state. On the other hand, metric tensors are the preferred measures for describing deformations in fluids, becuase fluids have no unique state of reference.

Strains are two-state fields that ideally possess four characteristic properties. The first property is: strain is a relative measure of deformation in that it vanishes whenever its two dependent states are coincident. The second property is: strain is additive and anti-symmetric in its dependency upon state. The third property is: strain exhibits tension/compression asymmetry; for example, axial extensions of λ and λ^{-1} correspond to strains that are equal in magnitude but opposite in sign. And the fourth property is: strain is an absolute field (i.e., without tensorial weight) although, for the most part, this is really a requirement of convience. The second and third criteria actually quite restrictive. Only Hencky strain is known to satisfy all four of these criteria.

The classic strain measures are defined below. The first two are tensor fields that relate to two distinct changes in length-of-line; the first tensor relates to a separation between neighboring particles, while the second tensor relates to a separation between neighboring material surfaces. The third strain measure is a scalar field that relates to the volume change of a mass element.

3.2.1 Covariant

The metric geometry of (3.1) can be rearranged in such a manner that (cf. Lodge [68, pp. 24–26])

$$(dS)^2 - (dS_0)^2 = 2\, d\underline{\boldsymbol{\xi}} \cdot \underline{\underline{\epsilon}} \cdot d\underline{\boldsymbol{\xi}}, \quad \underline{\underline{\epsilon}} := \tfrac{1}{2}\big(\underline{\underline{\gamma}} - \underline{\underline{\gamma}}_0\big), \tag{3.8}$$

where $\underline{\underline{\epsilon}}(\mathfrak{P};t_0,t)$ is an absolute, symmetric, covariant, strain tensor. It has properties: *i*) tensor $\underline{\underline{\epsilon}}$ vanishes in the reference state, $\underline{\underline{\epsilon}}(\mathfrak{P};t_0,t_0) = \underline{\underline{\mathbf{0}}}$; *ii*) it is additive and anti-symmetric in its time agruments, $\underline{\underline{\epsilon}}(\mathfrak{P};t_0,t) = \underline{\underline{\epsilon}}(\mathfrak{P};t_0,t') + \underline{\underline{\epsilon}}(\mathfrak{P};t',t)$ for all $t' \in [t_0,t]$, regardless of the extent of deformation; and *iii*) it has no tensorial weight; however, it does not possess tension/compression asymmetry. Typically one sets t_0 to zero, but for the time being, we shall leave it as t_0 for clarity of discussion.

The factor of 2 that appears in (3.8) is for historical reasons. Specifically, engineering strain is given by $(\ell - \ell_0)/\ell_0$ for the infinitesimal extension of a rod with length $\ell(t)$ whose gauge length is $\ell_0 := \ell(t_0)$. A normalized representation of the left-hand

side in (3.8) produces the relative strain measure

$$\frac{(dS)^2-(dS_0)^2}{2(dS_0)^2}=\frac{\big(dS+dS_0\big)}{2\,dS_0}\,\frac{\big(dS-dS_0\big)}{dS_0}\\ \approx\frac{dS-dS_0}{dS_0}\quad\text{whenever}\quad dS\sim dS_0,\tag{3.9}$$

demonstrating a consistency with the classic definition for engineering strain under conditions of infinitesimal deformation.

Rates

The covariant strain-rate tensor, $D\underline{\underline{\epsilon}}(\mathfrak{P};t)$, is a one-state tensor field given by

$$D\underline{\underline{\epsilon}}=\tfrac{1}{2}\,D\underline{\underline{\gamma}},\tag{3.10}$$

because $D\underline{\underline{\gamma}}_0=\underline{\underline{0}}$.

The covariant, fractal, strain-rate tensor, $D^\alpha_\star\underline{\underline{\epsilon}}(\mathfrak{P};t_0,t)$, depends on the path of straining incurred over the interval $[t_0,t]$ of integration, and is given by

$$D^\alpha_\star\underline{\underline{\epsilon}}=\tfrac{1}{2}\,D^\alpha_\star\underline{\underline{\gamma}},\tag{3.11}$$

because $D^\alpha_\star\underline{\underline{\gamma}}_0=\underline{\underline{0}}$ (the Caputo derivative of a constant is zero).

3.2.2 Contravariant

In similar fashion to (3.8), the metric geometry of (3.2) can be rearranged in such a manner that (cf. Lodge [68, pp. 26–32])

$$\left(\frac{dC}{dH_0}\right)^2-\left(\frac{dC}{dH}\right)^2=2\,\frac{\partial\sigma}{\partial\underline{\xi}}\cdot\underline{\underline{\zeta}}\cdot\frac{\partial\sigma}{\partial\underline{\xi}},\quad\underline{\underline{\zeta}}:=\tfrac{1}{2}\big(\underline{\underline{\gamma}}_0^{-1}-\underline{\underline{\gamma}}^{-1}\big),\tag{3.12}$$

where $\underline{\underline{\zeta}}(\mathfrak{P};t_0,t)$ is an absolute, symmetric, contravariant, strain tensor[†], which provides another acceptable representation for strain. Like $\underline{\underline{\epsilon}}$, the strain $\underline{\underline{\zeta}}$ is: *i*) a relative

[†]From (3.3), one can likewise define an alternative, symmetric, contravariant, strain measure as

$$(dA_0)^2-(dA)^2=2\big(d\underline{\xi}\times\widehat{d\underline{\xi}}\big)\cdot\underline{\underline{\beta}}\cdot\big(d\underline{\xi}\times\widehat{d\underline{\xi}}\big),\quad\underline{\underline{\beta}}:=\tfrac{1}{2}\Big(\big(\det\underline{\underline{\gamma}}_0\big)\,\underline{\underline{\gamma}}_0^{-1}-\big(\det\underline{\underline{\gamma}}\big)\,\underline{\underline{\gamma}}^{-1}\Big),$$

which is a relative measure of deformation in that $\underline{\underline{\beta}}(\mathfrak{P};t_0,t_0)=\underline{\underline{0}}$, and it is also additive and anti-symmetric in its time agruments because $\underline{\underline{\beta}}(\mathfrak{P};t_0,t)=\underline{\underline{\beta}}(\mathfrak{P};t_0,t')+\underline{\underline{\beta}}(\mathfrak{P};t',t)$ for all $t'\in[t_0,t]$, regardless of the magnitude of deformation; however, it has a tensorial weight of two (2). It can be converted into an absolute field (i.e., without tensorial weight), but the outcome will violate the second desirable property of a strain field (viz., additive and anti-symmetric in state dependence).

Because tensorial weights must equal amongst all additive terms in a tensor equation, and because all of the other tensor fields that we happen to use in constitutive development are absolute fields, it is therefore not practical to use $\underline{\underline{\beta}}$ as a strain measure, even though it has the desirable interpretation of relating to changes in area-of-surface.

measure of deformation in that $\underline{\underline{\boldsymbol{\zeta}}}(\mathfrak{P};t_0,t_0)=\underline{\underline{\mathbf{0}}}$; *ii*) it is additive and anti-symmetric in its time agruments because $\underline{\underline{\boldsymbol{\zeta}}}(\mathfrak{P};t_0,t)=\underline{\underline{\boldsymbol{\zeta}}}(\mathfrak{P};t_0,t')+\underline{\underline{\boldsymbol{\zeta}}}(\mathfrak{P};t',t)$ for all $t'\in[t_0,t]$, regardless of the extent of deformation, and *iii*) it has no tensorial weight; however, it does not possess tension/compression asymmetry.

Rates

The contravariant strain-rate tensor, $D\underline{\underline{\boldsymbol{\zeta}}}(\mathfrak{P};t)$, is a one-state tensor field given by

$$D\underline{\underline{\boldsymbol{\zeta}}}=-\tfrac{1}{2}\,D\underline{\underline{\boldsymbol{\gamma}}}^{-1}\equiv\underline{\underline{\boldsymbol{\gamma}}}^{-1}\cdot\big(D\underline{\underline{\boldsymbol{\epsilon}}}\big)\cdot\underline{\underline{\boldsymbol{\gamma}}}^{-1},\tag{3.13}$$

because $D\underline{\underline{\boldsymbol{\gamma}}}_0^{-1}=\underline{\underline{\mathbf{0}}}$.

The contravariant, fractal, strain-rate tensor, $D^\alpha_\star\underline{\underline{\boldsymbol{\zeta}}}(\mathfrak{P};t_0,t)$, depends on the path of straining incurred over the interval $[t_0,t]$ of integration, and is given by

$$D^\alpha_\star\underline{\underline{\boldsymbol{\zeta}}}=-\tfrac{1}{2}\,D^\alpha_\star\underline{\underline{\boldsymbol{\gamma}}}^{-1},\tag{3.14}$$

because $D^\alpha_\star\underline{\underline{\boldsymbol{\gamma}}}_0^{-1}=\underline{\underline{\mathbf{0}}}$ (the Caputo derivative of a constant is zero). Unlike the integer-order strain rates $D\underline{\underline{\boldsymbol{\epsilon}}}$ and $D\underline{\underline{\boldsymbol{\zeta}}}$, there is no identity relating the fractal strain rate $D^\alpha_\star\underline{\underline{\boldsymbol{\epsilon}}}$ to $D^\alpha_\star\underline{\underline{\boldsymbol{\zeta}}}$.

3.2.3 Dilatation

To acquire a volumetric strain measure that is additive and anti-symmetric in its time dependency and exhibits tension/compression asymmetry, too, requires taking a different tact. Using the conservation of mass as our guide (viz., integrating $D\ln\varrho=-\frac{1}{2}\operatorname{tr}D\underline{\underline{\boldsymbol{\gamma}}}$) leads to Hencky's [50] definition for dilatation, $\Delta(\mathfrak{P};t_0,t)$, which is a scalar field given by (cf. Oldroyd [83])

$$\Delta=\tfrac{1}{2}\ln\Big(\det\big(\underline{\underline{\boldsymbol{\gamma}}}_0^{-1}\cdot\underline{\underline{\boldsymbol{\gamma}}}\big)\Big)=\ln\big(\varrho_0/\varrho\big)\equiv\ln\big(dV/dV_0\big).\tag{3.15}$$

This is our third classic strain measure. Like the prior strain measures, dilatation: *i*) vanishes in the reference state, $\Delta(\mathfrak{P};t_0,t_0)=0$; *ii*) it is additive and anti-symmetric in its time dependence, $\Delta(\mathfrak{P};t_0,t)=\Delta(\mathfrak{P};t_0,t')+\Delta(\mathfrak{P};t',t)$ for all $t'\in[t_0,t]$, independent of the magnitude of deformation; and *iii*) it is without tensorial weight. Unlike the two prior strain measures, it *iv*) possesses tension/compression symmetry in that $\ln\big(dV_1/dV_2\big)=-\ln\big(dV_2/dV_1\big)$.

Scalar $\varrho(\mathfrak{P};t)$ denotes the density of mass element $\mathfrak{P}$, with $\varrho_0:=\varrho(\mathfrak{P};t_0)$ being its gauge density. Scalar $dV(\mathfrak{P};t)$ is the infinitesimal volume of mass element $\mathfrak{P}$ at time t, with $dV_0:=dV(\mathfrak{P};t_0)$ denoting its gauge volume. Because $\det\underline{\underline{\boldsymbol{\gamma}}}_0^{-1}$ has a tensorial weight of minus two (-2), while $\det\underline{\underline{\boldsymbol{\gamma}}}$ has a weight of plus two (2), it follows that $\det(\underline{\underline{\boldsymbol{\gamma}}}_0^{-1}\cdot\underline{\underline{\boldsymbol{\gamma}}})$ has no tensorial weight, and therefore Δ is an absolute scalar field.

Rates

Dilatation Δ is actually defined via its rate, $D\Delta(\mathfrak{P};t)$, according to the expression

$$D\Delta := \tfrac{1}{2}\operatorname{tr} D\underline{\underline{\gamma}} = -D\ln\varrho \equiv D\ln dV, \tag{3.16}$$

which arises from the conservation of mass. It has a fractal rate of $D^{\alpha}_{\star}\Delta(\mathfrak{P};t_0,t)$, where

$$D^{\alpha}_{\star}\Delta = \frac{1}{\Gamma(1-\alpha)}\int_{t_0}^{t}\frac{1}{(t-t')^{\alpha}}\big(D\Delta\big)(t')\,dt', \tag{3.17}$$

which is precisely the definition of a Caputo derivative (1.8a), assuming $0<\alpha<1$.

3.3 Stress Fields

Stress is a linear mapping function defined by

$$d\underline{\phi} = \underline{\underline{\pi}}\cdot\underline{\nu}\,dA, \quad \text{and is constrained so that} \quad \underline{\underline{\pi}} = \underline{\underline{\pi}}^{\mathrm{T}}, \tag{3.18}$$

where $\underline{\underline{\pi}}(\mathfrak{P};t)$ is the contravariant body-stress tensor introduced by Lodge [68, 70], which is taken to be symmetric (i.e., $\underline{\underline{\pi}} = \underline{\underline{\pi}}^{\mathrm{T}}$ where superscript 'T' denotes the transpose). Its matrix representation $\mathbb{\pi}$ $(= [\![\pi^{rc}]\!])$ in the body-coordinate system $\mathcal{B}$ has components $\pi^{ij} = \pi^{ji} = \pi^{ij}(\xi;t)$. The resulting contravariant vector $d\underline{\phi}(\mathfrak{P};t)$ is a differential force of contact acting on a material surface of infinitesimal area dA belonging to the mass element $\mathfrak{P}$ whose unit normal is given by $\underline{\nu}$ at time t.

The differential area dA is assumed to be small enough (on a macroscale) that the differential traction vector $d\underline{\phi}/dA$ (which ratios force to area) is independent of its area, yet it must be large enough (on the microscale) that the contact force $d\underline{\phi}$ exerted on area dA represents a statistical average taken over numerous inter-atomic and/or -molecular forces that comprise the mass element, thus granting us with a perspective, albeit vague, as to the (physical) size of a (mathematical) point in a continuum.

There are times when it is preferrable to decompose stress into a sum of hydrostatic and deviatoric (i.e., traceless) contributions, which can always be done. Here the contravariant, deviatoric, stress tensor, $\underline{\underline{\widetilde{\pi}}}(\mathfrak{P};t)$, is defined as

$$\underline{\underline{\widetilde{\pi}}} := \underline{\underline{\pi}} + p\,\underline{\underline{\gamma}}^{-1}, \quad \text{and is constrained so that} \quad \operatorname{tr}\underline{\underline{\widetilde{\pi}}} = 0, \tag{3.19a}$$

where the trace, $\operatorname{tr}\underline{\underline{\widetilde{\pi}}}$, is computed as $\underline{\underline{\widetilde{\pi}}} : \underline{\underline{\gamma}}$. From this expression follows the definition for hydrostatic pressure, $p(\mathfrak{P};t)$, which is a scalar field given by

$$p := -\tfrac{1}{3}\operatorname{tr}\underline{\underline{\pi}}, \tag{3.19b}$$

wherein $\operatorname{tr}\underline{\underline{\pi}}$ is determined as $\underline{\underline{\pi}} : \underline{\underline{\gamma}}$.

There are other times when it is preferrable to express stress as a contravariant extra-stress tensor, $\underline{\underline{\Pi}}(\mathfrak{P};t)$, defined by

$$\underline{\underline{\Pi}} := \underline{\underline{\pi}} + \wp\,\underline{\underline{\gamma}}^{-1}, \tag{3.20a}$$

with the scalar $\wp(\mathfrak{P};t)$ being a Lagrange multiplier that is subject to an isotropic constraint of material incompressiblity; namely,

$$\det \underline{\underline{\gamma}} = \det \underline{\underline{\gamma}}_0, \quad \text{or equivalently,} \quad \operatorname{tr} D\underline{\underline{\gamma}} = 0, \tag{3.20b}$$

recalling that $\operatorname{tr} D\underline{\underline{\gamma}} = \underline{\underline{\gamma}}^{-1} : D\underline{\underline{\gamma}}$. The extra stress is not, in general, a deviatoric tensor; that is, $\operatorname{tr} \underline{\underline{\mathbf{\Pi}}} = 3(\wp - p)$ need not be zero.

3.3.1 Rates

Like the metric-rate tensor, it is a straightforward matter to establish the stress-rate tensor, $D\underline{\underline{\pi}}$, via

$$D\underline{\underline{\pi}}(\mathfrak{P};t) = \lim_{t' \to t} \frac{\underline{\underline{\pi}}(\mathfrak{P};t) - \underline{\underline{\pi}}(\mathfrak{P};t')}{t - t'}, \tag{3.21a}$$

so that the rate of deviatoric stress, $D\underline{\underline{\widetilde{\pi}}}$, becomes

$$D\underline{\underline{\widetilde{\pi}}} = D\underline{\underline{\pi}} + (Dp)\underline{\underline{\gamma}}^{-1} + p\big(D\underline{\underline{\gamma}}^{-1}\big), \tag{3.21b}$$

which itself is not deviatoric because $D(\underline{\underline{\widetilde{\pi}}} : \underline{\underline{\gamma}}) = D(0) = 0$ implies that

$$\operatorname{tr} D\underline{\underline{\widetilde{\pi}}} \equiv \big(D\underline{\underline{\widetilde{\pi}}}\big) : \underline{\underline{\gamma}} = -\underline{\underline{\widetilde{\pi}}} : \big(D\underline{\underline{\gamma}}\big), \tag{3.21c}$$

and where hydrostatic pressure evolves according to

$$Dp = -\tfrac{1}{3}\Big(\big(D\underline{\underline{\pi}}\big) : \underline{\underline{\gamma}} + \underline{\underline{\pi}} : \big(D\underline{\underline{\gamma}}\big)\Big). \tag{3.21d}$$

To compute the fractal stress-rate tensor, $D^{\alpha}_{\star}\underline{\underline{\pi}}$, one must solve the integral equation

$$D^{\alpha}_{\star}\underline{\underline{\pi}}(\mathfrak{P};t_0,t) = \frac{1}{\Gamma(1-\alpha)} \int_{t_0}^{t} \frac{1}{(t-t')^{\alpha}} \big(D\underline{\underline{\pi}}\big)(\mathfrak{P};t')\, dt', \tag{3.22}$$

where $0 < \alpha < 1$, with like expressions applying for $D^{\alpha}_{\star}\underline{\underline{\widetilde{\pi}}}$ and $D^{\alpha}_{\star}p$.

Derivatives of the extra stress $\underline{\underline{\mathbf{\Pi}}}$ are handled differently, because the isotropic constraint $\wp\,\underline{\underline{\gamma}}^{-1}$ is actually a Lagrange multiplier and therefore it can be pulled outside the derivative.

Chapter 4

Field Transfer: Cartesian space-tensor fields

Body-tensor fields, space-tensor fields, Cartesian space-tensor fields, and the mappings between them, have all been carefully documented by Lodge in [68, 69, 70]. In Chp. 3 we presented the basic fields of body-tensor analysis. In this chapter we present an overview of Lodge's mappings from the body into Cartesian space. These results are stated without proof. An useful artifact of any such transfer of field (i.e., mapping from the body into Cartesian space) is that the resulting spatial fields are objective (viz., frame invariant). We also present a section containing new results for the field transfer of fractional-order derivatives and integrals.

The operation of field transfer makes it very plain as to whether a particular spatial field is Eulerian or Lagrangian. This characteristic of space tensors is affiliated with the time of field transfer. Eulerian fields result from a transfer of field at current time t, with this mapping being denoted by: *body field* $\overset{t}{\Longmapsto}$ *space field*; whereas, Lagrangian fields result from a transfer of field at some reference time—say, t_0 (which we arbitrarily take to be zero)—as denoted by: *body field* $\overset{t_0}{\Longmapsto}$ *space field*. Without a knowledge of these field transfers, it is often difficult to ascertain whether a particular space field is Eulerian or Lagrangian. Detailing the underlying mathematics of $\overset{t}{\Longmapsto}$ and $\overset{t_0}{\Longmapsto}$ is beyond the scope of this report. The interested reader is referred to either of the two texts by Lodge [68, 70].

4.1 Kinematics

In contrast with the constructs of the prior chapter, continuum $\mathbb{B}$ can also constitute an infinite set of point places, $\{\mathfrak{X}_0\}$, occupying a connected region in space, $\mathbb{S}$, at some arbitrary time t_0 denoting its reference state. Each place $\mathfrak{X}_0$ relates to a unique particle $\mathfrak{P}$ in $\mathbb{B}$ and is given a label of $\underline{X}$, which corresponds to the spatial position of $\mathfrak{X}_0$ (and therefore of $\mathfrak{P}$) in this reference configuration. Given an admissible, rectangular-Cartesian, coordinate system, $\mathcal{C}$, defined over $\mathbb{S}$, each place $\mathfrak{X}_0$ in $\mathbb{S}$ is thereby assigned a unique set of spatial coordinates, $\mathbb{X} = (\mathrm{X}_1, \mathrm{X}_2, \mathrm{X}_3)$, $\mathrm{X}_i \in \mathbb{R}$, such that $\mathcal{C}\colon \mathfrak{X}_0 \to \mathbb{X}$.

Later, at current time t ($t > t_0$), continuum $\mathbb{B}$ coincides with another infinite set of point places, $\{\mathfrak{X}\}$, that now occupies a different region in space, $\mathbb{S}$. Each place $\mathfrak{X}$ relates to a unique particle $\mathfrak{P}$ in $\mathbb{B}$ and is given a label of $\underline{x}$ with coordinates $x = (\mathrm{x}_1, \mathrm{x}_2, \mathrm{x}_3)$, which corresponds to the spatial position of $\mathfrak{X}$ (and therefore of $\mathfrak{P}$) in this current configuration. Consequently, $\mathcal{C}\colon \mathfrak{X} \to x$ where $\mathcal{C}$ is the same coordinate system used in the mapping $\mathcal{C}\colon \mathfrak{X}_0 \to \mathbb{X}$.

Particle $\mathfrak{P}$ moves through space $\mathbb{S}$ with a velocity, $\underline{v}(t)$, of

$$\underline{v} := \frac{\partial \underline{x}}{\partial t}, \tag{4.1}$$

whose matrix representation is given by $v = [\![\mathrm{v}_r]\!]$, with components, $\mathrm{v}_i = \partial \mathrm{x}_i / \partial t$, that are quantified in the Cartesian coordinate system $\mathcal{C}$.

The fundamental hypothesis of Cartesian continuum mechanics is that the motion at any location in the body is assumed to be sufficiently smooth in the sense that both

$$\delta \underline{x} = \underline{\underline{F}} \cdot \delta \underline{X} \quad \text{and} \quad \delta \underline{v} = \frac{\partial \underline{\underline{F}}}{\partial t} \cdot \delta \underline{X} = \frac{\partial \underline{\underline{F}}}{\partial t} \cdot \underline{\underline{F}}^{-1} \cdot \delta \underline{x} = \underline{\underline{L}} \cdot \delta \underline{x} \tag{4.2}$$

exist, where $\underline{\underline{F}}(t_0, t) := \partial \underline{x} / \partial \underline{X}$ defines the deformation-gradient tensor, and where $\underline{\underline{L}}(t) := \partial \underline{v} / \partial \underline{x}$ defines the velocity-gradient tensor, neither of which is symmetric. They have matrix representations of $\mathbb{F} = [\![\partial \mathrm{x}_r / \partial \mathrm{X}_c]\!]$ and $\mathbb{L} = [\![\partial \mathrm{v}_r / \partial \mathrm{x}_c]\!]$ in the coordinate system $\mathcal{C}$. The deformation gradient $\underline{\underline{F}}$ is positive definite because, from the conservation of mass,

$$0 < \frac{\varrho_0}{\varrho} = \det\left(\underline{\underline{F}}\right) < \infty, \tag{4.3}$$

and consequently, $\underline{\underline{F}}^{-1}(t_0, t) = \partial \underline{X} / \partial \underline{x}$ always exists. In contrast, $\underline{\underline{L}}$ is not positive definite, and as such, $\underline{\underline{L}}^{-1}$ does not exist, in general. A subtle yet important fact is that $\underline{\underline{F}}$ and $\underline{\underline{F}}^{-1}$ anchor to different locations; $\underline{\underline{F}}$ anchors to $\underline{X}$, while $\underline{\underline{F}}^{-1}$ anchors to $\underline{x}$.

Particle $\mathfrak{P}$ changes its motion through space $\mathbb{S}$ with an acceleration, $\underline{a}(t)$, of

$$\underline{a} := \frac{\partial \underline{v}}{\partial t} + \underline{\underline{L}} \cdot \underline{v}, \tag{4.4}$$

whose matrix representation is given by $\mathrm{a} = [\![\mathrm{a}_r]\!]$, with components a_i in coordinate system $\mathcal{C}$ quantified through the chain rule by $\mathrm{a}_i = \partial \mathrm{v}_i / \partial t + (\partial \mathrm{v}_i / \partial \mathrm{x}_k)(\partial \mathrm{x}_k / \partial t)$, where the repeated index k is summed over in the usual way.

Position, $\underline{x}$, velocity, $\underline{v}$, and acceleration, $\underline{a}$, are vector fields that establish kinematic attributes belonging to a point in space. The deformation gradient, $\underline{\underline{F}}$, and the velocity gradient, $\underline{\underline{L}}$, are tensor fields that establish additional kinematic attributes belonging to a point in a continuum.

4.2 Deformation Fields

In an Eulerian transfer of the various body-metric tensors into Cartesian space, Lodge [68, pg. 320] has shown that

$$\left.\begin{array}{ll} \underline{\underline{\gamma}} \overset{t}{\Longmapsto} \underline{\underline{I}}, & \underline{\underline{\gamma}}_0 \overset{t}{\Longmapsto} \underline{\underline{B}}^{-1} \\ \underline{\underline{\gamma}}^{-1} \overset{t}{\Longmapsto} \underline{\underline{I}}, & \underline{\underline{\gamma}}_0^{-1} \overset{t}{\Longmapsto} \underline{\underline{B}} \end{array}\right\}, \tag{4.5}$$

where $\underline{\underline{I}}$ is the unit tensor, and $\underline{\underline{B}}(\mathfrak{X}; t_0, t) := \underline{\underline{F}} \cdot \underline{\underline{F}}^{\mathrm{T}}$ is the symmetric, positive-definite, deformation tensor of Finger [32], today commonly referred to as the left, Cauchy-Green, deformation tensor. Its reciprocal field $\underline{\underline{B}}^{-1}(\mathfrak{X}; t_0, t) = \underline{\underline{F}}^{-\mathrm{T}} \cdot \underline{\underline{F}}^{-1}$ is the actual deformation tensor that was introduced by Cauchy [14, pp. 60–69].

A Lagrangian transfer of these same body-metric tensors produces

$$\left.\begin{array}{ll} \underline{\underline{\gamma}} \overset{t_0}{\Longmapsto} \underline{\underline{C}}, & \underline{\underline{\gamma}}_0 \overset{t_0}{\Longmapsto} \underline{\underline{I}} \\ \underline{\underline{\gamma}}^{-1} \overset{t_0}{\Longmapsto} \underline{\underline{C}}^{-1}, & \underline{\underline{\gamma}}_0^{-1} \overset{t_0}{\Longmapsto} \underline{\underline{I}} \end{array}\right\}, \tag{4.6}$$

where $\underline{\underline{C}}(\mathfrak{X}_0; t_0, t) := \underline{\underline{F}}^{\mathrm{T}} \cdot \underline{\underline{F}}$ is the symmetric, positive-definite, deformation tensor of Green [46], today commonly referred to as the right, Cauchy-Green, deformation tensor. The inverse of this metric, $\underline{\underline{C}}^{-1}(\mathfrak{X}_0; t_0, t)$, is computed as $\underline{\underline{F}}^{-1} \cdot \underline{\underline{F}}^{-\mathrm{T}}$.

It is apparent from the above results that the mappings $\overset{t}{\Longmapsto}$ and $\overset{t_0}{\Longmapsto}$ are many-to-one. This consequence arises from the fact that Cartesian vector and tensor fields do not distinguish between tensorial kind (i.e., between covariant and contravariant indices in their coordinate transformation laws, because the Jacobian is restricted to be orthogonal for Cartesian fields), and as such, there is a loss of this information during these mappings.*

4.2.1 Duals

Finger [32] introduced both dual-metric tensors (viz., $\underline{\underline{B}}$ and $\underline{\underline{C}}^{-1}$) into the literature. It is well known that the fundamental metric tensors of the Eulerian and Lagrangian frames (i.e., $\underline{\underline{B}}^{-1}$ and $\underline{\underline{C}}$, respectively) measure change in an infinitesimal length-of-line according to

$$(dS_0)^2 = d\underline{x} \cdot \underline{\underline{B}}^{-1} \cdot d\underline{x} \quad \text{and} \quad (dS)^2 = d\underline{X} \cdot \underline{\underline{C}} \cdot d\underline{X}. \tag{4.7}$$

Less known, and proven by Truesdell [108], is that the normalized inverse metrics $\underline{\underline{B}} \,/\, \det \underline{\underline{B}}$ and $\underline{\underline{C}}^{-1} / \det \underline{\underline{C}}^{-1}$ provide a like geometric interpretation; specifically, they

*General space-tensor fields do distinguish between kind in their coordinate transformation laws, and as such, field transfer between body-tensor fields and general space-tensor fields have mappings that are one-to-one. General space-tensor fields are not introduced in this report. The interested reader is referred to any one of the many excellent texts on the subject (e.g., Sokolnikoff [106]).

measure change in an infinitesimal area-of-surface according to[†]

$$(dA_0)^2 = \big(d\underline{x} \times \widehat{d\underline{x}}\big) \cdot \frac{\underline{\underline{B}}}{\det \underline{\underline{B}}} \cdot \big(d\underline{x} \times \widehat{d\underline{x}}\big) \quad \text{and} \quad (dA)^2 = \big(d\underline{X} \times \widehat{d\underline{X}}\big) \cdot \frac{\underline{\underline{C}}^{-1}}{\det \underline{\underline{C}}^{-1}} \cdot \big(d\underline{X} \times \widehat{d\underline{X}}\big), \tag{4.8a}$$

or equivalently, according to

$$\left(\frac{dA_0}{dA}\right)^2 = \underline{n} \cdot \frac{\underline{\underline{B}}}{\det \underline{\underline{B}}} \cdot \underline{n} \quad \text{and} \quad \left(\frac{dA}{dA_0}\right)^2 = \underline{N} \cdot \frac{\underline{\underline{C}}^{-1}}{\det \underline{\underline{C}}^{-1}} \cdot \underline{N}, \tag{4.8b}$$

where $\underline{n}$ and $\underline{N}$ are the Eulerian and Lagrangian unit-normal vectors to a material surface, which relate to one-another via the pull-back formula $\underline{N}\, dA_0 = d\underline{X} \times \widehat{d\underline{X}} = (\det \underline{\underline{F}})^{-1} \underline{\underline{F}}^{\mathrm{T}} \cdot (d\underline{x} \times \widehat{d\underline{x}}) = (\det \underline{\underline{F}})^{-1} \underline{\underline{F}}^{\mathrm{T}} \cdot \underline{n}\, dA$. Truesdell [108] closes his little-known paper with the following insightful theorem.

> "The elements of area suffering extremal changes are normal to the principal directions of stretch, and the greatest (least) change of area occurs in the plane normal to the axis of least (greatest) stretch; in fact, if the principal stretches dS/dS_0 satisfy $\lambda_1 \geq \lambda_2 \geq \lambda_3$ the corresponding ratios dA/dA_0 satisfy $\lambda_2\lambda_3 \leq \lambda_1\lambda_3 \leq \lambda_1\lambda_2$."

4.2.2 Rates

In an Eulerian transfer of field, Lodge [68, pp. 321–327] also determined that the various metric-rates of the body map into Cartesian space as

$$\left.\begin{aligned} D\underline{\underline{\gamma}} &\overset{t}{\longmapsto} 2\underline{\underline{D}}, & D\underline{\underline{\gamma}}_0 = \underline{\underline{0}} &\overset{t}{\longmapsto} \overset{\triangledown}{\underline{\underline{B}}}{}^{-1} = \underline{\underline{0}} \\ D\underline{\underline{\gamma}}^{-1} &\overset{t}{\longmapsto} -2\underline{\underline{D}}, & D\underline{\underline{\gamma}}_0^{-1} = \underline{\underline{0}} &\overset{t}{\longmapsto} \overset{\triangle}{\underline{\underline{B}}} = \underline{\underline{0}} \end{aligned}\right\}, \tag{4.9}$$

where

$$\underline{\underline{D}}(\mathfrak{X}; t) := \tfrac{1}{2}\big(\underline{\underline{L}} + \underline{\underline{L}}^{\mathrm{T}}\big) \tag{4.10}$$

is the symmetric rate-of-deformation tensor. The resulting rates, expressed below for some arbitrary tensor $\underline{\underline{J}}$, are defined by

$$\overset{\triangledown}{\underline{\underline{J}}} := \dot{\underline{\underline{J}}} + \underline{\underline{L}}^{\mathrm{T}} \cdot \underline{\underline{J}} + \underline{\underline{J}} \cdot \underline{\underline{L}} \quad \text{and} \quad \overset{\triangle}{\underline{\underline{J}}} := \dot{\underline{\underline{J}}} - \underline{\underline{L}} \cdot \underline{\underline{J}} - \underline{\underline{J}} \cdot \underline{\underline{L}}^{\mathrm{T}}, \tag{4.11}$$

which denote the lower- and upper-convected derivatives, respectively, of Oldroyd [83]. They reduce to Lie derivatives taken with respect to velocity $\underline{v}$ whenever $\partial \underline{\underline{J}}/\partial t = \underline{\underline{0}}$. The common contributing term in these two formulæ,

$$\dot{\underline{\underline{J}}} := \frac{\partial \underline{\underline{J}}}{\partial t} + \big(\underline{\nabla} \underline{\underline{J}}\big) \cdot \underline{v}, \tag{4.12}$$

[†]We arrived at (3.3) by field transfer. Specifically, we mapped the tensor relations derived by Truesdell [108] from general space into the body, which is a one-to-one operation. Then by executing another transfer of field, this time mapping the formulæ in (3.3) from the body into Cartesian space, which is a many-to-one operation, we arrived at (4.8a).

is called the material derivative of $\underline{\underline{J}}$, which has a matrix representation of $\dot{J} = [\![\partial \mathrm{J}_{rc}/\partial t + (\partial \mathrm{J}_{rc}/\partial \mathrm{x}_k)\mathrm{v}_k]\!]$ in the coordinate system $\mathcal{C}$. Here the vector operator $\underline{\nabla}$ denotes the spatial gradient $\partial/\partial \underline{x}$.

The formulæ $\overset{\vartriangle}{\underline{\underline{B}}} = \underline{\underline{0}}$ and $\overset{\triangledown}{\underline{\underline{B}}}^{-1} = \underline{\underline{0}}$ of (4.9) can be rewritten as quasi-linear evolution equations for the Finger, $\underline{\underline{B}}$, and Cauchy, $\underline{\underline{B}}^{-1}$, deformation tensors; specifically,

$$\overset{\circ}{\underline{\underline{B}}} = \underline{\underline{D}} \cdot \underline{\underline{B}} + \underline{\underline{B}} \cdot \underline{\underline{D}} \quad \text{and} \quad \overset{\circ}{\underline{\underline{B}}}^{-1} = -\underline{\underline{D}} \cdot \underline{\underline{B}}^{-1} - \underline{\underline{B}}^{-1} \cdot \underline{\underline{D}}, \tag{4.13}$$

where the resulting rate, when expressed for an arbitrary tensor $\underline{\underline{J}}$, is defined by

$$\overset{\circ}{\underline{\underline{J}}} := \dot{\underline{\underline{J}}} - \underline{\underline{W}} \cdot \underline{\underline{J}} + \underline{\underline{J}} \cdot \underline{\underline{W}}, \tag{4.14}$$

and is called the corotational derivative, which was introduced by Zaremba [110] and is usually credited to Jaumann‡, wherein

$$\underline{\underline{W}}(\mathfrak{X}; t) := \tfrac{1}{2}\big(\underline{\underline{L}} - \underline{\underline{L}}^{\mathrm{T}}\big) \tag{4.15}$$

is the skew-symmetric vorticity tensor. The quasi-linear evolution equation for Finger deformation in (4.13) lies at the heart of Leonov's [63] viscoelastic theory.

The corotational $\overset{\circ}{\underline{\underline{J}}}$ and lower-convected $\overset{\triangledown}{\underline{\underline{J}}}$ deriviatives of any tensor $\underline{\underline{J}}$ are related via

$$\overset{\circ}{\underline{\underline{J}}} = \overset{\triangledown}{\underline{\underline{J}}} - \underline{\underline{D}} \cdot \underline{\underline{J}} - \underline{\underline{J}} \cdot \underline{\underline{D}}. \tag{4.16a}$$

Similarly, the corotational $\overset{\circ}{\underline{\underline{J}}}$ and upper-convected $\overset{\vartriangle}{\underline{\underline{J}}}$ derivatives relate according to

$$\overset{\circ}{\underline{\underline{J}}} = \overset{\vartriangle}{\underline{\underline{J}}} + \underline{\underline{D}} \cdot \underline{\underline{J}} + \underline{\underline{J}} \cdot \underline{\underline{D}}, \tag{4.16b}$$

where $\underline{\underline{D}}$ is the rate-of-deformation tensor. From these identities, one quickly arrives at the evolution equations (4.13) for $\overset{\circ}{\underline{\underline{B}}}$ and $\overset{\circ}{\underline{\underline{B}}}^{-1}$, given the field transfer results of (4.9).

We point out that rates $\overset{\vartriangle}{\underline{\underline{B}}}(\mathfrak{X}; t_0, t)$, $\overset{\circ}{\underline{\underline{B}}}(\mathfrak{X}; t_0, t)$, $\overset{\triangledown}{\underline{\underline{B}}}^{-1}(\mathfrak{X}; t_0, t)$ and $\overset{\circ}{\underline{\underline{B}}}^{-1}(\mathfrak{X}; t_0, t)$ are all two-state tensor fields.

In Eulerian transfers of field where time-based derivatives of absolute, symmetric, second-rank, body-tensor fields are being mapped into Catesian space, the partial derivative of a covariant body tensor maps into a lower-convected derivative, while the partial derivative of a contravariant body tensor maps into an upper-convected derivative.

‡Contrary to numerous citations sprinkled throughout the literature, Jaumann did not publish the corotational derivative until 1911 [55], where it is given for both vector and tensor fields. An explicit definition of the corotational derivative does not appear in his book [54] of 1905. Zaremba [110] was the first to publish the corotational derivative of a tensor field, which he did in 1903. Nowhere (known to us) did Zeremba publish the corotational derivative of a vector field.

In a Lagrangian transfer of field, the body-metric rates map into Cartesian space according to

$$\left.\begin{aligned} D\underline{\underline{\gamma}} &\overset{t_0}{\Longmapsto} D\underline{\underline{C}} = 2\,\underline{\underline{F}}^{\mathrm{T}}\cdot\underline{\underline{D}}\cdot\underline{\underline{F}}, & D\underline{\underline{\gamma}}_0 = \underline{\underline{0}} &\overset{t_0}{\Longmapsto} D\underline{\underline{I}} = \underline{\underline{0}} \\ D\underline{\underline{\gamma}}^{-1} &\overset{t_0}{\Longmapsto} D\underline{\underline{C}}^{-1} = -2\,\underline{\underline{F}}^{-1}\cdot\underline{\underline{D}}\cdot\underline{\underline{F}}^{-\mathrm{T}}, & D\underline{\underline{\gamma}}_0^{-1} = \underline{\underline{0}} &\overset{t_0}{\Longmapsto} D\underline{\underline{I}} = \underline{\underline{0}} \end{aligned}\right\}, \tag{4.17}$$

where $D\underline{\underline{C}}(\mathfrak{X}_0;t_0,t)$ and $D\underline{\underline{C}}^{-1}(\mathfrak{X}_0;t_0,t)$ are two-state tensor rates, and by $D\underline{\underline{C}}^{-1}$ we mean $D(\underline{\underline{C}}^{-1})$ and not $(D\underline{\underline{C}})^{-1}$, the latter of which does not exist, in general.

Fractional order

Because the process of integration commutes with the operation of field transfer [70, pg. 111], it therefore follows from the preceeding formulæ that the Caputo derivative (1.3) of the metric tensor, $D^\alpha_\star\underline{\underline{\gamma}}(\mathfrak{P};t_0,t)$, maps into Cartesian space in a Lagrangian frame as $D^\alpha_\star\underline{\underline{C}}(\mathfrak{X}_0;t_0,t)$ according to

$$\begin{aligned} D^\alpha_\star\underline{\underline{\gamma}} &= \frac{1}{\Gamma(1-\alpha)}\int_{t_0}^t \frac{1}{(t-t')^\alpha}\,\frac{\partial\underline{\underline{\gamma}}(t')}{\partial t'}\,dt' \\ &\overset{t_0}{\Longmapsto} \begin{cases} D^\alpha_\star\underline{\underline{C}} = \dfrac{1}{\Gamma(1-\alpha)}\displaystyle\int_{t_0}^t \frac{1}{(t-t')^\alpha}\,\frac{\partial\underline{\underline{C}}(t_0,t')}{\partial t'}\,dt' \\ \qquad = \dfrac{2}{\Gamma(1-\alpha)}\displaystyle\int_{t_0}^t \frac{1}{(t-t')^\alpha}\,\underline{\underline{F}}_{t'}^{\mathrm{T}}\cdot\underline{\underline{D}}(t')\cdot\underline{\underline{F}}_{t'}\,dt'. \end{cases} \end{aligned} \tag{4.18a}$$

In like manner, the Caputo derivative of the dual metric, $D^\alpha_\star\underline{\underline{\gamma}}^{-1}(\mathfrak{P};t_0,t)$, maps as $D^\alpha_\star\underline{\underline{C}}^{-1}(\mathfrak{X}_0;t_0,t)$ according to

$$\begin{aligned} D^\alpha_\star\underline{\underline{\gamma}}^{-1} &= \frac{1}{\Gamma(1-\alpha)}\int_{t_0}^t \frac{1}{(t-t')^\alpha}\,\frac{\partial\underline{\underline{\gamma}}^{-1}(t')}{\partial t'}\,dt' \\ &\overset{t_0}{\Longmapsto} \begin{cases} D^\alpha_\star\underline{\underline{C}}^{-1} = \dfrac{1}{\Gamma(1-\alpha)}\displaystyle\int_{t_0}^t \frac{1}{(t-t')^\alpha}\,\frac{\partial\underline{\underline{C}}^{-1}(t_0,t')}{\partial t'}\,dt' \\ \qquad = \dfrac{-2}{\Gamma(1-\alpha)}\displaystyle\int_{t_0}^t \frac{1}{(t-t')^\alpha}\,\underline{\underline{F}}_{t'}^{-1}\cdot\underline{\underline{D}}(t')\cdot\underline{\underline{F}}_{t'}^{-\mathrm{T}}\,dt', \end{cases} \end{aligned} \tag{4.18b}$$

where the order of differentiation has been restricted to the range $0<\alpha<1$. The deformation tensors present in these formulæ are anchored to state t_0. These derivatives have units in time t of order $t^{-\alpha}$.

Given that $a<b$, the notation $\underline{\underline{F}}(a,b)$ implies $\partial\underline{x}(b)/\partial\underline{x}(a)$, while $\underline{\underline{F}}^{-1}(a,b)$ implies $\partial\underline{x}(a)/\partial\underline{x}(b)$, thereby establishing notation for a generalized deformation-gradient tensor. Changing the order of the arguments in the deformation gradient is equivalent to taking its inverse. So we adopt a notation for the deformation gradient wherein the numeric value of the first argument is always less than that of the second, and we invert the field, as needed, to satisfy this requirement. Whenever $a=t_0$, the

shortened notation of $\underline{\underline{F}}_{t'} := \underline{\underline{F}}(t_0, t')$ is used, and whenever $a = t_0$ and $b = t$, the accepted notation of $\underline{\underline{F}} := \underline{\underline{F}}(t_0, t)$ is used, otherwise $\underline{\underline{F}}(a, b)$ is used.

Following in this notation, let $\underline{\underline{B}}(a, b) := \underline{\underline{F}}(a, b) \cdot \underline{\underline{F}}^{\mathrm{T}}(a, b)$ define a generalized Finger deformation and let $\underline{\underline{C}}(a, b) := \underline{\underline{F}}^{\mathrm{T}}(a, b) \cdot \underline{\underline{F}}(a, b)$ define a generalized Green deformation. In their arguments, the first state, a, denotes the initial (or reference) state; whereas, the second state, b, denotes the final (or current) state.

In an Eulerian transfer of field, the Caputo derivatives $D^{\alpha}_{\star}\underline{\underline{\gamma}}$ and $D^{\alpha}_{\star}\underline{\underline{\gamma}}^{-1}$ map into Cartesian space according to

$$
\begin{aligned}
D^{\alpha}_{\star}\underline{\underline{\gamma}} &= \frac{1}{\Gamma(1-\alpha)} \int_{t_0}^{t} \frac{1}{(t-t')^{\alpha}} \frac{\partial \underline{\underline{\gamma}}(t')}{\partial t'}\, dt' \\
&\overset{t}{\longmapsto} \begin{cases} 2\,\overset{\alpha\downarrow}{\underline{\underline{D}}} := \dfrac{1}{\Gamma(1-\alpha)} \displaystyle\int_{t_0}^{t} \frac{1}{(t-t')^{\alpha}} \frac{\partial \underline{\underline{B}}^{-1}(t', t)}{\partial t'}\, dt' \\ \qquad = \dfrac{2}{\Gamma(1-\alpha)} \displaystyle\int_{t_0}^{t} \frac{1}{(t-t')^{\alpha}} \underline{\underline{F}}^{-\mathrm{T}}(t', t) \cdot \underline{\underline{D}}(t') \cdot \underline{\underline{F}}^{-1}(t', t)\, dt', \end{cases}
\end{aligned}
\tag{4.19a}
$$

and

$$
\begin{aligned}
D^{\alpha}_{\star}\underline{\underline{\gamma}}^{-1} &= \frac{1}{\Gamma(1-\alpha)} \int_{t_0}^{t} \frac{1}{(t-t')^{\alpha}} \frac{\partial \underline{\underline{\gamma}}^{-1}(t')}{\partial t'}\, dt' \\
&\overset{t}{\longmapsto} \begin{cases} -2\,\overset{\alpha\uparrow}{\underline{\underline{D}}} := \dfrac{1}{\Gamma(1-\alpha)} \displaystyle\int_{t_0}^{t} \frac{1}{(t-t')^{\alpha}} \frac{\partial \underline{\underline{B}}(t', t)}{\partial t'}\, dt' \\ \qquad = \dfrac{-2}{\Gamma(1-\alpha)} \displaystyle\int_{t_0}^{t} \frac{1}{(t-t')^{\alpha}} \underline{\underline{F}}(t', t) \cdot \underline{\underline{D}}(t') \cdot \underline{\underline{F}}^{\mathrm{T}}(t', t)\, dt', \end{cases}
\end{aligned}
\tag{4.19b}
$$

with $\overset{\alpha\uparrow}{\underline{\underline{D}}}$ first appearing in a paper written by Drozdov [27] but in a different notation. Notice that the deformation tensors in the integrands are now anchored to the floating state t', which is the dummy variable of integration, instead of to the fixed inital state t_0. Also notice that the derivatives in the integrands (e.g., $\partial \underline{\underline{B}}(t', t)/\partial t'$) are taken at the reference state of the field (i.e., t') instead of at its current state (viz. t).

The rate-of-deformation tensor, $\underline{\underline{D}}$, has no distinction between tensor kind; however, its fractional counterparts have covariant-like, $\overset{\alpha\downarrow}{\underline{\underline{D}}}$, and contravariant-like, $\overset{\alpha\uparrow}{\underline{\underline{D}}}$, constituents.

The above expressions for the fractional rate-of-deformation tensors can be changed to anchor to the reference state t_0 by an appropriate application of the chain rule for differentiation. In doing so, the lower-fractal rate-of-deformation tensor, $\overset{\alpha\downarrow}{\underline{\underline{D}}}(\mathfrak{X}; t_0, t)$, of order α, with $0 < \alpha < 1$, can be rewritten as

$$
\begin{aligned}
\overset{\alpha\downarrow}{\underline{\underline{D}}} &= \underline{\underline{F}}^{-\mathrm{T}} \cdot \left(\frac{1}{\Gamma(1-\alpha)} \int_{t_0}^{t} \frac{1}{(t-t')^{\alpha}} \underline{\underline{F}}^{\mathrm{T}}_{t'} \cdot \underline{\underline{D}}(t') \cdot \underline{\underline{F}}_{t'}\, dt' \right) \cdot \underline{\underline{F}}^{-1} \\
&= \tfrac{1}{2}\, \underline{\underline{F}}^{-\mathrm{T}} \cdot \left(D^{\alpha}_{\star}\underline{\underline{C}} \right) \cdot \underline{\underline{F}}^{-1},
\end{aligned}
\tag{4.20a}
$$

where the deformation gradients $\underline{\underline{F}}^{-\mathrm{T}}$ and $\underline{\underline{F}}^{-1}$ can be taken outside the integral because their state dependence corresponds with the limits of integration. Likewise,

the upper-fractal rate-of-deformation tensor, $\overset{\alpha\mathrm{f}}{\underline{\underline{D}}}(\mathfrak{X};t_0,t)$, can be expressed as

$$\begin{aligned}\overset{\alpha\mathrm{f}}{\underline{\underline{D}}} &= \underline{\underline{F}}\cdot\left(\frac{1}{\Gamma(1-\alpha)}\int_{t_0}^{t}\frac{1}{(t-t')^{\alpha}}\,\underline{\underline{F}}_{t'}^{-1}\cdot\underline{\underline{D}}(t')\cdot\underline{\underline{F}}_{t'}^{-\mathrm{T}}\,dt'\right)\cdot\underline{\underline{F}}^{\mathrm{T}} \\ &= -\tfrac{1}{2}\,\underline{\underline{F}}\cdot\left(D_{\star}^{\alpha}\underline{\underline{C}}^{-1}\right)\cdot\underline{\underline{F}}^{\mathrm{T}}.\end{aligned} \tag{4.20b}$$

From these results it is apparent that the Lagrangian fields $D_{\star}^{\alpha}\underline{\underline{C}}$ and $D_{\star}^{\alpha}\underline{\underline{C}}^{-1}$ are the fundamental (most basic) measures for fractional deformation rates in a spatial formulation in that they are actual Caputo derivatives.

The Lagrangian and Eulerian, fractal, deformation rates of (4.18 & 4.19) are compatible (in the limit as α goes to 1 from below) with their first-order counterparts, which are: $D\underline{\underline{C}} = 2\,\underline{\underline{F}}^{\mathrm{T}}\cdot\underline{\underline{D}}\cdot\underline{\underline{F}}$ and $D\underline{\underline{C}}^{-1} = -2\,\underline{\underline{F}}^{-1}\cdot\underline{\underline{D}}\cdot\underline{\underline{F}}^{-\mathrm{T}}$.

4.3 Field Transfer of Fractional Operators

We are now in a position to map fractional-order derivatives and integrals of any absolute, symmetric, body-tensor field into Cartesian space in both the Eulerian and Lagrangian frames of reference.

We begin by considering an arbitrary, symmetric, covariant, body tensor, $\underline{\underline{\boldsymbol{\mu}}}$, and an arbitrary, symmetric, contravariant, body tensor, $\underline{\underline{\boldsymbol{\eta}}}$, whose mappings into Cartesian space are known. For purposes of illustration, consider a transfer of covariant field that is given by

$$\underline{\underline{\boldsymbol{\mu}}}(\mathfrak{P};t)\ \begin{cases}\overset{t}{\longmapsto} & \underline{\underline{M}}(\mathfrak{X};t),\\ \overset{t_0}{\longmapsto} & \underline{\underline{N}}(\mathfrak{X}_0;t_0,t),\end{cases}\quad\text{such that}\quad \underline{\underline{N}} = \underline{\underline{F}}^{\mathrm{T}}\cdot\underline{\underline{M}}\cdot\underline{\underline{F}}, \tag{4.21a}$$

and consider a transfer of contravariant field that is given by

$$\underline{\underline{\boldsymbol{\eta}}}(\mathfrak{P};t)\ \begin{cases}\overset{t}{\longmapsto} & \underline{\underline{G}}(\mathfrak{X};t),\\ \overset{t_0}{\longmapsto} & \underline{\underline{H}}(\mathfrak{X}_0;t_0,t),\end{cases}\quad\text{such that}\quad \underline{\underline{H}} = \underline{\underline{F}}^{-1}\cdot\underline{\underline{G}}\cdot\underline{\underline{F}}^{-\mathrm{T}}, \tag{4.21b}$$

where $\underline{\underline{M}}$ and $\underline{\underline{G}}$ are some arbitrary (but known), symmetric, Eulerian, tensor fields, with $\underline{\underline{N}}$ and $\underline{\underline{H}}$ designating their respective, symmetric, Lagrangian, tensor fields. In these transformations of field, the deformation gradient $\underline{\underline{F}}$ serves as a Jacobian of transformation between the Cartesian frames that pulls a known Eulerian field backwards, out of the Eulerian frame and into the Lagrangian frame.

Lodge [68, pp. 321–327] has shown that the time rate-of-change D of a symmetric covariant tensor $\underline{\underline{\boldsymbol{\mu}}}$ maps into Cartesian space as

$$D\underline{\underline{\boldsymbol{\mu}}}\ \begin{cases}\overset{t}{\longmapsto} & \overset{\triangledown}{\underline{\underline{M}}},\\ \overset{t_0}{\longmapsto} & D\underline{\underline{N}},\end{cases}\quad\text{such that}\quad D\underline{\underline{N}} = \underline{\underline{F}}^{\mathrm{T}}\cdot\overset{\triangledown}{\underline{\underline{M}}}\cdot\underline{\underline{F}}, \tag{4.22a}$$

while the time rate-of-change of a symmetric contravariant tensor $\underline{\underline{\boldsymbol{\eta}}}$ maps as

$$D\underline{\underline{\boldsymbol{\eta}}} \begin{cases} \overset{t}{\longmapsto} & \overset{\vartriangle}{\underline{\underline{G}}}, \\ \overset{t_0}{\longmapsto} & D\underline{\underline{H}}, \end{cases} \quad \text{such that} \quad D\underline{\underline{H}} = \underline{\underline{F}}^{-1} \cdot \overset{\vartriangle}{\underline{\underline{G}}} \cdot \underline{\underline{F}}^{-\mathrm{T}}, \tag{4.22b}$$

where $\overset{\triangledown}{\underline{\underline{M}}}$ and $\overset{\vartriangle}{\underline{\underline{G}}}$ are the lower- and upper-convected derivatives defined in (4.11), while $D\underline{\underline{N}}$ and $D\underline{\underline{H}}$ are simple first-order derivatives, as their notation suggests. The pull-back formulæ in (4.22) can also be derived by differentiating the pull-back formulæ of (4.21), as one would expect.

Assuming that the above information is known to us, it is a straightforward matter to construct the special derivatives of interest.

4.3.1 Derivatives

Here we prove that the Caputo derivative $D^{\alpha}_{\star}$ (1.8a) of a symmetric covariant tensor $\underline{\underline{\boldsymbol{\mu}}}$ maps into Cartesian space as

$$D^{\alpha}_{\star}\underline{\underline{\boldsymbol{\mu}}} \begin{cases} \overset{t}{\longmapsto} & \mathfrak{D}^{\alpha\downarrow}_{\star}\underline{\underline{M}}, \\ \overset{t_0}{\longmapsto} & D^{\alpha}_{\star}\underline{\underline{N}}, \end{cases} \quad \text{such that} \quad D^{\alpha}_{\star}\underline{\underline{N}} = \underline{\underline{F}}^{\mathrm{T}} \cdot \left(\mathfrak{D}^{\alpha\downarrow}_{\star}\underline{\underline{M}}\right) \cdot \underline{\underline{F}}, \tag{4.23a}$$

while the Caputo derivative of a symmetric contravariant tensor $\underline{\underline{\boldsymbol{\eta}}}$ maps as

$$D^{\alpha}_{\star}\underline{\underline{\boldsymbol{\eta}}} \begin{cases} \overset{t}{\longmapsto} & \mathfrak{D}^{\alpha\uparrow}_{\star}\underline{\underline{G}}, \\ \overset{t_0}{\longmapsto} & D^{\alpha}_{\star}\underline{\underline{H}}, \end{cases} \quad \text{such that} \quad D^{\alpha}_{\star}\underline{\underline{H}} = \underline{\underline{F}}^{-1} \cdot \left(\mathfrak{D}^{\alpha\uparrow}_{\star}\underline{\underline{G}}\right) \cdot \underline{\underline{F}}^{-\mathrm{T}}. \tag{4.23b}$$

The Eulerian tensors $\mathfrak{D}^{\alpha\downarrow}_{\star}\underline{\underline{M}}$ and $\mathfrak{D}^{\alpha\uparrow}_{\star}\underline{\underline{G}}$ are objective rates of order α defined in (4.26), where notation '$\alpha\downarrow$' is affiliated with covariant-like fields, while notation '$\alpha\uparrow$' is affiliated with contravariant-like fields. Unlike $D^{\alpha}_{\star}\underline{\underline{N}}$ and $D^{\alpha}_{\star}\underline{\underline{H}}$, which are actual Caputo derivatives, derivatives $\mathfrak{D}^{\alpha\downarrow}_{\star}\underline{\underline{M}}$ and $\mathfrak{D}^{\alpha\uparrow}_{\star}\underline{\underline{G}}$ are not Caputo derivatives, in a strict sense of the definition, which is why they are given a different notation. For this reason, Lagrangian Caputo derivatives are considered the more fundamental of these fractional rates.

In the derivations that follow, which prove the above mappings, α is restricted to the range $0 < \alpha < 1$.

Proof: The Caputo derivative of symmetric body-tensor fields map into Cartesian space in a Lagrangian frame in an intuitive way. For example, for a covariant tensor $\underline{\underline{\boldsymbol{\mu}}}$, its fractional derivative maps as

$$\begin{aligned} D^{\alpha}_{\star}\underline{\underline{\boldsymbol{\mu}}} &= \frac{1}{\Gamma(1-\alpha)} \int_{t_0}^{t} \frac{1}{(t-t')^{\alpha}} \frac{\partial \underline{\underline{\boldsymbol{\mu}}}(t')}{\partial t'}\, dt' \\ \overset{t_0}{\longmapsto} D^{\alpha}_{\star}\underline{\underline{N}} &= \frac{1}{\Gamma(1-\alpha)} \int_{t_0}^{t} \frac{1}{(t-t')^{\alpha}} \frac{\partial \underline{\underline{N}}(t_0,t')}{\partial t'}\, dt', \end{aligned} \tag{4.24a}$$

whereas, for a contravariant tensor $\underline{\underline{\boldsymbol{\eta}}}$, its fractional derivative maps as

$$\begin{aligned} D^{\alpha}_{\star}\underline{\underline{\boldsymbol{\eta}}} &= \frac{1}{\Gamma(1-\alpha)}\int_{t_0}^{t}\frac{1}{(t-t')^{\alpha}}\frac{\partial\underline{\underline{\boldsymbol{\eta}}}(t')}{\partial t'}\,dt' \\ &\overset{t_0}{\Longmapsto} D^{\alpha}_{\star}\underline{\underline{H}} = \frac{1}{\Gamma(1-\alpha)}\int_{t_0}^{t}\frac{1}{(t-t')^{\alpha}}\frac{\partial\underline{\underline{H}}(t_0,t')}{\partial t'}\,dt'. \end{aligned} \tag{4.24b}$$

These mappings reproduce standard definitions for Caputo derivatives of spatial fields. What is noteworthy about these mappings is that the argument list belonging to the spatial fields being differentiated under the integral sign is (t_0, t'), designating a fixed referenced state at t_0 with differentiation under the integrand occurring at the second state t'.

The mappings of these same Caputo derivatives (i.e., $D^{\alpha}_{\star}\underline{\underline{\boldsymbol{\mu}}}$ and $D^{\alpha}_{\star}\underline{\underline{\boldsymbol{\eta}}}$) from the body into Cartesian space in an Eulerian frame is a more subtle process. Before one can proceed, we must know how body-tensor fields from a past state map into Cartesian space in the present state, which they do according to

$$\left.\begin{aligned} \underline{\underline{\boldsymbol{\mu}}}(t') &\overset{t}{\Longmapsto} \underline{\underline{F}}^{-\mathrm{T}}(t',t)\cdot\underline{\underline{M}}(t')\cdot\underline{\underline{F}}^{-1}(t',t) \\ \underline{\underline{\boldsymbol{\eta}}}(t') &\overset{t}{\Longmapsto} \underline{\underline{F}}(t',t)\cdot\underline{\underline{G}}(t')\cdot\underline{\underline{F}}^{\mathrm{T}}(t',t) \end{aligned}\right\} \quad t_0\le t'\le t, \tag{4.25a}$$

where

$$\underline{\underline{\boldsymbol{\mu}}}(t') \overset{t'}{\Longmapsto} \underline{\underline{M}}(t') \quad\text{and}\quad \underline{\underline{\boldsymbol{\eta}}}(t') \overset{t'}{\Longmapsto} \underline{\underline{G}}(t'). \tag{4.25b}$$

These transfers of field are distinct from the Eulerian transfers listed in (4.21). Here the deformation gradient $\underline{\underline{F}}(t',t)$ serves as a Jacobian of transformation that pushs-forward a field that was anchored at some prior time t' into a like field that is now anchored at present time t.

From the above formulæ, it readily follows that the Caputo derivative of a symmetric covariant tensor $\underline{\underline{\boldsymbol{\mu}}}$ maps into Cartesian space in the Eulerian frame as

$$\begin{aligned} D^{\alpha}_{\star}\underline{\underline{\boldsymbol{\mu}}} &= \frac{1}{\Gamma(1-\alpha)}\int_{t_0}^{t}\frac{1}{(t-t')^{\alpha}}\frac{\partial\underline{\underline{\boldsymbol{\mu}}}(t')}{\partial t'}\,dt' \\ &\overset{t}{\Longmapsto}\left\{\begin{aligned} \mathfrak{D}^{\alpha\mathrm{l}}_{\star}\underline{\underline{M}} &:= \frac{1}{\Gamma(1-\alpha)}\int_{t_0}^{t}\frac{1}{(t-t')^{\alpha}}\frac{\partial}{\partial t'}\Big(\underline{\underline{F}}^{-\mathrm{T}}(t',t)\cdot\underline{\underline{M}}(t')\cdot\underline{\underline{F}}^{-1}(t',t)\Big)dt' \\ &= \frac{1}{\Gamma(1-\alpha)}\int_{t_0}^{t}\frac{1}{(t-t')^{\alpha}}\underline{\underline{F}}^{-\mathrm{T}}(t',t)\cdot\overset{\triangledown}{\underline{\underline{M}}}(t')\cdot\underline{\underline{F}}^{-1}(t',t)\,dt' \\ &= \underline{\underline{F}}^{-\mathrm{T}}\cdot\left(\frac{1}{\Gamma(1-\alpha)}\int_{t_0}^{t}\frac{1}{(t-t')^{\alpha}}\underline{\underline{F}}^{\mathrm{T}}_{t'}\cdot\overset{\triangledown}{\underline{\underline{M}}}(t')\cdot\underline{\underline{F}}_{t'}\,dt'\right)\cdot\underline{\underline{F}}^{-1} \\ &= \underline{\underline{F}}^{-\mathrm{T}}\cdot\left(\frac{1}{\Gamma(1-\alpha)}\int_{t_0}^{t}\frac{1}{(t-t')^{\alpha}}\frac{\partial\underline{\underline{N}}(t_0,t')}{\partial t'}\,dt'\right)\cdot\underline{\underline{F}}^{-1} \\ &= \underline{\underline{F}}^{-\mathrm{T}}\cdot\big(D^{\alpha}_{\star}\underline{\underline{N}}\big)\cdot\underline{\underline{F}}^{-1}, \end{aligned}\right. \end{aligned} \tag{4.26a}$$

while the Caputo derivative of a symmetric contravariant tensor $\underline{\underline{\boldsymbol{\eta}}}$ maps as

$$
\begin{aligned}
D^{\alpha}_{\star}\underline{\underline{\boldsymbol{\eta}}} &= \frac{1}{\Gamma(1-\alpha)}\int_{t_0}^{t}\frac{1}{(t-t')^{\alpha}}\frac{\partial\underline{\underline{\boldsymbol{\eta}}}(t')}{\partial t'}\,dt' \\
&\overset{t}{\longmapsto}\begin{cases}
\mathfrak{D}^{\alpha\dagger}_{\star}\underline{\underline{G}} := \dfrac{1}{\Gamma(1-\alpha)}\displaystyle\int_{t_0}^{t}\frac{1}{(t-t')^{\alpha}}\frac{\partial}{\partial t'}\Big(\underline{\underline{F}}(t',t)\cdot\underline{\underline{G}}(t')\cdot\underline{\underline{F}}^{\mathrm{T}}(t',t)\Big)dt' \\
\qquad = \dfrac{1}{\Gamma(1-\alpha)}\displaystyle\int_{t_0}^{t}\frac{1}{(t-t')^{\alpha}}\underline{\underline{F}}(t',t)\cdot\overset{\vartriangle}{\underline{\underline{G}}}(t')\cdot\underline{\underline{F}}^{\mathrm{T}}(t',t)\,dt' \\
\qquad = \underline{\underline{F}}\cdot\left(\dfrac{1}{\Gamma(1-\alpha)}\displaystyle\int_{t_0}^{t}\frac{1}{(t-t')^{\alpha}}\underline{\underline{F}}_{t'}^{-1}\cdot\overset{\vartriangle}{\underline{\underline{G}}}(t')\cdot\underline{\underline{F}}_{t'}^{-\mathrm{T}}\,dt'\right)\cdot\underline{\underline{F}}^{\mathrm{T}} \\
\qquad = \underline{\underline{F}}\cdot\left(\dfrac{1}{\Gamma(1-\alpha)}\displaystyle\int_{t_0}^{t}\frac{1}{(t-t')^{\alpha}}\frac{\partial\underline{\underline{H}}(t_0,t')}{\partial t'}\,dt'\right)\cdot\underline{\underline{F}}^{\mathrm{T}} \\
\qquad = \underline{\underline{F}}\cdot\left(D^{\alpha}_{\star}\underline{\underline{H}}\right)\cdot\underline{\underline{F}}^{\mathrm{T}}.
\end{cases}
\end{aligned}
\tag{4.26b}
$$

What is noteworthy about these mappings is that the argument list for the spatial fields being differentiated under the integral sign is (t',t) in the defining integrals, designating a floating reference state at t'. In the equalities that follow the defining equality, this reference state is changed from floating (i.e., t') to fixed (viz., t_0).□

4.3.2 Integrals

With the above derivations in place, it is a straightforward matter to prove that the Riemann-Liouville integral J^{α} (1.2) of a symmetric covariant tensor $\underline{\underline{\boldsymbol{\mu}}}$ maps into Cartesian space as

$$
J^{\alpha}\underline{\underline{\boldsymbol{\mu}}}\ \begin{cases}\overset{t}{\longmapsto} & \mathfrak{J}^{\alpha\downarrow}\underline{\underline{M}}, \\ \overset{t_0}{\longmapsto} & J^{\alpha}\underline{\underline{N}},\end{cases}\quad\text{such that}\quad J^{\alpha}\underline{\underline{N}} = \underline{\underline{F}}^{\mathrm{T}}\cdot\left(\mathfrak{J}^{\alpha\downarrow}\underline{\underline{M}}\right)\cdot\underline{\underline{F}},
\tag{4.27a}
$$

while the Riemann-Liouville integral of a symmetric contravariant tensor $\underline{\underline{\boldsymbol{\eta}}}$ maps as

$$
J^{\alpha}\underline{\underline{\boldsymbol{\eta}}}\ \begin{cases}\overset{t}{\longmapsto} & \mathfrak{J}^{\alpha\dagger}\underline{\underline{G}}, \\ \overset{t_0}{\longmapsto} & J^{\alpha}\underline{\underline{H}},\end{cases}\quad\text{such that}\quad J^{\alpha}\underline{\underline{H}} = \underline{\underline{F}}^{-1}\cdot\left(\mathfrak{J}^{\alpha\dagger}\underline{\underline{G}}\right)\cdot\underline{\underline{F}}^{-\mathrm{T}}.
\tag{4.27b}
$$

The Eulerian tensors $\mathfrak{J}^{\alpha\downarrow}\underline{\underline{M}}$ and $\mathfrak{J}^{\alpha\dagger}\underline{\underline{G}}$ are objective integrals of order α defined in (4.29). Unlike $J^{\alpha}\underline{\underline{N}}$ and $J^{\alpha}\underline{\underline{H}}$, which are actual Riemann-Liouville integrals, integrals $\mathfrak{J}^{\alpha\downarrow}\underline{\underline{M}}$ and $\mathfrak{J}^{\alpha\dagger}\underline{\underline{G}}$ are not true Riemann-Liouville integrals, in a strict sense of the definition, which is why they are given a different notation. For this reason, Lagrangian Riemann-Liouville integrals are considered the more fundamental of these integrals.

Proof: Like the Caputo derivatives, a Lagrangian map of the Riemann-Liouville integral for some covariant tensor $\underline{\underline{\boldsymbol{\mu}}}$ is a straightforward process whose outcome takes

the form

$$
\begin{aligned}
J^{\alpha}\underline{\underline{\boldsymbol{\mu}}} &= \frac{1}{\Gamma(\alpha)}\int_{t_0}^{t}\frac{1}{(t-t')^{1-\alpha}}\,\underline{\underline{\boldsymbol{\mu}}}(t')\,dt' \\
&\overset{t_0}{\Longmapsto} J^{\alpha}\underline{\underline{N}} = \frac{1}{\Gamma(\alpha)}\int_{t_0}^{t}\frac{1}{(t-t')^{1-\alpha}}\,\underline{\underline{N}}(t_0,t')\,dt',
\end{aligned}
\tag{4.28a}
$$

while for some contravariant tensor $\underline{\underline{\boldsymbol{\eta}}}$ it becomes

$$
\begin{aligned}
J^{\alpha}\underline{\underline{\boldsymbol{\eta}}} &= \frac{1}{\Gamma(\alpha)}\int_{t_0}^{t}\frac{1}{(t-t')^{1-\alpha}}\,\underline{\underline{\boldsymbol{\eta}}}(t')\,dt' \\
&\overset{t_0}{\Longmapsto} J^{\alpha}\underline{\underline{H}} = \frac{1}{\Gamma(\alpha)}\int_{t_0}^{t}\frac{1}{(t-t')^{1-\alpha}}\,\underline{\underline{H}}(t_0,t')\,dt'.
\end{aligned}
\tag{4.28b}
$$

These mappings reproduce standard definitions for Riemann-Liouville integrals of spatial fields, and are valid for all $\alpha > 0$.

Using the mappings of (4.25), it follows that the Riemann-Liouville integral of a symmetric covariant tensor $\underline{\underline{\boldsymbol{\mu}}}$ maps into Cartesian space in the Eulerian frame as

$$
\begin{aligned}
J^{\alpha}\underline{\underline{\boldsymbol{\mu}}} &= \frac{1}{\Gamma(\alpha)}\int_{t_0}^{t}\frac{1}{(t-t')^{1-\alpha}}\,\underline{\underline{\boldsymbol{\mu}}}(t')\,dt' \\
&\overset{t}{\Longmapsto}\begin{cases}
\mathfrak{J}^{\alpha\rfloor}\underline{\underline{M}} := \dfrac{1}{\Gamma(\alpha)}\displaystyle\int_{t_0}^{t}\frac{1}{(t-t')^{1-\alpha}}\,\underline{\underline{F}}^{-\mathrm{T}}(t',t)\cdot\underline{\underline{M}}(t')\cdot\underline{\underline{F}}^{-1}(t',t)\,dt' \\
\qquad = \underline{\underline{F}}^{-\mathrm{T}}\cdot\left(\dfrac{1}{\Gamma(\alpha)}\displaystyle\int_{t_0}^{t}\frac{1}{(t-t')^{1-\alpha}}\,\underline{\underline{F}}_{t'}^{\mathrm{T}}\cdot\underline{\underline{M}}(t')\cdot\underline{\underline{F}}_{t'}\,dt'\right)\cdot\underline{\underline{F}}^{-1} \\
\qquad = \underline{\underline{F}}^{-\mathrm{T}}\cdot\left(J^{\alpha}\underline{\underline{N}}\right)\cdot\underline{\underline{F}}^{-1},
\end{cases}
\end{aligned}
\tag{4.29a}
$$

while the Riemann-Liouville integral of a symmetric contravariant tensor $\underline{\underline{\boldsymbol{\eta}}}$ maps as

$$
\begin{aligned}
J^{\alpha}\underline{\underline{\boldsymbol{\eta}}} &= \frac{1}{\Gamma(\alpha)}\int_{t_0}^{t}\frac{1}{(t-t')^{1-\alpha}}\,\underline{\underline{\boldsymbol{\eta}}}(t')\,dt' \\
&\overset{t}{\Longmapsto}\begin{cases}
\mathfrak{J}^{\alpha\rfloor}\underline{\underline{G}} := \dfrac{1}{\Gamma(\alpha)}\displaystyle\int_{t_0}^{t}\frac{1}{(t-t')^{1-\alpha}}\,\underline{\underline{F}}(t',t)\cdot\underline{\underline{G}}(t')\cdot\underline{\underline{F}}^{\mathrm{T}}(t',t)\,dt' \\
\qquad = \underline{\underline{F}}\cdot\left(\dfrac{1}{\Gamma(\alpha)}\displaystyle\int_{t_0}^{t}\frac{1}{(t-t')^{1-\alpha}}\,\underline{\underline{F}}_{t'}^{-1}\cdot\underline{\underline{G}}(t')\cdot\underline{\underline{F}}_{t'}^{-\mathrm{T}}\,dt'\right)\cdot\underline{\underline{F}}^{\mathrm{T}} \\
\qquad = \underline{\underline{F}}\cdot\left(J^{\alpha}\underline{\underline{H}}\right)\cdot\underline{\underline{F}}^{\mathrm{T}},
\end{cases}
\end{aligned}
\tag{4.29b}
$$

for all $\alpha > 0$.□

4.4 Strain Fields

Strain is not a unique concept in finite-deformation analysis. Here we present two, Cartesian, strain fields that relate to changes in length-of-line. The first pertains to a separation between material points, while the second pertains to a separation between

material planes. A third measure of strain accounts for changes in the volume of a material point. These concepts are presented in both their Eulerian and Lagrangian constructs.

As it turns out, the strain fields used in the constitutive theories of Chp. 5 are different from the classic strain fields that are discussed in this chapter. Be that as it may, the strain fields presented in this chapter are of historical significance, and seeing how they arrive from field transfer should aid the reader's understanding of how the spatial strain fields of Chp. 5 are arrived at.

4.4.1 Covariant-Like

The covariant strain tensor of (3.8) maps into spatial strain fields that are well known. In particular, in an Eulerian transfer of field,

$$\underline{\underline{\epsilon}} := \tfrac{1}{2}\big(\underline{\underline{\gamma}} - \underline{\underline{\gamma}}_0\big) \overset{t}{\Longmapsto} \underline{\underline{A}} := \tfrac{1}{2}\big(\underline{\underline{I}} - \underline{\underline{B}}^{-1}\big), \tag{4.30a}$$

where $\underline{\underline{A}}(\mathfrak{X}; t_0, t)$ is the Almansi [2] strain tensor, while in a Lagrangian transfer of field,

$$\underline{\underline{\epsilon}} := \tfrac{1}{2}\big(\underline{\underline{\gamma}} - \underline{\underline{\gamma}}_0\big) \overset{t_0}{\Longmapsto} \underline{\underline{E}} := \tfrac{1}{2}\big(\underline{\underline{C}} - \underline{\underline{I}}\big), \tag{4.30b}$$

where $\underline{\underline{E}}(\mathfrak{X}_0; t_0, t)$ is the popular Green [46] strain tensor.

The Almansi and Green strains are symmetric fields that measure a change in the distance-of-separation between a pair of neighboring material points.

Rates

From (4.22a), the time rate-of-change of strain $\underline{\underline{\epsilon}}$ maps into Cartesian space as

$$D\underline{\underline{\epsilon}} = \tfrac{1}{2}\, D\underline{\underline{\gamma}} \begin{cases} \overset{t}{\longmapsto} & \overset{\triangledown}{\underline{\underline{A}}} = \underline{\underline{D}}, \\ \overset{t_0}{\longmapsto} & D\underline{\underline{E}} = \tfrac{1}{2}\, D\underline{\underline{C}} = \underline{\underline{F}}^{\mathrm{T}} \cdot \underline{\underline{D}} \cdot \underline{\underline{F}}, \end{cases} \tag{4.31}$$

where $\overset{\triangledown}{\underline{\underline{A}}}$ is the lower-convected rate of Almansi strain, and $D\underline{\underline{E}}$ is the Green strain rate, both of which are well-known results. Formula $\overset{\triangledown}{\underline{\underline{A}}} = \underline{\underline{D}}$ can be rewritten in terms of the corotational derivative via (4.16a) as

$$\overset{\circ}{\underline{\underline{A}}} = \underline{\underline{D}} - \underline{\underline{D}} \cdot \underline{\underline{A}} - \underline{\underline{A}} \cdot \underline{\underline{D}}, \tag{4.32}$$

thereby producing a quasi-linear equation for the evolution of $\underline{\underline{A}}$ in terms of its Zaremba-Jaumann derivative.

Fractional order: The fractal, covariant, strain-rate tensor, $D^{\alpha}_{\star}\underline{\underline{\epsilon}}$, of (3.11) maps into Cartesian space according to (4.23a) as

$$D^{\alpha}_{\star}\underline{\underline{\epsilon}} = \tfrac{1}{2}\, D^{\alpha}_{\star}\underline{\underline{\gamma}} \begin{cases} \overset{t}{\longmapsto} & \mathfrak{D}^{\alpha\downarrow}_{\star}\underline{\underline{A}} = \overset{\alpha\downarrow}{\underline{\underline{D}}}, \\ \overset{t_0}{\longmapsto} & D^{\alpha}_{\star}\underline{\underline{E}} = \tfrac{1}{2}\, D^{\alpha}_{\star}\underline{\underline{C}} = \underline{\underline{F}}^{\mathrm{T}} \cdot \overset{\alpha\downarrow}{\underline{\underline{D}}} \cdot \underline{\underline{F}} \\ & \qquad = \frac{1}{\Gamma(1-\alpha)} \int_{t_0}^{t} \frac{1}{(t-t')^{\alpha}}\, \underline{\underline{F}}^{\mathrm{T}}_{t'} \cdot \underline{\underline{D}}(t') \cdot \underline{\underline{F}}_{t'}\, dt', \end{cases} \tag{4.33}$$

where $\mathfrak{D}^{\alpha\rfloor}_{\star}\underline{\underline{A}}$ is the lower-fractal, Almansi, strain-rate tensor, and $D^{\alpha}_{\star}\underline{\underline{E}}$ is the fractional, Green, strain-rate tensor, both of order α wherein α is restricted to the interval $0 < \alpha < 1$.

4.4.2 Contravariant-Like

The contravariant strain tensor of (3.12) maps into Cartesian space in an Eulerian frame as

$$\underline{\underline{\zeta}} := \tfrac{1}{2}\big(\underline{\underline{\gamma}}_0^{-1} - \underline{\underline{\gamma}}^{-1}\big) \overset{t}{\longmapsto} \underline{\underline{Z}} := \tfrac{1}{2}\big(\underline{\underline{B}} - \underline{\underline{I}}\big), \tag{4.34a}$$

where $\underline{\underline{Z}}(\mathfrak{X}; t_0, t)$ is a strain tensor that was introduced by Signorini [104], and whose appearance in the literature is scarce. A Lagrangian transfer of this same body field yeilds

$$\underline{\underline{\zeta}} := \tfrac{1}{2}\big(\underline{\underline{\gamma}}_0^{-1} - \underline{\underline{\gamma}}^{-1}\big) \overset{t_0}{\longmapsto} \underline{\underline{Y}} := \tfrac{1}{2}\big(\underline{\underline{I}} - \underline{\underline{C}}^{-1}\big), \tag{4.34b}$$

where $\underline{\underline{Y}}(\mathfrak{X}_0; t_0, t)$ is a strain tensor whose origin is unknown to us, and that we shall simply refer to as a Lagrangian strain tensor.

The Signorini and Lagrangian strains are symmetric fields that measure a change in the height-of-separation between a pair of neighboring material planes that are non-intersecting.

Rates

From (4.22b), the time rate-of-change of strain $\underline{\underline{\zeta}}$ maps into Cartesian space as

$$D\underline{\underline{\zeta}} = -\tfrac{1}{2}\, D\underline{\underline{\gamma}}^{-1} \begin{cases} \overset{t}{\longmapsto} & \overset{\vartriangle}{\underline{\underline{Z}}} = \underline{\underline{D}}, \\ \overset{t_0}{\longmapsto} & D\underline{\underline{Y}} = -\tfrac{1}{2}\, D\underline{\underline{C}}^{-1} = \underline{\underline{F}}^{-1} \cdot \underline{\underline{D}} \cdot \underline{\underline{F}}^{-\mathrm{T}}, \end{cases} \tag{4.35}$$

where $\overset{\vartriangle}{\underline{\underline{Z}}}$ is the upper-convected rate of Signorini strain, and $D\underline{\underline{Y}}$ is the Lagrangian strain-rate. Because of (4.16b), formula $\overset{\vartriangle}{\underline{\underline{Z}}} = \underline{\underline{D}}$ can be rewritten in terms of the corotational derivative as

$$\overset{\circ}{\underline{\underline{Z}}} = \underline{\underline{D}} + \underline{\underline{D}} \cdot \underline{\underline{Z}} + \underline{\underline{Z}} \cdot \underline{\underline{D}}, \tag{4.36}$$

thereby producing a quasi-linear equation for the evolution of $\underline{\underline{Z}}$ in terms of its corotational derivative.

Fractional order: According to (4.23b), the fractal, contravariant, strain-rate tensor, $D^{\alpha}_{\star}\underline{\underline{\zeta}}$, of (3.14) maps into Cartesian space as

$$D^{\alpha}_{\star}\underline{\underline{\zeta}} = -\tfrac{1}{2}\, D^{\alpha}_{\star}\underline{\underline{\gamma}}^{-1} \begin{cases} \overset{t}{\longmapsto} & \mathfrak{D}^{\alpha\rfloor}_{\star}\underline{\underline{Z}} = \overset{\alpha\rfloor}{\underline{\underline{D}}}, \\ \overset{t_0}{\longmapsto} & D^{\alpha}_{\star}\underline{\underline{Y}} = -\tfrac{1}{2}\, D^{\alpha}_{\star}\underline{\underline{C}}^{-1} = \underline{\underline{F}}^{-1} \cdot \overset{\alpha\rfloor}{\underline{\underline{D}}} \cdot \underline{\underline{F}}^{-\mathrm{T}} \\ & \qquad = \frac{1}{\Gamma(1-\alpha)} \int_{t_0}^{t} \frac{1}{(t-t')^{\alpha}}\, \underline{\underline{F}}_{t'}^{-1} \cdot \underline{\underline{D}}(t') \cdot \underline{\underline{F}}_{t'}^{-\mathrm{T}}\, dt', \end{cases} \tag{4.37}$$

where $\mathfrak{D}^{\alpha\rfloor}_{\star}\underline{\underline{Z}}$ is the upper-fractal strain-rate tensor of Signorini, and $D^{\alpha}_{\star}\underline{\underline{Y}}$ is the upper-eth, fractional, Lagrangian, strain-rate tensor, both of order α wherein $0 < \alpha < 1$.

4.4.3 Dilational

Using the preceeding results of this chapter, it is also a straightforward matter to map the dilatation $\Delta(t_0, t)$ of (3.15) from a body formulation into a spatial formulation, thereby producing

$$\Delta = \ln\Big(\det\big(\underline{\underline{\gamma}}_0^{-1} \cdot \underline{\underline{\gamma}}\big)^{1/2}\Big) \overset{t}{\Longmapsto} \Delta = \ln\Big(\big(\det \underline{\underline{\boldsymbol{B}}}\big)^{1/2}\Big) = \ln\big(\det \underline{\underline{\boldsymbol{F}}}\big) \tag{4.38a}$$

in an Eulerian setting, and

$$\Delta = \ln\Big(\det\big(\underline{\underline{\gamma}}_0^{-1} \cdot \underline{\underline{\gamma}}\big)^{1/2}\Big) \overset{t_0}{\Longmapsto} \Delta = \ln\Big(\big(\det \underline{\underline{\boldsymbol{C}}}\big)^{1/2}\Big) = \ln\big(\det \underline{\underline{\boldsymbol{F}}}\big) \tag{4.38b}$$

in a Lagrangian setting. There is no distinction between the Eulerian and Lagrangian descriptions for dilatation, as expected, because dilatation is an absolute scalar field, and is therefore independent of the Jacobian of transformation between these two frames.

Rates

A consequence of the above transfers for strain rate is that the time rate-of-change of dilatation (3.16) maps from the body into Cartesian space in an Eulerian frame as

$$D\Delta = \tfrac{1}{2} \operatorname{tr} D\underline{\underline{\gamma}} \overset{t}{\Longmapsto} D\Delta = \operatorname{tr} \underline{\underline{D}}, \tag{4.39a}$$

and it maps into Cartesian space in a Lagrangian frame as

$$D\Delta = \tfrac{1}{2} \operatorname{tr} D\underline{\underline{\gamma}} \overset{t_0}{\Longmapsto} D\Delta = \tfrac{1}{2} \underline{\underline{C}}^{-1} : D\underline{\underline{C}} = \operatorname{tr} \underline{\underline{D}}. \tag{4.39b}$$

Again, there is no distinction between configurations because the transferred field is an absolute scalar.

Fractional order: The fractal rate of dilatation, $D^\alpha_\star \Delta$, can be computed as

$$D^\alpha_\star \Delta = \frac{1}{\Gamma(1-\alpha)} \int_0^t \frac{1}{(t-t')^\alpha} \big(\operatorname{tr} \underline{\underline{D}}\big)(t')\, dt', \tag{4.40}$$

which follows straight away from (4.39), or equivalently, from a field transfer of (3.17). This equation applies to both spatial frames of reference.

Conservation of mass

From the results of (4.38 & 4.39) it follows that the conservation of mass, whose rate form is

$$D \ln \varrho = -\tfrac{1}{2} \operatorname{tr} D\underline{\underline{\gamma}} \overset{t}{\Longmapsto} D \ln \varrho = -\operatorname{tr} \underline{\underline{D}}, \tag{4.41a}$$

integrates to

$$\frac{\varrho_0}{\varrho} = \frac{dV}{dV_0} = \det \underline{\underline{F}}, \tag{4.41b}$$

in accordance with (3.15).

4.5 Stress Fields

In an Eulerian transfer of field, Lodge [68, pp. 327–328] has shown that the body-stress tensor $\underline{\underline{\pi}}$ maps into Cartesian space as

$$\underline{\underline{\pi}} \overset{t}{\Longmapsto} \underline{\underline{T}}, \tag{4.42a}$$

where $\underline{\underline{T}}(\mathfrak{X}; t)$ is the Cauchy [14, pp. 42–56] stress tensor. The equation for deviatoric stress (3.19) therefore maps to Eulerian space as

$$\left.\begin{aligned} \underline{\underline{\widetilde{\pi}}} := \underline{\underline{\pi}} + p\,\underline{\underline{\gamma}}^{-1} \overset{t}{\Longmapsto} \underline{\underline{\widetilde{T}}} := \underline{\underline{T}} + p\,\underline{\underline{I}} \\ p := -\tfrac{1}{3}\,\mathrm{tr}\,\underline{\underline{\pi}} \overset{t}{\Longmapsto} p := -\tfrac{1}{3}\,\mathrm{tr}\,\underline{\underline{T}} \end{aligned}\right\}, \tag{4.42b}$$

where $\underline{\underline{\widetilde{T}}}$ is the deviatoric stress associated with hydrostatic pressure p in Cartesian analysis.

In a Lagrangian transfer of field, the body stress maps into Cartesian space as

$$\tfrac{\varrho_0}{\varrho}\,\underline{\underline{\pi}} \overset{t_0}{\Longmapsto} \underline{\underline{P}}, \qquad \underline{\underline{\pi}} \overset{t_0}{\Longmapsto} \underline{\underline{P}}^{\star}, \tag{4.42c}$$

where $\underline{\underline{P}}(\mathfrak{X}_0; t_0, t) := \frac{\varrho_0}{\varrho}\,\underline{\underline{F}}^{-1} \cdot \underline{\underline{T}} \cdot \underline{\underline{F}}^{-\mathrm{T}}$ is commonly referred to as the second, Piola-Kirchhoff, stress tensor, named after the independent works of Piola [85] and Kirchhoff [58]. Tensor $\underline{\underline{P}}^{\star}(\mathfrak{X}_0; t_0, t) := \underline{\underline{F}}^{-1} \cdot \underline{\underline{T}} \cdot \underline{\underline{F}}^{-\mathrm{T}}$ is a Lagrangian stress tensor.[§] Both fields are symmetric, two-state, stress tensors. The deviatoric stress and the hydrostatic pressure of (3.19) therefore map into the Lagrangian frame as

$$\tfrac{\varrho_0}{\varrho}\,\underline{\underline{\widetilde{\pi}}} \overset{t_0}{\Longmapsto} \underline{\underline{\widetilde{P}}} := \underline{\underline{P}} + \tfrac{\varrho_0}{\varrho}\,p\,\underline{\underline{C}}^{-1} \quad \text{and} \quad \tfrac{\varrho_0}{\varrho}\,p \overset{t_0}{\Longmapsto} \tfrac{\varrho_0}{\varrho}\,p := -\tfrac{1}{3}\,\underline{\underline{P}} : \underline{\underline{C}}, \tag{4.42d}$$

both of which are widely used definitions.

4.5.1 Conservation Laws

The physical law that impacts stress is the conservation of momentum.

Balance of linear momentum

This law yeilds a vector formula, called the stress equations of motion, that in an Eulerian frame is given by

$$\varrho\,\underline{a} = \underline{\nabla} \cdot \underline{\underline{T}} + \varrho \underline{f}, \tag{4.43a}$$

where $\underline{\nabla} \cdot \underline{\underline{T}}$ is the divergence of stress, with a matrix representation of $[\![\partial \mathrm{T}_{rk}/\partial \mathrm{x}_k]\!]$ in coordinate system $\mathcal{C}$, and where vectors $\underline{a}$ and $\underline{f}$ denote acceleration and body force, respectively.

[§]In the literature, the notation $\underline{\underline{P}}^{\star}$ is often used to denote the first, Piola-Kirchhoff, stress tensor, $\frac{\varrho_0}{\varrho}\,\underline{\underline{F}}^{-1} \cdot \underline{\underline{T}}$, which is not symmetric. The stress tensor that we call $\underline{\underline{P}}^{\star}$ is seldom used. For us, tensor $\underline{\underline{P}}^{\star} = \underline{\underline{F}}^{-1} \cdot \underline{\underline{T}} \cdot \underline{\underline{F}}^{-\mathrm{T}}$ is a natural choice, since it arises directly from a field transfer of the body-stress tensor $\underline{\underline{\pi}}$.

In a Lagrangian setting, the balance of momentum can be expressed as

$$\varrho_0\, \underline{a} = \mathrm{Div}\big(\underline{\underline{F}} \cdot \underline{\underline{P}}\big) + \varrho_0 \underline{f}, \tag{4.43b}$$

where the divergence of stress is now taken with respect to the reference frame in that $\mathrm{Div}\,\underline{\underline{H}}$ has a matrix representation in $\mathcal{C}$ of $[\![\partial \mathrm{H}_{rk}/\partial \mathrm{X}_k]\!]$ for some tensor $\underline{\underline{H}}$. Vectors $\underline{a}$ and $\underline{f}$ are the same as those appearing in (4.43a).

Balance of angular momentum

In the absense of couple-stress effects, which we assume herein, a balance of angular momentum requires that Cauchy stress $\underline{\underline{T}}$ be symmetric, and therefore, $\widetilde{\underline{\underline{T}}}$, $\underline{\underline{P}}$, $\widetilde{\underline{\underline{P}}}$ and $\underline{\underline{P}}^\star$ must all be symmetric, too.

4.5.2 Rates

According to (4.22b), an Eulerian transfer of the body stress-rate tensor into Cartesian space leads to

$$D\underline{\underline{\boldsymbol{\pi}}} \overset{t}{\longmapsto} \overset{\vartriangle}{\underline{\underline{T}}}, \tag{4.44a}$$

where $\overset{\vartriangle}{\underline{\underline{T}}}$ is the upper-convected derivative of Cauchy stress. A Lagrangian transfer of this same body field produces

$$D\underline{\underline{\boldsymbol{\pi}}} \overset{t_0}{\longmapsto} D\underline{\underline{P}}^\star, \tag{4.44b}$$

where $D\underline{\underline{P}}^\star = \underline{\underline{F}}^{-1} \cdot \overset{\vartriangle}{\underline{\underline{T}}} \cdot \underline{\underline{F}}^{-\mathrm{T}}$, recalling that $\overset{\vartriangle}{\underline{\underline{T}}} = \partial \underline{\underline{T}}/\partial t + \big(\underline{\underline{T}}\boldsymbol{\nabla}\big) \cdot \underline{v} - \underline{\underline{L}} \cdot \underline{\underline{T}} - \underline{\underline{T}} \cdot \underline{\underline{L}}^{\mathrm{T}}$.

Fractional order

By constraining the fractal order so that $0 < \alpha < 1$, an application of (4.25) leads to an Eulerian transfer of field $D^\alpha_\star \underline{\underline{\boldsymbol{\pi}}}$ that produces

$$\begin{aligned} D^\alpha_\star \underline{\underline{\boldsymbol{\pi}}} &= \frac{1}{\Gamma(1-\alpha)} \int_0^t \frac{1}{(t-t')^\alpha} \frac{\partial \underline{\underline{\boldsymbol{\pi}}}(t')}{\partial t'}\, dt' \\ &\overset{t}{\longmapsto} \begin{cases} \mathfrak{D}^{\alpha\uparrow}_\star \underline{\underline{T}} = \dfrac{1}{\Gamma(1-\alpha)} \displaystyle\int_0^t \frac{1}{(t-t')^\alpha} \underline{\underline{F}}(t',t) \cdot \overset{\vartriangle}{\underline{\underline{T}}}(t') \cdot \underline{\underline{F}}^{\mathrm{T}}(t',t)\, dt' \\ \qquad = \underline{\underline{F}} \cdot \left(\dfrac{1}{\Gamma(1-\alpha)} \displaystyle\int_0^t \frac{1}{(t-t')^\alpha} \underline{\underline{F}}^{-1}_{t'} \cdot \overset{\vartriangle}{\underline{\underline{T}}}(t') \cdot \underline{\underline{F}}^{-\mathrm{T}}_{t'}\, dt' \right) \cdot \underline{\underline{F}}^{\mathrm{T}}, \end{cases} \end{aligned} \tag{4.45a}$$

where the upper-fractal stress-rate tensor, $\mathfrak{D}^{\alpha\uparrow}_\star \underline{\underline{T}}$, of order α first appeared in a paper written by Drozdov [27], but in different notation.

A Lagrangian transfer of the same field leads to

$$D^{\alpha}_{\star}\underline{\underline{\boldsymbol{\pi}}} = \frac{1}{\Gamma(1-\alpha)}\int_0^t \frac{1}{(t-t')^{\alpha}}\,\frac{\partial \underline{\underline{\boldsymbol{\pi}}}(t')}{\partial t'}\,dt'$$

$$\overset{t_0}{\Longmapsto} \begin{cases} D^{\alpha}_{\star}\underline{\underline{P}}^{\star} = \dfrac{1}{\Gamma(1-\alpha)}\displaystyle\int_0^t \frac{1}{(t-t')^{\alpha}}\,\frac{\partial \underline{\underline{P}}^{\star}(t_0,t')}{\partial t'}\,dt' \\ \qquad\quad = \dfrac{1}{\Gamma(1-\alpha)}\displaystyle\int_0^t \frac{1}{(t-t')^{\alpha}}\,\underline{\underline{F}}^{-1}_{t'}\cdot\overset{\vartriangle}{\underline{\underline{T}}}(t')\cdot\underline{\underline{F}}^{-\mathrm{T}}_{t'}\,dt', \end{cases} \tag{4.45b}$$

where $D^{\alpha}_{\star}\underline{\underline{P}}^{\star} = \underline{\underline{F}}^{-1}\cdot\mathfrak{D}^{\alpha}_{\star}\underline{\underline{T}}\cdot\underline{\underline{F}}^{-\mathrm{T}}$, which is compatible with its first-order counterpart $D\underline{\underline{P}}^{\star} = \underline{\underline{F}}^{-1}\cdot\overset{\vartriangle}{\underline{\underline{T}}}\cdot\underline{\underline{F}}^{-\mathrm{T}}$ in the limit as α goes to 1 from below.

Chapter 5

Constitutive Theories

Continuum theories are presented in this chapter that are suitable for elastic and viscoelastic materials. Both compressible and incompressible constructions are discussed. Each theoretical structure is reduced to cases of material isotropy and transverse isotropy. The resulting theories are mapped into Cartesian space in the Eulerian and Lagrangian frames of reference for use when solving boundary-value problems. Tangent moduli are also derived so these theories can be implemented into finite elements. Material functions are assigned to these theories in Chps. 7–??, thereby producing material models that can then be compared against experimental data.

5.1 Integrity Bases

The theory of invariants [107] is well developed as it pertains to our needs. In the case of a single tensor—say, $\underline{\underline{A}}$—having a matrix representation $\mathbb{A}$ in some admissible coordinate system affiliated with the underlying manifold, there exists an integrity basis that is comprised of three, irreducible, moment invariants:

$$\operatorname{tr}\mathbb{A}, \quad \operatorname{tr}\mathbb{A}^2, \quad \operatorname{tr}\mathbb{A}^3. \tag{5.1a}$$

This set constitutes an admissible, isotropic, integrity basis for any single, symmetric, 3×3 matrix $\mathbb{A}$. One advantage of using an integrity basis is that scalar fields can replace tensor fields as arguments in state functions. Another advantage is that an integrity basis leads to tensorial structure in a potential-based theory without having to introduce any ad hoc assumptions.

None of the above three invariants can be expressed solely in terms of the other two; they are orthogonal to one another. Even so, this basis is not unique. The Cayley-Hamilton theorem—$\mathbb{A}^3 - (\operatorname{tr}\mathbb{A})\mathbb{A}^2 + \frac{1}{2}\big((\operatorname{tr}\mathbb{A})^2 - \operatorname{tr}\mathbb{A}^2\big)\mathbb{A} - (\det\mathbb{A})\mathbb{I} = \mathbb{0}$, with invariants: $\operatorname{tr}\mathbb{A}$, $\frac{1}{2}\big((\operatorname{tr}\mathbb{A})^2 - \operatorname{tr}\mathbb{A}^2\big)$, and $\det\mathbb{A}$—permits an exchange of the cubic moment (i.e., $\operatorname{tr}\mathbb{A}^3$) with the determinant (viz., $\det\mathbb{A} \equiv \frac{1}{3}\{\operatorname{tr}\mathbb{A}^3 - \operatorname{tr}\mathbb{A}[(\operatorname{tr}\mathbb{A})^2 - 3\operatorname{tr}\mathbb{A}^2\}$) when assigning an integrity basis. Furthermore, if matrix $\mathbb{A}$ is non-singular (i.e., $\det\mathbb{A} \neq 0$), then another application of the Cayley-Hamilton theorem allows the quadratic moment, $\operatorname{tr}\mathbb{A}^2$, to be replaced by the moment of its inverse, $\operatorname{tr}\mathbb{A}^{-1}$. It is accepted practice to make use of both of these exchanges when assigning an

integrity basis for isotropic elasticity; specifically, $\operatorname{tr}\mathbb{A}$, $\operatorname{tr}\mathbb{A}^{-1}$, and $\det\mathbb{A}$ are often employed because they lead to practicle models, even though they do not consititute an irreducible set.

For the case of two distinct matrices—say, $\mathbb{A}$ and $\mathbb{B}$—then in addition to those invariants that involve a single matrix only, one must also consider the coupled traces

$$\operatorname{tr}\mathbb{AB}, \quad \operatorname{tr}\mathbb{A}^2\mathbb{B}, \quad \operatorname{tr}\mathbb{AB}^2, \quad \operatorname{tr}\mathbb{A}^2\mathbb{B}^2, \tag{5.1b}$$

making a total of ten invariants that now comprise this irreducible integrity basis.

When preference is given to one coordinate line above all other coordinate lines, then the resulting integrity basis is said to be transverse isotropic. Let vector a be a unit vector that is tangent to this coordinate line. Because there is no directional preference along a coordinate line, the integrity basis must be even in a, and as such, vector a can be represented by the symmetric dyadic matrix $\mathbb{B} := \mathrm{a}\otimes\mathrm{a}$ with components $\mathbb{B} = [\![a^r a^c]\!]$, wherein $\otimes$ denotes the outer product between two vectors. Because a is a unit vector, it follows that $\mathrm{a}\otimes\mathrm{a} = (\mathrm{a}\otimes\mathrm{a})^2 = (\mathrm{a}\otimes\mathrm{a})^3 = \ldots$, and it also follows that $\operatorname{tr}\mathrm{a}\otimes\mathrm{a} = 1$, $\operatorname{tr}\mathbb{A}\cdot(\mathrm{a}\otimes\mathrm{a}) = \mathrm{a}\cdot\mathbb{A}\cdot\mathrm{a}$, $\operatorname{tr}\mathbb{A}^2\cdot(\mathrm{a}\otimes\mathrm{a}) = \mathrm{a}\cdot\mathbb{A}^2\cdot\mathrm{a}$, etc. Consequently, of the ten invariants in (5.1a & 5.1b) only five are independent; they are:

$$\operatorname{tr}\mathbb{A}, \quad \operatorname{tr}\mathbb{A}^2, \quad \operatorname{tr}\mathbb{A}^3, \quad \mathrm{a}\cdot\mathbb{A}\cdot\mathrm{a}, \quad \mathrm{a}\cdot\mathbb{A}^2\cdot\mathrm{a}, \tag{5.1c}$$

which define the irreducible, transversely isotropic, integrity basis for matrix $\mathbb{A}$.

The intellectual process of selecting an integrity basis will lead to a constitutive theory. This is not a straightforward process because, although the irreducible integrity basis is unique, there are numerous, other, orthogonal, integrity bases that are also admissible and therefore may be considered. Mathematics alone is incapable of selecting an integrity basis; physics must also be addressed. Once a theory is in hand, the process of assigning/deriving a potential function appropriate for the selected integrity basis will produce a constitutive model. Only when such a model is available can the challenging process of characterization and (hopefully) verification against experimental data begin to take place. In physics, one cannot prove a theory/model to be correct. One can only, perhaps, disprove it, or more importantly, establish its domain of applicability.

5.2 Elasticity

Here we consider a mass element $\mathfrak{P}$ of density $\varrho(\mathfrak{P};t)$ in a state of stress $\underline{\underline{\boldsymbol{\pi}}}(\mathfrak{P};t)$ that is undergoing an infinitesimal change in shape of $d\underline{\underline{\boldsymbol{\gamma}}}(\mathfrak{P};t) := \underline{\underline{\boldsymbol{\gamma}}}(\mathfrak{P};t+dt) - \underline{\underline{\boldsymbol{\gamma}}}(\mathfrak{P};t)$ over an increment in time of dt. This induces a differential change in the work done, $dW(\mathfrak{P};t)$, on the mass element (including the energetic contribution due to its change in kinetic energy) that is quantified by the formula [70, pp. 194–195]

$$dW = \frac{1}{2\varrho}\,\underline{\underline{\boldsymbol{\pi}}} : d\underline{\underline{\boldsymbol{\gamma}}}. \tag{5.2}$$

From thermostatics, given an arbitrary reversible process, $\underline{\underline{\boldsymbol{\gamma}}} \to \underline{\underline{\boldsymbol{\gamma}}} + d\underline{\underline{\boldsymbol{\gamma}}}$, the increment of work done on a mass element minus the change in its kinetic energy (herein

denoted as dW) equates with a change in the internal energy of the mass element. For an isothermal reversible process, the increment dW equates with a change in the Helmholtz free-energy of the mass element.

Equation (5.2) leads to a potential-based constitutive equation for elasticity,

$$\tfrac{\varrho_0}{\varrho}\,\underline{\underline{\pi}} = 2\varrho_0\,\frac{\partial \mathfrak{W}}{\partial \underline{\underline{\gamma}}} = 2\varrho_0 \sum_{n=1}^{N} \frac{\partial \mathfrak{W}}{\partial I_n}\,\frac{\partial I_n}{\partial \underline{\underline{\gamma}}}, \tag{5.3}$$

which implies that (5.2) is an expression of the chain rule. The potential function representing elastic strain-energy density, $W(\mathfrak{P};0,t) = \mathfrak{W}(I_1, I_2, \ldots, I_N\colon \mathfrak{P};0,t)$, has arguments that make up an integrity basis comprised of N independent invariants $I_n(\underline{\underline{\gamma}}_0, \underline{\underline{\gamma}}, \underline{\underline{\chi}}_1, \underline{\underline{\chi}}_2, \cdots, \underline{\underline{\chi}}_{M-2}\colon \mathfrak{P};0,t)$, $n = 1,2,\ldots,N$, obtained from M separate tensor fields: the metric tensors $\underline{\underline{\gamma}}_0$ and $\underline{\underline{\gamma}}$ along with $M-2$ material tensors $\underline{\underline{\chi}}_m$, $m = 1,2,\ldots,M-2$. The tensor gradient $\partial\mathfrak{W}/\partial\underline{\underline{\gamma}}$ must be symmetric (i.e., $\partial\mathfrak{W}/\partial_{\mathfrak{O}} = \frac{1}{2}[\![\partial\mathfrak{W}/\partial\gamma_{rc} + \partial\mathfrak{W}/\partial\gamma_{cr}]\!]$ in every body-coordinate system $\mathcal{B}\colon \underline{\underline{\gamma}} \to \mathfrak{O}$) in order for it to satisfy the conservation of angular momentum. All anisotropic attributes, when present, are manifest through the gradient $\partial\mathfrak{W}/\partial\underline{\underline{\gamma}}$, which has units of stress on mass density. Unlike classical elasticity, there need not be a fourth-rank modulus tensor that assigns anisotropic characteristics in the theory of finite-strain elasticity; instead, the integrity basis introduces them through its gradients.

When elasticity is described by a potential function then the material model is called hyper-elastic, and although there is no mathematical proof for its existence, Leonov [66] has provided physical proof for its necessity (there is no know proof of sufficiency): non-potential, finite-strain, elastic (so called hypo-elastic) constitutive relations can be constructed that create energy from nothing (i.e., they can operate as perpetual motion machines); hyper-elastic constitutive relations cannot be constructed to violate thermodynamics in this way. This justifies referring to (5.3) as the fundamental constitutive equation governing elasticity.

Theromostatics places loose constraints on what are admissible functional forms for the potential function $\mathfrak{W}$. This is an important topic in constitutive modeling, but it lies outside the scope of this report.

5.3 Viscoelasticity

One can 'fluidize' the above, elastic, constitutive laws, moving them beyond the realm of reversible thermostatics and into the domain of irreversible thermodynamics, by introducing a memory function that bestows a loss of remembrance onto past states [18]. The contributions that can be recollected from each past state are then summed over a loading history. Stress and strain are taken to be causal functions of time during this integration, and as such, are zero valued for all times prior to time $t = 0$. However, loading histories may be discontinuous at time $t = 0$, as will be the case in creep and stress-relaxation experiments.

The well-known constitutive equation for linear viscoelasticity, restricted to infinitesimal strains and rotations, can be written as the following Volterra integral

equation [47],

$$\mathrm{T}_{ij}(t) = \mathrm{G}_{ijk\ell}(t)\,\mathrm{E}_{k\ell}(0,0^+) + \int_{0^+}^{t} \mathrm{G}_{ijk\ell}(t-t')\,\frac{\partial \mathrm{E}_{k\ell}(0,t')}{\partial t'}\,dt'.$$

After an integration by parts, this expression becomes

$$\mathrm{T}_{ij}(t) = \mathrm{G}_{ijk\ell}(0)\,\mathrm{E}_{k\ell}(0,t) - \int_{0}^{t} \mathrm{M}_{ijk\ell}(t-t')\,\mathrm{E}_{k\ell}(0,t')\,dt',$$

or equivalently, using the additive and anti-symmetric property of infinitesimal strain (i.e., $E_{k\ell}(0,t) = E_{k\ell}(0,t') + E_{k\ell}(t',t)$, $t' \in [0,t]$), it can also be written as

$$\mathrm{T}_{ij}(t) = \mathrm{G}_{ijk\ell}(t)\,\mathrm{E}_{k\ell}(0,t) + \int_{0}^{t} \mathrm{M}_{ijk\ell}(t-t')\,\mathrm{E}_{k\ell}(t',t)\,dt',$$

where $\mathrm{T}_{ij} = \mathrm{T}_{ji}$ are the symmetric components of stress, $\mathrm{E}_{k\ell} = \mathrm{E}_{\ell k}$ are the symmetric components of infinitesimal strain, $\mathrm{G}_{ijk\ell} = \mathrm{G}_{jik\ell} = \mathrm{G}_{ij\ell k}$ are the symmetric components of a relaxation modulus, and $\mathrm{M}_{ijk\ell}(t-t') \coloneqq \partial \mathrm{G}_{ijk\ell}(t-t')/\partial t'$ are the symmetric components of a memory modulus. Memory fades if $|\mathrm{M}_{ijk\ell}(t_2)| < |\mathrm{M}_{ijk\ell}(t_1)|$ for all $t_2 > t_1 \geq 0$. In classic viscoelasticity, the fourth-rank material functions $\mathrm{G}_{ijk\ell}$ and $\mathrm{M}_{ijk\ell}$ account for material anisotropy, when present.

The first of the three formulations listed above requires the strain to be continuous and differentiable over time. The second and third formulations are less restrictive in that they only require strain to be continuous over time. The last two formulations differ in the moduli of their elastic terms, and they also differ in the states that define strain in their viscoelastic (integral) terms. It is the third expression of these three equivalent expressions that we choose to analytically continue from the infinitesimal into the finite.

In all three of these classic formulations, strain is the controlled variable to which stress responds. Because the theory is linear, it can also be written so that stress is the control variable to which strain responds. But in our end application (finite elements), displacements are assigned to which forces respond, which motivates selecting strain for the cause and stress for the effect.

Using classical viscoelasticity as our guide, and adopting the hypothesis of Kaye [56] and Bernstein et al. [7] (which they applied to viscoelastic liquids) wherein strain is replaced by the gradient of strain energy, as in elasticity theory, we therefore consider a class of K-BKZ - like viscoelastic solids that obey the constitutive hypothesis

$$\tfrac{\varrho_0}{\varrho}\,\underline{\underline{\boldsymbol{\pi}}} = 2\varrho_0 \sum_{n=1}^{N} \left(\mathfrak{G}_n(t) \frac{\partial \mathfrak{W}}{\partial I_n}\,\frac{\partial I_n(0,t)}{\partial \underline{\underline{\boldsymbol{\gamma}}}(t)} + \int_0^t \mathfrak{M}_n(t-t') \frac{\partial \mathfrak{W}}{\partial I_n}\,\frac{\partial I_n(t',t)}{\partial \underline{\underline{\boldsymbol{\gamma}}}(t)}\,dt' \right), \qquad (5.4)$$

and as such, produce a work increment (5.2) of

$$dW = \sum_{n=1}^{N} \left(\mathfrak{G}_n(t) \frac{\partial \mathfrak{W}}{\partial I_n}\,\frac{\partial I_n(0,t)}{\partial \underline{\underline{\boldsymbol{\gamma}}}(t)} + \int_0^t \mathfrak{M}_n(t-t') \frac{\partial \mathfrak{W}}{\partial I_n}\,\frac{\partial I_n(t',t)}{\partial \underline{\underline{\boldsymbol{\gamma}}}(t)}\,dt' \right) : d\underline{\underline{\boldsymbol{\gamma}}}(t),$$

where the viscoelastic strain-energy density $W(\mathfrak{P};t',t) = \mathfrak{W}(I_1, I_2, \ldots, I_N\colon \mathfrak{P};t',t)$ with invariants $I_n(\underline{\underline{\gamma}}_{t'}, \underline{\underline{\gamma}}, \underline{\underline{\chi}}_1, \underline{\underline{\chi}}_2, \ldots, \underline{\underline{\chi}}_{M-2}\colon \mathfrak{P};t',t)$, $n = 1,2,\ldots,N$, is constrained such that $\partial\mathfrak{W}(\mathfrak{P};t,t)/\partial\underline{\underline{\gamma}} = \underline{\underline{0}}$ (there can be no strain when the two states defining strain are one in the same), and where $\underline{\underline{\gamma}}_{t'} := \underline{\underline{\gamma}}(\mathfrak{P};t')$ with $t' \in [0,t]$.

The n^{th} relaxation function, $\mathfrak{G}_n(t-t')$, which is positive and dimensionless, along with its associated memory function, $\mathfrak{M}_n(t-t') := \partial\mathfrak{G}_n(t-t')/\partial t'$, which is positive, has units of reciprocal time, and is monotone decreasing, do not specify anisotropic characteristics, when present, which is different from classical viscoelasticity. This task is relegated to the gradient of strain energy, $\partial\mathfrak{W}/\partial\underline{\underline{\gamma}}$, which has units of stress on mass density. The fact that the memory functions, $\mathfrak{M}_n$, are positive and monotonic, and that the state of integration, t', replaces the initial state, $t = 0$, as the reference state in the invariants of the integrand, are both in agreement with the hypothesis of a fading memory [18, 19].

It is because the memory function convolves with a first-order derivative (i.e., strain $\partial\mathfrak{W}/\partial\underline{\underline{\gamma}}$), whereas the relaxation function convolves with a second-order derivative (viz., strain rate $\partial^2\mathfrak{W}/\partial t\,\partial\underline{\underline{\gamma}}$), that motivated our selection of the K-BKZ - like constitutive structure presented in (5.4) as the phenomenological foundatation for our theory of viscoelastic solids.

This type of construction (based on an elastic strain-energy density) is particularly attractive for modeling solids that are predominantly elastic with some viscoelastic attributes, like the materials of interest to us (viz., elastomers and soft biological tissues).

Equation (5.4), which is applicable for viscoelastic solids, is slightly different from the construct that one would use for viscoelastic fluids [71], which is

$$\underline{\underline{\mathbf{\Pi}}} = -\eta_s\, D\underline{\underline{\gamma}}^{-1} + 2\varrho_0 \sum_{n=1}^{N} \int_{-\infty}^{t} \mathfrak{M}_n(t-t') \frac{\partial\mathfrak{W}}{\partial I_n} \frac{\partial I_n(t',t)}{\partial\underline{\underline{\gamma}}(t)}\, dt', \quad \operatorname{tr} D\underline{\underline{\gamma}}^{-1} = 0,$$

wherein η_s represents solvent viscosity. Fluids are usually considered to be incompressible, and as such, the extra stress $\underline{\underline{\mathbf{\Pi}}}$ replaces the body stress $\underline{\underline{\pi}}$ in its construction. Furthermore, the viscous response of the solvent present in a viscoelastic fluid replaces the elastic response that is present in a viscoelastic solid. Finally, the lower limit of integration is moved from zero to minus infinity in the fluid theory, because fluids do not have a unique reference state.

In contrast with the classic formulæ of viscoelasticity, the constitutive theories presented in this chapter place no restrictions on the extent of either strain or rotation.

Thermodynamics places loose constraints on what are admissible functional forms for the strain-energy density $\mathfrak{W}$, relaxation $\mathfrak{G}_n$, and memory $\mathfrak{M}_n$ functions. Like elasticity, this is an important topic, but it lies outside the scope of this report.

5.4 Tangent Operator

Commercial finite-element packages often require a user to supply a tangent operator (or modulus) for user-defined constitutive equations so that its solver can construct

an optimal stiffness matrix. Even though finite-element programs do not employ body tensors, it is still advantageous for us to construct this fourth-rank tensor in the body, and to then map it into the required frame of Cartesian space for later use in finite element analysis.

The tangent operator $\underline{\underline{\underline{\underline{\mathfrak{C}}}}}(\mathfrak{P};0,t)$ is a fourth-rank contravariant tensor defined by

$$\underline{\underline{\underline{\underline{\mathfrak{C}}}}} := 2\,\frac{\partial\big(\frac{\varrho_0}{\varrho}\,\underline{\underline{\pi}}\big)}{\partial\underline{\underline{\gamma}}}, \quad \text{so that} \quad d\big(\tfrac{\varrho_0}{\varrho}\,\underline{\underline{\pi}}\big) = \underline{\underline{\underline{\underline{\mathfrak{C}}}}} : \big(\tfrac{1}{2}\,d\underline{\underline{\gamma}}\big) = \underline{\underline{\underline{\underline{\mathfrak{C}}}}} : d\underline{\underline{\epsilon}}, \tag{5.5}$$

where $\underline{\underline{\epsilon}}$ is the strain tensor of (3.8). This operator has symmetries (in a body-coordinate system $\mathcal{B}$) of $\mathfrak{C}^{ijk\ell} = \mathfrak{C}^{jik\ell} = \mathfrak{C}^{ij\ell k} = \mathfrak{C}^{ji\ell k}$, because stress $\underline{\underline{\pi}}$ and strain $\underline{\underline{\epsilon}}$ are symmetric fields. In component form, (5.5) reads as $\mathfrak{C}^{ijk\ell} = 2\partial(\frac{\varrho_0}{\varrho}\,\pi^{ij})/\partial\gamma_{k\ell}$.

For the elastic constitutive equation of (5.3), the tangent modulus becomes

$$\underline{\underline{\underline{\underline{\mathfrak{C}}}}} = 4\varrho_0 \sum_{n=1}^{N}\left(\frac{\partial\mathfrak{W}}{\partial I_n}\,\frac{\partial^2 I_n}{\partial\underline{\underline{\gamma}}\,\partial\underline{\underline{\gamma}}} + \sum_{m=1}^{N}\frac{\partial^2\mathfrak{W}}{\partial I_m\,\partial I_n}\,\frac{\partial I_m}{\partial\underline{\underline{\gamma}}}\otimes\frac{\partial I_n}{\partial\underline{\underline{\gamma}}}\right), \tag{5.6a}$$

which mandates an additional symmetry of $\mathfrak{C}^{ijk\ell} = \mathfrak{C}^{k\ell ij}$. The tensor outer product $\underline{\underline{\eta}}\otimes\underline{\underline{\eta}}$ has components $\eta^{ij}\eta^{k\ell}$ in coodrinate system $\mathcal{B}$. In most material models, including those of this report, $\partial^2\mathfrak{W}/\partial I_m\,\partial I_n = 0$ for all $m \neq n$, thereby simplifying the above modulus so that it becomes

$$\underline{\underline{\underline{\underline{\mathfrak{C}}}}} = 4\varrho_0 \sum_{n=1}^{N}\left(\frac{\partial\mathfrak{W}}{\partial I_n}\,\frac{\partial^2 I_n}{\partial\underline{\underline{\gamma}}\,\partial\underline{\underline{\gamma}}} + \frac{\partial^2\mathfrak{W}}{\partial I_n^2}\,\frac{\partial I_n}{\partial\underline{\underline{\gamma}}}\otimes\frac{\partial I_n}{\partial\underline{\underline{\gamma}}}\right). \tag{5.6b}$$

In keeping with the assumption that there are no cross-coupling terms arising between the various invariants in the functions selected to represent strain-energy density, it follows that

$$\begin{aligned}\underline{\underline{\underline{\underline{\mathfrak{C}}}}} = 4\varrho_0 \sum_{n=1}^{N}\Bigg(&\mathfrak{G}_n(t)\frac{\partial\mathfrak{W}}{\partial I_n}\,\frac{\partial^2 I_n}{\partial\underline{\underline{\gamma}}\,\partial\underline{\underline{\gamma}}} + \int_0^t \mathfrak{M}_n(t-t')\frac{\partial\mathfrak{W}}{\partial I_n}\,\frac{\partial^2 I_n}{\partial\underline{\underline{\gamma}}\,\partial\underline{\underline{\gamma}}}\,dt' \\ &+ \mathfrak{G}_n(t)\frac{\partial^2\mathfrak{W}}{\partial I_n^2}\,\frac{\partial I_n}{\partial\underline{\underline{\gamma}}}\otimes\frac{\partial I_n}{\partial\underline{\underline{\gamma}}} + \int_0^t \mathfrak{M}_n(t-t')\frac{\partial^2\mathfrak{W}}{\partial I_n^2}\,\frac{\partial I_n}{\partial\underline{\underline{\gamma}}}\otimes\frac{\partial I_n}{\partial\underline{\underline{\gamma}}}\,dt'\Bigg),\end{aligned} \tag{5.7}$$

for the viscoelastic constitutive equation of (5.4). Some care is required here becuase $I_n = I_n(0,t)$ in the elastic terms; whereas, $I_n = I_n(t',t)$ in viscoelastic (integral) terms.

5.4.1 Stability

For an elastic or viscoelastic solid to be stable requires that it be Hadamard stable, and as such, satisfies a condition of strong ellipticity where it becomes necessary and sufficient that

$$\mathfrak{C}^{ijk\ell}x_i y_j x_k y_\ell > 0, \quad \forall\ \underline{\boldsymbol{x}},\underline{\boldsymbol{y}}. \tag{5.8a}$$

A more useful condition (in accordance with 5.5), which is necessary but not sufficient, is that

$$d\underline{\underline{\epsilon}} : \underline{\underline{\underline{\underline{\mathfrak{C}}}}} : d\underline{\underline{\epsilon}} = d\left(\tfrac{\varrho_0}{\varrho}\,\underline{\underline{\pi}}\right) : d\underline{\underline{\epsilon}} > 0, \quad \forall \; d\underline{\underline{\epsilon}}. \tag{5.8b}$$

This is a thermodynamic condition for stability, the so-called Drucker [28] stability postulate, which is not a physical law.

The necessary and sufficient conditions for strong ellipticity are extremely complex and awkward to verify for any given model. It is for this reason that attempts have been made to obtain sufficient conditions for strong ellipticity that are of ample generality to be useful to the model developer. Of note are the works of Renardy [92], Leonov [65] and Kwon and Cho [61], all of which address viscoelastic liquids.

Dissipative stability, pertinent for a stability analysis of viscoelastic liquids [65], has no role to play in the stability analysis of viscoelastic solids.

5.5 Isotropic Elasticity

An isotropic elastic solid can be formulated in terms of two, mixed, tensor fields when being described by body-tensor fields; in particular, consider $\mathbb{A} := \mathfrak{b}_0^{-1}\mathfrak{b}$ and $\mathbb{B} := \mathfrak{b}^{-1}\mathfrak{b}_0$,* where one field is the inverse of the other. The conservation of mass, $\det(\underline{\underline{\gamma}}^{-1}\cdot\underline{\underline{\gamma}}_0) = (\varrho/\varrho_0)^2 > 0$, guarentees that $\underline{\underline{\gamma}}^{-1}\cdot\underline{\underline{\gamma}}_0$ is non-singular, and consequently, invertible (and therefore, $\underline{\underline{\gamma}}_0^{-1}\cdot\underline{\underline{\gamma}}$ is non-singular and invertible, too). As such, only three of the ten possible invariants in (5.1a & 5.1b) are independent. In what follows, we will postulate the existance of an integrity basis that is comprised of sums of like invariants taken from these two deformation tensors, and in doing so, we average their characteristics.

From a mechanics perspective, there is no reason to choose the deformation variable $\underline{\underline{\gamma}}_0^{-1}\cdot\underline{\underline{\gamma}}$ over deformation variable $\underline{\underline{\gamma}}^{-1}\cdot\underline{\underline{\gamma}}_0$, or vice versa. However, from a physics perspective, the molecular network theory of rubber elasticity (i.e., the neo-Hookean solid [53]) produces a constitutive equation described soley in terms of $\underline{\underline{\gamma}}_0^{-1}\cdot\underline{\underline{\gamma}}$ [72]. This contrasts with the popular phenomenological model of Mooney [80] that utilizes both deformation fields in its description, and whose rigorous derivation from statistical mechanics continues to elude researchers.

Rivlin [93, 94, 95, 96, 97, 98] and his students, Saunders [99] and Gent [39, 40, 41], were amoung the first to derive constitutive equations from an integrity basis for finite-strain isotropic elasticity, and to perform multi-dimensional experiments to seek out admissible functional forms for the strain-energy density. Reiner [91] was the first to

*As is the norm in general tensor analysis, the trace of a tensor field (in this case, $\underline{\underline{\gamma}}_0^{-1}$ and $\underline{\underline{\gamma}}_0$) is achieved through a contraction with the metric $\underline{\underline{\gamma}} := \underline{\underline{\gamma}}(\mathfrak{P}, t)$, $t > 0$, or, when appropriate, its inverse $\underline{\underline{\gamma}}^{-1} := \underline{\underline{\gamma}}^{-1}(\mathfrak{P}, t)$. It is because of this fact that gradients (i.e., $\partial\mathfrak{W}/\partial\underline{\underline{\gamma}}$) can arise from a strain-energy density $W = \mathfrak{W}(I_i; i = 1, 2, \ldots, N)$ that may otherwise be considered as resulting from non-conservative sources, (e.g., one can introduce $D\underline{\underline{\gamma}}$ as a state variable). This is one very important reason why we prefer using body-tensor fields for the purpose of deriving constitutive theories.

actually derive constitutive equations from an integrity basis. Today they are called Reiner fluids.

Flory [34] proposed a multiplicative decomposition of the deformation field (defining $\underline{\underline{G}} := (\det \underline{\underline{F}})^{-1/3} \underline{\underline{F}}$ so that $\det \underline{\underline{G}} = 1$) as a way to uncouple deviatoric and hydrostatic responses, which has certain advantages from a computational perspective [105]. We choose not to make such a decomposition in this body of work because the invariants we have chosen have gradients that are strain fields, not deformation fields as is typically the case, and therefore, it is not certain if the added complexity of introducing such a decomposition is warrented at this time.

Adding respective invariants from the two deformation tensors, $\underline{\underline{\gamma}}_0^{-1} \cdot \underline{\underline{\gamma}}$ and $\underline{\underline{\gamma}}^{-1} \cdot \underline{\underline{\gamma}}_0$, each anchored to a different state, averages the effect of reference state that is tacitly held by these two measures for deformation and leads us to consider the following set of invariants as our integrity basis:

$$\left.\begin{aligned} I_1 &:= \tfrac{1}{4}\left(\underline{\underline{\gamma}}_0^{-1} : \underline{\underline{\gamma}} + \underline{\underline{\gamma}}^{-1} : \underline{\underline{\gamma}}_0\right) \\ I_2 &:= \tfrac{1}{16}\left(\underline{\underline{\gamma}}_0^{-1} \cdot \underline{\underline{\gamma}} \cdot \underline{\underline{\gamma}}_0^{-1} : \underline{\underline{\gamma}} + \underline{\underline{\gamma}}^{-1} \cdot \underline{\underline{\gamma}}_0 \cdot \underline{\underline{\gamma}}^{-1} : \underline{\underline{\gamma}}_0\right) \\ I_3 &:= \sqrt{\det\left(\underline{\underline{\gamma}}_0^{-1} \cdot \underline{\underline{\gamma}}\right)} + \sqrt{\det\left(\underline{\underline{\gamma}}^{-1} \cdot \underline{\underline{\gamma}}_0\right)} \end{aligned}\right\}, \tag{5.9a}$$

whose gradients,[†]

$$\left.\begin{aligned} \partial I_1/\partial \underline{\underline{\gamma}} &= \tfrac{1}{4}\left(\underline{\underline{\gamma}}_0^{-1} - \underline{\underline{\gamma}}^{-1} \cdot \underline{\underline{\gamma}}_0 \cdot \underline{\underline{\gamma}}^{-1}\right) \\ \partial I_2/\partial \underline{\underline{\gamma}} &= \tfrac{1}{8}\left(\underline{\underline{\gamma}}_0^{-1} \cdot \underline{\underline{\gamma}} \cdot \underline{\underline{\gamma}}_0^{-1} - \underline{\underline{\gamma}}^{-1} \cdot \underline{\underline{\gamma}}_0 \cdot \underline{\underline{\gamma}}^{-1} \cdot \underline{\underline{\gamma}}_0 \cdot \underline{\underline{\gamma}}^{-1}\right) \\ \partial I_3/\partial \underline{\underline{\gamma}} &= \tfrac{1}{2}\left(\sqrt{\det\left(\underline{\underline{\gamma}}_0^{-1} \cdot \underline{\underline{\gamma}}\right)} - \sqrt{\det\left(\underline{\underline{\gamma}}^{-1} \cdot \underline{\underline{\gamma}}_0\right)}\right) \underline{\underline{\gamma}}^{-1} \end{aligned}\right\}, \tag{5.9b}$$

[†]Here we have used the following results to derive the gradients $\partial I_n/\partial \underline{\underline{\gamma}}$ and $\partial^2 I_n/\partial \underline{\underline{\gamma}}\,\partial \underline{\underline{\gamma}}$:

$$\frac{\partial \underline{\underline{\gamma}}}{\partial \underline{\underline{\gamma}}} = \underline{\underline{\delta}} \boxtimes \underline{\underline{\delta}}, \quad \text{with components in } \mathcal{B} \text{ of } \quad \frac{\partial \gamma_{k\ell}}{\partial \gamma_{ij}} = \tfrac{1}{2}\left(\delta^i_k \delta^j_\ell + \delta^i_\ell \delta^j_k\right),$$

$$\frac{\partial \underline{\underline{\gamma}}^{-1}}{\partial \underline{\underline{\gamma}}} = -\underline{\underline{\gamma}}^{-1} \boxtimes \underline{\underline{\gamma}}^{-1}, \quad \text{with components in } \mathcal{B} \text{ of } \quad \frac{\partial \gamma^{k\ell}}{\partial \gamma_{ij}} = -\tfrac{1}{2}\left(\gamma^{ik}\gamma^{j\ell} + \gamma^{i\ell}\gamma^{jk}\right),$$

and

$$\frac{\partial |\underline{\underline{\gamma}}|}{\partial \underline{\underline{\gamma}}} = |\underline{\underline{\gamma}}|\, \underline{\underline{\gamma}}^{-1}, \quad \text{noting that} \quad |\underline{\underline{\gamma}}_0^{-1} \cdot \underline{\underline{\gamma}}| = |\underline{\underline{\gamma}}_0^{-1}|\, |\underline{\underline{\gamma}}| = \frac{|\underline{\underline{\gamma}}|}{|\underline{\underline{\gamma}}_0|}.$$

are symmetric strain fields, and whose second derivatives,

$$\left.\begin{aligned}
\partial^2 I_1/\partial\underline{\underline{\gamma}}\,\partial\underline{\underline{\gamma}} &= \tfrac{1}{4}\Big(\underline{\underline{\gamma}}^{-1}\boxtimes\underline{\underline{\gamma}}^{-1}\cdot\underline{\underline{\gamma}}_0\cdot\underline{\underline{\gamma}}^{-1}+\underline{\underline{\gamma}}^{-1}\cdot\underline{\underline{\gamma}}_0\cdot\underline{\underline{\gamma}}^{-1}\boxtimes\underline{\underline{\gamma}}^{-1}\Big)\\
\partial^2 I_2/\partial\underline{\underline{\gamma}}\,\partial\underline{\underline{\gamma}} &= \tfrac{1}{8}\Big(\underline{\underline{\gamma}}_0^{-1}\boxtimes\underline{\underline{\gamma}}_0^{-1}+\underline{\underline{\gamma}}^{-1}\cdot\underline{\underline{\gamma}}_0\cdot\underline{\underline{\gamma}}^{-1}\boxtimes\underline{\underline{\gamma}}^{-1}\cdot\underline{\underline{\gamma}}_0\cdot\underline{\underline{\gamma}}^{-1}\\
&\quad+\underline{\underline{\gamma}}^{-1}\boxtimes\underline{\underline{\gamma}}^{-1}\cdot\underline{\underline{\gamma}}_0\cdot\underline{\underline{\gamma}}^{-1}\cdot\underline{\underline{\gamma}}_0\cdot\underline{\underline{\gamma}}^{-1}+\underline{\underline{\gamma}}^{-1}\cdot\underline{\underline{\gamma}}_0\cdot\underline{\underline{\gamma}}^{-1}\cdot\underline{\underline{\gamma}}_0\cdot\underline{\underline{\gamma}}^{-1}\boxtimes\underline{\underline{\gamma}}^{-1}\Big)\\
\partial^2 I_3/\partial\underline{\underline{\gamma}}\,\partial\underline{\underline{\gamma}} &= \tfrac{1}{4}\Big(\sqrt{\det\big(\underline{\underline{\gamma}}^{-1}\cdot\underline{\underline{\gamma}}_0\big)}+\sqrt{\det\big(\underline{\underline{\gamma}}_0^{-1}\cdot\underline{\underline{\gamma}}\big)}\Big)\,\underline{\underline{\gamma}}^{-1}\otimes\underline{\underline{\gamma}}^{-1}\\
&\quad+\tfrac{1}{2}\Big(\sqrt{\det\big(\underline{\underline{\gamma}}^{-1}\cdot\underline{\underline{\gamma}}_0\big)}-\sqrt{\det\big(\underline{\underline{\gamma}}_0^{-1}\cdot\underline{\underline{\gamma}}\big)}\Big)\,\underline{\underline{\gamma}}^{-1}\boxtimes\underline{\underline{\gamma}}^{-1}
\end{aligned}\right\}, \qquad (5.9c)$$

appear in the tangent moduli of (5.6). At first glance, these invariants and their gradients appear to be somewhat complex but, as we shall soon discover, these definitions produce relatively simple constitutive formulæ in the Eulerian frame. The coefficients imposed on these invariants scale their associated strain measures so that they coincide with the definition of infinitesimal strain in the small-strain limit. The fact that a square root can be used directly in I_3, but not in I_1 or I_2, has to do with some unique properties of the determinant that are not shared by the trace.[‡]

Each strain measure in (5.9b) vanishes in the reference state; however, not one of these strains is additive and anti-symmetric in its dependence upon state; yet they all possess the desirable property of producing an asymmetric tension/compression response—a property that first appeared in finite-strain theory with Hencky's [49] definition for strain, which is $\frac{1}{2}\ln\big(\underline{\underline{\gamma}}_0^{-1}\cdot\underline{\underline{\gamma}}\big) = \ln\underline{\underline{\Lambda}}$ when expressed in terms of body-tensor fields [36].

Utilizing the gradients in (5.9b) obtained from the postulated invariants of (5.9a), the constitutive equation for an isotropic elastic solid derived from the work potential

---

[‡]Instead of using the mixed deformation tensors $\underline{\underline{\gamma}}_0^{-1}\cdot\underline{\underline{\gamma}}$ and $\underline{\underline{\gamma}}^{-1}\cdot\underline{\underline{\gamma}}_0$ as state variables, it may be preferable (especially for viscoelastic liquids) to use the mixed stretch tensors

$$\underline{\underline{\Lambda}} \coloneqq \sqrt{\underline{\underline{\gamma}}_0^{-1}\cdot\underline{\underline{\gamma}}} \quad\text{and}\quad \underline{\underline{\Lambda}}^{-1} = \sqrt{\underline{\underline{\gamma}}^{-1}\cdot\underline{\underline{\gamma}}_0},$$

as state variables. From the identity $\underline{\underline{\Lambda}}^{-1}\cdot\underline{\underline{\Lambda}} = \underline{\underline{\delta}}$, it follows that

$$\frac{\partial\underline{\underline{\Lambda}}^{-1}}{\partial\underline{\underline{\gamma}}} = -\underline{\underline{\Lambda}}^{-1}\cdot\frac{\partial\underline{\underline{\Lambda}}}{\partial\underline{\underline{\gamma}}}\cdot\underline{\underline{\Lambda}}^{-1},$$

and likewise, from the identity $\underline{\underline{\Lambda}}\cdot\underline{\underline{\Lambda}} = \underline{\underline{\gamma}}_0^{-1}\cdot\underline{\underline{\gamma}}$, it follows that

$$\frac{\partial\underline{\underline{\Lambda}}}{\partial\underline{\underline{\gamma}}}\cdot\underline{\underline{\Lambda}}+\underline{\underline{\Lambda}}\cdot\frac{\partial\underline{\underline{\Lambda}}}{\partial\underline{\underline{\gamma}}} = \underline{\underline{\gamma}}_0\boxtimes\underline{\underline{\delta}}.$$

Like relations exist in the case of time derivatives. Only when a solution can be found for $\partial\underline{\underline{\Lambda}}/\partial\underline{\underline{\gamma}}$, assuming that a solution does indeed exist, will it be possible to construct a theory using stretches instead of deformations as the state variables.

in (5.2) has a stress response of

$$\begin{aligned}\tfrac{\varrho_0}{\varrho}\,\underline{\underline{\pi}} = 2\varrho_0\Big(&\mathfrak{W}_{,1}\,\tfrac{1}{4}\Big(\underline{\underline{\gamma}}_0^{-1} - \underline{\underline{\gamma}}^{-1}\cdot\underline{\underline{\gamma}}_0\cdot\underline{\underline{\gamma}}^{-1}\Big)\\ &+\mathfrak{W}_{,2}\,\tfrac{1}{8}\Big(\underline{\underline{\gamma}}_0^{-1}\cdot\underline{\underline{\gamma}}\cdot\underline{\underline{\gamma}}_0^{-1} - \underline{\underline{\gamma}}^{-1}\cdot\underline{\underline{\gamma}}_0\cdot\underline{\underline{\gamma}}^{-1}\cdot\underline{\underline{\gamma}}_0\cdot\underline{\underline{\gamma}}^{-1}\Big)\\ &+\mathfrak{W}_{,3}\,\tfrac{1}{2}\Big(\sqrt{\det\big(\underline{\underline{\gamma}}_0^{-1}\cdot\underline{\underline{\gamma}}\big)} - \sqrt{\det\big(\underline{\underline{\gamma}}^{-1}\cdot\underline{\underline{\gamma}}_0\big)}\Big)\underline{\underline{\gamma}}^{-1}\Big),\end{aligned} \tag{5.10a}$$

whose trace defines a state of hydrostatic pressure (3.19b)

$$\begin{aligned}\tfrac{\varrho_0}{\varrho}\,p = -\tfrac{2}{3}\,\varrho_0\Big(&\mathfrak{W}_{,1}\,\tfrac{1}{4}\Big(\underline{\underline{\gamma}}_0^{-1}:\underline{\underline{\gamma}} - \underline{\underline{\gamma}}^{-1}:\underline{\underline{\gamma}}_0\Big)\\ &+\mathfrak{W}_{,2}\,\tfrac{1}{8}\Big(\underline{\underline{\gamma}}_0^{-1}\cdot\underline{\underline{\gamma}}\cdot\underline{\underline{\gamma}}_0^{-1}:\underline{\underline{\gamma}} - \underline{\underline{\gamma}}^{-1}\cdot\underline{\underline{\gamma}}_0\cdot\underline{\underline{\gamma}}^{-1}:\underline{\underline{\gamma}}_0\Big)\\ &+3\,\mathfrak{W}_{,3}\,\tfrac{1}{2}\Big(\sqrt{\det\big(\underline{\underline{\gamma}}_0^{-1}\cdot\underline{\underline{\gamma}}\big)} - \sqrt{\det\big(\underline{\underline{\gamma}}^{-1}\cdot\underline{\underline{\gamma}}_0\big)}\Big)\Big),\end{aligned} \tag{5.10b}$$

that for materials whose bulk moduli are many times more stiff than their shear moduli becomes[§]

$$\tfrac{\varrho_0}{\varrho}\,p \approx -\varrho_0\,\mathfrak{W}_{,3}\Big(\sqrt{\det\big(\underline{\underline{\gamma}}_0^{-1}\cdot\underline{\underline{\gamma}}\big)} - \sqrt{\det\big(\underline{\underline{\gamma}}^{-1}\cdot\underline{\underline{\gamma}}_0\big)}\Big). \tag{5.10c}$$

Here $\mathfrak{W}_{,i} := \partial\mathfrak{W}(0,t)/\partial I_i$, $i = 1,2,3$, are three material functions that can, at most, depend upon the three scalar invariants $I_1(0,t)$, $I_2(0,t)$ and $I_3(0,t)$. The invariants in (5.9a) are defined as sums between like invariants taken from the two stretch tensors, $\underline{\underline{\gamma}}_0^{-1}\cdot\underline{\underline{\gamma}}$ and $\underline{\underline{\gamma}}^{-1}\cdot\underline{\underline{\gamma}}_0$. Cureously, hydrostatic pressure p is described in terms of differences taken between these same, fundamental, stretch invariants.

For the special case of an (ideally) incompressible material, the above theoretical structure reduces to

$$\underline{\underline{\mathbf{\Pi}}} = 2\varrho_0\Big(\mathfrak{W}_{,1}\,\tfrac{1}{4}\Big(\underline{\underline{\gamma}}_0^{-1} - \underline{\underline{\gamma}}^{-1}\cdot\underline{\underline{\gamma}}_0\cdot\underline{\underline{\gamma}}^{-1}\Big) + \mathfrak{W}_{,2}\,\tfrac{1}{8}\Big(\underline{\underline{\gamma}}_0^{-1}\cdot\underline{\underline{\gamma}}\cdot\underline{\underline{\gamma}}_0^{-1} - \underline{\underline{\gamma}}^{-1}\cdot\underline{\underline{\gamma}}_0\cdot\underline{\underline{\gamma}}^{-1}\cdot\underline{\underline{\gamma}}_0\cdot\underline{\underline{\gamma}}^{-1}\Big)\Big), \tag{5.10d}$$

which is similar to setting $\mathfrak{W}_{,3} = 0$. Tensor $\underline{\underline{\mathbf{\Pi}}}$ $(= \wp\,\underline{\underline{\gamma}}^{-1} + \underline{\underline{\pi}})$ is the extra-stress of (3.20a), with $\wp$ being a Lagrange multiplier that forces a constraint for incompressibility, $\det\underline{\underline{\gamma}} = \det\underline{\underline{\gamma}}_0$.

The tensorial nature of (5.10) is fixed. Its structure is a direct consequence of the chosen integrity basis listed in (5.9). Only the three scalar functions $\mathfrak{W}_{,i}$ are adjustable. Their specification will turn this theory for elasticity into a material model, which is the primary topic of Chps. 7–??.

[§]It is for this reason that we do not find it necessary to decouple strain into separate hydrostatic and deviatoric parts.

5.5.1 Field transfer

Using the results of Chp. 4, it is a straightforward process to map this theory for isotropic elasticity from the body manifold where it was derived into Cartesian space where it will be used to solve boundary-value problems. The main results from these mappings are outlined below.

Lagrangian frame

When the time of field transfer coincides with initial time $t = 0$, then the resulting Cartesian fields are referenced to the Lagrangian (or material) configuration. In this frame of reference, the isotropic elastic invariants of (5.9a) are computed as

$$\left.\begin{aligned} I_1 &= \tfrac{1}{4}\Big(\operatorname{tr}\underline{\underline{C}} + \operatorname{tr}\underline{\underline{C}}^{-1}\Big) \\ I_2 &= \tfrac{1}{16}\Big(\big(\operatorname{tr}\underline{\underline{C}}^2\big) + \big(\operatorname{tr}\underline{\underline{C}}^{-2}\big)\Big) \\ I_3 &= \sqrt{\det\underline{\underline{C}}} + \sqrt{\det\underline{\underline{C}}^{-1}} = \det\underline{\underline{F}} + \det\underline{\underline{F}}^{-1} \end{aligned}\right\}, \tag{5.11}$$

where $\underline{\underline{C}}$ $(= \underline{\underline{F}}^{\mathrm{T}} \cdot \underline{\underline{F}})$ is the symmetric deformation tensor of Green (4.6), often called the right, Cauchy-Green, deformation tensor, in which tensor $\underline{\underline{F}}$ $(= \partial\underline{x}/\partial\underline{X})$ denotes the deformation gradient defined in (4.2).

An isotropic elastic solid whose invariants are so defined has a stress response (mapped from Eqn. 5.10a) of

$$\underline{\underline{P}} = 2\varrho_0\Big(\mathfrak{W}_{,1}\,\tfrac{1}{4}\big(\underline{\underline{I}} - \underline{\underline{C}}^{-2}\big) + \mathfrak{W}_{,2}\,\tfrac{1}{8}\big(\underline{\underline{C}} - \underline{\underline{C}}^{-3}\big) + \mathfrak{W}_{,3}\,\tfrac{1}{2}\big(\det\underline{\underline{F}} - \det\underline{\underline{F}}^{-1}\big)\underline{\underline{C}}^{-1}\Big), \tag{5.12a}$$

with $\underline{\underline{P}}$ being the second, Piola-Kirchhoff, stress tensor defined in (4.42c). In the incompressible case, (5.10c) maps to space as the constitutive formula

$$\underline{\underline{P}}^{\star} + \wp\,\underline{\underline{C}}^{-1} = 2\varrho_0\Big(\mathfrak{W}_{,1}\,\tfrac{1}{4}\big(\underline{\underline{I}} - \underline{\underline{C}}^{-2}\big) + \mathfrak{W}_{,2}\,\tfrac{1}{8}\big(\underline{\underline{C}} - \underline{\underline{C}}^{-3}\big)\Big), \tag{5.12b}$$

subject to a constraint for incompressibility, $\det\underline{\underline{F}} = 1$. Tensor $\underline{\underline{P}}^{\star}$ $(= \frac{\varrho}{\varrho_0}\underline{\underline{P}})$ represents the Lagrangian stress tensor of (4.42c) that, in the incompressible limit, is equivalent to the second Piola-Kirchhoff stress $\underline{\underline{P}}$ becuase $\varrho = \varrho_0$.

Eulerian frame

When the time of field transfer coincides with current time t, then the resulting fields in Cartesian space are referenced to the Eulerian (or spatial) configuration. In this frame of reference, the isotropic elastic invariants of (5.9a) are computed as

$$\left.\begin{aligned} I_1 &= \tfrac{1}{4}\Big(\operatorname{tr}\underline{\underline{B}} + \operatorname{tr}\underline{\underline{B}}^{-1}\Big) \\ I_2 &= \tfrac{1}{16}\Big(\big(\operatorname{tr}\underline{\underline{B}}^2\big) + \big(\operatorname{tr}\underline{\underline{B}}^{-2}\big)\Big) \\ I_3 &= \sqrt{\det\underline{\underline{B}}} + \sqrt{\det\underline{\underline{B}}^{-1}} = \det\underline{\underline{F}} + \det\underline{\underline{F}}^{-1} \end{aligned}\right\}, \tag{5.13}$$

where $\underline{\underline{B}}$ ($= \underline{\underline{F}} \cdot \underline{\underline{F}}^{\mathrm{T}}$) is the symmetric deformation tensor of Finger (4.5), often called the left, Cauchy-Green, deformation tensor. Because the trace of a matrix product is independent of the order in which the product is taken, these Eulerian invariants equal their Lagrangian counterparts, which is why they are called invariants.

An isotropic elastic solid whose invariants are defined by (5.13) has a stress response (mapped from Eqn. 5.10a) of

$$\tfrac{\varrho_0}{\varrho}\,\underline{\underline{T}} = 2\varrho_0\Big(\mathfrak{W}_{,1}\,\tfrac{1}{4}\big(\underline{\underline{B}} - \underline{\underline{B}}^{-1}\big) + \mathfrak{W}_{,2}\,\tfrac{1}{8}\big(\underline{\underline{B}}^2 - \underline{\underline{B}}^{-2}\big) + \mathfrak{W}_{,3}\,\tfrac{1}{2}\big(\det\underline{\underline{F}} - \det\underline{\underline{F}}^{-1}\big)\underline{\underline{I}}\Big), \quad (5.14a)$$

with $\underline{\underline{T}}$ denoting the Cauchy stress defined in (4.42a). For the incompressible case (from a mapping of 5.10c), the stress response of (5.14a) reduces to an extra-stress response of

$$\underline{\underline{T}} + \wp\,\underline{\underline{I}} = 2\varrho_0\Big(\mathfrak{W}_{,1}\,\tfrac{1}{4}\big(\underline{\underline{B}} - \underline{\underline{B}}^{-1}\big) + \mathfrak{W}_{,2}\,\tfrac{1}{8}\big(\underline{\underline{B}}^2 - \underline{\underline{B}}^{-2}\big)\Big), \quad (5.14b)$$

where the Lagrange multiplier $\wp$ forces a constraint for incompressiblity, $\det\underline{\underline{F}} = 1$. Special care must be taken when implementing this constitutive equation (in fact, when implementing any nearly incompressible material model) into finite elements so as to avoid possible ill-conditioning of the stiffness matrix leading to a potential locking of the mesh caused by an overconstrained displacement field.

It is here, in the Eulerian frame, that the full simplicity of our constitutive theory for isotropic elasticity (derived from the integrity basis of 5.9a) is most apparent.

Equation (5.12a) can be pushed forward into the Eulerian frame producing (5.14a) by contracting (5.12a) with $\underline{\underline{F}}$ from the left and $\underline{\underline{F}}^{\mathrm{T}}$ from the right. Conversely, (5.14a) can be pulled backward into the Lagrangian frame producing (5.12a) by contracting (5.14a) with $\underline{\underline{F}}^{-1}$ from the left and $\underline{\underline{F}}^{-\mathrm{T}}$ from the right. These are appropriate push-forward/pull-back mappings for contravariant-like tensor fields. Because these mappings apply to $\underline{\underline{T}}$ and $\underline{\underline{P}}^{\star}$, and also to $\frac{\varrho_0}{\varrho}\,\underline{\underline{T}}$ and $\underline{\underline{P}}$, it is sufficient to obtain a single transfer of field from the body into Cartesian space (hereafter, we will provide mappings into the Eulerian frame) from which the corresponding formulation in the other (viz., Lagrangian) frame can then be readily acquired by applying the appropriate (i.e., pull-back) mapping between these two Cartesian configurations.

Generalized strain fields: The elastic theory presented above is constructed with generalized strain fields of the type

$$\underline{\underline{E}}^{(n)} := \tfrac{1}{4n}\big(\underline{\underline{B}}^{n} - \underline{\underline{B}}^{-n}\big), \quad n \in \mathbb{R}, \quad (5.15a)$$

with dilatation being approximated by the scalar measure

$$e := \tfrac{1}{2}\big(\det\underline{\underline{F}} - \det\underline{\underline{F}}^{-1}\big), \quad (5.15b)$$

where instances $n = 1$ and $n = 2$ are the strain fields present in (5.14) so that[¶]

$$\tfrac{\varrho_0}{\varrho}\,\underline{\underline{T}} = 2\varrho_0\big(\mathfrak{W}_{,1}\,\underline{\underline{E}}^{(1)} + \mathfrak{W}_{,2}\,\underline{\underline{E}}^{(2)} + \mathfrak{W}_{,3}\,e\,\underline{\underline{I}}\big), \quad (5.16a)$$

[¶]Another constitutive theory that may prove useful is

$$\tfrac{\varrho_0}{\varrho}\,\underline{\underline{T}} = 2\varrho_0\big(a\,\underline{\underline{E}}^{(1/2)} + b\,\underline{\underline{E}}^{(1)} + c\,e\,\underline{\underline{I}}\big),$$

with a hydrostatic pressure of

$$\tfrac{\varrho_0}{\varrho}\, p = -\tfrac{2}{3}\varrho_0\big(\mathfrak{W}_{,1}\,\mathrm{tr}\,\underline{\underline{E}}^{(1)} + \mathfrak{W}_{,2}\,\mathrm{tr}\underline{\underline{E}}^{(2)} + 3\,\mathfrak{W}_{,3}\,e\big) \approx -2\varrho_0\mathfrak{W}_{,3}\,e, \tag{5.16b}$$

that for incompressible materials becomes

$$\underline{\underline{T}} + \wp\,\underline{\underline{I}} = 2\varrho_0\big(\mathfrak{W}_{,1}\,\underline{\underline{E}}^{(1)} + \mathfrak{W}_{,2}\,\underline{\underline{E}}^{(2)}\big), \tag{5.16c}$$

satisfying a constraint for incompressiblity, $\det \underline{\underline{F}} = 1$. We will explore the capabilities of these elastic constitutive formulæ in the remaining chapters of this report. The notation $\underline{\underline{E}}^{(n)}$ ($\neq D^n\underline{\underline{E}}$) does not imply a derivative of order n, as it is often understood to mean.

Equation (5.15) is distinct from the generalized strain fields introduced by Doyle and Ericksen [26], where they define $\underline{\underline{E}}^{(n)}_{DE} := \frac{1}{2n}\big(\underline{\underline{C}}^n - \underline{\underline{I}}\big)$. Equation (5.15) is similar to, but still distinct from, the generalized strain fields of Bažant [6], where he defines $\underline{\underline{E}}^{(n)}_{B} := \frac{1}{4n}\big(\underline{\underline{C}}^n - \underline{\underline{C}}^{-n}\big)$. Actually, $\underline{\underline{E}}^{(n)} = \underline{\underline{R}}\cdot\underline{\underline{E}}^{(n)}_{B}\cdot\underline{\underline{R}}^{\mathrm{T}}$ with $\underline{\underline{R}}$ denoting the orthogonal rotation tensor (i.e., $\underline{\underline{R}}^{\mathrm{T}}\cdot\underline{\underline{R}} = \underline{\underline{I}}$) gotten from a polar decompostion of $\underline{\underline{F}}$ such that $\underline{\underline{F}} = \underline{\underline{V}}\cdot\underline{\underline{R}} = \underline{\underline{R}}\cdot\underline{\underline{U}}$, where $\underline{\underline{V}}$ and $\underline{\underline{U}}$ are symmetric positive-definite tensors called the left- and right-stretch tensors, respectively. It is easily verified that $\underline{\underline{B}} = \underline{\underline{V}}^2$ and $\underline{\underline{C}} = \underline{\underline{U}}^2$.

Taylor expansions (expressed as series in infinitesimal strain) of any Doyle-Ericksen strain field and of Hencky [49] strain, $\frac{1}{2}\ln\underline{\underline{C}} = \ln\underline{\underline{U}}$, are coincident only in their linear terms; they differ in all other terms in their expansions. In contrast, Taylor expansions of any Bažant strain field and of Hencky strain are coincident through their quadratic terms, differing thereafter [6]. Taylor expansions of (5.15) and $\frac{1}{2}\ln\underline{\underline{B}} = \ln\underline{\underline{V}}$ are likewise coincident through their quadratic terms, independent of n. This makes $\underline{\underline{E}}^{(n)}$ a reasonable approximation for logarithmic (true) strain, without having to deal with the complexities that otherwise accompany Hencky strain [51].

The strain fields of Hencky, Bažant, and Eqn. (5.15) all possess the desirable property of tension/compression asymmetry; for example, stretches of λ and λ^{-1} in uniaxial extension have strains that are equal in magnitude but opposite in sign.

Tangent operator: In an Eulerian frame where, for example, tangent moduli are constructed in updated-Lagrangian finite-element codes, the tangent operator of (5.5) maps into Cartesian space as[‖]

$$\big(\tfrac{\varrho_0}{\varrho}\,\underline{\underline{T}}\big)^{\vartriangle} = \underline{\underline{\underline{\underline{\mathcal{C}}}}} : \underline{\underline{D}}, \tag{5.17}$$

---

where a, b and c are material functions of some set of invariants yet to be determined. Such a theory could be constructed from a work (or strain energy) potential if one knew how to solve

$$\frac{\partial \underline{\underline{U}}}{\partial \underline{\underline{C}}}\cdot\underline{\underline{U}} + \underline{\underline{U}}\cdot\frac{\partial \underline{\underline{U}}}{\partial \underline{\underline{C}}} = \underline{\underline{I}}\boxtimes\underline{\underline{I}},$$

which here is represented in terms of Lagrangian fields.

[‖]In a Lagrangian frame, the tangent operator of (5.5) maps into Cartesian space as $d\underline{\underline{P}} = \underline{\underline{\underline{\underline{\mathrm{C}}}}} : d\underline{\underline{E}}$, where $\underline{\underline{P}}$ is the second, Piola-Kirchhoff, stress tensor and $\underline{\underline{E}}$ is the Green strain tensor. The Lagrangian and Eulerian tangent moduli have components that relate according to $\mathrm{C}_{ijk\ell} = \mathrm{F}^{-1}_{im}\mathrm{F}^{-1}_{jn}\mathrm{F}^{-1}_{kp}\mathrm{F}^{-1}_{\ell q}\mathcal{C}_{mnpq}$.

where $\underline{\underline{D}}$ is the rate-of-deformation tensor defined in (4.9), $\overset{\vartriangle}{\underline{\underline{T}}}$ is the upper-convected rate of Cauchy stress given in (4.44a), and where the fourth-rank tensor $\underline{\underline{\underline{\underline{\mathcal{C}}}}}$ is the Eulerian tangent operator obtained through the field transfer $\underline{\underline{\underline{\underline{\mathfrak{C}}}}} \overset{t}{\longmapsto} \underline{\underline{\underline{\underline{\mathcal{C}}}}}$.

The tangent operator for the isotropic elastic solid of (5.14) is given by

$$\begin{aligned}\underline{\underline{\underline{\underline{\mathcal{C}}}}} = 4\varrho_0\Big(& \mathfrak{W}_{,1}\,\tfrac{1}{4}\Big((\underline{\underline{I}}\boxtimes\underline{\underline{B}}^{-1}) + (\underline{\underline{B}}^{-1}\boxtimes\underline{\underline{I}})\Big) + \mathfrak{W}_{,11}(\underline{\underline{E}}^{(1)}\otimes\underline{\underline{E}}^{(1)}) \\ & + \mathfrak{W}_{,2}\,\tfrac{1}{8}\Big((\underline{\underline{B}}\boxtimes\underline{\underline{B}}) + (\underline{\underline{B}}^{-1}\boxtimes\underline{\underline{B}}^{-1}) + (\underline{\underline{I}}\boxtimes\underline{\underline{B}}^{-2}) + (\underline{\underline{B}}^{-2}\boxtimes\underline{\underline{I}})\Big) + \mathfrak{W}_{,22}(\underline{\underline{E}}^{(2)}\otimes\underline{\underline{E}}^{(2)}) \\ & + \mathfrak{W}_{,3}\,e(\underline{\underline{I}}\boxtimes\underline{\underline{I}}) + \big(\mathfrak{W}_{,3}\,\tfrac{1}{4}\,I_3 + \mathfrak{W}_{,33}\,e^2\big)(\underline{\underline{I}}\otimes\underline{\underline{I}})\Big),\end{aligned} \tag{5.18}$$

where $\mathfrak{W}_{,i} = \partial\mathfrak{W}/\partial I_i$ and $\mathfrak{W}_{,ij} = \partial^2\mathfrak{W}/\partial I_i\partial I_j$, $i,j = 1,2,3$, and where tensor products $\underline{\underline{M}}\boxtimes\underline{\underline{N}}$ and $\underline{\underline{M}}\otimes\underline{\underline{N}}$ have matrix representations of $M\boxtimes N = [\![\frac{1}{2}(\mathrm{M}_{ik}\mathrm{N}_{j\ell} + \mathrm{M}_{i\ell}\mathrm{N}_{jk})]\!]$ and $\overline{M}\otimes\overline{N} = \overline{[\![\mathrm{M}_{ij}\mathrm{N}_{k\ell}]\!]}$ in the coordinate system $\mathcal{C}$. This tangent modulus was obtained by substituting (5.9b & 5.9c) into (5.6b) and mapping the resultant into Cartesian space. Not all of the terms in (5.18) will be contributing in any given model; furthermore, additional terms will be required if the function representing strain-energy density has a cross-coupling of $I_m I_n$, $m \neq n$, in its definition.

5.6 Isotropic Viscoelasticity

With a general structure for isotropic elasticity in place, it is a straightforward process to extend this structure to a theory for isotropic viscoelasticity using the constructs of (5.4), which is based upon the K-BKZ [7, 56] hypothesis. As in the case of isotropic elasticity, the stress response has three constituent parts, one related to each invariant, that combine to quantify the total state of stress according to

$$\begin{aligned}\tfrac{\varrho_0}{\varrho}\,\underline{\underline{\pi}} = 2\varrho_0\Big(& \mathfrak{G}_1(t)\,\mathfrak{W}_{,1}(0,t)\,\tfrac{1}{4}\Big(\underline{\underline{\gamma}}_0^{-1} - \underline{\underline{\gamma}}^{-1}\cdot\underline{\underline{\gamma}}_0\cdot\underline{\underline{\gamma}}^{-1}\Big) \\ & + \int_0^t \mathfrak{M}_1(t-t')\,\mathfrak{W}_{,1}(t',t)\,\tfrac{1}{4}\Big(\underline{\underline{\gamma}}_{t'}^{-1} - \underline{\underline{\gamma}}^{-1}\cdot\underline{\underline{\gamma}}_{t'}\cdot\underline{\underline{\gamma}}^{-1}\Big)\,dt' \\ & + \mathfrak{G}_2(t)\,\mathfrak{W}_{,2}(0,t)\,\tfrac{1}{8}\Big(\underline{\underline{\gamma}}_0^{-1}\cdot\underline{\underline{\gamma}}\cdot\underline{\underline{\gamma}}_0^{-1} - \underline{\underline{\gamma}}^{-1}\cdot\underline{\underline{\gamma}}_0\cdot\underline{\underline{\gamma}}^{-1}\cdot\underline{\underline{\gamma}}_0\cdot\underline{\underline{\gamma}}^{-1}\Big) \\ & + \int_0^t \mathfrak{M}_2(t-t')\,\mathfrak{W}_{,2}(t',t)\,\tfrac{1}{8}\Big(\underline{\underline{\gamma}}_{t'}^{-1}\cdot\underline{\underline{\gamma}}\cdot\underline{\underline{\gamma}}_{t'}^{-1} - \underline{\underline{\gamma}}^{-1}\cdot\underline{\underline{\gamma}}_{t'}\cdot\underline{\underline{\gamma}}^{-1}\cdot\underline{\underline{\gamma}}_{t'}\cdot\underline{\underline{\gamma}}^{-1}\Big)\,dt' \\ & + \mathfrak{G}_3(t)\,\mathfrak{W}_{,3}(0,t)\,\tfrac{1}{2}\Big(\sqrt{\det(\underline{\underline{\gamma}}_0^{-1}\cdot\underline{\underline{\gamma}})} - \sqrt{\det(\underline{\underline{\gamma}}^{-1}\cdot\underline{\underline{\gamma}}_0)}\Big)\underline{\underline{\gamma}}^{-1} \\ & + \int_0^t \mathfrak{M}_3(t-t')\,\mathfrak{W}_{,3}(t',t)\,\tfrac{1}{2}\Big(\sqrt{\det(\underline{\underline{\gamma}}_{t'}^{-1}\cdot\underline{\underline{\gamma}})} - \sqrt{\det(\underline{\underline{\gamma}}^{-1}\cdot\underline{\underline{\gamma}}_{t'})}\Big)\,dt'\,\underline{\underline{\gamma}}^{-1}\Big),\end{aligned} \tag{5.19}$$

where the invariants of (5.9a), adjusted for time interval $[t',t]$, lead to constitutive formulæ that satisfy the required constraint of $\partial\mathfrak{W}(t,t)/\partial\underline{\underline{\gamma}} = \underline{\underline{0}}$ whenever $t' = t$.

There are three, independent, scalar-valued, relaxation functions $\mathfrak{G}_i$, $i = 1, 2, 3$, in this consitutive equation whose associated memory functions are computed as $\mathfrak{M}_i(t - t') := \partial \mathfrak{G}_i(t - t')/\partial t'$. The three $\mathfrak{G}_i$ are dimensionless, positive and bounded. Their memory functions $\mathfrak{M}_i(t - t')$ have dimensions of reciprocal time, they can possess a weak singularity at $t' = t$, they must be positive, and they must decrease monotonically with a sufficiently rapid rate of decay towards zero as t goes to infinity, all in accordance with the hypothesis of a fading memory [18, 19]. The fact that the memory function can be weakly singular at $t' = t$ is offset by the required constraint that $\partial \mathfrak{W}(t', t)/\partial \underline{\underline{\gamma}} = \underline{\underline{0}}$ whenever $t' = t$, so the integrand as a whole remains regular over the entire interval of integration.

One possible simplifying assumption that can be considered is to set the relaxation moduli $\mathfrak{G}_1$ and $\mathfrak{G}_2$ equal to one another, indicating that shear flow is governed by a single relaxation mechanism, independent of the order of strain.

5.6.1 Field transfer

Using the results of Chp. 4 and, in particular, Eqn. (4.25), the stress response of the isotropic viscoelastic solid listed in (5.19) has an Eulerian description of

$$\begin{aligned} \tfrac{\varrho_0}{\varrho}\,\underline{\underline{T}} = 2\varrho_0\Big(& \mathfrak{G}_1(t)\,\mathfrak{W}_{,1}(0,t)\,\underline{\underline{E}}^{(1)}(0,t) + \int_0^t \mathfrak{M}_1(t-t')\,\mathfrak{W}_{,1}(t',t)\,\underline{\underline{E}}^{(1)}(t',t)\,dt' \\ & + \mathfrak{G}_2(t)\,\mathfrak{W}_{,2}(0,t)\,\underline{\underline{E}}^{(2)}(0,t) + \int_0^t \mathfrak{M}_2(t-t')\,\mathfrak{W}_{,2}(t',t)\,\underline{\underline{E}}^{(2)}(t',t)\,dt' \\ & + \mathfrak{G}_3(t)\,\mathfrak{W}_{,3}(0,t)\,e(0,t)\,\underline{\underline{I}} + \int_0^t \mathfrak{M}_3(t-t')\,\mathfrak{W}_{,3}(t',t)\,e(t',t)\,dt'\,\underline{\underline{I}}\Big), \end{aligned} \tag{5.20a}$$

that, for materials whose bulk modulus is much greater than its shear modulus, produces a hydrostatic pressure that (approximately) satisfies

$$\tfrac{\varrho_0}{\varrho}\,p = -2\varrho_0\Big(\mathfrak{G}_3(t)\,\mathfrak{W}_{,3}(0,t)\,e(0,t) + \int_0^t \mathfrak{M}_3(t-t')\,\mathfrak{W}_{,3}(t',t)\,e(t',t)\,dt'\Big). \tag{5.20b}$$

For incompressible materials, this constitutive description simplifies to

$$\begin{aligned} \underline{\underline{T}} + \wp\,\underline{\underline{I}} = 2\varrho_0\Big(& \mathfrak{G}_1(t)\,\mathfrak{W}_{,1}(0,t)\,\underline{\underline{E}}^{(1)}(0,t) + \int_0^t \mathfrak{M}_1(t-t')\,\mathfrak{W}_{,1}(t',t)\,\underline{\underline{E}}^{(1)}(t',t)\,dt' \\ & + \mathfrak{G}_2(t)\,\mathfrak{W}_{,2}(0,t)\,\underline{\underline{E}}^{(2)}(0,t) + \int_0^t \mathfrak{M}_2(t-t')\,\mathfrak{W}_{,2}(t',t)\,\underline{\underline{E}}^{(2)}(t',t)\,dt'\Big), \end{aligned} \tag{5.20c}$$

subject to a constraint for incompressiblity: either $\det \underline{\underline{F}} = 1$ or $\operatorname{tr} \underline{\underline{D}} = 0$. Here $\underline{\underline{F}}(t', t) := \partial \underline{x}(t)/\partial \underline{x}(t') = \underline{\underline{F}}(0, t) \cdot \underline{\underline{F}}^{-1}(0, t')$ and $\underline{\underline{B}}(t', t) := \underline{\underline{F}}(t', t) \cdot \underline{\underline{F}}^{\mathrm{T}}(t', t)$ so that $\underline{\underline{E}}^{(n)}(t', t) = \frac{1}{4n}\big(\underline{\underline{B}}^{n}(t', t) - \underline{\underline{B}}^{-n}(t', t)\big)$ and $e(t', t) = \frac{1}{2}\big(\det \underline{\underline{F}}(t', t) - \det \underline{\underline{F}}^{-1}(t', t)\big)$. This is the theory for isotropic viscoelasticity that we employ for solving boundary-value problems.

Tangent operator

The tangent operator (5.7) is composed of two parts for each invariant—an elastic part and a viscoelastic part—whose sum produces the overall tangent modulus for the isotropic viscoelastic solid of (5.20); specifically,

$$\underline{\underline{\underline{\underline{\mathcal{C}}}}} = \underline{\underline{\underline{\underline{\mathcal{C}}}}}^{e} + \underline{\underline{\underline{\underline{\mathcal{C}}}}}^{v}, \tag{5.21a}$$

such that upon substituting (5.9b & 5.9c) into (5.7), and then mapping the resultant into Cartesian space, one obtains an elastic part that when expressed in the Eulerian frame is given by

$$\begin{aligned}
\underline{\underline{\underline{\underline{\mathcal{C}}}}}^{e} = 4\varrho_0 \Big(& \mathcal{G}_1(t) \Big(\mathfrak{W}_{,1}\, \tfrac{1}{4} \Big(\big(\underline{\underline{I}} \boxtimes \underline{\underline{B}}^{-1}\big) + \big(\underline{\underline{B}}^{-1} \boxtimes \underline{\underline{I}}\big) \Big) + \mathfrak{W}_{,11} \big(\underline{\underline{E}}^{(1)} \otimes \underline{\underline{E}}^{(1)}\big) \Big) \\
& + \mathcal{G}_2(t) \Big(\mathfrak{W}_{,2}\, \tfrac{1}{8} \Big(\big(\underline{\underline{B}} \boxtimes \underline{\underline{B}}\big) + \big(\underline{\underline{B}}^{-1} \boxtimes \underline{\underline{B}}^{-1}\big) + \big(\underline{\underline{I}} \boxtimes \underline{\underline{B}}^{-2}\big) + \big(\underline{\underline{B}}^{-2} \boxtimes \underline{\underline{I}}\big) \Big) \\
& \qquad + \mathfrak{W}_{,22} \big(\underline{\underline{E}}^{(2)} \otimes \underline{\underline{E}}^{(2)}\big) \Big) \\
& + \mathcal{G}_3(t) \Big(\mathfrak{W}_{,3}\, e \big(\underline{\underline{I}} \boxtimes \underline{\underline{I}}\big) + \big(\mathfrak{W}_{,3}\, \tfrac{1}{4} I_3 + \mathfrak{W}_{,33}\, e^2\big) \big(\underline{\underline{I}} \otimes \underline{\underline{I}}\big) \Big) \Big),
\end{aligned} \tag{5.21b}$$

and a corresponding viscoelastic part that is given by

$$\begin{aligned}
\underline{\underline{\underline{\underline{\mathcal{C}}}}}^{v} = 4\varrho_0 \Big(& \int_0^t \mathfrak{M}_1(t-t')\, \mathfrak{W}_{,1}(t',t)\, \tfrac{1}{4} \Big(\big(\underline{\underline{I}} \boxtimes \underline{\underline{B}}^{-1}(t',t)\big) + \big(\underline{\underline{B}}^{-1}(t',t) \boxtimes \underline{\underline{I}}\big) \Big) dt' \\
& + \int_0^t \mathfrak{M}_1(t-t')\, \mathfrak{W}_{,11}(t',t) \big(\underline{\underline{E}}^{(1)}(t',t) \otimes \underline{\underline{E}}^{(1)}(t',t)\big) dt' \\
& + \int_0^t \mathfrak{M}_2(t-t')\, \mathfrak{W}_{,2}(t',t)\, \tfrac{1}{8} \Big(\big(\underline{\underline{B}}(t',t) \boxtimes \underline{\underline{B}}(t',t)\big) + \big(\underline{\underline{B}}^{-1}(t',t) \boxtimes \underline{\underline{B}}^{-1}(t',t)\big) \\
& \qquad + \big(\underline{\underline{I}} \boxtimes \underline{\underline{B}}^{-2}(t',t)\big) + \big(\underline{\underline{B}}^{-2}(t',t) \boxtimes \underline{\underline{I}}\big) \Big) dt' \\
& + \int_0^t \mathfrak{M}_2(t-t')\, \mathfrak{W}_{,22}(t',t) \big(\underline{\underline{E}}^{(2)}(t',t) \otimes \underline{\underline{E}}^{(2)}(t',t)\big) dt' \\
& + \int_0^t \mathfrak{M}_3(t-t')\, \mathfrak{W}_{,3}(t',t) \Big(e \big(\underline{\underline{I}} \boxtimes \underline{\underline{I}}\big) + \tfrac{1}{4} I_3(t',t) \big(\underline{\underline{I}} \otimes \underline{\underline{I}}\big) \Big) dt' \\
& + \int_0^t \mathfrak{M}_3(t-t')\, \mathfrak{W}_{,33}(t',t)\, e^2(t',t) \big(\underline{\underline{I}} \otimes \underline{\underline{I}}\big) dt' \Big),
\end{aligned} \tag{5.21c}$$

with additional terms required whenever the function representing strain-energy density has a cross-coupled dependence between its invariants.

5.7 Transversely Isotropic Elasticity

We now address materials composed of a single family of fibers, or showing a single preferred orientation. Let the contravariant vector $\underline{\boldsymbol{\alpha}}_0 := \underline{\boldsymbol{\alpha}}(\mathfrak{P}, 0)$ be a tangent to this

material line of anisotropy at a particle $\mathfrak{P}$ in the reference state of time $t = 0$, and let this vector have unit length in this state so that it satisfies

$$\underline{\boldsymbol{\alpha}}_0 \cdot \underline{\underline{\gamma}}_0 \cdot \underline{\boldsymbol{\alpha}}_0 = 1. \tag{5.22a}$$

At current time t, the fibers along this material line will have stretched by an amount λ according to

$$\lambda^2 = \underline{\boldsymbol{\alpha}}_0 \cdot \underline{\underline{\gamma}} \cdot \underline{\boldsymbol{\alpha}}_0. \tag{5.22b}$$

Any material obeying such a symmetry property is called transversely isotropic, because the transverse material plane (defined by a normal vector that is coaxial with the covariant vector $\underline{\underline{\gamma}}_0 \cdot \underline{\boldsymbol{\alpha}}_0$) remains isotropic. Virtually all biological tissues are at least transversely isotropic. Many are orthotropic, and therefore exhibit two preferential directions, but we will not address this or any other higher level of anisotropy in this report.

In order to construct an elastic theory for transverse isotropy, in accordance with (5.1c), we need to introduce two additional invariants to the three isotropic invariants that already exist and which are defined in (5.9). The two additional invariants that we propose to use are defined by

$$\left.\begin{aligned} I_4 &:= \tfrac{1}{4}\, \underline{\boldsymbol{\alpha}}_0 \cdot \left(\underline{\underline{\gamma}} + \underline{\underline{\gamma}}_0 \cdot \underline{\underline{\gamma}}^{-1} \cdot \underline{\underline{\gamma}}_0 \right) \cdot \underline{\boldsymbol{\alpha}}_0 \\ I_5 &:= \tfrac{1}{16}\, \underline{\boldsymbol{\alpha}}_0 \cdot \left(\underline{\underline{\gamma}} \cdot \underline{\underline{\gamma}}_0^{-1} \cdot \underline{\underline{\gamma}} + \underline{\underline{\gamma}}_0 \cdot \underline{\underline{\gamma}}^{-1} \cdot \underline{\underline{\gamma}}_0 \cdot \underline{\underline{\gamma}}^{-1} \cdot \underline{\underline{\gamma}}_0 \right) \cdot \underline{\boldsymbol{\alpha}}_0 \end{aligned}\right\}, \tag{5.23a}$$

whose gradients are anisotropic strain measures given by

$$\left.\begin{aligned} \partial I_4 / \partial \underline{\underline{\gamma}} &= \tfrac{1}{4} \Big((\underline{\boldsymbol{\alpha}}_0 \otimes \underline{\boldsymbol{\alpha}}_0) - \underline{\underline{\gamma}}^{-1} \cdot \underline{\underline{\gamma}}_0 \cdot (\underline{\boldsymbol{\alpha}}_0 \otimes \underline{\boldsymbol{\alpha}}_0) \cdot \underline{\underline{\gamma}}_0 \cdot \underline{\underline{\gamma}}^{-1} \Big) \\ \partial I_5 / \partial \underline{\underline{\gamma}} &= \tfrac{1}{16} \Big((\underline{\boldsymbol{\alpha}}_0 \otimes \underline{\boldsymbol{\alpha}}_0) \cdot \underline{\underline{\gamma}} \cdot \underline{\underline{\gamma}}_0^{-1} - \underline{\underline{\gamma}}^{-1} \cdot \underline{\underline{\gamma}}_0 \cdot (\underline{\boldsymbol{\alpha}}_0 \otimes \underline{\boldsymbol{\alpha}}_0) \cdot \underline{\underline{\gamma}}_0 \cdot \underline{\underline{\gamma}}^{-1} \cdot \underline{\underline{\gamma}}_0 \cdot \underline{\underline{\gamma}}^{-1} \\ &\quad + \underline{\underline{\gamma}}_0^{-1} \cdot \underline{\underline{\gamma}} \cdot (\underline{\boldsymbol{\alpha}}_0 \otimes \underline{\boldsymbol{\alpha}}_0) - \underline{\underline{\gamma}}^{-1} \cdot \underline{\underline{\gamma}}_0 \cdot \underline{\underline{\gamma}}^{-1} \cdot \underline{\underline{\gamma}}_0 \cdot (\underline{\boldsymbol{\alpha}}_0 \otimes \underline{\boldsymbol{\alpha}}_0) \cdot \underline{\underline{\gamma}}_0 \cdot \underline{\underline{\gamma}}^{-1} \Big) \end{aligned}\right\}, \tag{5.23b}$$

and whose second-order derivatives, present in the tangent moduli, are

$$\left.\begin{aligned} \partial^2 I_4 / \partial \underline{\underline{\gamma}} \, \partial \underline{\underline{\gamma}} &= \tfrac{1}{4} \Big(\underline{\underline{\gamma}}^{-1} \boxtimes \underline{\underline{\gamma}}^{-1} \cdot \underline{\underline{\gamma}}_0 \cdot (\underline{\boldsymbol{\alpha}}_0 \otimes \underline{\boldsymbol{\alpha}}_0) \cdot \underline{\underline{\gamma}}_0 \cdot \underline{\underline{\gamma}}^{-1} \\ &\quad + \underline{\underline{\gamma}}^{-1} \cdot \underline{\underline{\gamma}}_0 \cdot (\underline{\boldsymbol{\alpha}}_0 \otimes \underline{\boldsymbol{\alpha}}_0) \cdot \underline{\underline{\gamma}}_0 \cdot \underline{\underline{\gamma}}^{-1} \boxtimes \underline{\underline{\gamma}}^{-1} \Big) \\ \partial^2 I_5 / \partial \underline{\underline{\gamma}} \, \partial \underline{\underline{\gamma}} &= \tfrac{1}{16} \Big((\underline{\boldsymbol{\alpha}}_0 \otimes \underline{\boldsymbol{\alpha}}_0) \boxtimes \underline{\underline{\gamma}}_0^{-1} + \underline{\underline{\gamma}}_0^{-1} \boxtimes (\underline{\boldsymbol{\alpha}}_0 \otimes \underline{\boldsymbol{\alpha}}_0) \\ &\quad + \underline{\underline{\gamma}}^{-1} \boxtimes \underline{\underline{\gamma}}^{-1} \cdot \underline{\underline{\gamma}}_0 \cdot (\underline{\boldsymbol{\alpha}}_0 \otimes \underline{\boldsymbol{\alpha}}_0) \cdot \underline{\underline{\gamma}}_0 \cdot \underline{\underline{\gamma}}^{-1} \cdot \underline{\underline{\gamma}}_0 \cdot \underline{\underline{\gamma}}^{-1} \\ &\quad + \underline{\underline{\gamma}}^{-1} \cdot \underline{\underline{\gamma}}_0 \cdot (\underline{\boldsymbol{\alpha}}_0 \otimes \underline{\boldsymbol{\alpha}}_0) \cdot \underline{\underline{\gamma}}_0 \cdot \underline{\underline{\gamma}}^{-1} \boxtimes \underline{\underline{\gamma}}^{-1} \cdot \underline{\underline{\gamma}}_0 \cdot \underline{\underline{\gamma}}^{-1} \\ &\quad + \underline{\underline{\gamma}}^{-1} \cdot \underline{\underline{\gamma}}_0 \cdot (\underline{\boldsymbol{\alpha}}_0 \otimes \underline{\boldsymbol{\alpha}}_0) \cdot \underline{\underline{\gamma}}_0 \cdot \underline{\underline{\gamma}}^{-1} \cdot \underline{\underline{\gamma}}_0 \cdot \underline{\underline{\gamma}}^{-1} \boxtimes \underline{\underline{\gamma}}^{-1} \\ &\quad + \underline{\underline{\gamma}}^{-1} \boxtimes \underline{\underline{\gamma}}^{-1} \cdot \underline{\underline{\gamma}}_0 \cdot \underline{\underline{\gamma}}^{-1} \cdot \underline{\underline{\gamma}}_0 \cdot (\underline{\boldsymbol{\alpha}}_0 \otimes \underline{\boldsymbol{\alpha}}_0) \cdot \underline{\underline{\gamma}}_0 \cdot \underline{\underline{\gamma}}^{-1} \\ &\quad + \underline{\underline{\gamma}}^{-1} \cdot \underline{\underline{\gamma}}_0 \cdot \underline{\underline{\gamma}}^{-1} \boxtimes \underline{\underline{\gamma}}^{-1} \cdot \underline{\underline{\gamma}}_0 \cdot (\underline{\boldsymbol{\alpha}}_0 \otimes \underline{\boldsymbol{\alpha}}_0) \cdot \underline{\underline{\gamma}}_0 \cdot \underline{\underline{\gamma}}^{-1} \\ &\quad + \underline{\underline{\gamma}}^{-1} \cdot \underline{\underline{\gamma}}_0 \cdot \underline{\underline{\gamma}}^{-1} \cdot \underline{\underline{\gamma}}_0 \cdot (\underline{\boldsymbol{\alpha}}_0 \otimes \underline{\boldsymbol{\alpha}}_0) \cdot \underline{\underline{\gamma}}_0 \cdot \underline{\underline{\gamma}}^{-1} \boxtimes \underline{\underline{\gamma}}^{-1} \Big) \end{aligned}\right\}. \tag{5.23c}$$

Collectively, the five invariants of (5.9a & 5.23a) constitute an admissible integrity basis for transversely isotropic materials.** Gradients $\partial I_1/\partial \underline{\underline{\gamma}}$ and $\partial I_4/\partial \underline{\underline{\gamma}}$ are strains of first order; whereas, gradients $\partial I_2/\partial \underline{\underline{\gamma}}$ and $\partial I_5/\partial \underline{\underline{\gamma}}$ are strains of second order.

From these five invariants, one arrives at the constitutive equation for an elastic solid with transverse isotropy derived from the work potential in (5.3); it has a stress response of

$$\begin{aligned}
\tfrac{\varrho_0}{\varrho}\,\underline{\underline{\pi}} = 2\varrho_0\Big(& \mathfrak{W}_{,1}\,\tfrac{1}{4}\Big(\underline{\underline{\gamma}}_0^{-1} - \underline{\underline{\gamma}}^{-1}\cdot\underline{\underline{\gamma}}_0\cdot\underline{\underline{\gamma}}^{-1}\Big) \\
& + \mathfrak{W}_{,2}\,\tfrac{1}{8}\Big(\underline{\underline{\gamma}}_0^{-1}\cdot\underline{\underline{\gamma}}\cdot\underline{\underline{\gamma}}_0^{-1} - \underline{\underline{\gamma}}^{-1}\cdot\underline{\underline{\gamma}}_0\cdot\underline{\underline{\gamma}}^{-1}\cdot\underline{\underline{\gamma}}_0\cdot\underline{\underline{\gamma}}^{-1}\Big) \\
& + \mathfrak{W}_{,3}\,\tfrac{1}{2}\Big(\sqrt{\det\big(\underline{\underline{\gamma}}_0^{-1}\cdot\underline{\underline{\gamma}}\big)} - \sqrt{\det\big(\underline{\underline{\gamma}}^{-1}\cdot\underline{\underline{\gamma}}_0\big)}\Big)\underline{\underline{\gamma}}^{-1} \\
& + \mathfrak{W}_{,4}\,\tfrac{1}{4}\Big(\big(\underline{\alpha}_0\otimes\underline{\alpha}_0\big) - \underline{\underline{\gamma}}^{-1}\cdot\underline{\underline{\gamma}}_0\cdot\big(\underline{\alpha}_0\otimes\underline{\alpha}_0\big)\cdot\underline{\underline{\gamma}}_0\cdot\underline{\underline{\gamma}}^{-1}\Big) \\
& + \mathfrak{W}_{,5}\,\tfrac{1}{16}\Big(\big(\underline{\alpha}_0\otimes\underline{\alpha}_0\big)\cdot\underline{\underline{\gamma}}\cdot\underline{\underline{\gamma}}_0^{-1} - \underline{\underline{\gamma}}^{-1}\cdot\underline{\underline{\gamma}}_0\cdot\big(\underline{\alpha}_0\otimes\underline{\alpha}_0\big)\cdot\underline{\underline{\gamma}}_0\cdot\underline{\underline{\gamma}}^{-1}\cdot\underline{\underline{\gamma}}_0\cdot\underline{\underline{\gamma}}^{-1} \\
& \qquad + \underline{\underline{\gamma}}_0^{-1}\cdot\underline{\underline{\gamma}}\cdot\big(\underline{\alpha}_0\otimes\underline{\alpha}_0\big) - \underline{\underline{\gamma}}^{-1}\cdot\underline{\underline{\gamma}}_0\cdot\underline{\underline{\gamma}}^{-1}\cdot\underline{\underline{\gamma}}_0\cdot\big(\underline{\alpha}_0\otimes\underline{\alpha}_0\big)\cdot\underline{\underline{\gamma}}_0\cdot\underline{\underline{\gamma}}^{-1}\Big)\Big).
\end{aligned} \tag{5.24}$$

There is an apparent symmetry in tensorial structure between the contravariant fields: $\underline{\underline{\gamma}}_0^{-1}$ and $\underline{\alpha}_0\otimes\underline{\alpha}_0$, and between the covariant fields: $\underline{\underline{\gamma}}_0$ and $\underline{\underline{\gamma}}_0\cdot\big(\underline{\alpha}_0\otimes\underline{\alpha}_0\big)\cdot\underline{\underline{\gamma}}_0$.

5.7.1 Field transfer

Before one can proceed with a mapping of this constitutive equation from the body into Cartesian space, it is necessary to determine how the unit vector $\underline{\alpha}_0$ of (5.22) maps into space. In a Lagrangian transfer of field, let the Lagrangian unit vector $\underline{a}_0$ be defined by the field transfer

$$\left.\begin{aligned}
\underline{\alpha}_0 &\overset{t_0}{\Longmapsto} \underline{a}_0 \\
\underline{\alpha}_0\cdot\underline{\underline{\gamma}}_0\cdot\underline{\alpha}_0 = 1 &\overset{t_0}{\Longmapsto} \underline{a}_0\cdot\underline{a}_0 = 1 \\
\underline{\alpha}_0\cdot\underline{\underline{\gamma}}\cdot\underline{\alpha}_0 = \lambda^2 &\overset{t_0}{\Longmapsto} \underline{a}_0\cdot\underline{\underline{C}}\cdot\underline{a}_0 = \lambda^2
\end{aligned}\right\}, \tag{5.25a}$$

**It was our desire to construct meaningful, anisotropic, finite-strain measures that led us to choose invariants that are themselves a sum of like invariants constructed from fields with opposing variance (e.g., one constituent invariant arises from the contravariant form of a state variable, while the other arises from the covariant form for that same state variable). Constructing meaningful, isotropic, strain measures is not a difficult task; there are many admissible choices. However, there are few admissible choices to select from when attempting to construct meaningful, anisotropic, strain measures. Equation (5.23b) presents one such pair of acceptable strain fields.

so that in an Eulerian transfer of field one gets

$$\left.\begin{aligned} \underline{\alpha}_0 &\overset{t}{\Longmapsto} \lambda\,\underline{a} \\ \underline{\alpha}_0\cdot\underline{\underline{\gamma}}_0\cdot\underline{\alpha}_0 = 1 &\overset{t}{\Longmapsto} \underline{a}\cdot\underline{\underline{B}}^{-1}\cdot\underline{a} = \lambda^{-2} \\ \underline{\alpha}_0\cdot\underline{\underline{\gamma}}\cdot\underline{\alpha}_0 = \lambda^2 &\overset{t}{\Longmapsto} \underline{a}\cdot\underline{a} = 1 \end{aligned}\right\}, \tag{5.25b}$$

and therefore $\underline{a} = \lambda^{-1}\underline{\underline{F}}\cdot\underline{a}_0$, or equivalently, $\underline{a}_0 = \lambda\,\underline{\underline{F}}^{-1}\cdot\underline{a}$. Material curves defined by the trajectory of $\underline{a}_0$ are indicative of fiber direction. After a deformation $\underline{\underline{F}}$, these fibers have a new direction of $\underline{a}$, and they have stretched by a factor of λ. Vectors $\underline{a}_0$ and $\underline{a}$ are the same vector fields that were utilized by Spencer [107, pg. 13].

To the invariants of (5.11 or 5.13) we add (gotten by a field transfer of Eqn. 5.23a)

$$I_4 = \tfrac{1}{4}\,\underline{a}_0\cdot\left(\underline{\underline{C}} + \underline{\underline{C}}^{-1}\right)\cdot\underline{a}_0 \quad\text{and}\quad I_5 = \tfrac{1}{16}\,\underline{a}_0\cdot\left(\underline{\underline{C}}^2 + \underline{\underline{C}}^{-2}\right)\cdot\underline{a}_0, \tag{5.26}$$

which are different in form from the invariants used by Spencer: $\underline{a}_0\cdot\underline{\underline{C}}\cdot\underline{a}_0$ and $\underline{a}_0\cdot\underline{\underline{C}}^2\cdot\underline{a}_0$. Affiliated with the invariants of (5.26) are the two, anisotropic, Eulerian, strain fields

$$\left.\begin{aligned} \underline{\underline{A}}^{(1)} &:= \tfrac{1}{4}\lambda^2\Big(\left(\underline{a}\otimes\underline{a}\right) - \underline{\underline{B}}^{-1}\cdot\left(\underline{a}\otimes\underline{a}\right)\cdot\underline{\underline{B}}^{-1}\Big) \\ \underline{\underline{A}}^{(2)} &:= \tfrac{1}{16}\lambda^2\Big(\left(\left(\underline{a}\otimes\underline{a}\right)\cdot\underline{\underline{B}} + \underline{\underline{B}}\cdot\left(\underline{a}\otimes\underline{a}\right)\right) \\ &\qquad - \underline{\underline{B}}^{-1}\cdot\left(\left(\underline{a}\otimes\underline{a}\right)\cdot\underline{\underline{B}}^{-1} + \underline{\underline{B}}^{-1}\cdot\left(\underline{a}\otimes\underline{a}\right)\right)\cdot\underline{\underline{B}}^{-1}\Big) \end{aligned}\right\}, \tag{5.27a}$$

which result from a transfer of the fields in (5.23b). Recalling that

$$\lambda^2 = \underline{a}_0\cdot\underline{\underline{C}}\cdot\underline{a}_0 \quad\text{and}\quad \underline{a} = \lambda^{-1}\,\underline{\underline{F}}\cdot\underline{a}_0, \tag{5.27b}$$

allows these anisotropic strain fields to be recast as

$$\left.\begin{aligned} \underline{\underline{A}}^{(1)} &= \tfrac{1}{4}\Big(\left(\underline{\underline{F}}\cdot\underline{a}_0\right)\otimes\left(\underline{\underline{F}}\cdot\underline{a}_0\right) - \left(\underline{\underline{F}}^{-\mathrm{T}}\cdot\underline{a}_0\right)\otimes\left(\underline{\underline{F}}^{-\mathrm{T}}\cdot\underline{a}_0\right)\Big) \\ \underline{\underline{A}}^{(2)} &= \tfrac{1}{16}\Big(\left(\underline{\underline{F}}\cdot\underline{a}_0\right)\otimes\left(\underline{\underline{B}}\cdot\underline{\underline{F}}\cdot\underline{a}_0\right) + \left(\underline{\underline{B}}\cdot\underline{\underline{F}}\cdot\underline{a}_0\right)\otimes\left(\underline{\underline{F}}\cdot\underline{a}_0\right) \\ &\qquad - \left(\underline{\underline{F}}^{-\mathrm{T}}\cdot\underline{a}_0\right)\otimes\left(\underline{\underline{B}}^{-1}\cdot\underline{\underline{F}}^{-\mathrm{T}}\cdot\underline{a}_0\right) - \left(\underline{\underline{B}}^{-1}\cdot\underline{\underline{F}}^{-\mathrm{T}}\cdot\underline{a}_0\right)\otimes\left(\underline{\underline{F}}^{-\mathrm{T}}\cdot\underline{a}_0\right)\Big) \end{aligned}\right\}. \tag{5.27c}$$

These are still Eulerian strain fields, it is just that they are represented in terms of the material vector $\underline{a}_0$ instead of its spatial variant $\underline{a}$. In the deformed state, vector $\underline{\underline{F}}\cdot\underline{a}_0$ is tangent to the material line of anisotropy, while vector $\underline{\underline{F}}^{-\mathrm{T}}\cdot\underline{a}_0$ is normal to the plane of isotropy, as illustrated in Fig. 5.1, and these vectors need not be coaxial.

A compressible, transversely isotropic, elastic solid whose invariants are so defined has a stress response (mapped from Eqn. 5.24) of

$$\tfrac{\varrho_0}{\varrho}\,\underline{\underline{T}} = 2\varrho_0\Big(\mathfrak{W}_{,1}\,\underline{\underline{E}}^{(1)} + \mathfrak{W}_{,2}\,\underline{\underline{E}}^{(2)} + \mathfrak{W}_{,3}\,e\,\underline{\underline{I}} + \mathfrak{W}_{,4}\,\underline{\underline{A}}^{(1)} + \mathfrak{W}_{,5}\,\underline{\underline{A}}^{(2)}\Big), \tag{5.28a}$$

that in the incompressible case becomes

$$\underline{\underline{T}} + \wp\,\underline{\underline{I}} = 2\varrho_0\Big(\mathfrak{W}_{,1}\,\underline{\underline{E}}^{(1)} + \mathfrak{W}_{,2}\,\underline{\underline{E}}^{(2)} + \mathfrak{W}_{,4}\,\underline{\underline{A}}^{(1)} + \mathfrak{W}_{,5}\,\underline{\underline{A}}^{(2)}\Big), \tag{5.28b}$$

where the Lagrange multiplier $\wp$ forces a constraint for incompressiblity, $\det\underline{\underline{F}} = 1$. These are the formulations for transverse-isotropic elasticity that we investigate in the remaining chapters of this report.

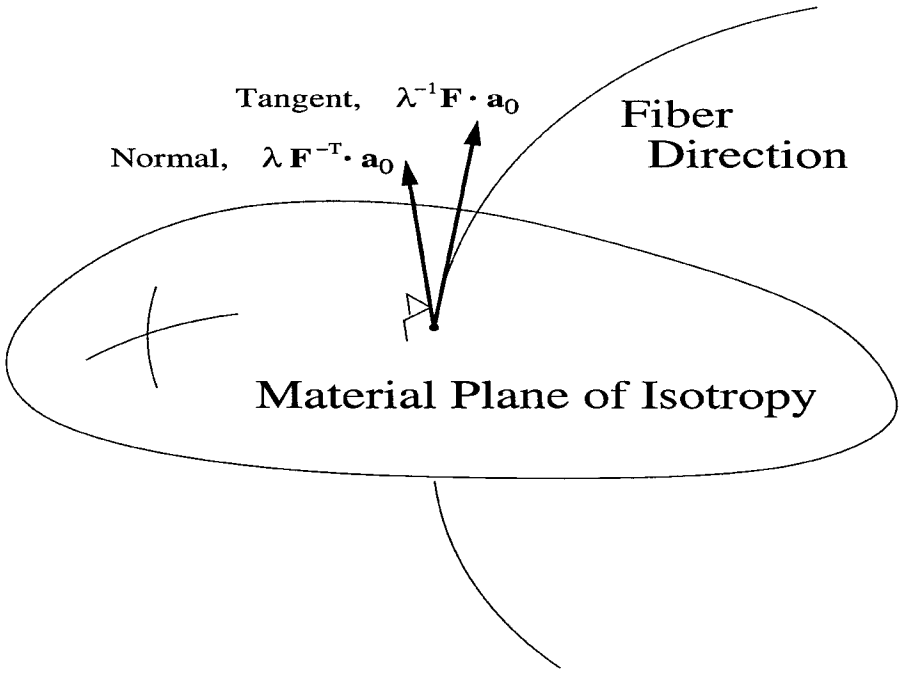

Figure 5.1: Kinematics of a transverse-isotropic material.

Tangent operator

To the isotropic, elastic, tangent operator listed in (5.18), one must add an anisotropic, elastic, tangent operator (obtained from substituting Eqns. 5.23b & 5.23c into Eqn. 5.6, and then mapping the resultant into Cartesian space), which is given by

$$
\begin{aligned}
\underline{\underline{\underline{\underline{\mathcal{C}}}}}^{a} = 4\varrho_0 \Bigg(& \tfrac{1}{4}\,\mathfrak{W}_{,4}\,\lambda^2 \Big(\underline{\underline{I}} \boxtimes \big(\underline{\underline{B}}^{-1}\cdot(\underline{a}\otimes\underline{a})\cdot\underline{\underline{B}}^{-1}\big) + \big(\underline{\underline{B}}^{-1}\cdot(\underline{a}\otimes\underline{a})\cdot\underline{\underline{B}}^{-1}\big) \boxtimes \underline{\underline{I}} \Big) \\
& + \tfrac{1}{16}\,\mathfrak{W}_{,5}\,\lambda^2 \Big(\underline{\underline{B}} \boxtimes (\underline{a}\otimes\underline{a}) + (\underline{a}\otimes\underline{a}) \boxtimes \underline{\underline{B}} \\
& \quad + \underline{\underline{I}} \boxtimes \Big(\underline{\underline{B}}^{-1}\cdot\big((\underline{a}\otimes\underline{a})\cdot\underline{\underline{B}}^{-1} + \underline{\underline{B}}^{-1}\cdot(\underline{a}\otimes\underline{a})\big)\cdot\underline{\underline{B}}^{-1} \Big) \\
& \quad\quad + \Big(\underline{\underline{B}}^{-1}\cdot\big((\underline{a}\otimes\underline{a})\cdot\underline{\underline{B}}^{-1} + \underline{\underline{B}}^{-1}\cdot(\underline{a}\otimes\underline{a})\big)\cdot\underline{\underline{B}}^{-1} \Big) \boxtimes \underline{\underline{I}} \\
& \quad + \underline{\underline{B}}^{-1} \boxtimes \Big(\underline{\underline{B}}^{-1}\cdot(\underline{a}\otimes\underline{a})\cdot\underline{\underline{B}}^{-1} \Big) + \Big(\underline{\underline{B}}^{-1}\cdot(\underline{a}\otimes\underline{a})\cdot\underline{\underline{B}}^{-1} \Big) \boxtimes \underline{\underline{B}}^{-1} \Big) \\
& + \mathfrak{W}_{,44}\Big(\underline{\underline{A}}^{(1)} \otimes \underline{\underline{A}}^{(1)} \Big) + \mathfrak{W}_{,55}\Big(\underline{\underline{A}}^{(2)} \otimes \underline{\underline{A}}^{(2)} \Big) \Bigg).
\end{aligned}
\tag{5.29}
$$

Again, additional components will need to be included into this expression if there exists a cross-product dependence between the invariants in the function representing strain-energy density that is being considered.

5.8 Transversely Isotropic Viscoelasticity

In accordance with our elastic theory for tansverse isotropy (5.24), an application of the K-BKZ - like constitutive hypothesis for viscoelasticity (5.4) produces a viscoelastic constitutive relation governing the stress response of a transversely isotropic material that has five constituent parts, one associated with each invariant, and is given by

$$
\begin{aligned}
\tfrac{\varrho_0}{\varrho}\,\underline{\underline{\pi}} = 2\varrho_0\Big(
&\mathfrak{G}_1(t)\,\mathfrak{W}_{,1}(0,t)\,\tfrac{1}{4}\Big(\underline{\underline{\gamma}}_0^{-1} - \underline{\underline{\gamma}}^{-1}\cdot\underline{\underline{\gamma}}_0\cdot\underline{\underline{\gamma}}^{-1}\Big)\\
&+\int_0^t \mathfrak{M}_1(t-t')\,\mathfrak{W}_{,1}(t',t)\,\tfrac{1}{4}\Big(\underline{\underline{\gamma}}_{t'}^{-1} - \underline{\underline{\gamma}}^{-1}\cdot\underline{\underline{\gamma}}_{t'}\cdot\underline{\underline{\gamma}}^{-1}\Big)\,dt'\\
&+\mathfrak{G}_2(t)\,\mathfrak{W}_{,2}(0,t)\,\tfrac{1}{8}\Big(\underline{\underline{\gamma}}_0^{-1}\cdot\underline{\underline{\gamma}}\cdot\underline{\underline{\gamma}}_0^{-1} - \underline{\underline{\gamma}}^{-1}\cdot\underline{\underline{\gamma}}_0\cdot\underline{\underline{\gamma}}^{-1}\cdot\underline{\underline{\gamma}}_0\cdot\underline{\underline{\gamma}}^{-1}\Big)\\
&+\int_0^t \mathfrak{M}_2(t-t')\,\mathfrak{W}_{,2}(t',t)\,\tfrac{1}{8}\Big(\underline{\underline{\gamma}}_{t'}^{-1}\cdot\underline{\underline{\gamma}}\cdot\underline{\underline{\gamma}}_{t'}^{-1} - \underline{\underline{\gamma}}^{-1}\cdot\underline{\underline{\gamma}}_{t'}\cdot\underline{\underline{\gamma}}^{-1}\cdot\underline{\underline{\gamma}}_{t'}\cdot\underline{\underline{\gamma}}^{-1}\Big)\,dt'\\
&+\mathfrak{G}_3(t)\,\mathfrak{W}_{,3}(0,t)\,\tfrac{1}{2}\Big(\sqrt{\det\big(\underline{\underline{\gamma}}_0^{-1}\cdot\underline{\underline{\gamma}}\big)} - \sqrt{\det\big(\underline{\underline{\gamma}}^{-1}\cdot\underline{\underline{\gamma}}_0\big)}\Big)\underline{\underline{\gamma}}^{-1}\\
&+\int_0^t \mathfrak{M}_3(t-t')\,\mathfrak{W}_{,3}(t',t)\,\tfrac{1}{2}\Big(\sqrt{\det\big(\underline{\underline{\gamma}}_{t'}^{-1}\cdot\underline{\underline{\gamma}}\big)} - \sqrt{\det\big(\underline{\underline{\gamma}}^{-1}\cdot\underline{\underline{\gamma}}_{t'}\big)}\Big)\,dt'\,\underline{\underline{\gamma}}^{-1}\\
&+\mathfrak{G}_4(t)\,\mathfrak{W}_{,4}(0,t)\,\tfrac{1}{4}\Big(\big(\underline{\boldsymbol{\alpha}}_0\otimes\underline{\boldsymbol{\alpha}}_0\big) - \underline{\underline{\gamma}}^{-1}\cdot\underline{\underline{\gamma}}_0\cdot\big(\underline{\boldsymbol{\alpha}}_0\otimes\underline{\boldsymbol{\alpha}}_0\big)\cdot\underline{\underline{\gamma}}_0\cdot\underline{\underline{\gamma}}^{-1}\Big)\\
&+\int_0^t \mathfrak{M}_4(t-t')\,\mathfrak{W}_{,4}(t',t)\,\tfrac{1}{4}\Big(\big(\underline{\boldsymbol{\alpha}}_{t'}\otimes\underline{\boldsymbol{\alpha}}_{t'}\big) - \underline{\underline{\gamma}}^{-1}\cdot\underline{\underline{\gamma}}_{t'}\cdot\big(\underline{\boldsymbol{\alpha}}_{t'}\otimes\underline{\boldsymbol{\alpha}}_{t'}\big)\cdot\underline{\underline{\gamma}}_{t'}\cdot\underline{\underline{\gamma}}^{-1}\Big)\,dt'\\
&+\mathfrak{G}_5(t)\,\mathfrak{W}_{,5}(0,t)\,\tfrac{1}{16}\Big(\big(\underline{\boldsymbol{\alpha}}_0\otimes\underline{\boldsymbol{\alpha}}_0\big)\cdot\underline{\underline{\gamma}}\cdot\underline{\underline{\gamma}}_0^{-1} - \underline{\underline{\gamma}}^{-1}\cdot\underline{\underline{\gamma}}_0\cdot\big(\underline{\boldsymbol{\alpha}}_0\otimes\underline{\boldsymbol{\alpha}}_0\big)\cdot\underline{\underline{\gamma}}_0\cdot\underline{\underline{\gamma}}^{-1}\cdot\underline{\underline{\gamma}}_0\cdot\underline{\underline{\gamma}}^{-1}\\
&\qquad+\underline{\underline{\gamma}}_0^{-1}\cdot\underline{\underline{\gamma}}\cdot\big(\underline{\boldsymbol{\alpha}}_0\otimes\underline{\boldsymbol{\alpha}}_0\big) - \underline{\underline{\gamma}}^{-1}\cdot\underline{\underline{\gamma}}_0\cdot\underline{\underline{\gamma}}^{-1}\cdot\underline{\underline{\gamma}}_0\cdot\big(\underline{\boldsymbol{\alpha}}_0\otimes\underline{\boldsymbol{\alpha}}_0\big)\cdot\underline{\underline{\gamma}}_0\cdot\underline{\underline{\gamma}}^{-1}\Big)\\
&+\int_0^t \mathfrak{M}_5(t-t')\,\mathfrak{W}_{,5}(t',t)\\
&\qquad\times\tfrac{1}{16}\Big(\big(\underline{\boldsymbol{\alpha}}_{t'}\otimes\underline{\boldsymbol{\alpha}}_{t'}\big)\cdot\underline{\underline{\gamma}}\cdot\underline{\underline{\gamma}}_{t'}^{-1} - \underline{\underline{\gamma}}^{-1}\cdot\underline{\underline{\gamma}}_{t'}\cdot\big(\underline{\boldsymbol{\alpha}}_{t'}\otimes\underline{\boldsymbol{\alpha}}_{t'}\big)\cdot\underline{\underline{\gamma}}_{t'}\cdot\underline{\underline{\gamma}}^{-1}\cdot\underline{\underline{\gamma}}_{t'}\cdot\underline{\underline{\gamma}}^{-1}\\
&\qquad\quad+\underline{\underline{\gamma}}_{t'}^{-1}\cdot\underline{\underline{\gamma}}\cdot\big(\underline{\boldsymbol{\alpha}}_{t'}\otimes\underline{\boldsymbol{\alpha}}_{t'}\big) - \underline{\underline{\gamma}}^{-1}\cdot\underline{\underline{\gamma}}_{t'}\cdot\underline{\underline{\gamma}}^{-1}\cdot\underline{\underline{\gamma}}_{t'}\cdot\big(\underline{\boldsymbol{\alpha}}_{t'}\otimes\underline{\boldsymbol{\alpha}}_{t'}\big)\cdot\underline{\underline{\gamma}}_{t'}\cdot\underline{\underline{\gamma}}^{-1}\Big)\,dt'\Big),
\end{aligned}
\tag{5.30}
$$

which contains isotropic viscoelasticity (5.19) as a special case.

A possible simplifying assumption that one may choose to consider would be to set $\mathfrak{G}_1 = \mathfrak{G}_2$ and $\mathfrak{G}_4 = \mathfrak{G}_5$, thereby implying that relaxation behavior does not discriminate between the first- and second-order strain fields, yet it does discern a difference in the relaxation behaviors along the strong direction and in the plane of isotropy.

Another simplifying assumption to consider, which is applicable for at least some biological tissues [101], is that $\mathfrak{G}_1 = \mathfrak{G}_4$ and $\mathfrak{G}_2 = \mathfrak{G}_5$, with the implication being that relaxation behavior does not vary between the strong direction and the plane of isotropy, even though the elastic response can possess a strong anisotropy; yet,

unless $\mathfrak{G}_1 = \mathfrak{G}_2$, too, (and therefore $\mathfrak{G}_1 = \mathfrak{G}_2 = \mathfrak{G}_4 = \mathfrak{G}_5$) the material can discern a difference between the relaxation behaviors due to first- and second-order strain effects.

A more useful assumption would be to eliminate the higher-order invariants I_2 and I_5 that introduce nonlinear capabilities, provided that experiments, or the boundary-value problems to be solved, justify making such a simplification.

5.8.1 Field transfer

The vector of anisotropy in the reference state of integration, $\underline{\boldsymbol{\alpha}}_{t'}$, maps into Cartesian space in this floating frame of reference as follows,

$$\left.\begin{aligned} \underline{\boldsymbol{\alpha}}_{t'} &\overset{t'}{\longmapsto} \underline{a}_{t'} \\ \underline{\boldsymbol{\alpha}}_{t'} \cdot \underline{\underline{\gamma}}_{t'} \cdot \underline{\boldsymbol{\alpha}}_{t'} = 1 &\overset{t'}{\longmapsto} \underline{a}_{t'} \cdot \underline{a}_{t'} = 1 \\ \underline{\boldsymbol{\alpha}}_{t'} \cdot \underline{\underline{\gamma}} \cdot \underline{\boldsymbol{\alpha}}_{t'} = \lambda^2(t',t) &\overset{t'}{\longmapsto} \underline{a}_{t'} \cdot \underline{\underline{C}}(t',t) \cdot \underline{a}_{t'} = \lambda^2(t',t) \end{aligned}\right\}, \tag{5.31a}$$

and consequently, it maps into the Eulerian frame as

$$\left.\begin{aligned} \underline{\boldsymbol{\alpha}}_{t'} &\overset{t}{\longmapsto} \lambda(t',t)\,\underline{a} \\ \underline{\boldsymbol{\alpha}}_{t'} \cdot \underline{\underline{\gamma}}_{t'} \cdot \underline{\boldsymbol{\alpha}}_{t'} = 1 &\overset{t}{\longmapsto} \underline{a} \cdot \underline{\underline{B}}^{-1}(t',t) \cdot \underline{a} = \lambda^{-2}(t',t) \\ \underline{\boldsymbol{\alpha}}_{t'} \cdot \underline{\underline{\gamma}} \cdot \underline{\boldsymbol{\alpha}}_{t'} = \lambda^2(t',t) &\overset{t}{\longmapsto} \underline{a} \cdot \underline{a} = 1 \end{aligned}\right\}, \tag{5.31b}$$

where $\lambda(t',t)$ denotes the stretch along the fiber axis over the time interval $[t',t]$. Furthermore, the anisotropic strain fields are given by

$$\left.\begin{aligned} \underline{\underline{A}}^{(1)}(t',t) &= \tfrac{1}{4}\lambda^2(t',t)\Big((\underline{a}\otimes\underline{a}) - \big(\underline{\underline{B}}^{-1}(t',t)\cdot(\underline{a}\otimes\underline{a})\cdot\underline{\underline{B}}^{-1}(t',t)\big)\Big) \\ \underline{\underline{A}}^{(2)}(t',t) &= \tfrac{1}{16}\lambda^2(t',t)\Big(\Big(\big((\underline{a}\otimes\underline{a})\cdot\underline{\underline{B}}(t',t)\big) + \big(\underline{\underline{B}}(t',t)\cdot(\underline{a}\otimes\underline{a})\big)\Big) \\ &\qquad - \underline{\underline{B}}^{-1}(t',t)\cdot\Big(\big((\underline{a}\otimes\underline{a})\cdot\underline{\underline{B}}^{-1}(t',t)\big) + \big(\underline{\underline{B}}^{-1}(t',t)\cdot(\underline{a}\otimes\underline{a})\big)\Big)\cdot\underline{\underline{B}}^{-1}(t',t)\Big) \end{aligned}\right\}, \tag{5.32a}$$

wherein

$$\lambda^2(t',t) = \underline{a}_{t'}\cdot\underline{\underline{C}}(t',t)\cdot\underline{a}_{t'} \quad \text{and} \quad \underline{a} = \lambda^{-1}(t',t)\,\underline{\underline{F}}(t',t)\cdot\underline{a}_{t'}, \tag{5.32b}$$

with

$$\lambda^2(0,t') = \underline{a}_0\cdot\underline{\underline{C}}(0,t')\cdot\underline{a}_0 \quad \text{yielding} \quad \underline{a}_{t'} = \lambda^{-1}(0,t')\,\underline{\underline{F}}(0,t')\cdot\underline{a}_0, \tag{5.32c}$$

which generalize the formulæ of (5.27).

The stress response of the transversely isotropic viscoelastic solid given in (5.30) has an Eulerian description of

$$\begin{aligned}\tfrac{\varrho_0}{\varrho}\,\underline{\underline{T}} = 2\varrho_0\Big(&\mathfrak{G}_1(t)\,\mathfrak{W}_{,1}(0,t)\,\underline{\underline{E}}^{(1)}(0,t) + \int_0^t \mathfrak{M}_1(t-t')\,\mathfrak{W}_{,1}(t',t)\,\underline{\underline{E}}^{(1)}(t',t)\,dt' \\ &+ \mathfrak{G}_2(t)\,\mathfrak{W}_{,2}(0,t)\,\underline{\underline{E}}^{(2)}(0,t) + \int_0^t \mathfrak{M}_2(t-t')\,\mathfrak{W}_{,2}(t',t)\,\underline{\underline{E}}^{(2)}(t',t)\,dt' \\ &+ \mathfrak{G}_3(t)\,\mathfrak{W}_{,3}(0,t)\,e(0,t)\,\underline{\underline{I}} + \int_0^t \mathfrak{M}_3(t-t')\,\mathfrak{W}_{,3}(t',t)\,e(t',t)\,dt'\,\underline{\underline{I}} \\ &+ \mathfrak{G}_4(t)\,\mathfrak{W}_{,4}(0,t)\,\underline{\underline{A}}^{(1)}(0,t) + \int_0^t \mathfrak{M}_4(t-t')\,\mathfrak{W}_{,4}(t',t)\,\underline{\underline{A}}^{(1)}(t',t)\,dt' \\ &+ \mathfrak{G}_5(t)\,\mathfrak{W}_{,5}(0,t)\,\underline{\underline{A}}^{(2)}(0,t) + \int_0^t \mathfrak{M}_5(t-t')\,\mathfrak{W}_{,5}(t',t)\,\underline{\underline{A}}^{(2)}(t',t)\,dt'\Big),\end{aligned} \tag{5.33a}$$

that, for an incompressible material, reduces to

$$\begin{aligned}\underline{\underline{T}} + \wp\,\underline{\underline{I}} = 2\varrho_0\Big(&\mathfrak{G}_1(t)\,\mathfrak{W}_{,1}(0,t)\,\underline{\underline{E}}^{(1)}(0,t) + \int_0^t \mathfrak{M}_1(t-t')\,\mathfrak{W}_{,1}(t',t)\,\underline{\underline{E}}^{(1)}(t',t)\,dt' \\ &+ \mathfrak{G}_2(t)\,\mathfrak{W}_{,2}(0,t)\,\underline{\underline{E}}^{(2)}(0,t) + \int_0^t \mathfrak{M}_2(t-t')\,\mathfrak{W}_{,2}(t',t)\,\underline{\underline{E}}^{(2)}(t',t)\,dt' \\ &+ \mathfrak{G}_4(t)\,\mathfrak{W}_{,4}(0,t)\,\underline{\underline{A}}^{(1)}(0,t) + \int_0^t \mathfrak{M}_4(t-t')\,\mathfrak{W}_{,4}(t',t)\,\underline{\underline{A}}^{(1)}(t',t)\,dt' \\ &+ \mathfrak{G}_5(t)\,\mathfrak{W}_{,5}(0,t)\,\underline{\underline{A}}^{(2)}(0,t) + \int_0^t \mathfrak{M}_5(t-t')\,\mathfrak{W}_{,5}(t',t)\,\underline{\underline{A}}^{(2)}(t',t)\,dt'\Big),\end{aligned} \tag{5.33b}$$

subject to a constraint for incompressiblity: either $\det\underline{\underline{F}} = 1$ or $\mathrm{tr}\,\underline{\underline{D}} = 0$. These are the formulations for transverse isotropic viscoelasticity that we exercise in the remaining chapters of this report.

Tangent operator

To the two parts already listed for the isotropic, viscoelastic, tangent operator in (5.21), two additional parts must be considered to account for transverse isotropy, such that

$$\underline{\underline{\underline{\underline{\mathcal{C}}}}} = \underline{\underline{\underline{\underline{\mathcal{C}}}}}^{e} + \underline{\underline{\underline{\underline{\mathcal{C}}}}}^{ea} + \underline{\underline{\underline{\underline{\mathcal{C}}}}}^{v} + \underline{\underline{\underline{\underline{\mathcal{C}}}}}^{va}, \tag{5.34a}$$

where the isotropic components $\underline{\underline{\underline{\underline{\mathcal{C}}}}}^{e}$ and $\underline{\underline{\underline{\underline{\mathcal{C}}}}}^{v}$ are found in (5.21b & 5.21c), and where the anisotropic components are given by

$$\begin{aligned}
\underline{\underline{\underline{\underline{\mathcal{C}}}}}^{ea} = 4\varrho_0 \Bigg(& \mathfrak{G}_4(t) \Bigg(\mathfrak{W}_{,4\,\frac{1}{4}\lambda^2} \Big(\underline{\underline{I}} \boxtimes \big(\underline{\underline{B}}^{-1} \cdot (\underline{a} \otimes \underline{a}) \cdot \underline{\underline{B}}^{-1} \big) + \big(\underline{\underline{B}}^{-1} \cdot (\underline{a} \otimes \underline{a}) \cdot \underline{\underline{B}}^{-1} \big) \boxtimes \underline{\underline{I}} \Big) \\
& + \mathfrak{W}_{,44} \big(\underline{\underline{A}}^{(1)} \otimes \underline{\underline{A}}^{(1)} \big) \Bigg) \\
& + \mathfrak{G}_5(t)\, \mathfrak{W}_{,5\,\frac{1}{16}\lambda^2} \Bigg(\underline{\underline{B}} \boxtimes (\underline{a} \otimes \underline{a}) + (\underline{a} \otimes \underline{a}) \boxtimes \underline{\underline{B}} \\
& \quad + \underline{\underline{B}}^{-1} \boxtimes \big(\underline{\underline{B}}^{-1} \cdot (\underline{a} \otimes \underline{a}) \cdot \underline{\underline{B}}^{-1} \big) + \big(\underline{\underline{B}}^{-1} \cdot (\underline{a} \otimes \underline{a}) \cdot \underline{\underline{B}}^{-1} \big) \boxtimes \underline{\underline{B}}^{-1} \\
& \quad + \underline{\underline{I}} \boxtimes \Big(\underline{\underline{B}}^{-1} \cdot \big((\underline{a} \otimes \underline{a}) \cdot \underline{\underline{B}}^{-1} + \underline{\underline{B}}^{-1} \cdot (\underline{a} \otimes \underline{a}) \big) \cdot \underline{\underline{B}}^{-1} \Big) \\
& \qquad + \Big(\underline{\underline{B}}^{-1} \cdot \big((\underline{a} \otimes \underline{a}) \cdot \underline{\underline{B}}^{-1} + \underline{\underline{B}}^{-1} \cdot (\underline{a} \otimes \underline{a}) \big) \cdot \underline{\underline{B}}^{-1} \Big) \boxtimes \underline{\underline{I}} \Big) \\
& + \mathfrak{G}_5(t)\, \mathfrak{W}_{,55} \big(\underline{\underline{A}}^{(2)} \otimes \underline{\underline{A}}^{(2)} \big) \Bigg),
\end{aligned} \tag{5.34b}$$

and

$$\begin{aligned}
\underline{\underline{\underline{\underline{\mathcal{C}}}}}^{va} = 4\varrho_0 \Bigg(& \int_0^t \mathfrak{M}_4(t-t')\, \mathfrak{W}_{,4}(t',t)\, \tfrac{1}{4}\lambda^2(t',t) \Big(\underline{\underline{I}} \boxtimes \big(\underline{\underline{B}}^{-1}(t',t) \cdot (\underline{a} \otimes \underline{a}) \cdot \underline{\underline{B}}^{-1}(t',t) \big) \\
& \quad + \big(\underline{\underline{B}}^{-1}(t',t) \cdot (\underline{a} \otimes \underline{a}) \cdot \underline{\underline{B}}^{-1}(t',t) \big) \boxtimes \underline{\underline{I}} \Big) dt' \\
& + \int_0^t \mathfrak{M}_4(t-t')\, \mathfrak{W}_{,44}(t',t) \big(\underline{\underline{A}}^{(1)}(t',t) \otimes \underline{\underline{A}}^{(1)}(t',t) \big) dt' \\
& + \int_0^t \mathfrak{M}_5(t-t')\, \mathfrak{W}_{,5}(t',t)\, \tfrac{1}{16}\lambda^2(t',t) \Bigg(\underline{\underline{B}}(t',t) \boxtimes (\underline{a} \otimes \underline{a}) + (\underline{a} \otimes \underline{a}) \boxtimes \underline{\underline{B}}(t',t) \\
& \quad + \underline{\underline{B}}^{-1}(t',t) \boxtimes \big(\underline{\underline{B}}^{-1}(t',t) \cdot (\underline{a} \otimes \underline{a}) \cdot \underline{\underline{B}}^{-1}(t',t) \big) \\
& \qquad + \big(\underline{\underline{B}}^{-1}(t',t) \cdot (\underline{a} \otimes \underline{a}) \cdot \underline{\underline{B}}^{-1}(t',t) \big) \boxtimes \underline{\underline{B}}^{-1}(t',t) \\
& \quad + \underline{\underline{I}} \boxtimes \Big(\underline{\underline{B}}^{-1}(t',t) \cdot \big((\underline{a} \otimes \underline{a}) \cdot \underline{\underline{B}}^{-1}(t',t) + \underline{\underline{B}}^{-1}(t',t) \cdot (\underline{a} \otimes \underline{a}) \big) \cdot \underline{\underline{B}}^{-1}(t',t) \Big) \\
& \qquad + \Big(\underline{\underline{B}}^{-1}(t',t) \cdot \big((\underline{a} \otimes \underline{a}) \cdot \underline{\underline{B}}^{-1}(t',t) + \underline{\underline{B}}^{-1}(t',t) \cdot (\underline{a} \otimes \underline{a}) \big) \cdot \underline{\underline{B}}^{-1}(t',t) \Big) \boxtimes \underline{\underline{I}} \Big) dt' \\
& + \int_0^t \mathfrak{M}_5(t-t')\, \mathfrak{W}_{,55}(t',t) \big(\underline{\underline{A}}^{(2)}(t',t) \otimes \underline{\underline{A}}^{(2)}(t',t) \big) dt' \Bigg),
\end{aligned} \tag{5.34c}$$

with additional terms required if the function representing strain-energy density happens to depend on cross products between its invariants.

Chapter 6

Finite-Strain Experiments

Although many characterization experiments are 1D in concept, they are 3D in reality and often require 3D analysis, even for the simplest of deformation histories, especially when finite strains are being considered. We restrict our discussion to those experiments whose stress and strain fields remain spatially uniform (homogeneous) throughout the specimen. Furthermore, deformations are assumed to be controlled to which forces are measured as reactions, while temperature is held constant. This restriction of controlling deformations and measuring forces, although imposed herein, is by no means a requirement of characterization experiments. Shear-free extensions and simple shearing are the deformations considered.

Deformation rates and strain rates are known because they are controlled. Force rates and stress rates, on the other hand, are usually not measured. Whenever stress rates are present in a constitutive equation, be they of integer or fractional order, a system of differential equations ensues that needs to be integrated to arrive at a predicted stress that can then be contrasted with the observed stress. This requires that stress rates be handled different than strain rates for purposes of characterization.

6.1 Shear-Free Extensions

A deformation is said to be shear free if there exists a convected coordinate system (e.g., $\mathcal{B}$: $\mathfrak{P} \rightarrow \mathfrak{E}$) that is always orthogonal [70, pg. 81]. In this class of experiments, a uniform material element in the shape of a unit cube is deformed into a rectangular parallelepiped causing tractions to set up on the various material faces, dependent upon boundary conditions, as illustrated in Fig. 6.1. These experiments are technologically important for solids because of their relative ease of execution. They are, however, extremely difficult to execute on fluids, where they have only met with some success when testing polymer fluids of high molecular weight.

6.1.1 Kinematics

The deformation just described locates an arbitrary particle $\mathfrak{P}$ in test sample $\mathbb{B}$ with a set of spatial coordinates X—say, $X = (X_1, X_2, X_3)$—in some rectangular-Cartesian

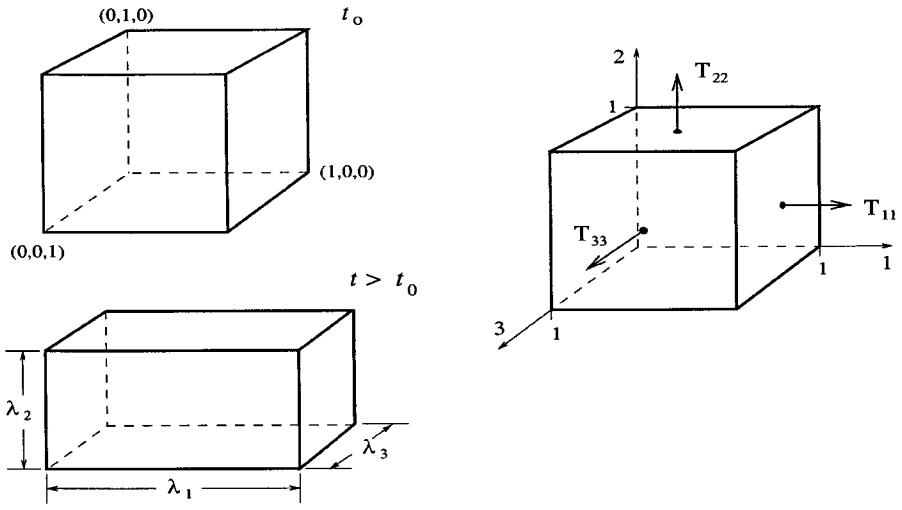

Figure 6.1: Shear-free extension of a material element.

coordinate system $\mathcal{C}$ at a reference state of t_0. Later, this same particle is located at a different place with coordinates $\mathbf{x}$—say, $\mathbf{x} = (x_1, x_2, x_3)$—in the same coordinate system $\mathcal{C}$, but now at the current state of t. These two coordinate pairs relate to one another through the motion

$$x_1 = \lambda_1 X_1, \quad x_2 = \lambda_2 X_2 \quad \text{and} \quad x_3 = \lambda_3 X_3, \tag{6.1}$$

where λ_i is the principal stretch in the i^{th} direction.

The deformation gradient tensors, $\underline{\underline{F}}$ and $\underline{\underline{F}}^{-1}$, therefore have components of

$$\mathbb{F} = \begin{bmatrix} \lambda_1 & 0 & 0 \\ 0 & \lambda_2 & 0 \\ 0 & 0 & \lambda_3 \end{bmatrix} \quad \text{and} \quad \mathbb{F}^{-1} = \begin{bmatrix} \lambda_1^{-1} & 0 & 0 \\ 0 & \lambda_2^{-1} & 0 \\ 0 & 0 & \lambda_3^{-1} \end{bmatrix}, \tag{6.2}$$

whose polar decompostion has a rotation matrix of

$$\mathbb{R} = \begin{bmatrix} 1 & 0 & 0 \\ 0 & 1 & 0 \\ 0 & 0 & 1 \end{bmatrix}, \tag{6.3}$$

leading to stretch tensors $\underline{\underline{V}}$ and $\underline{\underline{U}}$ with identical components of

$$\mathbb{V} = \begin{bmatrix} \lambda_1 & 0 & 0 \\ 0 & \lambda_2 & 0 \\ 0 & 0 & \lambda_3 \end{bmatrix} \quad \text{and} \quad \mathbb{U} = \begin{bmatrix} \lambda_1 & 0 & 0 \\ 0 & \lambda_2 & 0 \\ 0 & 0 & \lambda_3 \end{bmatrix}, \tag{6.4}$$

whose inverses are trivially

$$\mathbb{V}^{-1} = \begin{bmatrix} \lambda_1^{-1} & 0 & 0 \\ 0 & \lambda_2^{-1} & 0 \\ 0 & 0 & \lambda_3^{-1} \end{bmatrix} \quad \text{and} \quad \mathbb{U}^{-1} = \begin{bmatrix} \lambda_1^{-1} & 0 & 0 \\ 0 & \lambda_2^{-1} & 0 \\ 0 & 0 & \lambda_3^{-1} \end{bmatrix}. \tag{6.5}$$

Obviously, there is insufficient information in these components to exploit the full richness of these kinematic fields.

The velocity gradient, $\underline{\underline{L}}$, and the rate-of-deformation, $\underline{\underline{D}}$, tensors have like components of

$$\mathbb{L} = \begin{bmatrix} D\ln\lambda_1 & 0 & 0 \\ 0 & D\ln\lambda_2 & 0 \\ 0 & 0 & D\ln\lambda_3 \end{bmatrix} \quad \text{and} \quad \mathbb{D} = \begin{bmatrix} D\ln\lambda_1 & 0 & 0 \\ 0 & D\ln\lambda_2 & 0 \\ 0 & 0 & D\ln\lambda_3 \end{bmatrix}. \tag{6.6}$$

There is no vorticity (i.e., $\mathbb{W} = \mathbb{0}$) because the eigenvectors of strain are fixed in $\mathbb{B}$.

The lower-fractal rate-of-deformation tensor, $\overset{\alpha\downarrow}{\underline{\underline{D}}}$, has a matrix representation of

$$\overset{\alpha\downarrow}{\mathbb{D}} = \begin{bmatrix} \frac{1}{2}\lambda_1^{-2}D_\star^\alpha\lambda_1^2 & 0 & 0 \\ 0 & \frac{1}{2}\lambda_2^{-2}D_\star^\alpha\lambda_2^2 & 0 \\ 0 & 0 & \frac{1}{2}\lambda_3^{-2}D_\star^\alpha\lambda_3^2 \end{bmatrix}, \tag{6.7}$$

while the upper-fractal rate-of-deformation tensor, $\overset{\alpha\uparrow}{\underline{\underline{D}}}$, has a representation of

$$\overset{\alpha\uparrow}{\mathbb{D}} = \begin{bmatrix} -\frac{1}{2}\lambda_1^{2}D_\star^\alpha\lambda_1^{-2} & 0 & 0 \\ 0 & -\frac{1}{2}\lambda_2^{2}D_\star^\alpha\lambda_2^{-2} & 0 \\ 0 & 0 & -\frac{1}{2}\lambda_3^{2}D_\star^\alpha\lambda_3^{-2} \end{bmatrix}, \tag{6.8}$$

such that in the limit, as α goes to one from below, both $\overset{\alpha\downarrow}{\underline{\underline{D}}}$ and $\overset{\alpha\uparrow}{\underline{\underline{D}}}$ yield $\underline{\underline{D}}$ as expected.

6.1.2 Deformation Fields

In the Eulerian frame, the contravariant-like, Finger, deformation tensor, $\underline{\underline{B}}$, and the covariant-like, Cauchy, deformation tensor, $\underline{\underline{B}}^{-1}$, have components of

$$\mathbb{B} = \begin{bmatrix} \lambda_1^2 & 0 & 0 \\ 0 & \lambda_2^2 & 0 \\ 0 & 0 & \lambda_3^2 \end{bmatrix} \quad \text{and} \quad \mathbb{B}^{-1} = \begin{bmatrix} \lambda_1^{-2} & 0 & 0 \\ 0 & \lambda_2^{-2} & 0 \\ 0 & 0 & \lambda_3^{-2} \end{bmatrix}. \tag{6.9}$$

In the Lagrangian frame, the covariant-like, Green, deformation tensor, $\underline{\underline{C}}$, and its rate, $D\underline{\underline{C}}$, have matrix representations of

$$\mathbb{C} = \begin{bmatrix} \lambda_1^2 & 0 & 0 \\ 0 & \lambda_2^2 & 0 \\ 0 & 0 & \lambda_3^2 \end{bmatrix} \quad \text{and} \quad D\mathbb{C} = \begin{bmatrix} 2\lambda_1 D\lambda_1 & 0 & 0 \\ 0 & 2\lambda_2 D\lambda_2 & 0 \\ 0 & 0 & 2\lambda_3 D\lambda_3 \end{bmatrix}, \tag{6.10}$$

while the contravariant-like inverse, $\underline{\underline{C}}^{-1}$, and its rate, $D\underline{\underline{C}}^{-1}$, have representations of

$$\mathbb{C}^{-1} = \begin{bmatrix} \lambda_1^{-2} & 0 & 0 \\ 0 & \lambda_2^{-2} & 0 \\ 0 & 0 & \lambda_3^{-2} \end{bmatrix} \quad \text{and} \quad D\mathbb{C}^{-1} = \begin{bmatrix} -2\lambda_1^{-3} D\lambda_1 & 0 & 0 \\ 0 & -2\lambda_2^{-3} D\lambda_2 & 0 \\ 0 & 0 & -2\lambda_3^{-3} D\lambda_3 \end{bmatrix}. \tag{6.11}$$

The Caputo derivatives of these deformation fields have components of

$$D_\star^\alpha \mathbb{C} = \begin{bmatrix} D_\star^\alpha \lambda_1^2 & 0 & 0 \\ 0 & D_\star^\alpha \lambda_2^2 & 0 \\ 0 & 0 & D_\star^\alpha \lambda_3^2 \end{bmatrix} \quad \text{and} \quad D_\star^\alpha \mathbb{C}^{-1} = \begin{bmatrix} D_\star^\alpha \lambda_1^{-2} & 0 & 0 \\ 0 & D_\star^\alpha \lambda_2^{-2} & 0 \\ 0 & 0 & D_\star^\alpha \lambda_3^{-2} \end{bmatrix}, \tag{6.12}$$

for $0 < \alpha < 1$.

The fact that the deformation fields $\mathbb{B}$ and $\mathbb{C}$ have identical components is a direct consequence of the deformation gradient $\mathbb{F}$ being diagonal. In general, the Finger and Green deformation tensors have matrix representations that are different from one another, but not for shear-free extensions.

6.1.3 Strain Fields

With the deformation tensors and their rates now known, it is a simple matter to quantify any strain or strain-rate field of interest. In what follows, we determine the five Eulerian strain fields used in our models.

The three isotropic invariants defined in (5.13) have values of

$$\left.\begin{aligned} I_1 &= \tfrac{1}{4}\big(\lambda_1^2 + \lambda_2^2 + \lambda_3^2 + \lambda_1^{-2} + \lambda_2^{-2} + \lambda_3^{-2}\big) \\ I_2 &= \tfrac{1}{16}\big(\lambda_1^4 + \lambda_2^4 + \lambda_3^4 + \lambda_1^{-4} + \lambda_2^{-4} + \lambda_3^{-4}\big) \\ I_3 &= \lambda_1\lambda_2\lambda_3 + \lambda_1^{-1}\lambda_2^{-1}\lambda_3^{-1} \end{aligned}\right\}, \tag{6.13}$$

which are observed to be insensitive to tensions versus compressions, an achievement that other classic invariants can only obtain through squaring, whereby making them even functions. Associated with these invariants are the isotropic strains from (5.15) that in component form are given by

$$\mathbb{E}^{(1)} = \tfrac{1}{4}\big(\mathbb{B} - \mathbb{B}^{-1}\big) = \begin{bmatrix} \frac{1}{4}\big(\lambda_1^2 - \lambda_1^{-2}\big) & 0 & 0 \\ 0 & \frac{1}{4}\big(\lambda_2^2 - \lambda_2^{-2}\big) & 0 \\ 0 & 0 & \frac{1}{4}\big(\lambda_3^2 - \lambda_3^{-2}\big) \end{bmatrix}, \tag{6.14}$$

$$\mathbb{E}^{(2)} = \tfrac{1}{8}\big(\mathbb{B}^2 - \mathbb{B}^{-2}\big) = \begin{bmatrix} \frac{1}{8}\big(\lambda_1^4 - \lambda_1^{-4}\big) & 0 & 0 \\ 0 & \frac{1}{8}\big(\lambda_2^4 - \lambda_2^{-4}\big) & 0 \\ 0 & 0 & \frac{1}{8}\big(\lambda_3^4 - \lambda_3^{-4}\big) \end{bmatrix}, \tag{6.15}$$

and

$$e = \tfrac{1}{2}\big(|\mathbb{F}| - |\mathbb{F}|^{-1}\big) = \tfrac{1}{2}\big(\lambda_1\lambda_2\lambda_3 - \lambda_1^{-1}\lambda_2^{-1}\lambda_3^{-1}\big), \tag{6.16}$$

where the mass densities ratio as

$$\frac{\varrho_0}{\varrho} = \lambda_1\lambda_2\lambda_3, \tag{6.17}$$

in accordance with the conservation of mass.

Figure 6.2 plots stretch against strain for the deformation of simple extension where curves for $\mathrm{E}_{11}^{(1)}$, $\mathrm{E}_{11}^{(2)}$ and (infinitesimal) engineering strain are presented. What is observed is that $\mathrm{E}_{11}^{(1)}$ is a very good approximation for engineering strain to quite

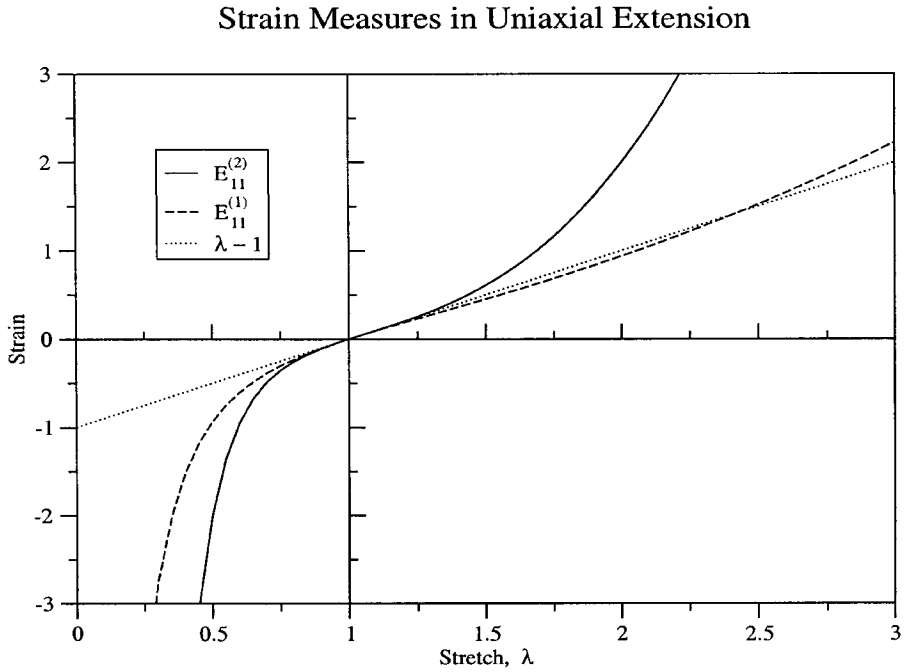

Figure 6.2: A comparison of various strain measures for the 1D extension of a rod.

large extensions, while $E_{11}^{(2)}$ is true nonlinear measure of strain. All have the same slope at $\lambda = 1$ by design.

We consider three individual cases for the anisotropic strains of (5.27) where the initial strong direction of the material $\underline{a}_0$ aligns with each one of the three coordinate axes in Fig. 6.1. In the first case,

$$\mathbf{a}_0 = \{1 \quad 0 \quad 0\}^{\mathrm{T}}, \tag{6.18}$$

leading to

$$\mathbb{A}^{(1)} = \begin{bmatrix} \frac{1}{4}(\lambda_1^2 - \lambda_1^{-2}) & 0 & 0 \\ 0 & 0 & 0 \\ 0 & 0 & 0 \end{bmatrix} \quad \text{and} \quad \mathbb{A}^{(2)} = \begin{bmatrix} \frac{1}{8}(\lambda_1^4 - \lambda_1^{-4}) & 0 & 0 \\ 0 & 0 & 0 \\ 0 & 0 & 0 \end{bmatrix}, \tag{6.19}$$

which are associated with the anisotropic invariants (5.26)

$$I_4 = \tfrac{1}{4}(\lambda_1^2 + \lambda_1^{-2}) \quad \text{and} \quad I_5 = \tfrac{1}{16}(\lambda_1^4 + \lambda_1^{-4}). \tag{6.20}$$

In the second case,

$$\mathbf{a}_0 = \{0 \quad 1 \quad 0\}^{\mathrm{T}}, \tag{6.21}$$

with

$$\mathbb{A}^{(1)} = \begin{bmatrix} 0 & 0 & 0 \\ 0 & \frac{1}{4}(\lambda_2^2 - \lambda_2^{-2}) & 0 \\ 0 & 0 & 0 \end{bmatrix} \quad \text{and} \quad \mathbb{A}^{(2)} = \begin{bmatrix} 0 & 0 & 0 \\ 0 & \frac{1}{8}(\lambda_2^4 - \lambda_2^{-4}) & 0 \\ 0 & 0 & 0 \end{bmatrix}, \tag{6.22}$$

so that

$$I_4 = \tfrac{1}{4}\left(\lambda_2^2 + \lambda_2^{-2}\right) \quad \text{and} \quad I_5 = \tfrac{1}{16}\left(\lambda_2^4 + \lambda_2^{-4}\right). \tag{6.23}$$

And in the third case,

$$\mathbb{a}_0 = \left\{0 \;\; 0 \;\; 1\right\}^{\mathrm{T}}, \tag{6.24}$$

producing

$$\mathbb{A}^{(1)} = \begin{bmatrix} 0 & 0 & 0 \\ 0 & 0 & 0 \\ 0 & 0 & \frac{1}{4}\left(\lambda_3^2 - \lambda_3^{-2}\right) \end{bmatrix} \quad \text{and} \quad \mathbb{A}^{(2)} = \begin{bmatrix} 0 & 0 & 0 \\ 0 & 0 & 0 \\ 0 & 0 & \frac{1}{8}\left(\lambda_3^4 - \lambda_3^{-4}\right) \end{bmatrix}, \tag{6.25}$$

with

$$I_4 = \tfrac{1}{4}\left(\lambda_3^2 + \lambda_3^{-2}\right) \quad \text{and} \quad I_5 = \tfrac{1}{16}\left(\lambda_3^4 + \lambda_3^{-4}\right). \tag{6.26}$$

In all three of these cases the non-zero anisotropic strain component equals the corresponding isotropic strain component; they have the same strength. In fact, the coefficients appearing in the definitions of I_4 and I_5 were chosen to specifically achieve this scaling.

It is possible to run experiments where $\underline{a}_0$ does not align with a coordinate axis, but care is required here because the ensueing deformations will not remain homogeneous and they certainly will no longer be shear free.

6.1.4 Stress Fields

The actual state of stress is dictated by the boundary conditions imposed on the specimen. When tractions are present on a particular material plane they can lead to non-zero components of stress acting in that direction, otherwise these planes are stress (traction) free.

For isotropic materials and transversely isotropic materials whose strong direction aligns with one of the three coordinate axes, the Cauchy stress, $\underline{\underline{T}}$, is characterized by

$$\mathbb{T} = \begin{bmatrix} \mathrm{T}_{11} & 0 & 0 \\ 0 & \mathrm{T}_{22} & 0 \\ 0 & 0 & \mathrm{T}_{33} \end{bmatrix} = \begin{bmatrix} f_1/\lambda_2\lambda_3 A_{1,0} & 0 & 0 \\ 0 & f_2/\lambda_1\lambda_3 A_{2,0} & 0 \\ 0 & 0 & f_3/\lambda_1\lambda_2 A_{3,0} \end{bmatrix}, \tag{6.27}$$

which for incompressible materials (i.e., $\lambda_1\lambda_2\lambda_3 = 1$) simplifies to

$$\mathbb{T} = \begin{bmatrix} \lambda_1 f_1/A_{1,0} & 0 & 0 \\ 0 & \lambda_2 f_2/A_{2,0} & 0 \\ 0 & 0 & \lambda_3 f_3/A_{3,0} \end{bmatrix}, \tag{6.28}$$

where f_i, $i = 1, 2, 3$, are the contact forces at current time $t > t_0$ applied in the i^{th} coordinate directions onto surfaces whose initial areas $A_{i,0}$ $(= \ell_{j,0}\,\ell_{k,0}, i \neq j \neq k)$ are measured in the reference state of t_0.

6.1.5 Special Cases

Except for dilational compression, these experiments are considered to be done on (nearly) incompressible materials in the sense that their bulk moduli are order(s) in magnitude greater than their shear moduli.

Simple tension

Uniaxial tension/compression experiments done on isotropic materials have a deformation gradient and a state of stress with components that are described by

$$\mathbb{F} = \begin{bmatrix} \lambda & 0 & 0 \\ 0 & \lambda^{-1/2} & 0 \\ 0 & 0 & \lambda^{-1/2} \end{bmatrix}, \quad \mathbb{T} = \begin{bmatrix} \sigma = \lambda f/A_0 & 0 & 0 \\ 0 & 0 & 0 \\ 0 & 0 & 0 \end{bmatrix}, \tag{6.29}$$

where λ $(= \lambda_1 = \ell/\ell_0)$ is the applied stretch, with σ being the resulting applied state of Cauchy stress.

Biaxial tension

When a sheet is stretched in orthogonal directions by amounts λ_1 and λ_2, the deformation that ensues is described by a deformation gradient and Cauchy stress whose matrix representations are

$$\mathbb{F} = \begin{bmatrix} \lambda_1 & 0 & 0 \\ 0 & \lambda_2 & 0 \\ 0 & 0 & \lambda_1^{-1}\lambda_2^{-1} \end{bmatrix}, \quad \mathbb{T} = \begin{bmatrix} \sigma_1 = \lambda_1 f_1/A_{1,0} & 0 & 0 \\ 0 & \sigma_2 = \lambda_2 f_2/A_{2,0} & 0 \\ 0 & 0 & 0 \end{bmatrix}, \tag{6.30}$$

where σ_1 and σ_2 are the corresponding applied stresses. Equibiaxial tension implies that $\lambda_1 = \lambda_2$.

Pure shear

When performed in a state of tension, this experiment is called pure shear; whereas, when performed in a state of compression, it is often called planar or channel compression. These experiments produce a state whose deformation gradient and stress fields have components given by

$$\mathbb{F} = \begin{bmatrix} \lambda & 0 & 0 \\ 0 & 1 & 0 \\ 0 & 0 & \lambda^{-1} \end{bmatrix}, \quad \mathbb{T} = \begin{bmatrix} \sigma = \lambda f/A_0 & 0 & 0 \\ 0 & \varsigma & 0 \\ 0 & 0 & 0 \end{bmatrix}, \tag{6.31}$$

where it is under a condition of incompressibility that these kinematics conform with the classic notion of pure shear (in the sense of strains). Here λ and λ^{-1} are the applied and reaction stretches, respectively, while σ and ς are the resulting applied and reaction stresses, respectively.

Dispite its name, pure shear is a shear-free deformation because the principal axes of stress and strain do not rotate, but remain orthogonal. Pure shear is therefore not a shearing deformation. Simple shear, defined in the next section, is a shearing deformation.

Dilational compression

To be able to justify using the constraint of incompressibility, as we have done in the preceeding cases, one should experimentally demonstrate that the shear response of the material is orders of magnitude less stiff than its bulk response. A dilational compression experiment is usually performed to quantify bulk behavior. It is this experiment that earned Bridgman his Nobel Prize for Physics in 1946.* Here the deformation gradient and stress fields have matrix representations of

$$\mathbb{F} = \begin{bmatrix} \lambda & 0 & 0 \\ 0 & 1 & 0 \\ 0 & 0 & 1 \end{bmatrix}, \quad \mathbb{T} = \begin{bmatrix} \sigma = f/A_0 & 0 & 0 \\ 0 & \varsigma & 0 \\ 0 & 0 & \varsigma \end{bmatrix}, \tag{6.32}$$

where λ is the applied stretch, σ is the resulting applied stress, while ς is the reaction stress, which Bridgman did not measure.

This experiment does not, in general, impose a state of pure hydrostatic pressure. It is only when the bulk effects drown the shear effects that the resulting stress state becomes approximately isotropic (i.e., hydrostatic).

6.2 Simple Shear

This is a technologically important experiment for fluids and solids alike because the eigenvectors of stress and strain rotate in the body, yet the stress and strain fields themselves remain spatially uniform throughout the sample being tested. In this experiment, a homogeneous material element in the shape of a unit cube is deformed into a parallelepiped of unit height and with square shear planes by displacing the top shear plane a horizontal distance s, as illustrated in Fig. 6.3. This causes a reactionary shear stress, T_{12}, to set up along this shear plane. Furthermore, second-order effects gradually appear in the normal directions as an artifact of these kinematics; effects first studied by Poynting [88].

The angle of shear, γ, and the magnitude of shear, s, are two common measures of shear deformation that relate to one another through the expression

$$s = \tan\gamma = \gamma + \tfrac{1}{3}\gamma^3 + \tfrac{2}{15}\gamma^5 + \tfrac{17}{315}\gamma^7 + \cdots, \tag{6.33}$$

with γ being typically refered to as the engineering shear strain.

6.2.1 Kinematics

The deformation describing simple shear locates an arbitrary particle $\mathfrak{P}$ in test sample $\mathbb{B}$ with a set of spatial coordinates X—say, $X = (X_1, X_2, X_3)$—in rectangular-Cartesian coordinate system $\mathcal{C}$ in a reference state at t_0. Later, this particle occupies

*Bridgman's Nobel Prize citation reads:

"For the invention of an apparatus to produce extremely high pressures, and for the discoveries he made therewith in the field of high pressure physics."

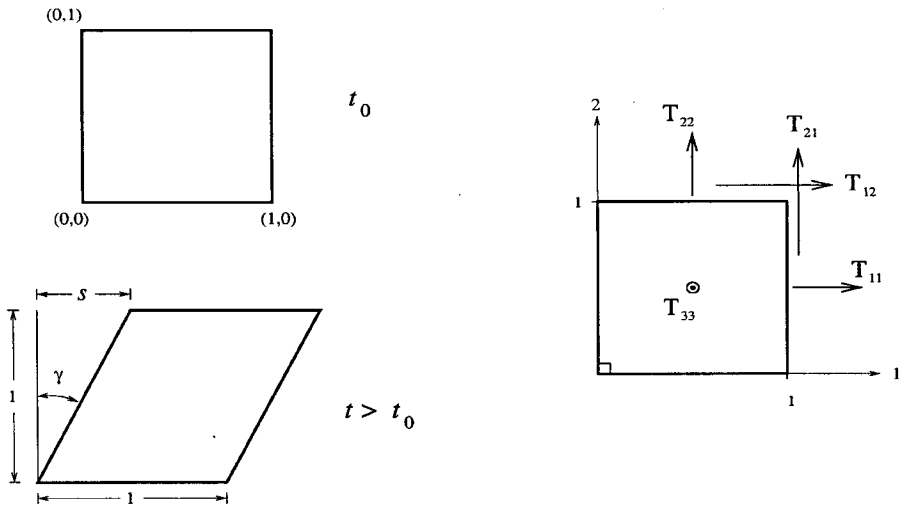

Figure 6.3: Simple shearing of a material element.

a different location with coordinates $\mathbf{x}$—say, $\mathbf{x} = (x_1, x_2, x_3)$—in the same coordinate system $\mathcal{C}$, but in the current state of t. These coordinates relate to one another via the motion

$$x_1 = X_1 + s\,X_2, \quad x_2 = X_2 \quad \text{and} \quad x_3 = X_3, \tag{6.34}$$

so that the deformation gradient tensors, $\underline{\underline{F}}$ and $\underline{\underline{F}}^{-1}$, have components of

$$\mathbb{F} = \begin{bmatrix} 1 & s & 0 \\ 0 & 1 & 0 \\ 0 & 0 & 1 \end{bmatrix} \quad \text{and} \quad \mathbb{F}^{-1} = \begin{bmatrix} 1 & -s & 0 \\ 0 & 1 & 0 \\ 0 & 0 & 1 \end{bmatrix}, \tag{6.35}$$

whose rotation matrix in turn has components

$$\mathbb{R} = \begin{bmatrix} \cos\theta & \sin\theta & 0 \\ -\sin\theta & \cos\theta & 0 \\ 0 & 0 & 1 \end{bmatrix}, \quad \text{wherein} \quad \theta = \tan^{-1}(s/2) = \tan^{-1}\left(\tfrac{1}{2}\tan\gamma\right). \tag{6.36}$$

The left-stretch tensor has a matrix representation of

$$\mathbb{V} = \begin{bmatrix} (1+\sin^2\theta)/\cos\theta & \sin\theta & 0 \\ \sin\theta & \cos\theta & 0 \\ 0 & 0 & 1 \end{bmatrix}, \tag{6.37}$$

with inverse

$$\mathbb{V}^{-1} = \begin{bmatrix} \cos\theta & -\sin\theta & 0 \\ -\sin\theta & (1+\sin^2\theta)/\cos\theta & 0 \\ 0 & 0 & 1 \end{bmatrix}, \tag{6.38}$$

while the right-stretch tensor has components of

$$\mathbb{U} = \begin{bmatrix} \cos\theta & \sin\theta & 0 \\ \sin\theta & (1+\sin^2\theta)/\cos\theta & 0 \\ 0 & 0 & 1 \end{bmatrix}, \tag{6.39}$$

with inverse

$$\mathbb{U}^{-1} = \begin{bmatrix} (1+\sin^2\theta)/\cos\theta & -\sin\theta & 0 \\ -\sin\theta & \cos\theta & 0 \\ 0 & 0 & 1 \end{bmatrix}. \tag{6.40}$$

The richness of tensor fields for describing the kinematics of deformation is fully realized in simple shear making it a more informative experiment than those with shear-free deformation histories.

The velocity gradient tensor, $\underline{\underline{L}}$, has values of

$$\mathbb{L} = \begin{bmatrix} 0 & Ds & 0 \\ 0 & 0 & 0 \\ 0 & 0 & 0 \end{bmatrix}, \tag{6.41}$$

leading to rate-of-deformation, $\underline{\underline{D}}$, and vorticity, $\underline{\underline{W}}$, tensors whose matrix representations are

$$\mathbb{D} = \begin{bmatrix} 0 & \frac{1}{2}Ds & 0 \\ \frac{1}{2}Ds & 0 & 0 \\ 0 & 0 & 0 \end{bmatrix} \quad \text{and} \quad \mathbb{W} = \begin{bmatrix} 0 & \frac{1}{2}Ds & 0 \\ -\frac{1}{2}Ds & 0 & 0 \\ 0 & 0 & 0 \end{bmatrix}. \tag{6.42}$$

It is the simplistic form of the vorticity tensor that makes simple shear such an important experiment for material characterization.

The lower-fractal rate-of-deformation tensor, $\overset{\alpha\downarrow}{\underline{\underline{D}}}$, has a representation of

$$\overset{\alpha\downarrow}{\mathbb{D}} = \begin{bmatrix} 0 & \frac{1}{2}D^\alpha_\star s & 0 \\ \frac{1}{2}D^\alpha_\star s & \frac{1}{2}\left(D^\alpha_\star s^2 - 2s\,D^\alpha_\star s\right) & 0 \\ 0 & 0 & 0 \end{bmatrix}, \tag{6.43}$$

while the upper-fractal rate-of-deformation tensor, $\overset{\alpha\uparrow}{\underline{\underline{D}}}$, has a representation of

$$\overset{\alpha\uparrow}{\mathbb{D}} = \begin{bmatrix} \frac{1}{2}\left(2s\,D^\alpha_\star s - D^\alpha_\star s^2\right) & \frac{1}{2}D^\alpha_\star s & 0 \\ \frac{1}{2}D^\alpha_\star s & 0 & 0 \\ 0 & 0 & 0 \end{bmatrix}, \tag{6.44}$$

for $0 < \alpha < 1$. The component $\frac{1}{2}\left(2s\,D^\alpha_\star s - D^\alpha_\star s^2\right)$ goes to zero in the limit as α goes to one (1) from below, which it must in order for $\overset{\alpha\downarrow}{\underline{\underline{D}}}$ and $\overset{\alpha\uparrow}{\underline{\underline{D}}}$ to be consistent with $\underline{\underline{D}}$ in this limit.

Simple shear is isochoric because $\det(\underline{\underline{F}}) = 1$, implying that this deformation is a volume preserving process, independent of constitutive assumption.

6.2.2 Deformation Fields

In the Eulerian frame, the contravariant-like, Finger, deformation tensor, $\underline{\underline{B}}$, and the covariant-like, Cauchy, deformation tensor, $\underline{\underline{B}}^{-1}$, have components of

$$\mathbb{B} = \begin{bmatrix} 1+s^2 & s & 0 \\ s & 1 & 0 \\ 0 & 0 & 1 \end{bmatrix} \quad \text{and} \quad \mathbb{B}^{-1} = \begin{bmatrix} 1 & -s & 0 \\ -s & 1+s^2 & 0 \\ 0 & 0 & 1 \end{bmatrix}. \tag{6.45}$$

In the Lagrangian frame, the covariant-like, Green, deformation tensor, $\underline{\underline{C}}$, and its contravariant-like inverse, $\underline{\underline{C}}^{-1}$, have matrix representations of

$$C = \begin{bmatrix} 1 & s & 0 \\ s & 1+s^2 & 0 \\ 0 & 0 & 1 \end{bmatrix} \quad \text{and} \quad C^{-1} = \begin{bmatrix} 1+s^2 & -s & 0 \\ -s & 1 & 0 \\ 0 & 0 & 1 \end{bmatrix}, \tag{6.46}$$

that evolve as

$$DC = \begin{bmatrix} 0 & Ds & 0 \\ Ds & 2s\,Ds & 0 \\ 0 & 0 & 0 \end{bmatrix} \quad \text{and} \quad DC^{-1} = \begin{bmatrix} 2s\,Ds & -Ds & 0 \\ -Ds & 0 & 0 \\ 0 & 0 & 0 \end{bmatrix}, \tag{6.47}$$

and whose Caputo derivatives are

$$D^\alpha_\star C = \begin{bmatrix} 0 & D^\alpha_\star s & 0 \\ D^\alpha_\star s & D^\alpha_\star s^2 & 0 \\ 0 & 0 & 0 \end{bmatrix} \quad \text{and} \quad D^\alpha_\star C^{-1} = \begin{bmatrix} D^\alpha_\star s^2 & -D^\alpha_\star s & 0 \\ -D^\alpha_\star s & 0 & 0 \\ 0 & 0 & 0 \end{bmatrix}, \tag{6.48}$$

for $0 < \alpha < 1$.

Simple shear is the simplest experiment wherein the four deformation tensors $\underline{\underline{B}}$, $\underline{\underline{B}}^{-1}$, $\underline{\underline{C}}$ and $\underline{\underline{C}}^{-1}$ have matrix representations $\mathcal{B}$, $\mathcal{B}^{-1}$, C and C^{-1} that are all different.

6.2.3 Strain Fields

Now that the various kinematic and deformation tensors and their rates have been quantified for simple shear, it is a straightforward process to establish any strain or strain-rate field of interest. Here we provide the five strain fields used in our material models.

The three isotropic invariants of (5.13) are determined to be

$$I_1 = \tfrac{1}{2}\big(3+s^2\big), \quad I_2 = \tfrac{1}{8}\big(3+4s^2+s^4\big) \quad \text{and} \quad I_3 = 2, \tag{6.49}$$

whose associated strains (5.15) have components of

$$\mathcal{E}^{(1)} = \tfrac{1}{4}\big(\mathcal{B}-\mathcal{B}^{-1}\big) = \begin{bmatrix} \frac{1}{4}s^2 & \frac{1}{2}s & 0 \\ \frac{1}{2}s & -\frac{1}{4}s^2 & 0 \\ 0 & 0 & 0 \end{bmatrix}, \tag{6.50}$$

$$\mathcal{E}^{(2)} = \tfrac{1}{8}\big(\mathcal{B}^2-\mathcal{B}^{-2}\big) = \begin{bmatrix} \frac{1}{8}s^2(2+s^2) & \frac{1}{4}s(2+s^2) & 0 \\ \frac{1}{4}s(2+s^2) & -\frac{1}{8}s^2(2+s^2) & 0 \\ 0 & 0 & 0 \end{bmatrix} = (1+\tfrac{1}{2}s^2)\mathcal{E}^{(1)}, \tag{6.51}$$

and

$$e = \tfrac{1}{2}\big(|F|-|F|^{-1}\big) = 0, \tag{6.52}$$

the latter of which is zero because the deformation is isochoric, and therefore

$$\varrho = \varrho_0, \tag{6.53}$$

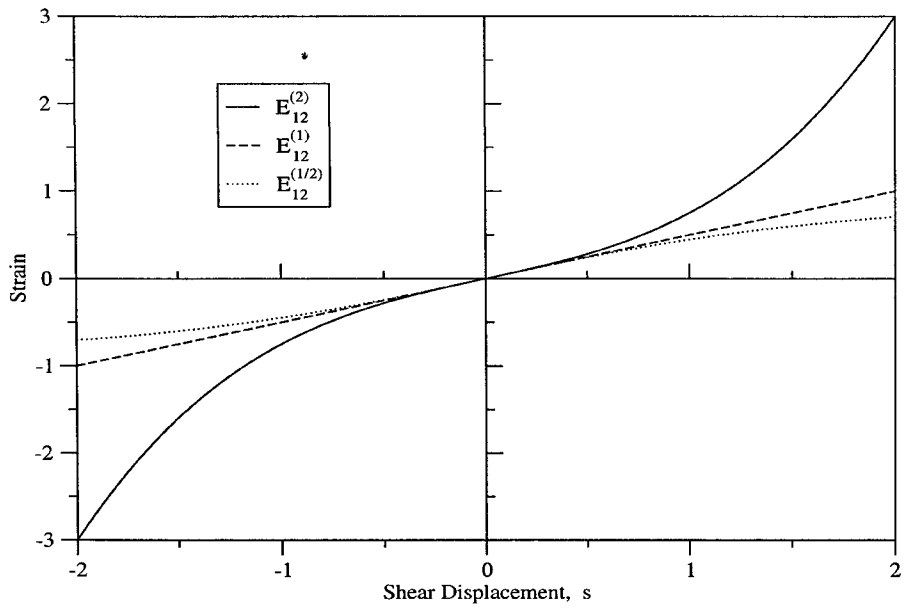

Figure 6.4: A comparison of $E_{12}^{(1/2)}$, $E_{12}^{(1)}$ and $E_{12}^{(2)}$ for simple shearing.

in accordance with the conservation of mass. The fact that $\mathbb{E}^{(2)}$ is proportional to $\mathbb{E}^{(1)}$ within a scalar factor is unique to the deformation of simple shear. In other deformations, like shear-free flows, $\mathbb{E}^{(1)}$ and $\mathbb{E}^{(2)}$ are distinct measures of strain.

Figure 6.4 presents a comparison between the shear components of $\mathbb{E}^{(1/2)}$, $\mathbb{E}^{(1)}$ and $\mathbb{E}^{(2)}$ during a deformation of simple shear. Contrasting these plots with experimental data will provide the modeler with an indication as to which strain fields to include in a model for that material. Like shear-free deformations, $E_{12}^{(1)}$ is a linear strain measure while $E_{12}^{(2)}$ is a nonlinear strain measure.

Even though we do not presently know how to derive $\underline{\underline{E}}^{(1/2)}$ from a free-energy expression, we still present $\mathbb{E}_{12}^{(1/2)}$ in Fig. 6.4 for comparison purposes. Of particular note is the fact that $E_{12}^{(1/2)} \to 1$ as $s \to \infty$. If stress is to be proportional to strain, then the strain field $\underline{\underline{E}}^{(1/2)}$ is characteristic of fluid-like behavior, not solid-like behavior, thereby lending additional support for our selection of the integrity basis listed in (5.9a & 5.23a) for isotropic and transversely isotropic solids. If we were developing a theory for viscoelastic fluids instead of one for viscoelastic solids, then seeking an integrity basis that would lead to strains $\underline{\underline{E}}^{(n)}$, $0 < n \leq 1$, would be an appropriate exercise.

As with shear-free extensions, we investigate those instances where the strong material direction $\underline{a}_0$ aligns with one of the three coordinate axes of Fig. 6.3. In the case where $\underline{a}_0$ aligns with the direction of shearing, there

$$a_0 = \{1 \quad 0 \quad 0\}^{\mathrm{T}}, \tag{6.54}$$

and this direction remains fixed throughout the deformation. This produces a longi-

tudinal shearing along the fibers, which themselves lie in the plane of shearing. Here the anisotropic strain tensors of (5.27) have components

$$\mathbb{A}^{(1)} = \begin{bmatrix} 0 & \frac{1}{4}s & 0 \\ \frac{1}{4}s & -\frac{1}{4}s^2 & 0 \\ 0 & 0 & 0 \end{bmatrix}, \tag{6.55}$$

and

$$\mathbb{A}^{(2)} = (1+\tfrac{1}{2}s^2)\mathbb{A}^{(1)} = \begin{bmatrix} 0 & \frac{1}{8}s(2+s^2) & 0 \\ \frac{1}{8}s(2+s^2) & -\frac{1}{8}s^2(2+s^2) & 0 \\ 0 & 0 & 0 \end{bmatrix}, \tag{6.56}$$

whose associated invariants (5.26) are

$$I_4 = \tfrac{1}{4}\big(2+s^2\big) \quad \text{and} \quad I_5 = \tfrac{1}{16}\big(2+4s^2+s^4\big), \tag{6.57}$$

indicating that an anisotropic effect is being picked up by this mode of shearing.

In the second case, the strong direction is initially normal to the shearing plane and therefore aligns with the coordinate direction

$$a_0 = \big\{0 \quad 1 \quad 0\big\}^{\mathrm{T}}. \tag{6.58}$$

Unlike the prior mode of shearing, here the material direction of strength rotates in the body during the deformation to a new direction of

$$a_0 = \big\{s/\sqrt{1+s^2} \quad 1/\sqrt{1+s^2} \quad 0\big\}^{\mathrm{T}}. \tag{6.59}$$

In the presence of this cross-axis shearing, the anisotropic strain tensors have components of

$$\mathbb{A}^{(1)} = \begin{bmatrix} \frac{1}{4}s^2 & \frac{1}{4}s & 0 \\ \frac{1}{4}s & 0 & 0 \\ 0 & 0 & 0 \end{bmatrix}, \tag{6.60}$$

and

$$\mathbb{A}^{(2)} = \begin{bmatrix} \frac{1}{8}s^2(2+s^2) & \frac{1}{8}s(2+s^2) & 0 \\ \frac{1}{8}s(2+s^2) & 0 & 0 \\ 0 & 0 & 0 \end{bmatrix} = (1+\tfrac{1}{2}s^2)\mathbb{A}^{(1)}, \tag{6.61}$$

associated with invariants

$$I_4 = \tfrac{1}{4}\big(2+s^2\big) \quad \text{and} \quad I_5 = \tfrac{1}{16}\big(2+4s^2+s^4\big). \tag{6.62}$$

Consequently, longitudinal and cross-axis shearing have the same, first-order, anisotropic response, differing only in their second-order normal responses. Unlike shear-free extensions, where the strength of the isotropic and anisotropic strains are the same, here the anisotropic shear component has half the strength of the isotropic shear component. This means that the simple shear experiment has half the sensitivity to material anisotropy that the simple extension experiment has.

The third case, called transverse shearing, places the strong direction in the shear plane lying normal to the shearing direction, so that

$$\mathbb{a}_0 = \{0 \quad 0 \quad 1\}^{\mathrm{T}}. \tag{6.63}$$

Like longitudinal shearing, here the strong direction remains fixed throughout the deformation. Unlike the other two shearing modes, this mode of simple shear leads to anisotropic strain tensors that do not contribute to the overall strain field in that

$$\mathbb{A}^{(1)} = \mathbb{A}^{(2)} = \mathbb{0}, \tag{6.64}$$

because the invariants are fixed,

$$I_4 = 1/2 \quad \text{and} \quad I_5 = 1/8, \tag{6.65}$$

implying that transverse shearing occurs in the plane of isotropy.

6.2.4 Stress Fields

For isotropic materials and for transversely isotropic materials where the strong direction $\underline{a}_0$ aligns with any one of the three coordinate directions, the most general state of stress that can arise from simple shearing produces components for Cauchy stress of [68, pp. 62–64]

$$\mathbb{T} = \begin{bmatrix} \mathrm{T}_{11} & \mathrm{T}_{12} & 0 \\ \mathrm{T}_{21} & \mathrm{T}_{22} & 0 \\ 0 & 0 & \mathrm{T}_{33} \end{bmatrix} = \begin{bmatrix} f_{11}/A_1 & f_{12}/A_2 & 0 \\ f_{21}/A_1 & f_{22}/A_2 & 0 \\ 0 & 0 & f_{33}/A_3 \end{bmatrix}, \tag{6.66}$$

where $f_{12}/A_2 = f_{21}/A_1$ because of symmetry in stress (i.e., because $\mathrm{T}_{12} = \mathrm{T}_{21}$). Notation f_{mn} denotes a force acting in the m direction on a material surface of area A_n whose unit normal is in the n direction in the rectangular-Cartesian coordinate system $\mathcal{C}$ displayed in Fig. 6.3. The third normal stress, T_{33}, will generally be zero valued except for incompressible materials where T_{33} will equal $-\wp$ with $\wp$ denoting a Lagrange multiplier that has been introduced to secure an incompressible deformation.

Incompressible materials

If a material is incompressible (i.e., its bulk response is orders of magnitude more stiff than its shear response), then the isotropic constraint of (3.20b) that enforces this condition will not permit all three normal components of stress to be uniquely determined. For this reason, simple shear experiments done on (apparently) incompressible materials result in at most three, independent, stress-like quantities that can be measured via experiment; they are:

$$\tau := \mathrm{T}_{12} = \mathrm{T}_{21}, \quad \Psi_1 := \mathrm{T}_{11} - \mathrm{T}_{22}, \quad \Psi_2 := \mathrm{T}_{22} - \mathrm{T}_{33}, \tag{6.67}$$

where τ is the shear stress, Ψ_1 is the first normal-stress difference, and Ψ_2 is the second normal-stress difference. Taking the difference between any two normal-stress components subtracts out the unknown contribution arising from $\wp$, the Lagrange multiplier. Data from shear experiments done on viscoelastic fluids are usually reported in terms of these three stress measures.

Chapter 7

Bulk Material Models

In this report we are primarily concerned with biological and synthetic, polymeric elastomers whose bulk moduli are at least an order in magnitude more stiff than their shear moduli. For the purpose of materials characterization, it is therefore reasonable to assume that the bulk and shear responses are uncoupled. However, for the purpose of numeric computation in finite elements, it is advantageous to treat these materials as being compressible, even if only slightly so.

In this chapter elastic and viscoelastic constitutive formulæ that quantify pressure in terms of dilatation are presented and then used to solve the boundary-value problem of Bridgman's experiment (6.32). There is much that the reader can learn about constructing fractional-order, viscoelastic, material models by first studying the simpler one-dimensional case of isotropic bulk behavior.

7.1 Elastic Response

In his early studies done shortly after the first world war, Bridgman [11] used the method of least squares to fit his isothermal experimental data to the empirical formula

$$\delta := \frac{dV - dV_0}{dV_0} = -a\,p + b\,p^2 - c\,p^3, \tag{7.1}$$

where he reported fitted parameters for a, b and c instead of presenting plots of the raw data. Even then his peak pressures were well in excess of 1 GPa. In his later works, Bridgman presented raw data in graphical form; fitted expressions were not given. In the above formula, $\delta(\mathfrak{P}; t_0, t)$ represents a definition for dilatation used in the linear theory of elasticity, which is different from Hencky's definition (3.15) given by $\Delta(\mathfrak{P}; t_0, t)$ $\big(= \ln(dV/dV_0)\big)$, and which is different from our definition (5.15b) given by $e(\mathfrak{P}; t_0, t)$ $\big(= \frac{1}{2}(dV/dV_0 - dV_0/dV)\big)$. Scalar $p(\mathfrak{P}, t)$ $(= -\frac{1}{3}\operatorname{tr}\underline{\underline{\boldsymbol{\pi}}})$ denotes hydrostatic pressure and dV represents the volume of mass element $\mathfrak{P}$ whose gauge volume is dV_0. In most cases, Bridgman had only to fit his data with a quadratic polynomial in order to obtain a quality approximation to the data. In all cases, a linear fit was inadequate.

Hencky [50] derived a governing equation for pressure from thermodynamics (viz., $\frac{\varrho_0}{\varrho}\,p = -\varrho_0\,\partial W/\partial\Delta$), and then proceeded to propose two constitutive equations, the

simpler being

$$\tfrac{\varrho_0}{\varrho}\, p = -\kappa\, \Delta, \tag{7.2}$$

wherein κ (> 0) is the bulk modulus, p is the hydrostatic pressure, and Δ is his measure for dilatation. We point out that $\frac{\varrho_0}{\varrho} = e^{\Delta}$ from the conservation of mass. Equation (7.2) is linear; it is Hencky's definition for dilatation that is non-linear. This is a good example of what we are striving to achieve in this document: simple constitutive relations whose complexity (non-linearity) lies within the definitions of the fields themselves.

Hencky's constitutive equation has a strain-energy density of

$$\begin{aligned} \mathfrak{W} &= \frac{\kappa}{2\varrho_0}\Big(\ln\sqrt{\det\big(\underline{\underline{\gamma}}_0^{-1}\cdot\underline{\underline{\gamma}}\big)}\Big)^2 \\ &\equiv \frac{\kappa}{2\varrho_0}\Big(\ln\big(\det\underline{\underline{F}}\big)\Big)^2 \\ &= \frac{\kappa}{2\varrho_0}\,\Delta^2, \end{aligned} \tag{7.3}$$

which is quadratic in structure, like the strain-energy density from classic elasticity. Substituting (7.3) into (5.3)*, and taking its trace, reproduces Hencky's constitutive equation of (7.2).

Expanding Hencky's constitutive formula (7.2) for pressure as a power series in the measure of dilatation used in infinitesimal strain analysis (i.e., in terms of δ) gives

$$p/\kappa = -\delta + \tfrac{3}{2}\delta^2 - \tfrac{11}{6}\delta^3 + \tfrac{25}{12}\delta^4 - \tfrac{137}{60}\delta^5 + O\big(\delta^6\big). \tag{7.4a}$$

The inverted form of this series is

$$\delta = -p/\kappa + \tfrac{3}{2}(p/\kappa)^2 - \tfrac{8}{3}(p/\kappa)^3 + O\big((p/\kappa)^4\big), \tag{7.4b}$$

which allows Hencky's formula to be expressed in the format of Bridgman's polynomial (7.1), where coefficients b and c can now be expressed in terms of constant a after an assignment of $\kappa := 1/a$. A tabulation of such comparisons is provided in Table 7.1, where perfect fits have reported ratios of one. Over half of these comparison ratios are within a factor of two (i.e., between $1/2$ and 2) which, given the fact that these are coefficients to second- and third-order terms in p/κ, is remarkable testimony as to the accuracy of Hencky's simple formula for describing the bulk, elastic, material response. Not one of these ratios has a negative value; hence, the predicted and observed curvatures in these pressure-volume plots are in agreement.

The values that Bridgman [11] measured for bulk moduli in 1923, and which are reported in Table 7.1, are about five to ten percent larger, on average, than their accepted values of today (see, e.g., `http://www.webelements.com`). Unavoidable

*This derivation makes use of the following properties of determinants:

$$\frac{\partial|\underline{\underline{\gamma}}|}{\partial\underline{\underline{\gamma}}} = |\underline{\underline{\gamma}}|\,\underline{\underline{\gamma}}^{-1} \quad \text{and} \quad |\underline{\underline{\gamma}}_0^{-1}\cdot\underline{\underline{\gamma}}| = |\underline{\underline{\gamma}}_0^{-1}|\,|\underline{\underline{\gamma}}| = \frac{|\underline{\underline{\gamma}}|}{|\underline{\underline{\gamma}}_0|}.$$

Metal	Name	Atomic Number	Bulk Modulus κ (GPa)	2nd order $b/\left(3/(2\kappa^2)\right)$	3rd order $c/\left(8/(3\kappa^3)\right)$
Li	Lithium	3	12	0.86	—
Na	Sodium	11	6.5	0.82	16
Mg	Magnesium	12	34	1.5	—
Al	Aluminum	13	78	1.3	—
K	Potassium	19	2.9	1.5	1.7
Ca	Calcium	20	17	0.92	—
Fe	Iron	26	180	4.1	—
Co	Cobalt	27	200	4.8	—
Ni	Nickel	28	190	5.1	—
Cu	Copper	29	150	3.4	—
Ge	Germanium	32	82	2.4	—
Sr	Strontium	38	12	0.72	—
Mo	Molybdenum	42	280	6.6	—
Pd	Palladium	46	200	5.2	—
Ag	Silver	47	110	3.0	—
Cd	Cadmium	48	52–72	2.5	—
Sn	Tin	50	60	1.7	—
Sb	Antimony	51	42	1.9	—
Ce	Cerium	58	29	0.99	—
Ta	Tantalum	73	210	0.73	—
W	Tungsten	74	330	12	—
Pt	Platinum	78	290	9.3	—
Au	Gold	79	180	4.1	—
Pb	Lead	82	43	2.0	—
Bi	Bismuth	83	36	1.5	—
U	Uranium	92	110	1.8	—

Table 7.1: Bulk moduli, as reported by Bridgman [11], and ratios of Bridgman's higher-order coefficients (7.1) to those predicted by Hencky's formula (7.2).

frictional forces that were likely present in his testing apparatus, and which he could not measure, are the probable cause of these errors. This does not in any way belittle his experimental results, nor diminish the significance of his findings. After all, twenty-three years after publishing Ref. [11], Bridgman was awarded the Nobel prize in physics for the invention of his testing apparatus and for the discoveries he made therewith.

We can conclude from the comparisons presented in Table 7.1 that Hencky's formula (7.2) is a viable material model for representing bulk material behavior to extremely large states of pressure. Because most engineering applications do not experience such enormous volume changes, it is reasonable to consider an approximation of the above construction.

7.1.1 Theory for pressure

Taking the trace of (5.16a), which is our phenomenological theory for isotropic elasticity, produces the following constitutive equation for hydrostatic pressure,

$$\tfrac{\varrho_0}{\varrho}\, p = \tfrac{-2}{3}\varrho_0\Big(\mathfrak{W}_{,1}\,\mathrm{tr}\,\underline{\underline{E}}^{(1)} + \mathfrak{W}_{,2}\,\mathrm{tr}\,\underline{\underline{E}}^{(2)} + 3\,\mathfrak{W}_{,3}\,e\Big). \tag{7.5a}$$

For materials whose bulk moduli are many times larger than their shear moduli, like those we are interested in, this expression simplifies to

$$\tfrac{\varrho_0}{\varrho}\, p \approx -\kappa\, e \quad \text{given that} \quad \mathfrak{W}_{,3} = \kappa/2\varrho_0, \tag{7.5b}$$

which is a quadratic approximation to Hencky's constitutive equation (7.2). Figure 7.1 demonstrates that $\frac{1}{2}(\det\underline{\underline{F}} - \det\underline{\underline{F}}^{-1}) \simeq \ln\det\underline{\underline{F}}$ over the interval $1/2 < \det\underline{\underline{F}} < 3/2$. This is a huge range for volume change from a practical point of view, recalling that $\det\underline{\underline{F}} = dV/dV_0$, and as such, the constitutive formulæ of (7.5b) and (7.2) are essentially equivalent in the realm of present-day engineering applications.

From the conservation of mass, the dilational strain measure of (7.5b) can be expressed as

$$\begin{aligned} e = \tfrac{1}{2}\big(\det\underline{\underline{F}} - \det\underline{\underline{F}}^{-1}\big) &= \frac{1}{2}\left(\frac{dV}{dV_0} - \frac{dV_0}{dV}\right) \\ &= \frac{\big(dV - dV_0\big)}{dV_0}\,\frac{\big(dV + dV_0\big)}{2\,dV} \\ &\approx \frac{dV - dV_0}{dV_0} \quad \text{whenever} \quad dV \sim dV_0, \end{aligned} \tag{7.6}$$

so that for infinitesimal volume changes

$$\tfrac{\varrho_0}{\varrho}\, p = -\kappa\,\frac{dV - dV_0}{dV_0} \quad \text{or equivalently} \quad p = -\kappa\,\frac{dV - dV_0}{dV}, \tag{7.7}$$

which is in agreement with the classical theory of elasticity.

There will be instances when non-elastic aspects of a pressure/dilatation response need consideration (e.g., in capillary flows of viscoelastic liquids [64]) but, for most applications, the assumption of an elastic bulk response will be adequate whenever compressiblity effects need to be addressed.

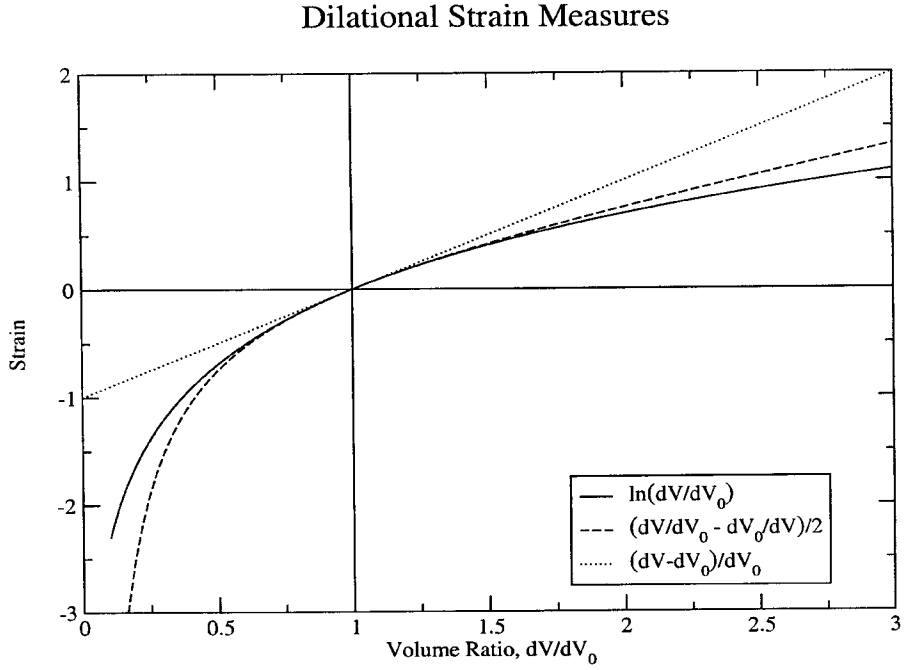

Figure 7.1: Comparison of strain measures used to represent dilatation in constitutive equations for hydrostatic pressure: Hencky's theory (7.2), our theory (7.5b), and linear elasticity.

7.2 Viscoelastic Response

Because pressure does not relax to zero at a fixed dilation, even in infinite time, fluids and solids both behave like solids in their bulk response. In what follows, we seek a solid-like representation within the constructs of Boltzmann's [9] linear theory of viscoelasticity.

Rewriting Hencky's strain-energy density (7.3) as

$$\mathfrak{W} = \frac{\kappa}{4\varrho_0}\left(\ln\sqrt{\det\left(\underline{\underline{\gamma}}_{t'}^{-1}\cdot\underline{\underline{\gamma}}\right)}\right)^2, \tag{7.8}$$

substituting it into (5.4), and then taking its trace, leads to

$$\tfrac{\varrho_0}{\varrho}\,p = -\kappa\left(\mathfrak{G}(t)\,\Delta(0,t) + \int_0^t \mathfrak{M}(t-t')\,\Delta(t',t)\,dt'\right), \tag{7.9a}$$

where $\mathfrak{G}(t-t')$ and $\mathfrak{M}(t-t') := \partial\mathfrak{G}(t-t')/\partial t'$ are the bulk relaxation and memory functions, respectively, which are material properties to be acquired from experimental data, and where Δ is Hencky's definition (3.15) for dilatation. By envoking the additive and anti-symmetric property $\Delta(a,c) = \Delta(a,b) + \Delta(b,c)$, $\forall\ b \in [a,c]$, which applies to this strain definition, the above formula can also be expressed as

$$\tfrac{\varrho_0}{\varrho}\,p = -\kappa\left(\mathfrak{G}(0)\,\Delta(0,t) - \int_0^t \mathfrak{M}(t-t')\,\Delta(0,t')\,dt'\right), \tag{7.9b}$$

that after an integration by parts becomes

$$\tfrac{\varrho_0}{\varrho}\, p = -\kappa\Big(\mathfrak{G}(t)\, \Delta(0,0^+) + \int_{0^+}^{t} \mathfrak{G}(t-t')\, D\Delta(t')\, dt' \Big). \tag{7.9c}$$

All three formulæ in (7.9) are mathematically equivalent. The first two expressions require dilatation to be continuous in time (i.e., $\Delta \in C^0$), while the third expression is more restrictive in that it requires dilatation to be both continuous and differentiable in time (viz., $\Delta \in C^1$).

It is also possible to construct a viscoelastic theory where dilatation is given in terms of pressure, but in our end application (finite elements), displacements are assigned to which forces respond, thereby placing (7.9) in the desired format.

The above constitutive theory is, in and of itself, too general. To have engineering utility, one needs to assign appropriate functional forms to $\mathfrak{G}$ and $\mathfrak{M}$ (i.e., one needs to create a model). There are a variety of ways that this can be done. One approach is to convert a known differential equation into the format of (7.9), which can always be done through, for example, an application of Laplace transform techniques, provided that the differential equation is linear. As an outcome of this procedure, the bulk relaxation and memory functions can be determined for that particular differential equation.

7.2.1 Voigt solid

The simplest viscoelastic solid of the differential type that one can consider is the Voigt solid,

$$\tfrac{\varrho_0}{\varrho}\, p(t) = -\kappa\big(1 + \bar{\rho}\, D\big)\Delta(t), \tag{7.10a}$$

satisfying a homogeneous initial condition. The two material constants in the model are κ and $\bar{\rho}$. A bar is placed over the viscoelastic material constant to designate that it is associated with bulk deformation. The Voigt solid has a relaxation function given by

$$\mathfrak{G}(t-t') = \big(1 + \bar{\rho}\big)\delta(t-t'), \tag{7.10b}$$

where δ is the Dirac delta distribution (function). Consequently, its memory function, $\mathfrak{M}(t-t') = \partial\mathfrak{G}(t-t')/\partial t'$, is undefined.

The Voigt solid is therefore dismissed on physical grounds. It predicts that sound waves travel with infinite speed. For this reason, if this constitutive equation is to be used, the constraint of a homogeneous initial condition must be adhered to. Beware, this material model can cause instabilities to arise that are artifacts of the model. These are not physical instabilities; rather, they are numeric instabilities.

7.2.2 Kelvin solid

The next simplest material model that can be used to describe bulk viscoelatic behavior is the Kelvin (or standard viscoelastic) solid,

$$\big(1 + \bar{\tau}\, D\big)\big(\tfrac{\varrho_0}{\varrho}\, p\big)(t) = -\kappa\big(1 + \bar{\rho}\, D\big)\Delta(t), \quad \tfrac{\varrho_0}{\varrho_{0^+}}\, p_{0^+} = -\kappa\, \frac{\bar{\rho}}{\bar{\tau}}\, \Delta_{0^+}, \tag{7.11a}$$

which can handle an inhomogeneous initial condition, and therefore predicts a finite speed for sound. The bulk relaxation function is determined to be

$$\mathfrak{G}(t-t') = 1 + \frac{\bar{\rho}-\bar{\tau}}{\bar{\tau}} \exp\bigl(-(t-t')/\bar{\tau}\bigr), \quad 1 \leq \mathfrak{G}(t-t') \leq \frac{\bar{\rho}}{\bar{\tau}}, \tag{7.11b}$$

which has an associated memory function of

$$\mathfrak{M}(t-t') = \frac{\bar{\rho}-\bar{\tau}}{\bar{\tau}^2} \exp\bigl(-(t-t')/\bar{\tau}\bigr), \quad 0 \leq \mathfrak{M}(t-t') \leq \frac{\bar{\rho}-\bar{\tau}}{\bar{\tau}^2}. \tag{7.11c}$$

Both material functions are monotonic and bounded on the positive real line whenever $t \geq 0$, $t' \in [0,t]$, and $\bar{\rho} > \bar{\tau} > 0$. Here κ (> 0) denotes the rubbery (quasi-static) bulk modulus; $\kappa(\bar{\rho}/\bar{\tau})$ $(> \kappa)$ represents the glassy (dynamic) bulk modulus; $\bar{\tau}$ (> 0) is the characteristic, bulk, relaxation time; and $\bar{\rho}$ $(> \bar{\tau})$ is the characteristic, bulk, retardation (or creep) time.

The differential equation in (7.11a) and the integral equations of (7.9) with material functions (7.11b & 7.11c) are equivalent formulations. Whether one chooses the differential or integral form of a particular model for use in analysis is largely a matter of personal taste that may be swayed by factors like: the boundary-value problem being solved, and the solution (e.g., numerical) methods available for solving it.

The limited data that are available for characterizing bulk viscoelasticity suggest that the bulk response of a material is not as viscoelastic as its shear response. For example, the bulk viscoelastic response of polyisobutylene [77] has a ratio for $\bar{\rho}/\bar{\tau}$ (i.e., the ratio of dynamic to quasi-static moduli) that is less than 10; whereas, for the same material, the shear response has a ratio of dynamic to quasi-static moduli (e.g., ρ/τ) that exceeds 10^4 [33].

For this material model, sound is predicted to travel at a speed of $v_s = \sqrt{\kappa\bar{\rho}/\bar{\tau}\varrho}$ (with ϱ denoting mass density). This is a direct consequence of the fact that there exists a finite, inhomogeneous, elastic, initial condition whose effective (i.e., dynamic) bulk modulus happens to be $\kappa(\bar{\rho}/\bar{\tau})$. Measuring both v_s and ϱ is therefore a viable way for experimentally evaluating the dynamic bulk modulus, $\kappa(\bar{\rho}/\bar{\tau})$, in isotropic compressible materials. The static bulk modulus, κ, can be obtained from a dilational compression test, like what Bridgman used. The time constants $\bar{\rho}$ and $\bar{\tau}$ can then be extracted from their ratio $\bar{\rho}/\bar{\tau}$ by performing, for example, an additional stress relaxation experiment in dilational compression using the same compression fixture used previously to establish κ.

Measuring wave speeds to quantify the dynamic bulk modulus works well for fluids, where there is typically one type of wave present. However, additional care is warrented when this approach is applied to solids, because solids propagate two types of waves: logitudinal (bulk) and transverse (shear).

7.2.3 Fractional-order models

It is a straightforward matter to extend (7.10 & 7.11) to fractional order. The greater flexibility afforded by fractional models over their classical counterparts, when it comes time to correlate with experimental data, is justification enough for us to consider such extensions.

Fractional Voigt solid

The simplest fractional-order viscoelastic solid that one can consider is the fractional Voigt solid introduced by Caputo [12] which, for dilatation, takes on the form

$$\tfrac{\varrho_0}{\varrho}\, p(t) = -\kappa\big(1 + \bar{\rho}^{\bar{\alpha}} D_\star^{\bar{\alpha}}\big)\Delta(t), \tag{7.12a}$$

and satisfies a homogeneous initial condition. This model has an additional constant $\bar{\alpha}$ that controls the rate of evolution. Equation (7.12a) has a relaxation function of

$$\mathfrak{G}(t-t') = 1 + \bar{\rho}^{\bar{\alpha}}\, \frac{1}{\Gamma(1-\bar{\alpha})}\, \frac{1}{(t-t')^{\bar{\alpha}}}, \tag{7.12b}$$

that can be extracted directly from the definition of Caputo's derivative (1.8a). When differentiated, the memory function is found to be

$$\mathfrak{M}(t-t') = \bar{\rho}^{\bar{\alpha}}\, \frac{\bar{\alpha}}{\Gamma(1-\bar{\alpha})}\, \frac{1}{(t-t')^{1+\bar{\alpha}}}. \tag{7.12c}$$

Material function $\mathfrak{G}$ is weakly singular at the upper limit of integration where $t' = t$, while $\mathfrak{M}$ is strongly singular.

The fractional Voigt solid is also dismissed on physical grounds, because it too propagates a sound wave with infinite speed due to the weak singularity present in the relaxation function.

Fractional Kelvin solid

The simplest, fractional-order, differential equation that is physically admissible for representing a viscoelastic solid is the standard FOV solid of (2.2) introduced by Caputo and Mainardi [13] which, as it applies to bulk response, is given by

$$\big(1 + \bar{\tau}^{\bar{\alpha}} D_\star^{\bar{\alpha}}\big)\big(\tfrac{\varrho_0}{\varrho}\, p\big)(t) = -\kappa\big(1 + \bar{\rho}^{\bar{\alpha}} D_\star^{\bar{\alpha}}\big)\Delta(t), \quad \tfrac{\varrho_0}{\varrho_{0+}}\, p_{0+} = -\kappa \left(\frac{\bar{\rho}}{\bar{\tau}}\right)^{\bar{\alpha}} \Delta_{0+}, \tag{7.13a}$$

and it can satisfy an inhomogeneous initial condition. This model has a bulk relaxation function of [75]

$$\mathfrak{G}(t-t') = 1 + \frac{\bar{\rho}^{\bar{\alpha}} - \bar{\tau}^{\bar{\alpha}}}{\bar{\tau}^{\bar{\alpha}}}\, E_{\bar{\alpha}}\Big(-\big((t-t')/\bar{\tau}\big)^{\bar{\alpha}}\Big), \quad 1 \le \mathfrak{G}(t-t') \le \left(\frac{\bar{\rho}}{\bar{\tau}}\right)^{\bar{\alpha}}, \tag{7.13b}$$

obtained by taking the Laplace transform of (7.13a). Equation (7.13b) is a dimensionless version of (2.5), which is the relaxation modulus for an FOV solid. Associated with $\mathfrak{G}$ is the memory function $\mathfrak{M}$, which is computed to be[†]

$$\mathfrak{M}(t-t') = -\frac{\bar{\rho}^{\bar{\alpha}} - \bar{\tau}^{\bar{\alpha}}}{\bar{\tau}^{\bar{\alpha}}}\, \frac{E_{\bar{\alpha},0}\Big(-\big((t-t')/\bar{\tau}\big)^{\bar{\alpha}}\Big)}{t-t'}, \quad 0 \le \mathfrak{M}(t-t') \le \infty. \tag{7.13c}$$

[†]Confer with Mainardi and Gorenflo [76] or Podlubny [86, pp. 21–22], for example, for a listing of derivatives and other useful properties of the Mittag-Leffler function.

Like (7.11b & 7.11c), (7.13b & 7.13c) are both positive monotone-decreasing functions provided that $t \geq 0$, $t' \in [0,t]$, $\bar{\rho} > \bar{\tau} > 0$, and $0 < \bar{\alpha} \leq 1$; however, because $-E_{\bar{\alpha},0}\big(-((t-t')/\bar{\tau})^{\bar{\alpha}}\big)/(t-t') \asymp (t-t')^{\bar{\alpha}-1}$ as $t' \to t$, it is apparent that this memory function becomes unbounded at time t exhibiting a weak singularity. Here $E_\alpha(x) \equiv E_{\alpha,1}(x)$ is the Mittag-Leffler function in one parameter, α, which reduces to the exponential function e^x whenever $\alpha = 1$, while $E_{\alpha,\beta}(x)$ is the Mittag-Leffler function in two parameters, α and β, (cf. §1.5). Again, κ (> 0) is the rubbery bulk modulus; now $\kappa(\bar{\rho}/\bar{\tau})^{\bar{\alpha}}$ $(> \kappa)$ represents the glassy bulk modulus; parameters $\bar{\tau}$ and $\bar{\rho}$ are still the characteristic, bulk, relaxation and retardation times, respectively; and $\bar{\alpha}$ is a new material constant accounting for the fractal order of evolution. Their values can be extracted from the same set of experiments used to quantify the constants of (7.11).

Experimental data [103] suggests that the bulk time constants $\bar{\tau}$ and $\bar{\rho}$ are much smaller than their counterparts τ and ρ for shear (bulk transients fade faster), and that the fractal order for bulk evolution $\bar{\alpha}$ is smaller than the fractal order for shear evolution α (bulk behavior is less rate sensitive), both being bound to the interval $(0, 1]$. In other words, the bulk response tends to be more solid-like, while the shear response is more fluid-like.

Surface plots of $y = E_{\alpha,1}(-x^\alpha)$ and $y = -E_{\alpha,0}(-x^\alpha)/x$, which are representative of $\mathfrak{G}$ and $\mathfrak{M}$ in (7.13), respectively, are presented in Figs. 7.2 & 7.3. In both plots $0.001 \leq \alpha \leq 1$, while $0 \leq x$ in the first plot and $0.001 \leq x$ in the second plot. Figure 7.2 is characteristic of stress-relaxation curves, while Fig. 7.3 is indicative of the extent of remembrance of past events. These plots clearly illustrate the influence that the fractal order of evolution, α, has on the (material) response function, y.

When α is very small, but still greater than zero, the normalized relaxation function $y = E_\alpha(-x^\alpha)$ of Fig. 7.2 drops immediately from a value of $y = 1$ at $x = 0$ to a value of $y \approx 1/2$ at $x = 0^+$, from which it slowly asymptotes to zero as x goes to infinity. Strictly speaking, the Mittag-Leffler function is not defined for $\alpha = 0$. This would be the elastic boundary where, if the Mittag-Leffer function were defined, it would have to exhibit a discontinuous jump so that at $\alpha = 0$ the response would be $y = 1$ for all $x \geq 0$ (i.e., there can be no relaxation in the elastic limit). At the other boundary of $\alpha = 1$, relaxation is smooth and occurs at an exponential rate (viz., $E_1(-x^1) \equiv e^{-x}$). For all values of α that lie inbetween, the Mittag-Leffler function provides a smooth monotone transition from elastic to nearly classic viscoelastic.

Examining the normalized memory function $y = -E_{\alpha,0}(-x^\alpha)/x$ of Fig. 7.3, when α is very small but still greater than zero, the response y is observed to behave like an impulse function indicating that the material has a perfect knownledge of the current state, but it has almost no recollection of even the most recent of past states. As α grows toward a value of unity, the memory function continues to maintain a nearly perfect knowledge of the current state (i.e., y is infinite at $x = 0$, but the strength of this singularity diminishes as α moves toward one), and to this, it adds some recollection of past events—albeit a memory that rapidly fades away with the passing of time. At the upper boundary of $\alpha = 1$, memory is lost at an exponential rate which, cureously, is the slowest rate of memory loss over the interval $0 < \alpha \leq 1$. Because $y = \infty$ at $x = 0$ for $0 < \alpha < 1$, this kernel (7.13c) representing the memory function $\mathfrak{M}$ of the bulk constitutive equation (7.9) produces an integral that has a

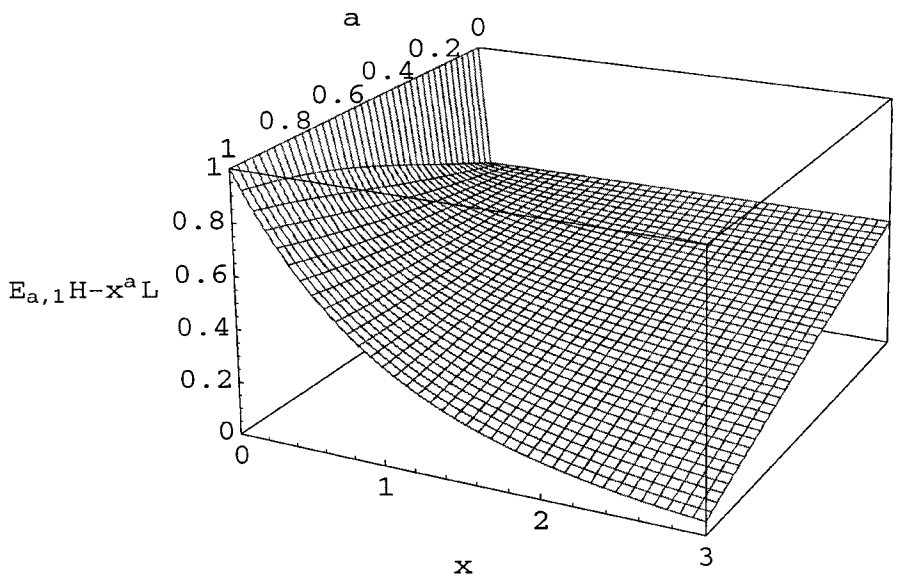

Figure 7.2: A 3D surface plot of $y = E_{\alpha,1}(-x^\alpha)$, which appears in the relaxation function $\mathfrak{G}$ of the standard FOV solid.

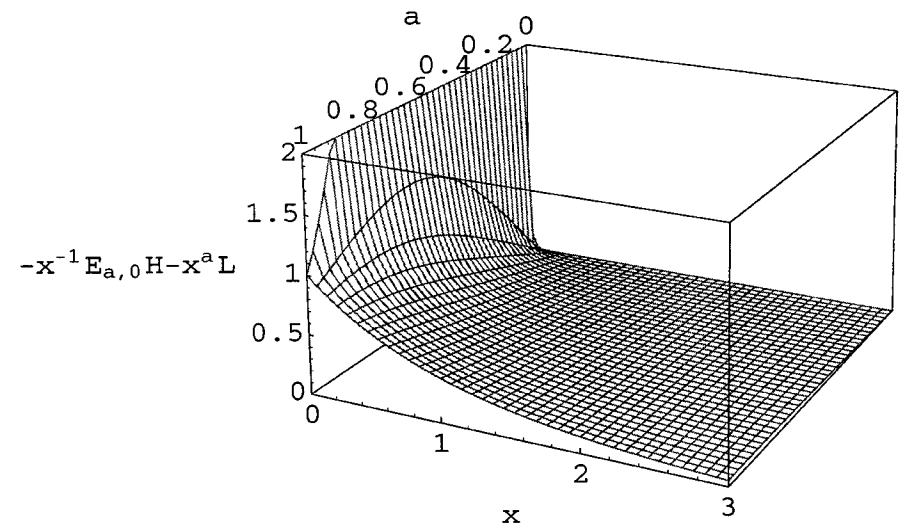

Figure 7.3: A 3D surface plot of $y = -E_{\alpha,0}(-x^\alpha)/x$, which appears in the memory function $\mathfrak{M}$ of the standard FOV solid.

weak singularity at the upper limit of integration, like the fractional derivative (cf. Eqn. 1.8a).

Choosing the integral equation of (7.9) (with the bulk relaxation and memory functions being given by Eqns. 7.13b & 7.13c) over its equivalent, fractional, differential equation (7.13a) has an advantage of disguising the fractal nature of the constitutive equation. However, selecting $\mathfrak{G}$ (7.13b) and $\mathfrak{M}$ (7.13c) without a priori knowledge of the fractional differential equation (7.13a) would be unlikely, at least they have not appeared in the literature as such.[‡] For this reason, our preferred method for constitutive construction is to begin with a fractional differential equation, ensuring that it possesses physically meaningful initial conditions, and to then convert it into an equivalent integral expression (i.e., to solve the differential equation).

Furthermore, using the integral formulation of (7.9a) with memory function $\mathfrak{M}$ as the kernel of integraion, instead of employing its variant (7.9c) that uses the relaxation function $\mathfrak{G}$ as its kernel, leads to a convolution integral whose recollection of past events fades much more rapidly, and as such, should be better suited for numerical analysis.

Alternate model: The viscoelastic models presented in (7.9–7.13) are all based on Hencky's definition for dilatation, $\Delta = \ln\det\underline{\underline{F}}$, defined in (4.38). In contrast, our viscoelastic theory (5.20) introduces a dilational strain measure defined by $e = \frac{1}{2}\big(\det\underline{\underline{F}} - \det\underline{\underline{F}}^{-1}\big)$, as established in (5.15b), which is a second-order accurate approximate to Hencky dilatation. In fact, whenever the bulk modulus is much stiffer than the shear modulus for a given material, the trace of (5.20a) produces a hydrostatic pressure response of

$$\tfrac{\varrho_0}{\varrho}\,p = -\kappa\left(\mathfrak{G}_3(t)\,e(0,t) + \int_0^t \mathfrak{M}_3(t-t')\,e(t',t)\,dt'\right) \quad \text{when} \quad \mathfrak{M}_{,3} = \frac{\kappa}{2\varrho_0}, \tag{7.14a}$$

wherein

$$e(t',t) = \frac{1}{2}\left(\frac{\det\underline{\underline{F}}}{\det\underline{\underline{F}}_{t'}} - \frac{\det\underline{\underline{F}}_{t'}}{\det\underline{\underline{F}}}\right),$$

with $\underline{\underline{F}} = \underline{\underline{F}}(0,t)$ and $\underline{\underline{F}}_{t'} = \underline{\underline{F}}(0,t')$. Assigning to this constitutive equation the following material functions

$$\mathfrak{G}_3(t-t') = 1 + \beta_3\,E_{\alpha_3}\Big(-\big((t-t')/\tau_3\big)^{\alpha_3}\Big), \tag{7.14b}$$

and

$$\mathfrak{M}_3(t-t') = -\beta_3\,\frac{E_{\alpha_3,0}\Big(-\big((t-t')/\tau_3\big)^{\alpha_3}\Big)}{t-t'}, \tag{7.14c}$$

[‡]This is the first appearance of a memory function that is representative of a fractional-order viscoelastic model. Relaxation functions representative of fractional-order viscoelastic models have been in the literature since Caputo's [12] and Mainardi's [13] pioneering papers, but they have not appeared (e.g., phenomenologically) in the general viscoelastic literature, excluding that subset of papers which makes use of the fractional calculus.

results in an admissible material model for bulk viscoelasticity with constants α_3, β_3 and τ_3. This is the bulk, viscoelastic, material model that we advocate using.

It is easily verified that $e(a,c) \neq e(a,b) + e(b,c)$ for any $b \in (a,c)$; in words, dilatation e is not additive and anti-symmetric in its dependency upon state. This means that (7.14a) and

$$\tfrac{\varrho_0}{\varrho}\, p = -\kappa\left(\mathfrak{G}_3(t)\, e(0,0^+) + \int_{0^+}^{t} \mathfrak{G}_3(t-t')\, \frac{\partial e(0,t')}{\partial t'}\, dt' \right) \tag{7.15a}$$

are not equivalent constitutive formulæ; (7.14a & 7.15a) are distinct. However, the integral equation in (7.15a), employing the material functions of (7.14b & 7.14c), and the fractional differential equation

$$\big(1+\tau_3^{\alpha_3} D_\star^{\alpha_3}\big)\big(\tfrac{\varrho_0}{\varrho}\, p\big)(t) = -\kappa\big(1+\rho_3^{\alpha_3} D_\star^{\alpha_3}\big) e(0,t), \quad \tfrac{\varrho_0}{\varrho_{0^+}}\, p_{0^+} = -\kappa \left(\frac{\rho_3}{\tau_3}\right)^{\alpha_3} e(0,0^+), \tag{7.15b}$$

are equivalent formulæ upon setting $\beta_3 = \big((\rho_3-\tau_3)/\tau_3\big)^{\alpha_3}$. Consequently, the integral form of our viscoelastic model for bulk response (7.14) and the fractional differential equation (7.15b) are different material models, which is why we introduced constant β_3 in place of (but not equivalent to) ρ_3. To what extent and under what conditions they do differ remains to be determined.

7.3 Bridgman's Experiment

Dilational compression is described by the boundary-value problem of (6.32). The state of stress given in (6.32) becomes hydrostatic (i.e., $\sigma = \varsigma = f/A_0$, wherein f is the force applied over an area of A_0) whenever shear effects can be neglected (e.g., the bulk modulus is significantly larger than the shear modulus).

Under these conditions, and when expressed in terms of the parameters measured in an actual experiment, the elastic constitutive equation (7.5b) becomes

$$\lambda \frac{f}{A_0} = -\kappa\, \tfrac{1}{2}\big(\lambda - \lambda^{-1}\big), \tag{7.16}$$

where stretch λ ratios the current specimen length ℓ to its gauge length ℓ_0. This is a material model in one constant—the bulk modulus κ.

Likewise, the viscoelastic constitutive equation (7.14a) is given by

$$\lambda \frac{f}{A_0} = -\kappa \left(\mathfrak{G}_3(t)\, \tfrac{1}{2}\big(\lambda - \lambda^{-1}\big) + \int_0^t \mathfrak{M}_3(t-t')\, \frac{1}{2}\left(\frac{\lambda}{\lambda_{t'}} - \frac{\lambda_{t'}}{\lambda} \right) dt' \right), \tag{7.17}$$

where $\lambda = \ell(t)/\ell_0$ and $\lambda_{t'} = \ell(t')/\ell_0$ are the stretch ratios, and where the material functions $\mathfrak{G}_3$ and $\mathfrak{M}_3$ are given by (7.14b & 7.14c), respectively. This model has four material constants: κ, α_3, β_3 and τ_3.

Appendix A

Table of Caputo Derivatives

For the convenience of the reader, we provide this appendix where we give some Caputo-type derivatives of certain important functions.* We do not strive for completeness in any sense, but we do want to give at least the derivatives of the classical examples.

Throughout this appendix, α will always denote the order of the Caputo-type differential operator under consideration. We shall only consider the case $\alpha > 0$ and $\alpha \notin \mathbb{N}$, where $\mathbb{N} := \{1, 2, 3, \ldots\}$ while $\mathbb{N}_0 := \{0, 1, 2, \ldots\}$. We use the ceiling function $\lceil \alpha \rceil$ to denote the smallest integer greater than (or equal to) α, and the floor function $\lfloor \alpha \rfloor$ $(= \lceil \alpha \rceil - 1)$ to denote the largest integer (strictly) less than α. Recall that for $\alpha \in \mathbb{N}$, the Caputo differential operator coincides with the usual differential operator of integer order.

Moreover, $E_{\nu,\mu}$ denotes the Mittag-Leffler function of the two parameters μ and $\nu > 0$, given by (cf. [31, Chp. 18])

$$E_{\nu,\mu}(t) = \sum_{k=0}^{\infty} \frac{t^k}{\Gamma(\nu k + \mu)},$$

ψ is the Digamma function, given by

$$\psi(x) = \frac{\Gamma'(x)}{\Gamma(x)}.$$

${}_1F_1$ and ${}_2F_1$ denote the usual hypergeometric functions, i.e.,

$${}_1F_1(a; b; z) = \frac{\Gamma(b)}{\Gamma(a)} \sum_{k=0}^{\infty} \frac{\Gamma(a+k)}{\Gamma(b+k)k!} z^k, \qquad a \in \mathbb{R}, \quad -b \notin \mathbb{N}_0,$$

(sometimes called the Kummer confluent hypergeometric function [1, Chp. 13]), the power series being convergent for arbitrary complex z, and

$${}_2F_1(a, b; c; z) = \frac{\Gamma(c)}{\Gamma(a)\Gamma(b)} \sum_{k=0}^{\infty} \frac{\Gamma(a+k)\Gamma(b+k)}{\Gamma(c+k)k!} z^k, \qquad a, b \in \mathbb{R}, \quad -c \notin \mathbb{N}_0,$$

*Tables of Riemann-Liouville integrals and derivatives can be found in various places in the literature (cf. e.g., Podlubny [86] or Samko et al. [102]). We do not repeat those results here.

(the Gauss hypergeometric function [1, Chp. 15]), in which case the power series converges for all complex z with $|z| < 1$ and may be extended analytically into the entire complex plane with a branch cut along the positive real axis from $+1$ to $+\infty$. (Note that in the formulæ below, we only need to evaluate this function for negative values of z, so the branch cut for positive z gives no problems.) Finally, $i = \sqrt{-1}$ is the imaginary unit.

1. Let $f(x) = x^j$. Here we have to distinguish some cases:

$$(D_\star^\alpha f)(x) = \begin{cases} 0 \text{ if } j \in \mathbb{N}_0 \text{ and } j < \lceil\alpha\rceil, \\ \dfrac{\Gamma(j+1)}{\Gamma(j+1-\alpha)} x^{j-\alpha} \text{ if } j \in \mathbb{N}_0 \text{ and } j \geq \lceil\alpha\rceil \\ \qquad\qquad \text{or } j \notin \mathbb{N} \text{ and } j > \lfloor\alpha\rfloor. \end{cases}$$

2. Let $f(x) = (x+c)^j$ for arbitrary $c > 0$ and $j \in \mathbb{R}$. Then

$$(D_\star^\alpha f)(x) = \frac{\Gamma(j+1)}{\Gamma(j-\lfloor\alpha\rfloor)} \frac{c^{j-\lceil\alpha\rceil-1}}{\Gamma(\lceil\alpha\rceil-\alpha+1)} x^{\lceil\alpha\rceil-\alpha} {}_2F_1(1, \lceil\alpha\rceil - j; \lceil\alpha\rceil - \alpha + 1; -x/c).$$

3. Let $f(x) = x^j \ln x$ for some $j > \lfloor\alpha\rfloor$. Then

$$\begin{aligned} (D_\star^\alpha f)(x) &= \sum_{k=0}^{\lfloor\alpha\rfloor} (-1)^{\lceil\alpha\rceil-k+1} \binom{j}{k} \frac{\lceil\alpha\rceil!}{\lceil\alpha\rceil - k} \frac{\Gamma(j-\lfloor\alpha\rfloor)}{\Gamma(j-\alpha+1)} x^{j-\alpha} \\ &\quad + \frac{\Gamma(j+1)}{\Gamma(j-\alpha+1)} x^{k-\alpha} (\psi(j-\lfloor\alpha\rfloor) - \psi(j-\alpha+1) + \ln x). \end{aligned}$$

4. Let $f(x) = \exp(jx)$ for some $j \in \mathbb{R}$. Then

$$(D_\star^\alpha f)(x) = j^{\lceil\alpha\rceil} x^{\lceil\alpha\rceil-\alpha} E_{1,\lceil\alpha\rceil-\alpha+1}(jx).$$

5. Let $f(x) = \sin jx$ for some $j \in \mathbb{R}$. Here again we have two cases:

$$(D_\star^\alpha f)(x) = \begin{cases} -\dfrac{j^{\lceil\alpha\rceil} i (-1)^{\lceil\alpha\rceil/2} x^{\lceil\alpha\rceil-\alpha}}{2\Gamma(\lceil\alpha\rceil-\alpha+1)} [{}_1F_1(1; \lceil\alpha\rceil-\alpha+1; ijx) \\ \qquad\qquad - {}_1F_1(1; \lceil\alpha\rceil-\alpha+1; -ijx)] \text{ if } \lceil\alpha\rceil \text{ is even}, \\ \dfrac{j^{\lceil\alpha\rceil} (-1)^{\lfloor\alpha\rfloor/2} x^{\lceil\alpha\rceil-\alpha}}{2\Gamma(\lceil\alpha\rceil-\alpha+1)} [{}_1F_1(1; \lceil\alpha\rceil-\alpha+1; ijx) \\ \qquad\qquad + {}_1F_1(1; \lceil\alpha\rceil-\alpha+1; -ijx)] \text{ if } \lceil\alpha\rceil \text{ is odd}. \end{cases}$$

6. Finally we consider $f(x) = \cos jx$ with some $j \in \mathbb{R}$. As in the previous example, we obtain two cases:

$$(D_\star^\alpha f)(x) = \begin{cases} \dfrac{j^{\lceil\alpha\rceil} (-1)^{\lceil\alpha\rceil/2} x^{\lceil\alpha\rceil-\alpha}}{2\Gamma(\lceil\alpha\rceil-\alpha+1)} [{}_1F_1(1; \lceil\alpha\rceil-\alpha+1; ijx) \\ \qquad\qquad + {}_1F_1(1; \lceil\alpha\rceil-\alpha+1; -ijx)] \text{ if } \lceil\alpha\rceil \text{ is even}, \\ \dfrac{j^{\lceil\alpha\rceil} i (-1)^{\lfloor\alpha\rfloor/2} x^{\lceil\alpha\rceil-\alpha}}{2\Gamma(\lceil\alpha\rceil-\alpha+1)} [{}_1F_1(1; \lceil\alpha\rceil-\alpha+1; ijx) \\ \qquad\qquad - {}_1F_1(1; \lceil\alpha\rceil-\alpha+1; -ijx)] \text{ if } \lceil\alpha\rceil \text{ is odd}. \end{cases}$$

Appendix B

Automatic Integration

In §1.5.2 we had found the need to calculate two integrals numerically in order to complete the evaluation of the Mittag-Leffler function. In this appendix we outline a possible strategy for the solution of these integrals. Essentially we will follow the ideas explained in QUADPACK [84]. The routines introduced in that book are the generally accepted standard when looking for efficient and reliable quadrature algorithms. They are in the public domain, but they can also be found in many commercially distributed software packages. The source code is written in FORTRAN77 and may be obtained, for example, from the URL `http://www.netlib.org/quadpack`. For integrands of the form encountered in §1.5.2, it turns out that the routine DQAG (Double precision Quadrature, Adaptive, General purpose) is the method of choice. Our description of this routine follows a top-down structure (i.e., we first explain the general strategy without giving much information on the details, and at a later stage we fill in those details).

B.1 The Fundamental Strategy

The fundamental idea of automatic integration is the following. The user supplies the integrand function and the bounds for the interval of integration (i.e., the data that define the integral in question) and a desired accuracy (i.e., a bound for the relative or absolute error that he/she is willing to accept). The routine is then supposed to return either an approximation for the correct value of the integral that is sufficiently accurate to satify the user's requirements or an error flag if it fails to find such an approximation.

Typically the algorithms try to achieve this goal by sub-dividing the interval of integration in an adaptive way, thus concentrating more quadrature nodes in areas where the integrand is difficult to approximate. This leads to a structure indicated in Alg. B.1.

In practice, one may also terminate the WHILE loop in this algorithm when; for example, too many sub-divisions have taken place thereby using up all available memory, or too much computing time has been consumed. In such cases the algorithm should return an error flag.

Algorithm B.1 Automatic Integration

GIVEN two real numbers a and b, a function $f : [a, b] \to \mathbb{C}$,
and some tolerance $\epsilon > 0$ THEN
Calculate an approximation $Q[f]$ for $\int_a^b f(x)dx$ and an estimate $\hat{\epsilon}$ for the
error $\int_a^b f(x)dx - Q[f]$
Initialize a list L of the approximations obtained so far
by $L := \{([a, b], Q[f], \hat{\epsilon})\}$
WHILE error tolerance is not satified DO
Take the interval from L with the largest error estimate
and remove it from the list;
Bisect this interval;
Calculate approximations and error estimates for the two newly obtained
subintervals;
Add these subintervals, their corresponding approximations,
and their error estimates to the list L
END of while loop
RETURN the sum of the approximations obtained for all the intervals.

B.2 Approximation of the Integral

In Alg. B.1 we have left open some of the key details. Specifically, we have not said how the approximation of the integral itself will be performed, and we have not indicated how the required error estimates can be found. We now turn our attention to these two questions.

The basic idea behind the solution is the concept of Gauss-Kronrod integration. That is, we calculate two different approximations for the integral, both of which are of the form

$$\sum_{j=1}^{n} a_{j,n} f(x_{j,n}),$$

with suitably chosen values of n, $a_{j,n}$, and $x_{j,n}$ $(j = 1, \ldots, n)$. In particular, we begin with a first approximation that is just a Gauss quadrature formula with n_1 nodes, which is the (uniquely determined) quadrature formula that gives the exact value of the integral whenever the integrand is a polynomial of degree not exceeding $2n_1 - 1$. This formula has been thoroughly investigated. For a recent survey we refer to Ref. [10] and the references cited therein. Specifically, there is no quadrature formula with the same number of nodes that is exact for a larger class of polynomials. Moreover, as stated in [10], both theoretical and practical evidence suggest that this method is a very good one.

B.3 Approximation of Error Estimates

From rather general considerations, it is known that one, single, quadrature formula can only give an approximation, but not both an approximation and an error estimate.

Therefore, to derive also an error estimate, it is necessary to introduce a second quadrature formula. The heuristic argument is as follows. Assuming that the second quadrature formula is much more accurate than the first, then the difference between the two approximations will be a good approximation for the error of the cruder of the two approximations, and therefore, a rather conservative (and thus quite reliable) upper bound for the error of the finer of the two approximations. Hence, we need a second quadrature formula that is significantly better than the first (Gauss-type) formula. In view of the quality of the Gauss formula, this can only be achieved by selecting a formula with n_2 nodes, where $n_2 > n_1$. In principle, one could use a Gauss formula again, but this would be very uneconomical because a Gauss formula with n_1 nodes would have at most one node in common with a Gauss formula with n_2 nodes, and so almost none of the information gathered so far (i.e., the function values $f(x_{j,n_1})$, whose calculation is typically the most computationally expensive part of the algorithm) could be reused. To overcome this difficulty, Kronrod [59, 60] suggested to construct a formula that is nowadays called the Kronrod extension of the Gauss formula or, shortly, the Gauss-Kronrod formula. His formula is based on the Gauss formula with n_1 nodes; it uses $n_2 = 2n_1 + 1$ nodes and is constructed according to the following criteria:

- The n_1 nodes x_{j,n_1} of the Gauss method form a subset of the n_2 nodes x_{j,n_2} of the Gauss-Kronrod method.
- The remaining nodes and the weights a_{j,n_2} of the of the Gauss-Kronrod scheme are determined in such a way that the resulting method is exact for all polynomials of degree not exceeding $3n_1 + 1$.

A recent survey on Gauss-Kronrod formulas is given in [29].

Algorithms for the concrete calculation of the required nodes and weights are available (cf. the survey papers mentioned above and the references cited therein). For our purposes, it is sufficient to use the tabulated values given in [84]. In particular, following the suggestions made there, we propose using the Gaussian method with 15 points in combination with the 31-point Kronrod extension for computing the integral with function K mentioned in Alg. 1.4 (the monotonic part). In view of the nice smoothness properties of the integrand, this gives us an approximation with quite high accuracy without too much computational effort. For the other integral in that algorithm, with the oscillatory integrand function P, these formulæ may be unable to follow the oscillations properly; thus, we propose using the 30-point Gauss method together with its 61-point Kronrod extension. This is essentially also the method suggested for oscillatory integrals in the NAG Library [81] (see the documentation for routine D01AKF).

Appendix C

Table of Padé Approximates for Mittag-Leffler Function

This appendix presents a scheme for fast computations of

$$E_\alpha(-x^\alpha), \quad 0 < \alpha < 1, \quad x \geq 0,$$

suitable for finite elements. This function appears in the relaxation functions of both the FOV fluid (2.1) and solid (2.2).

The defining series (1.11) is used on the interval $0 < x < 0.1$, and an asymptotic series (1.16) is used whenever $x > 15$, as in Alg. 1.4, but in contrast with Alg. 1.4, a Padé approximate (or rational polynomial) is applied inbetween where $0.1 \leq x \leq 15$; specifically,

$$E_\alpha(-x^\alpha) \approx \begin{cases} \sum_{k=0}^{4} \frac{(-x)^{\alpha k}}{\Gamma(1+\alpha k)} & 0 \leq x \leq 0.1 \\ \frac{a_0+a_1 x+a_2 x^2}{1+b_1 x+b_2 x^2+b_3 x-0^3} & 0.1 < x < 15 \\ -\sum_{k=1}^{4} \frac{(-x)^{-\alpha k}}{\Gamma(1-\alpha k)} & x \geq 15 \end{cases} \tag{C.1}$$

where the coefficients a_0, a_1, a_2, b_1, b_2 and b_3 are listed in Table C.1 for values of α varying between 0.01 and 0.99 by increments of 0.01. Also listed are the r^2 resultants from each nonlinear regression with the tolerance set sufficient to achieve accuracies of $r^2 > 0.999$, except for $\alpha > 0.9$ where such tight r^2 values could not be achieved for the order of approximate employed. The Padé approximates were obtained from fits to exact values (within machine precision) for the Mittag-Leffler function (obtained from Alg. 1.4) at 150 evenly spaced grid points over the interval $[0.1, 15]$. The form of this rational polynomial was selected after a study of numerous tables for function approximation listed in the appendices of Hart et al. [48]. Our fits were constrained to be exact at the end points so that transitions will be smooth when crossing a boundary between solution domains.

A number written as 0.123456(7) stands for $0.123456 \cdot 10^7 = 1,234,560$.

Table C.1: Coefficients for Padé approximates of Mittag-Leffler function.

α	a_0	a_1	a_2	b_1	b_2	b_3	r^2
0.01	-.424129(3)	-.695856(6)	-.391944(6)	-.138637(7)	-.795778(6)	-.207400(3)	0.999371
0.02	-.291078(4)	-.231705(7)	-.121393(7)	-.460100(7)	-.250385(7)	-.127923(4)	0.999345
0.03	-.159594(4)	-.883786(6)	-.485177(6)	-.174711(7)	-.101562(7)	-.832687(3)	0.999381
0.04	-.401668(4)	-.151329(7)	-.678102(6)	-.298958(7)	-.144743(7)	-.138260(4)	0.999114
0.05	-.480619(4)	-.145550(7)	-.643881(6)	-.286638(7)	-.139751(7)	-.171118(4)	0.999129
0.06	-.358700(4)	-.953746(6)	-.452754(6)	-.186815(7)	-.996694(6)	-.160873(4)	0.999313
0.07	-.431271(4)	-.958824(6)	-.424475(6)	-.187447(7)	-.952144(6)	-.175012(4)	0.999215
0.08	-.104813(5)	-.220562(7)	-.109649(7)	-.427837(7)	-.248747(7)	-.594850(4)	0.999401
0.09	-.113182(5)	-.204162(7)	-.931135(6)	-.395568(7)	-.215524(7)	-.560193(4)	0.999340
0.10	-.100534(5)	-.165546(7)	-.753470(6)	-.319371(7)	-.177305(7)	-.527749(4)	0.999361
0.11	-.771890(4)	-.116952(7)	-.530686(6)	-.224658(7)	-.126954(7)	-.429168(4)	0.999382
0.12	-.209949(4)	-.331485(6)	-.178194(6)	-.628014(6)	-.428531(6)	-.183967(4)	0.999349
0.13	-.201966(5)	-.264628(7)	-.118361(7)	-.503944(7)	-.292906(7)	-.123451(5)	0.999408
0.14	-.144185(5)	-.177380(7)	-.787251(6)	-.336281(7)	-.198184(7)	-.923408(4)	0.999420
0.15	-.358699(4)	-.414163(6)	-.180624(6)	-.782040(6)	-.463020(6)	-.235432(4)	0.999423
0.16	-.367384(5)	-.387982(7)	-.157708(7)	-.732069(7)	-.414017(7)	-.218683(5)	0.999358
0.17	-.834348(4)	-.877610(6)	-.381391(6)	-.163991(7)	-.101120(7)	-.619007(4)	0.999453
0.18	-.665920(4)	-.661019(6)	-.279508(6)	-.123090(7)	-.755801(6)	-.495376(4)	0.999452
0.19	-.880313(4)	-.839225(6)	-.352670(6)	-.155465(7)	-.970538(6)	-.689880(4)	0.999463
0.20	-.516937(4)	-.463982(6)	-.186660(6)	-.857478(6)	-.525412(6)	-.391939(4)	0.999446
0.21	-.181654(5)	-.159929(7)	-.655973(6)	-.293380(7)	-.187316(7)	-.153968(5)	0.999480
0.22	-.287739(5)	-.241617(7)	-.962412(6)	-.441685(7)	-.280701(7)	-.244057(5)	0.999477
0.23	-.283969(5)	-.233523(7)	-.935683(6)	-.423970(7)	-.277398(7)	-.261404(5)	0.999497
0.24	-.218950(5)	-.174274(7)	-.687682(6)	-.314803(7)	-.207911(7)	-.208550(5)	0.999503
0.25	-.184865(5)	-.142847(7)	-.555414(6)	-.256670(7)	-.171282(7)	-.182554(5)	0.999510
0.26	-.154930(5)	-.116572(7)	-.448241(6)	-.208289(7)	-.140906(7)	-.159998(5)	0.999520
0.27	-.252656(5)	-.187367(7)	-.720787(6)	-.332362(7)	-.230555(7)	-.280571(5)	0.999534
0.28	-.348286(5)	-.250157(7)	-.938597(6)	-.441764(7)	-.306951(7)	-.392527(5)	0.999538
0.29	-.223178(5)	-.158819(7)	-.597404(6)	-.278265(7)	-.198723(7)	-.272201(5)	0.999553
0.30	-.262152(5)	-.180630(7)	-.659350(6)	-.315184(7)	-.224602(7)	-.321389(5)	0.999556
0.31	-.110316(5)	-.741001(6)	-.263517(6)	-.128658(7)	-.919175(6)	-.137449(5)	0.999558
0.32	-.344887(5)	-.231540(7)	-.831618(6)	-.398374(7)	-.294522(7)	-.473795(5)	0.999578
0.33	-.253440(5)	-.165943(7)	-.579558(6)	-.284133(7)	-.210336(7)	-.352888(5)	0.999583
0.34	-.320037(5)	-.206983(7)	-.712936(6)	-.351975(7)	-.264342(7)	-.467058(5)	0.999592
0.35	-.788648(5)	-.506620(7)	-.172863(7)	-.854865(7)	-.654223(7)	-.122026(6)	0.999604
0.36	-.289781(5)	-.195379(7)	-.707274(6)	-.324061(7)	-.268137(7)	-.555978(5)	0.999616
0.37	-.142051(5)	-.971770(6)	-.354821(6)	-.159385(7)	-.136569(7)	-.302386(5)	0.999617
0.38	-.816551(5)	-.523578(7)	-.175872(7)	-.860767(7)	-.705295(7)	-.156056(6)	0.999642
0.39	-.575871(5)	-.348533(7)	-.107617(7)	-.574012(7)	-.450994(7)	-.991720(5)	0.999625
0.40	-.173808(5)	-.117277(7)	-.408516(6)	-.187857(7)	-.167833(7)	-.429558(5)	0.999651
0.41	-.103477(5)	-.686777(6)	-.231234(6)	-.109392(7)	-.977034(6)	-.258727(5)	0.999700
0.42	-.195086(5)	-.129617(7)	-.429282(6)	-.204698(7)	-.185582(7)	-.514821(5)	0.999681
0.43	-.333165(5)	-.221252(7)	-.718492(6)	-.346552(7)	-.318194(7)	-.922518(5)	0.999693
0.44	-.473286(5)	-.311742(7)	-.981295(6)	-.484992(7)	-.447200(7)	-.134275(6)	0.999708
0.45	-.147598(5)	-.982326(6)	-.304968(6)	-.151324(7)	-.142189(7)	-.447789(5)	0.999719
0.46	-.152914(5)	-.104712(7)	-.326140(6)	-.159246(7)	-.154553(7)	-.517302(5)	0.999725
0.47	-.167037(5)	-.114533(7)	-.346912(6)	-.172774(7)	-.169118(7)	-.587605(5)	0.999740
0.48	-.142611(5)	-.991368(6)	-.293586(6)	-.148061(7)	-.147062(7)	-.531760(5)	0.999752
0.49	-.654706(5)	-.455618(7)	-.130849(7)	-.675094(7)	-.675481(7)	-.253173(6)	0.999766
0.50	-.188800(3)	-.135370(5)	-.383675(4)	-.198223(5)	-.202768(5)	-.797517(3)	0.999777
0.51	-.516448(5)	-.373170(7)	-.102716(7)	-.541357(7)	-.559798(7)	-.228252(6)	0.999790
0.52	-.392154(5)	-.289687(7)	-.780114(6)	-.415703(7)	-.437101(7)	-.185908(6)	0.999801
0.53	-.135449(5)	-.106392(7)	-.289899(6)	-.150142(7)	-.164334(7)	-.749106(5)	0.999802
0.54	-.953841(4)	-.748349(6)	-.193214(6)	-.104887(7)	-.114460(7)	-.530462(5)	0.999822
0.55	-.793386(3)	-.639333(5)	-.159875(5)	-.886439(5)	-.979799(5)	-.469973(4)	0.999835
0.56	-.599232(4)	-.443865(6)	-.952614(5)	-.619108(6)	-.646389(6)	-.288690(5)	0.999847

Table C.1: Coefficients for Padé approximates of Mittag-Leffler function.

α	a_0	a_1	a_2	b_1	b_2	b_3	r^2
0.57	-.337393(5)	-.286190(7)	-.663678(6)	-.388535(7)	-.438767(7)	-.223581(6)	0.999859
0.58	-.463960(5)	-.405168(7)	-.899289(6)	-.544254(7)	-.620515(7)	-.324201(6)	0.999871
0.59	-.151791(4)	-.125852(6)	-.241507(5)	-.169238(6)	-.185486(6)	-.904156(4)	0.999886
0.60	-.502729(4)	-.464569(6)	-.919187(5)	-.611566(6)	-.705142(6)	-.377940(5)	0.999896
0.61	-.480103(5)	-.461103(7)	-.860143(6)	-.600297(7)	-.697998(7)	-.378472(6)	0.999907
0.62	-.671512(4)	-.708363(6)	-.131044(6)	-.906252(6)	-.108843(7)	-.626832(5)	0.999908
0.63	-.312780(5)	-.328986(7)	-.533551(6)	-.418611(7)	-.494518(7)	-.268704(6)	0.999928
0.64	-.567954(5)	-.632239(7)	-.945394(6)	-.794766(7)	-.947107(7)	-.509518(6)	0.999937
0.65	-.149230(4)	-.182752(6)	-.259499(5)	-.226154(6)	-.275373(6)	-.151317(5)	0.999939
0.66	-.433396(5)	-.549988(7)	-.664464(6)	-.674519(7)	-.815645(7)	-.407908(6)	0.999953
0.67	-.752321(4)	-.109682(7)	-.126030(6)	-.132094(7)	-.164296(7)	-.843703(5)	0.999948
0.68	-.503149(5)	-.782828(7)	-.716973(6)	-.932883(7)	-.115421(8)	-.500161(6)	0.999960
0.69	-.113475(5)	-.204800(7)	-.158167(6)	-.240096(7)	-.301897(7)	-.117538(6)	0.999955
0.70	-.277604(3)	-.535397(5)	-.226639(4)	-.621910(5)	-.768192(5)	-.150446(4)	0.999976
0.71	-.551694(5)	-.158192(8)	-.673086(6)	-.178833(8)	-.232888(8)	-.532630(6)	0.999919
0.72	-.310305(5)	-.102892(8)	0.663348(5)	-.115056(8)	-.146317(8)	0.202771(6)	0.99994
0.73	-.160766(4)	-.449254(7)	-.116371(6)	-.482429(7)	-.682061(7)	-.111373(6)	0.999719
0.74	0.341935(4)	-.241906(7)	-.669717(5)	-.252295(7)	-.376790(7)	-.808538(5)	0.999510
0.75	0.173763(4)	-.103357(7)	-.513330(6)	-.106853(7)	-.212490(7)	-.787594(6)	0.999166
0.76	-.198004(4)	-.170209(6)	-.546410(6)	-.212224(6)	-.727938(6)	-.906762(6)	0.999483
0.77	-.255574(4)	-.399973(6)	-.408010(6)	-.461840(6)	-.889107(6)	-.736776(6)	0.999574
0.78	-.107310(4)	-.102865(6)	-.104591(6)	-.125079(6)	-.207143(6)	-.205284(6)	0.999673
0.79	-.494450(4)	-.463767(6)	-.357502(6)	-.563528(6)	-.802633(6)	-.767703(6)	0.999707
0.80	-.218066(4)	-.219047(6)	-.128115(6)	-.262855(6)	-.339154(6)	-.302753(6)	0.999721
0.81	-.534378(4)	-.539996(6)	-.258539(6)	-.645497(6)	-.766988(6)	-.675138(6)	0.999723
0.82	-.675467(4)	-.688012(6)	-.275764(6)	-.819312(6)	-.908437(6)	-.800006(6)	0.999715
0.83	-.702848(3)	-.690578(5)	-.240789(5)	-.824283(5)	-.847142(5)	-.779293(5)	0.999699
0.84	-.609980(4)	-.583751(6)	-.176849(6)	-.697471(6)	-.667838(6)	-.642815(6)	0.999674
0.85	-.103053(5)	-.915547(6)	-.247199(6)	-.110278(7)	-.963517(6)	-.101397(7)	0.999639
0.86	-.774771(4)	-.667011(6)	-.156824(6)	-.805409(6)	-.651177(6)	-.733497(6)	0.999594
0.87	-.838904(4)	-.693431(6)	-.141730(6)	-.840712(6)	-.624128(6)	-.763282(6)	0.999538
0.88	-.447750(4)	-.359964(6)	-.629983(5)	-.437447(6)	-.299094(6)	-.396021(6)	0.999468
0.89	-.390787(4)	-.296304(6)	-.446099(5)	-.362820(6)	-.222076(6)	-.331368(6)	0.999382
0.90	-.724688(4)	-.509096(6)	-.654940(5)	-.630388(6)	-.335377(6)	-.584487(6)	0.999277
0.91	-.152262(5)	-.100158(7)	-.106340(6)	-.125254(7)	-.574996(6)	-.117309(7)	0.999150
0.92	-.150108(5)	-.942028(6)	-.792810(5)	-.118669(7)	-.467003(6)	-.112366(7)	0.998998
0.93	-.106495(5)	-.626399(6)	-.398859(5)	-.797901(6)	-.255226(6)	-766267(6)	0.998816
0.94	-.153906(5)	-.847297(6)	-371308(5)	-.109242(7)	-.268144(6)	-.106481(7)	0.998600
0.95	-.600332(4)	-.311566(6)	0.756057(4)	-.406277(6)	-.710353(5)	-.401715(6)	0.998343
0.96	-.445797(5)	-.214492(7)	-.119855(5)	-.284119(7)	-.270455(6)	-.285641(7)	0.998041
0.97	-.355171(5)	-.159674(7)	0.206708(5)	-.214673(7)	-.423690(5)	-.219239(7)	0.997685
0.98	-.145397(5)	-.610793(6)	0.190402(5)	-.834188(6)	0.464083(5)	-.865369(6)	0.997270
0.99	-.105996(5)	-.416113(6)	0.204340(5)	-.577797(6)	0.755603(5)	-.608788(6)	0.996786

Bibliography

[1] M. Abramowitz and I. A. Stegun (eds.), *Handbook of mathematical functions: With formulas, graphs, and mathematical tables*, NBS Applied Mathematics Series, vol. 55, National Bureau of Standards, Washington, D.C., 1964, Second printing with corrections. Republished by Dover, New York, 1965.

[2] E. Almansi, *Sulle deformazioni finite dei solidi elastici isotropi*, Rendiconti della Reale Accademia dei Lincei: Classe di scienze fisiche, matematiche e naturali **20** (1911), 705–714.

[3] R. L. Bagley and R. A. Calico, *Fractional order state equations for the control of viscoelastically damped structures*, Journal of Guidance, Control, and Dynamics **14** (1991), 304–311.

[4] R. L. Bagley and P. J. Torvik, *A theoretical basis for the application of fractional calculus to viscoelasticity*, Journal of Rheology **27** (1983), 201–210.

[5] ———, *On the fractional calculus model of viscoelastic behavior*, Journal of Rheology **30** (1986), 133–155.

[6] Z. P. Bažant, *Easy-to-compute tensors with symmetric inverse approximating Hencky finite strain and its rate*, Journal of Engineering Materials and Technology **120** (1998), 131–136.

[7] B. Bernstein, E. A. Kearsley, and L. J. Zapas, *A study of stress relaxation with finite strain*, Transactions of the Society of Rheology **7** (1963), 391–410.

[8] G. W. Scott Blair, *Analytical and integrative aspects of the stress-strain-time problem*, Journal of Scientific Instruments **21** (1944), 80–84.

[9] L. Boltzmann, *Zur Theorie der elastischen Nachwirkung*, Sitzungsberichte der Kaiserlichen Akademie der Wissenschaften: Mathematisch-naturwissenschaftlichen klasse, Wien **70** (1874), 275–300.

[10] H. Brass, J.-W. Fischer, and K. Petras, *The Gaussian quadrature method*, Abhandlungen der Braunschweigischen Wissenschaftlichen Gesellschaft **47** (1996), 115–150.

[11] P. W. Bridgman, *The compressibility of thirty metals as a function of pressure and temperature*, Proceedings of the American Academy of Arts and Sciences **58** (1923), 165–242.

[12] M. Caputo, *Linear models of dissipation whose Q is almost frequency independent–II*, The Geophysical Journal of the Royal Astronomical Society **13** (1967), 529–539.

[13] M. Caputo and F. Mainardi, *Linear models of dissipation in anelastic solids*, Rivista del Nuovo Cimento **1** (1971), 161–198.

[14] A.-L. Cauchy, *Exercices de mathématiques*, vol. 2, de Bure Frères, Paris, 1827.

[15] J.-T. Chern, *Finite element modeling of viscoelastic materials on the theory of fractional calculus*, Ph.D. thesis, The Pennsylvania State University, December 1993, University Microfilms No. 9414260.

[16] R. M. Christensen, *Theory of viscoelasticity: An introduction*, Academic Press, New York, 1971.

[17] K. S. Cole and R. H. Cole, *Dispersion and absorption in dielectrics: I. alternating current characteristics*, Journal of Chemical Physics **9** (1941), 341–351.

[18] B. D. Coleman, *Thermodynamics of materials with memory*, Archive for Rational Mechanics and Analysis **17** (1964), 1–46.

[19] B. D. Coleman and V. J. Mizel, *On the general theory of fading memory*, Archive for Rational Mechanics and Analysis **29** (1968), 18–31.

[20] K. Diethelm, *Generalized compound quadrature formulæ for finite-part integrals*, IMA Journal of Numerical Analysis **17** (1997), 479–493.

[21] K. Diethelm and N. J. Ford, *Analysis of fractional differential equations*, Journal of Mathematical Analysis and Applications **265** (2002), in press.

[22] K. Diethelm, N. J. Ford, and A. D. Freed, *Detailed error analysis for a fractional Adams method*, In review.

[23] ———, *A predictor-corrector approach for the numerical solution of fractional differential equations*, Nonlinear Dynamics **??** (2002), in press.

[24] K. Diethelm and G. Walz, *Numerical solution of fractional order differential equations by extrapolation*, Numerical Algorithms **16** (1997), 231–253.

[25] J. F. Douglas, *Polymer science applications of path-integration, integral equations, and fractional calculus*, Applications of Fractional Calculus in Physics (R. Hilfer, ed.), World Scientific, Singapore, 2000, pp. 241–330.

[26] T. C. Doyle and J. E. Ericksen, *Nonlinear elasticity*, Advances in Applied Mechanics (H. L. Dryden and T. von Kármán, eds.), vol. 4, Academic Press, New York, 1956, pp. 53–115.

[27] A. D. Drozdov, *Fractional differential models in finite viscoelasticity*, Acta Mechanica **124** (1997), 155–180.

[28] D. C. Drucker, *A definition of stable inelastic material*, Journal of Applied Mechanics **27** (1959), 101–106.

[29] S. Ehrich, *Stieltjes polynomials and the error of Gauss-Kronrod quadrature formulas*, Applications and Computation of Orthogonal Polynomials (W. Gautschi, G. Golub, and G. Opfer, eds.), International Series of Numerical Mathematics, no. 131, Birkhäuser, Basel, 1999, pp. 57–77.

[30] D. Elliott, *An asymptotic analysis of two algorithms for certain Hadamard finite-part integrals*, IMA Journal of Numerical Analysis **13** (1993), 445–462.

[31] A. Erdélyi, W. Magnus, F. Oberhettinger, and F. G. Tricomi (eds.), *Higher transcendental functions*, Bateman manuscript project, vol. 2, McGraw-Hill, New York, 1955.

[32] J. Finger, *Über die allgemeinsten Beziehungen zwischen endlichen Deformationen und den zugehörigen Spannungen in aeolotropen und isotropen Substanzen*, Sitzungsberichte der Akademie der Wissenschaften, Wien **103** (1894), 1073–1100.

[33] E. R. Fitzgerald, Jr. L. D. Grandine, and J. D. Ferry, *Dynamic mechanical properties of polyisobutylene*, Journal of Applied Physics **24** (1953), 650–655.

[34] P. J. Flory, *Thermodynamic relations for high elastic materials*, Transactions of the Faraday Society **57** (1961), 829–838.

[35] N. J. Ford and A. C. Simpson, *The numerical solution of fractional differential equations: Speed versus accuracy*, Numerical Algorithms **26** (2001), 333–346.

[36] A. D. Freed, *Natural strain*, Journal of Engineering Materials and Technology **117** (1995), 379–385.

[37] S. Fujiwara and F. Yonezawa, *Anomalous relaxation in fractal structures*, Physical Review E **51** (1995), 2277–2285.

[38] A. Gemant, *A method of analyzing experimental results obtained from elasto-viscous bodies*, Physics **7** (1936), 311–317.

[39] A. N. Gent and R. S. Rivlin, *Experiments on the mechanics of rubber I: Eversion of a tube*, Proceedings of the Physical Society, London **B 65** (1952), 118–121.

[40] ———, *Experiments on the mechanics of rubber II: The torsion, inflation and extension of a tube*, Proceedings of the Physical Society, London **B 65** (1952), 487–501.

[41] ———, *Experiments on the mechanics of rubber III: Small torsions of stretched prisms*, Proceedings of the Physical Society, London **B 65** (1952), 645–648.

[42] A. N. Gerasimov, *A generalization of linear laws of deformation and its application to inner friction problems*, Prikladnaëiìa Matematika i Mekhanika **12** (1948), 251–260.

[43] S. Gomi and F. Yonezawa, *Anomalous relaxation in the fractal time random walk model*, Physical Review Letters **74** (1975), 4125–4128.

[44] R. Gorenflo, *Fractional calculus: Some numerical methods*, Fractals and Fractional Calculus in Continuum Mechanics (A. Carpinteri and F. Mainardi, eds.), CISM Courses and Lectures, no. 378, Springer, Wien, 1997, pp. 277–290.

[45] R. Gorenflo, I. Loutchko, and Yu. Luchko, *Numerische Berechnung der Mittag-Leffler - Funktion $E_{\alpha,\beta}(z)$ und ihrer Ableitung*, Tech. Report A–6–99, Freie Universität Berlin, Berlin, 1999.

[46] G. Green, *On the propagation of light in crystallized media*, Transactions of the Cambridge Philosophical Society **7** (1841), 121–140.

[47] M. E. Gurtin and E. Sternberg, *On the linear theory of viscoelasticity*, Archive for Rational Mechanics and Analysis **11** (1962), 291–356.

[48] J. F. Hart, E. W. Cheney, C. L. Lawson, H. J. Maehly, C. K. Mesztenyi, J. R. Rice, H. G. Thacher, Jr., and C. Witzgall, *Computer approximations*, The SIAM Series in Applied Mathematics, John Wiley & Sons, New York, 1968.

[49] H. Hencky, *Über die Form des Elastizitätsgesetzes bei ideal elastischen Stoffen*, Zeitschrift für technische Physik **9** (1928), 215–220.

[50] ———, *The law of elasticity for isotropic and quasi-isotropic substances by finite deformations*, Journal of Rheology **2** (1931), 169–176.

[51] A. Hoger, *The material time derivative of logarithmic strain*, International Journal of Solids and Structures **22** (1986), 1019–1032.

[52] F. de Hoog and R. Weiss, *Asymptotic expansions for product integration*, Mathematics of Computation **27** (1973), 295–306.

[53] H. M. James and E. Guth, *Theory of the elastic properties of rubber*, The Journal of Chemical Physics **11** (1943), 455–481.

[54] G. Jaumann, *Die Grundlagen der Bewegungslehre von einem modernen Standpunkte aus*, Verlag, Leipzig, 1905.

[55] ———, *Geschlossenes System physikalischer und chemischer Differentialgesetze*, Sitzungsberichte der Kaiserlichen Akademie der Wissenschaften: Mathematisch - naturwissenschaftliche klasse **120** (1911), 385–530.

[56] A. Kaye, *Non-Newtonian flow in incompressible fluids*, Tech. Report 134, The College of Aeronautics, Cranfield, October 1962.

[57] A. A. Kilbas and J. J. Trujillo, *Differential equations of fractional order: Methods, results and problems–I*, Applicable Analysis **78** (2001), 153–192.

[58] G. Kirchhoff, *über die Gleichungen des Gleichgewichtes eines elastischen Körpers bei nicht unendlich kleinen Verschiebungen seiner Theile*, Sitzungsberichte der Akademie der Wissenschaften, Wien **9** (1852), 763–773.

[59] A. S. Kronrod, *Integration with control of accuracy*, Soviet Physics Doklady **9** (1964), no. 1, 17–19.

[60] ———, *Nodes and weights for quadrature formulæ: Sixteen place tables*, Nauka, Moscow, 1964, In Russian.

[61] Y. Kwon and K. S. Cho, *Time-strain nonseparability in viscoelastic constitutive equations*, Journal of Rheology **45** (2001), 1441–1452.

[62] R. S. Lakes, *Viscoelastic solids*, CRC Press, Boca Raton, 1998.

[63] A. I. Leonov, *On a class of constitutive equations for viscoelastic liquids*, Journal of Non-Newtonian Fluid Mechanics **25** (1987), 1–59.

[64] ———, *On the constitutive equations for nonisothermal bulk relaxation*, Macromolecules **29** (1996), 8383–8386.

[65] ———, *Constitutive equations for viscoelastic liquids: Formulation, analysis and comparison with data*, Advances in the Flow and Rheology of Non-Newtonian Fluids (D. A. Siginer, D. DeKee, and R. P. Chalra, eds.), vol. A, Elsevier, New York, 1999, pp. 519–575.

[66] ———, *On the conditions of potentiality in finite elasticity and hypo-elasticity*, International Journal of Solids and Structures **37** (2000), 2565–2576.

[67] J. Liouville, *Mémoire sur quelques questions de géométrie et de mécanique, et sur un nouveau genre de calcul pour résoudre ces questions*, Journal de l'École Polytechnique **13** (1832), no. cahier 21, 1–66.

[68] A. S. Lodge, *Elastic liquids: An introductory vector treatment of finite-strain polymer rheology*, Academic Press, London, 1964.

[69] ———, *On the description of rheological properties of viscoelastic continua. I. Body-, space-, and Cartesian-space - tensor fields*, Rheological Acta **11** (1972), 106–118.

[70] ———, *Body tensor fields in continuum mechanics: With applications to polymer rheology*, Academic Press, New York, 1974.

[71] ———, 1980, Course notes, University of Wisconsin, Madison.

[72] ———, *An introduction to elastomer molecular network theory*, Bannatek Press, PO Box 44133, Madison, WI, 1999, Has no ISBN.

[73] C. F. Lorenzo and T. T. Hartley, *Initialized fractional calculus*, TP 2000-209943, NASA Glenn Research Center, Cleveland, February 2000.

[74] J. Lützen, 2001, Personal communication.

[75] F. Mainardi, *Fractional calculus: Some basic problems in continuum and statistical mechanics*, Fractals and Fractional Calculus in Continuum Mechanics (A. Carpinteri and F. Mainardi, eds.), CISM Courses and Lectures, no. 378, Springer, Wien, 1997, pp. 291–348.

[76] F. Mainardi and R. Gorenflo, *The Mittag-Leffler function in the Riemann-Liouville fractional calculus*, Boundary Value Problems, Special Functions and Fractional Calculus. Proceedings of international conference dedicated to 90th birthday of Prof. F. D. Gakhov (Minsk) (A. A. Kilbas, ed.), Belarusian State University, February 1996, pp. 215–225.

[77] R. S. Marvin, R. Aldrich, and H. S. Sack, *The dynamic bulk viscosity of polyisobutylene*, Journal of Applied Physics **25** (1954), 1213–1218.

[78] K. S. Miller and B. Ross, *An introduction to the fractional calculus and fractional differential equations*, John Wiley & Sons, New York, 1993.

[79] G. Mittag-Leffler, *Sur la représentation analytique d'une branche uniforme d'une fonction monogène*, Acta Mathematica **29** (1904), 101–168.

[80] M. Mooney, *A theory of large elastic deformations*, Journal of Applied Physics **11** (1940), 582–592.

[81] Numerical Algorithms Group, Ltd., Oxford, *NAG FORTRAN library mark 17*, 1995.

[82] K. B. Oldham and J. Spanier, *The fractional calculus*, Mathematics in Science and Engineering, Academic Press, New York, 1974.

[83] J. G. Oldroyd, *On the formulation of rheological equations of state*, Proceedings of the Royal Society, London **A 200** (1950), 523–541.

[84] R. Piessens, E. de Doncker-Kapenga, C. Überhuber, and D. K. Kahaner, *QUADPACK—A subroutine package for automatic integration*, Springer Series in Computational Mathematics, Springer, Berlin, 1983.

[85] G. Piola, *La meccanica dé corpi naturalmente estesi: Trattata col calcolo delle variazioni*, Opuscoli Matematici e Fisici di Diversi Autori **1** (1833), 201–236.

[86] I. Podlubny, *Fractional differential equations: An introduction to fractional derivatives, fractional differential equations, to methods of their solution and some of their applications*, Mathematics in Science and Engineering, vol. 198, Academic Press, San Diego, 1999.

[87] ———, *Geometric and physical interpretation of fractional integration and fractional differentiation*, Tech. report, Department of Informatics and Control Engineering, Technical University of Kosice, 2001.

[88] J. H. Poynting, *On pressure perpendicular to the shear planes in finite pure shears, and on the lengthening of loaded wires when twisted*, Proceedings of the Royal Society, London **A 82** (1909), 546–559.

[89] W. H. Press, S. A. Teukolsky, W. T. Vetterling, and B. P. Flannery, *Numerical recipes in C: The art oft scientific computing*, 2nd ed., Cambridge University Press, Cambridge, 1999, Reprinted, corrected to software version 2.08.

[90] Yu. N. Rabotnov, *Creep problems in structural members*, North-Holland Series in Applied Mathematics and Mechanics, vol. 7, North-Holland Publishing Company, Amsterdam, 1969, Originally published in Russian as: *Polzuchest Elementov Konstruktsii*, Nauka, Moscow, 1966.

[91] M. Reiner, *A mathematical theory of dilatancy*, American Journal of Mathematics **67** (1945), 350–362.

[92] M. Renardy, *A local existence and uniqueness theorem for a K-BKZ-fluid*, Archives for Rational Mechanics and Analysis **88** (1985), 83–94.

[93] R. S. Rivlin, *Large elastic deformations of isotropic materials I. Fundamental concepts*, Philosophical Transactions of the Royal Society, London **A 240** (1948), 459–490.

[94] ———, *Large elastic deformations of isotropic materials II. Some uniqueness theorems for pure, homogeneous deformation*, Philosophical Transactions of the Royal Society, London **A 240** (1948), 491–508.

[95] ———, *Large elastic deformations of isotropic materials III. Some simple problems in cylindrical polar co-ordinates*, Philosophical Transactions of the Royal Society, London **A 240** (1948), 509–525.

[96] ———, *Large elastic deformations of isotropic materials IV. Further developments of the general theory*, Philosophical Transactions of the Royal Society, London **A 241** (1948), 379–397.

[97] ———, *Large elastic deformations of isotropic materials. V. The problem of flexture*, Proceedings of the Royal Society, London **A 195** (1949), 463–473.

[98] ———, *Large elastic deformations of isotropic materials VI. Further results in the theory of torsion, shear and flexture*, Philosophical Transactions of the Royal Society, London **A 242** (1949), 173–195.

[99] R. S. Rivlin and D. W. Saunders, *Large elastic deformations of isotropic materials VII. Experiments on the deformation of rubber*, Philosophical Transactions of the Royal Society, London **A 243** (1951), 251–288.

[100] B. Ross, *The development of fractional calculus 1695–1900*, Historia Mathematica **4** (1977), 75–89.

[101] M. S. Sacks, *Biaxial mechanical evaluation of planar biological materials*, Journal of Elasticity **61** (2000), 199–246.

[102] S. G. Samko, A. Kilbas, and O. I. Marichev, *Fractional integrals and derivatives: Theory and applications*, Gordon and Breach, Yverdon, 1993.

[103] S. B. Sane and W. G. Knauss, *The time-dependent bulk response of poly (methyl methacrylate)*, Mechanics of Time-Dependent Materials **5** (2001), 293–324.

[104] A. Signorini, *Sulle deformazioni thermoelastiche finite*, Proceedings of the 3rd International Congress for Applied Mechanics (Stockholm) (C. W. Oseen and W. Weibull, eds.), vol. 2, Ab. Sveriges Litografiska Tryckerier, 1930, pp. 80–89.

[105] J. C. Simo and R. L. Taylor, *Quasi-incompressible finite elasticity in principal stretches. Continuum basis and numerical algorithms*, Computer Methods in Applied Mechanics and Engineering **85** (1991), 273–310.

[106] I. S. Sokolnikoff, *Tensor analysis: Theory and applications to geometry and mechanics of continua*, 2nd ed., John Wiley & Sons, New York, 1964.

[107] A. J. M. Spencer, *Deformations of fibre-reinforced materials*, Clarendon Press, Oxford, 1972.

[108] C. Truesdell, *Geometric interpretation for the reciprocal deformation tensors*, Quarterly Journal of Applied Mathematics **15** (1958), 434–435.

[109] S. W. J. Welch, R. A. L. Ropper, and Jr. R. G. Duren, *Application of time-based fractional calculus methods to viscoelastic creep and stress relaxation of materials*, Mechanics of Time-Dependent Materials **3** (1999), 279–303.

[110] S. Zaremba, *Sur une forme perfectionnée de la théorie de la relaxation*, Bulletin de l'Académie de Cracovie (1903), 594–614.

[111] C. Zener, *Elasticity and anelasticity of metals*, The University of Chicago Press, Chicago, 1948.

REPORT DOCUMENTATION PAGE

Form Approved
OMB No. 0704-0188

1. AGENCY USE ONLY (*Leave blank*)	2. REPORT DATE	3. REPORT TYPE AND DATES COVERED
	December 2002	Technical Memorandum

4. TITLE AND SUBTITLE

Fractional-Order Viscoelasticity (FOV): Constitutive Development Using the Fractional Calculus: First Annual Report

5. FUNDING NUMBERS

WU–708–24–13–00

6. AUTHOR(S)

Alan Freed, Kai Diethelm, and Yury Luchko

7. PERFORMING ORGANIZATION NAME(S) AND ADDRESS(ES)

National Aeronautics and Space Administration
John H. Glenn Research Center at Lewis Field
Cleveland, Ohio 44135–3191

8. PERFORMING ORGANIZATION REPORT NUMBER

E–13607

9. SPONSORING/MONITORING AGENCY NAME(S) AND ADDRESS(ES)

National Aeronautics and Space Administration
Washington, DC 20546–0001

10. SPONSORING/MONITORING AGENCY REPORT NUMBER

NASA TM—2002-211914

11. SUPPLEMENTARY NOTES

Alan Freed, NASA Glenn Research Center, Cleveland, Ohio; Kai Diethelm, Technische Universität Braunschweig, Braunschweig, Germany; and Yury Luchko, Europe University Viadrina, Frankfurt, Germany. Responsible person, Alan Freed, organization code 5150, 216–433–8747.

12a. DISTRIBUTION/AVAILABILITY STATEMENT

Unclassified - Unlimited
Subject Category: 27 Distribution: Nonstandard

Available electronically at http://gltrs.grc.nasa.gov

This publication is available from the NASA Center for AeroSpace Information, 301–621–0390.

12b. DISTRIBUTION CODE

13. ABSTRACT ***(Maximum 200 words)***

This is the first annual report to the U.S. Army Medical Research and Material Command for the three year project "Advanced Soft Tissue Modeling for Telemedicine and Surgical Simulation" supported by grant No. DAMD17–01–1–0673 to The Cleveland Clinic Foundation, to which the NASA Glenn Research Center is a subcontractor through Space Act Agreement SAA 3–445. The objective of this report is to extend popular one-dimensional (1D) fractional-order viscoelastic (FOV) materials models into their three-dimensional (3D) equivalents for finitely deforming continua, and to provide numerical algorithms for their solution.

14. SUBJECT TERMS	15. NUMBER OF PAGES
Elasticity; Viscoelasticity; Stress; Strain; Numerical differentiation; Numerical integration	137
	16. PRICE CODE

17. SECURITY CLASSIFICATION OF REPORT	18. SECURITY CLASSIFICATION OF THIS PAGE	19. SECURITY CLASSIFICATION OF ABSTRACT	20. LIMITATION OF ABSTRACT
Unclassified	Unclassified	Unclassified	